



**UNIwersYTET
MIKOŁAJA KOPERNIKA
W TORUNIU**

Collegium Medicum
im. Ludwika Rydygiera w Bydgoszczy

Bydgoszcz 2023 r.



**UNIWERSYTET
MIKOŁAJA KOPERNIKA
W TORUNIU**
Wydział Lekarski
Collegium Medicum w Bydgoszczy

Karolina Matulewicz

**Modifications of selected cytostatics
in genitourinary cancers**

Rozprawa na stopień doktora nauk medycznych

Promotor:

Dr hab. n. med. Anna Bajek, prof. UMK

Drugi Promotor:

Associated Prof. Bartosz Tylkowski

Bydgoszcz 2023 r.

*Składam serdeczne podziękowania
Moim Promotorom, Prof. Annie Bajek i Prof. Bartoszowi Tylkowskiemu
za poświęcony czas, cenne wskazówki oraz ogrom wiedzy naukowej
przekazanej mi podczas realizacji niniejszej pracy,*

*Panu dr Łukaszowi Kaźmierskiemu,
za życzliwą atmosferę i nieocenioną pomoc w realizacji badań
oraz **moim najbliższym** za ogrom cierpliwości i wsparcia.*

The table of contents

Summary in English	7
Summary in Polish	8
1. Introduction	9
1.1. Growing need for new cancer therapies.....	9
1.2. Biopolymers.....	12
1.3. Chemopreventive and natural compounds in cancer treatment	14
1.4. Biologically active compounds - polyphenols and flavonoids.....	15
1.5. Circular economy as a new trend in medicine	16
1.6. Norway spruce extract <i>Picea abies</i> (L.)	17
1.7. Ciprofloxacin.....	18
1.8. Levofloxacin.....	20
1.9. <i>In vitro</i> studies - barriers and opportunities for development	20
2. Aim of the study	23
3. Material and methods	24
3.1. Cell culture	24
3.1.1. T24 cell line.....	24
3.1.2. DU145 cell line.....	24
3.2. Cell passage.....	24
3.3. Preparation of multicellular tumor spheroids	25
3.4. Assessment of cell viability in a microscope with inverted optics	26
3.5. Drugs solutions.....	27
3.6. Chitosan solution preparation and characterization	28
3.7. Transmission Electron Microscope (TEM).....	29
3.8. Natural compounds extracts preparation.....	29
3.9. Biologically active compounds characterization	30
3.10. Spheroids kinetics growth.....	30
3.11. Imaging technique and training a neural network.....	31
3.12. Live/Dead Assay	31
3.13. Cell viability assessment by thiazolyl blue tetrazolium bromide assay (MTT).....	32
3.14. Cell viability assessment by WST8 assay	33
3.15. Assessment of apoptosis - identification of caspase 3 and 7 activity	33
3.16. Cell proliferation by thymidine analogue 5-Bromo-2'-deoxyuridine method	34
3.17. pH of the cell culture medium measurement.....	35

3.18. Statistical analysis.....	36
4. Results.....	37
4.1. Chitosan drugs' modification	37
4.2. Chitosan drugs' modification – adherent cell culture.....	38
4.2.1. Assessment of cell viability in a microscope with inverted optics.....	38
4.2.2. Live/Dead Assay	46
4.2.3. Cell viability assessment by thiazolyl blue tetrazolium bromide assay (MTT).....	54
4.2.4. Cell viability assessment by WST8 assay	59
4.2.5. Assessment of apoptosis - identification of caspase 3 and 7 activity.....	64
4.2.6. Cell proliferation by thymidine analogue 5-Bromo-2'-deoxyuridine method	71
4.2.7. pH of the cell culture medium measurement.....	75
4.3. <i>Picea abies</i> tree extract drugs modification – adherent cell culture	79
4.3.1. Biologically active compounds characterization.....	79
4.3.1. Assessment of cell viability in a microscope with inverted optics.....	80
4.4.2. Live/Dead Assay	88
4.4.3. Cell viability assessment by thiazolyl blue tetrazolium bromide assay (MTT).....	94
4.4.4. Cell viability assessment by WST8 assay	99
4.4.5. Assessment of apoptosis - identification of caspase 3 and 7 activity.....	103
4.4.6. Cell proliferation by thymidine analogue 5-Bromo-2'-deoxyuridine method	109
4.4.7. pH of the cell culture medium measurement.....	113
4.5. Multicellular tumor spheroids – cell culture optimalization.....	116
4.5.1. Preparation of multicellular tumor spheroids	116
4.5.2. Spheroids kinetics growth.....	119
4.5.3. Live/Dead Assay of Cellular Spheroids.....	120
4.5.4. Live spheroids assessment - WST8 and MTT assay.....	120
4.6. Multicellular spheroids - chitosan drugs' modification.....	122
4.6.1. Assessment of cell viability in a microscope with inverted optics.....	122
4.6.2. Live/Dead Assay	125
4.6.3. Cell viability assessment by thiazolyl blue tetrazolium bromide assay (MTT).....	130
4.6.4. Multicellular spheroids growth kinetics analysis	133
4.7. Multicellular spheroids - <i>Picea abies</i> tree extract drugs modification	137
4.7.1. Assessment of cell viability in a microscope with inverted optics.....	137
4.7.2. Live/Dead Assay	140
4.7.3. Cell viability assessment by thiazolyl blue tetrazolium bromide assay (MTT).....	144
4.7.4. Multicellular spheroids growth kinetics analysis	147
5. Discussion	150

5.1.	Chitosan as a biopolymer in drug modification	150
5.2.	Polyphenols and flavonoids in cancer therapy	154
5.3.	New cell models for <i>in vitro</i> research	157
6.	Conclusions	161
7.	Attachments	162
7.1.	Approval of the Bioethics Committee	162
7.2.	List of abbreviations	164
7.3.	List of tables	165
7.4.	List of figures	166
8.	Bibliography	171

Summary in English

The growing mortality rate resulting from the incidence of cancer requires the search for new methods of treatment. One of the most common cancers are cancers of the genitourinary system, including bladder and prostate, which are the cause of about 3.8% of all deaths caused by cancer in men.

The aim of the research was to search for new methods of treating cancers of the genitourinary system and to use biotechnology in the development of modifications of anticancer drugs. Moreover, the research was aimed at examining the effect of biomaterials and substrates of natural origin on cancerous cells of the genitourinary system *in vitro* in a 2D and 3D model of cell culture. Second and third generation fluoroquinolones: ciprofloxacin and levofloxacin were used in the study. The first biomaterial used in the research was chitosan. For many years, it was considered as a useful bioadhesive material due to its ability to form non-covalent bonds with biological tissues, moreover, it is considered biocompatible and non-toxic, biodegradable by enzymes. The research used another current trend in medicine - natural extracts and the reuse of raw materials. Polyphenols, including flavonoids, are organic compounds. These compounds are found in large amounts in plants and trees (popularly growing in Poland). Norway spruce (*Picea abies*) extract was used in this study. Commercially available cell lines T24 (bladder cancer) and DU145 (prostate cancer) were selected as cell models. Metabolic activity, rate of proliferation, growth kinetics, apoptosis level, changes in pH of culture medium, ratio of live/dead cells were studied. In response to the need to develop new *in vitro* test models, an additional analysis was also performed on the 3D model of the T24 line.

Depending on the analysis, the most toxic drugs turned out to be combinations of ciprofloxacin in concentrations of 1000 μM with 5% *Picea abies* extract. All combinations of drugs had a very large impact on the tested parameters of cancer cells, showing particularly cytotoxic effects in the last time points of the modified drugs. The highest sensitivity in detecting changes indicating the cytotoxic nature of drugs was observed on multicellular spheroids, which seem to be a promising model for future research.

The conducted analyzes proved that the modification of drugs with biopolymers and natural extracts may be a promising direction in the fight against cancers of the genitourinary system. However, it is necessary to carry out further analyses, also based on new methods of chemical modification of drugs and their optimization for further *in vitro* studies on 3D models.

Key words: *fluoroquinolones, bladder cancer, prostate cancer, chitosan, polyphenols.*

Summary in Polish

Rosnąca śmiertelność wynikająca z zachorowalności na nowotwory wymaga poszukiwania nowych metod leczenia. Jednymi z najczęściej występujących nowotworów są nowotwory układu moczowo-płciowego, w tym pęcherza moczowego i prostaty, będących przyczyną około 3,8% zgonów wśród mężczyzn.

Celem badań było poszukiwanie nowych metod leczenia nowotworów układu moczowo-płciowego i zastosowanie biotechnologii w rozwoju modyfikacji leków przeciwnowotworowych. Co więcej, badania miały na celu analizę wpływu biomateriałów oraz substratów pochodzenia naturalnego na zmienione nowotworowo komórki układu moczowo-płciowego *in vitro* w modelu 2D oraz 3D hodowli komórkowej. W badaniu zostały wykorzystane fluorochinolony drugiej i trzeciej generacji: ciprofloksacyna i lewofloksacyna. Pierwszym zastosowanym w badaniach biomateriałem był chitozan. Przez wiele lat był uważany za przydatny jako materiał bioadhezyjny ze względu na jego zdolność do tworzenia niekowalencyjnych wiązań z tkankami biologicznymi, ponadto jest uznawany za biokompatybilny i nietoksyczny, ulegający biodegradacji przez enzymy. W badaniach wykorzystano kolejny obecny trend w medycynie – naturalne ekstrakty oraz ponowne wykorzystanie surowców. Polifenole, a wśród nich także flawonoidy są związkami organicznymi. W dużych ilościach związki te występują w roślinach oraz drzewach (popularnie rosnących w Polsce). W niniejszej pracy wykorzystano ekstrakt ze świerku pospolitego (*Picea abies*). Jako modele komórkowe wybrano komercyjnie dostępne linie komórkowe T24 (rak pęcherza moczowego) oraz DU145 (rak prostaty). Badano aktywność metaboliczną, tempo proliferacji, kinetykę wzrostu, poziom apoptozy, zmiany w pH medium hodowlanego, stosunek żywych/martwych komórek. W odpowiedzi na potrzebę opracowania nowych modeli testów *in vitro*, dodatkowo przeprowadzono również analizę na modelu 3D linii T24.

W zależności od przeprowadzonej analizy najbardziej toksycznymi lekami okazały się połączenia ciprofloksacyny w stężeniach 1000 μM z 5% ekstraktem *Picea abies*. Wszystkie kombinacje leków miały bardzo duży wpływ na badane parametry komórek nowotworowych, wykazując w przypadku modyfikowanych leków szczególnie cytotoksyczne działanie w ostatnich badanych punktach czasowych. Najwyższą czułość w wykrywaniu zmian świadczących o cytotoksycznym charakterze leków zaobserwowano na sferoidach wielokomórkowych, które wydają się być obiecującym modelem do przyszłych badań.

Przeprowadzone analizy dowodzą, że modyfikacja leków biopolimerami oraz naturalnymi ekstraktami może być obiecującym kierunkiem w walce z nowotworami układu moczowo-płciowego. Jednak konieczne jest przeprowadzenie dalszych analiz, również w oparciu o nowe metody modyfikacji chemicznej leków i optymalizacja ich pod dalszym kątem badań *in vitro* na modelach 3D.

Słowa kluczowe: *fluorochinolony, rak pęcherza moczowego, rak prostaty, chitozan, polifenole.*

1. Introduction

1.1. Growing need for new cancer therapies

The recent years show that cancer is a major public health problem worldwide and the leading cause of death in the United States [1]. In 2020, the diagnosis and treatment of cancer was adversely affected by the COVID-19 pandemic. Reduced access to care, because of health care setting closures and fear of COVID-19, exposure resulted in delays in diagnosis and treatment that may lead to an increase in the number of cases of advanced disease despite the illusory decline in cancer incidence [2]. It is expected to increase to an incidence of 15.5 million deaths by 2030 due to the cancer [3]. It can be claimed that, cancer is leading cause of death and an huge barrier to increasing life expectancy in each country of the world [4] (Fig. 1).

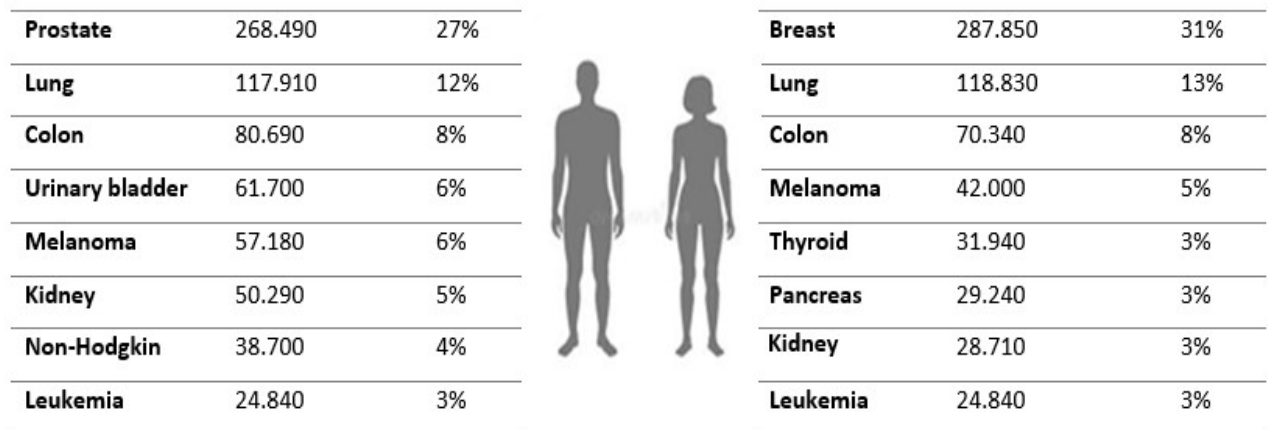


Figure 1. Ten Leading Cancer Types for the Estimated New Cancer Cases by Sex, United States, 2022.

According to estimates from the World Health Organization (WHO) in 2019 [5] cancer is the first or second leading cause of death before the age of 70 years [6]. The lifetime probability of being diagnosed with an invasive cancer is more than 40% [7]. Right behind the most common cancers (such as lung and breast cancer) are cancers of the genitourinary system [8]. Among them, bladder cancer and prostate show the greatest mortality. More than 350.000 new cases of bladder cancer are diagnosed worldwide each year [9]. Based on the latest GLOBOCAN data, bladder cancer accounts around 3% of global cancer diagnoses and is especially prevalent in the developed world [10]. In the United States, bladder cancer is the sixth most incident neoplasm [11, 12]. A total of 90% of bladder cancer diagnoses are made in those 55 years of age and older, and the disease is four times more common in men than

women [13]. Based on data provided from the Surveillance, Epidemiology, and End Results Program (SEER) sample data show that a 50-year old man has an average risk of 0.28% to be diagnosed with bladder cancer before his 60th birthday [14]. A 60-year old woman has an average risk of 1.15% to be diagnosed with bladder cancer in the remainder of her life (Fig. 2) [15].

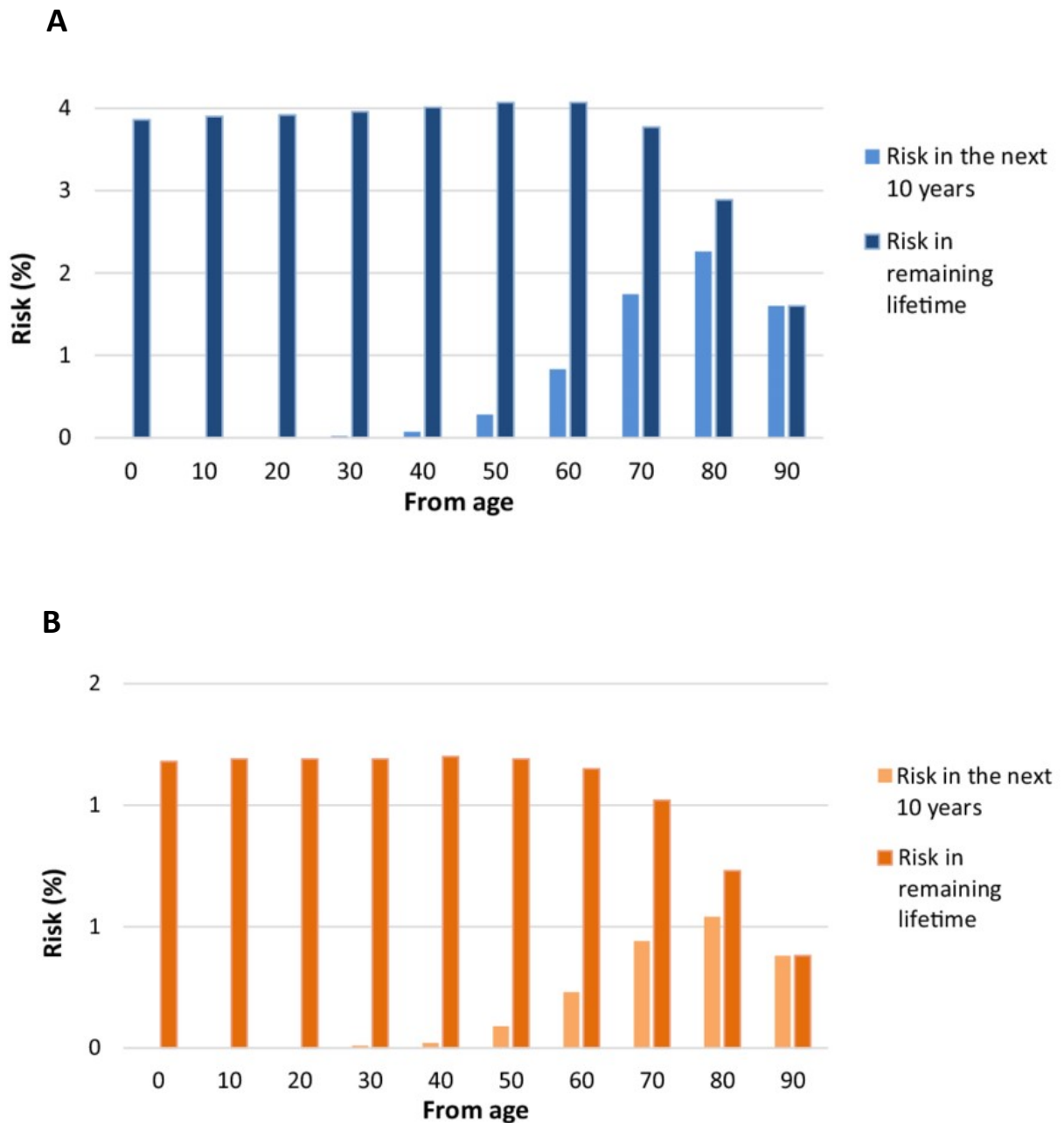


Figure 2. Diagrams show the risk of developing urinary bladder cancer for males (A) and females (B) in the United States of America. Data for 2020. [Richters A. et al., 2020].

Prostate cancer (PC) is undeniably the most frequently diagnosed malignant neoplasm in men, with annual statistics of 1.276.106 new cases and 358.989 deaths (3.8% of all deaths caused by cancer in men) in last years [16, 17]. Furthermore, it is estimated that 1 in 6 American men will be affected by this cancer during their lifetimes. Despite the fact that 2.293.818 new cases are estimated before 2040, a small variation in mortality will be observed (an increase of 1.05%) [18]. Prostate cancer is often slow and may require minimal treatment and may be asymptomatic at an early stage over a long period of time. Often, initial symptoms, such as discomfort, difficulty urinating, more frequent urination, and nocturia, are mistaken for an enlarged prostate gland. The diagnosis is often made at an advanced stage of the disease, which is manifested by urinary retention or back pain, as the axial skeleton is the most common site of bone metastases [19]. Treatment of such a common neoplasm entails a number of challenges, it should be available, cheap and low-toxic due to the advanced age of the patients.

Rapid advances in biotechnology has driven the field of drug discovery and led to the development of many new highly potent and target-specific drug candidates [20]. The growing mortality resulting from the increasing incidence of cancer requires the search for new methods of treatment. Although well-known conventional chemotherapy has been successful to some extent, the main drawbacks of chemotherapy are its high-dose requirements, poor bioavailability, adverse side effects, low therapeutic indices and development of multiple drug resistance [21, 22]. The main goal of developing drug delivery vehicles is to effectively address these problems in delivering and transporting drugs to the desired sites of therapeutic action while minimizing side effects [23]. Unfortunately, the fast pace of research and early-stage discovery, many drug candidates fail during preclinical evaluation due to limited bioavailability, and other challenges associated with effective drug delivery [24]. One of the way is rapid developments of various modified drugs by polymers because of their potential in a wide range of biotechnological applications, especially in advance biomedical one [25].

1.2. Biopolymers

In recent years, biopolymer development has become one of the main areas of drug delivery research. An impressive library of different drug delivery vehicles of different sizes, models and surface physicochemical properties with targeting strategies was developed [26, 27, 28] (Fig. 3). Recent years of biopolymer research have driven the successful formulations of various novel drug delivery devices with increased therapeutic efficacy, improved patient compliance and, importantly, cost effectiveness [29]. Polymer drug delivery systems are of great interest to scientists as they show great advantages in drug delivery systems due to optimized drug loading and release properties. The common side effects of synthetic polymers far exceed those that lead to some difficulties such as dose reduction, treatment delay, or an intermittent therapy [30, 31]. With this in mind, and with the need for a protective drug delivery system, natural polymeric substances such as biopolymers and their composites are selected for research as an excipient due to their low toxicity, biodegradability, stability and renewable nature [32, 33]. Moreover, they have many different structures, different physiological functions and can provide a wide variety of biomedical applications due to their distinctive properties [34].

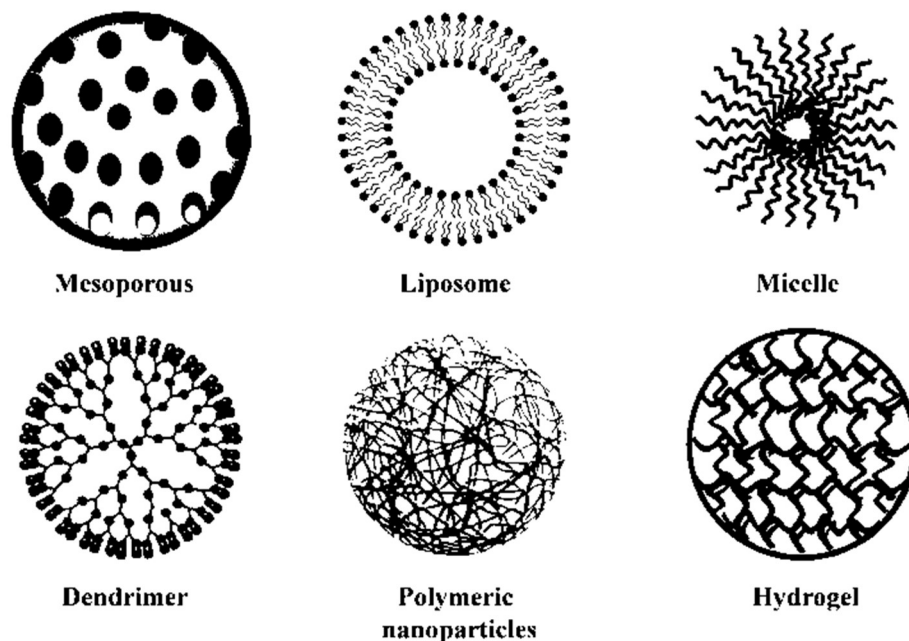


Figure 3. Different types of nanocarriers used as controlled delivery vehicles for cancer treatment [modified: Senapati S, 2018].

A wide variety of biodegradable polymers are widely used in the drug delivery field because these polymers are biodegradable into non-toxic components inside the body [34]. One such well-known and widely used biopolymer is chitosan [35] (Fig. 4).

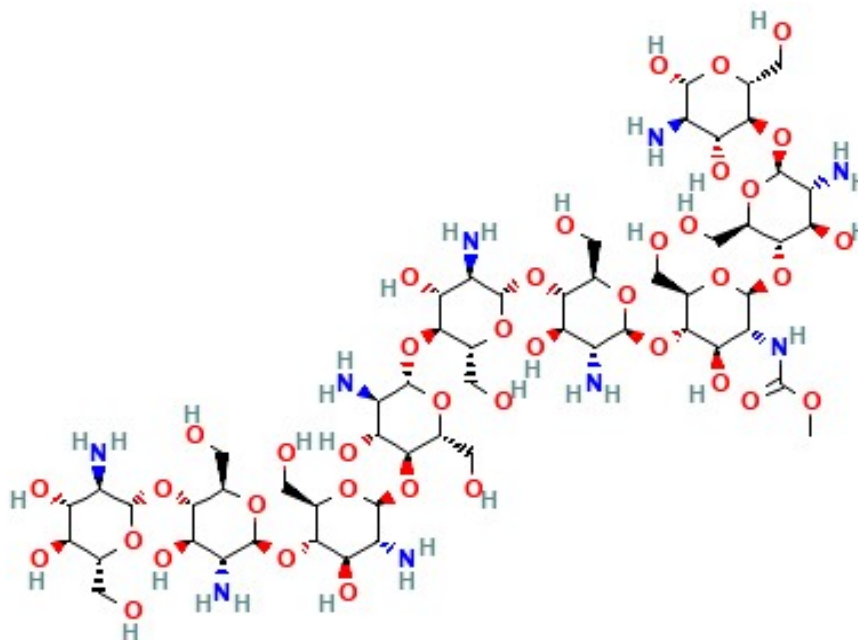


Figure 4. Chitosan's structure (source: <https://pubchem.ncbi.nlm.nih.gov/compound/Chitosan>).

For many years chitosan was considered as a useful bio-adhesive material because of its ability to form non-covalent bonds with biological tissues, mainly epithelia and mucous membranes [36]. Bio-adhesions formed using natural polymers, have unique properties as a carrier because they can prolong residence time and, therefore, increase the absorbance of loaded drugs [37]. Chitosan is hydrophilic and soluble in acidic solutions through the protonation of its amine groups [38]. Modified and unmodified chitosan has been widely used, although with different molecular weights and chemical modifications, in biomedical, pharmaceutical, metal chelation, food additive and other industrial applications [38, 39, 40]. Chitosan is biocompatible and can be biodegraded by enzymes such as lysozymes, some lipases, and proteases [41]. Compared to all other polysaccharides, chitosan has a cationic character due to its key amino groups. These primary amino groups are responsible for properties such as controlled drug release, transfection or inhibitory properties of the efflux pump [42]. What is more, chitosan's protection in medicinal and therapeutic applications has also been approved by the Food and Drug Administration (FDA) [43]. Any of these properties may also be further

enhanced due to chemical modifications. These properties, as well as its positive charge in physiological conditions, endow chitosan with a promising future as a biomaterial.

1.3. Chemopreventive and natural compounds in cancer treatment

Since antiquity, numerous plants have been used worldwide in traditional and folk medicine, in addition to their common usage for food purposes. With the development of civilization, people return to what is natural and known for centuries on many levels of life, including medicine [44]. Lately, the need for new biologically active substances and the need for research to support the empirical use of various plants in folk medicine has increased interest and spurred the study of several of these plants [45]. Botanical and nutritional compounds have been used in the treatment and prevention of cancer for centuries. Population studies suggest that a reduced risk of cancer is associated with high consumption of fruits and vegetables. Thus, the cancer chemo-preventive potential of naturally occurring phytochemicals is of great interest. There are numerous reports of cancer chemopreventive activity of dietary botanicals, including cruciferous vegetables such as broccoli, garlic and onion [46], green tea [47], citrus fruits [48], tomatoes [49], berries, and ginger, as well as medicinal plants [50]. Several lead compounds, such as lycopene (from tomatoes), indole-3-carbinol (from broccoli), sulforaphane (from asparagus), and resveratrol (from grapes and peanuts) are in preclinical or clinical trials for cancer chemoprevention [51] (Tab. 1). Phytochemicals have great potential in cancer prevention because of their low cost, safety, and oral bioavailability [52].

Table 1. Examples of clinical trials used polyphenols and flavonoids treatment potential (source: www.clinicaltrials.gov).

ClinicalTrials.gov Identifier:	Agent	Trial Type	Cancer Type	Phase
NCT00685516	Green tea	Therapy	Prostate	II
NCT00005828	Green tea	Therapy	Prostate	II
NCT01108003	Broccoli Sprout Extract	Therapy	Bladder cancer	II
NCT00253643	Green tea	Therapy	Prostate	II
NCT00088946	Green tea	Therapy	Bladder cancer	II
NCT00666562	Green tea	Therapy	Bladder cancer	II
NCT03986398	Cranberry Fruit Juice Extract	Prevention	Bladder cancer	Not applicable

1.4. Biologically active compounds - polyphenols and flavonoids

Polyphenols are compounds of plant secondary metabolism that accumulate in plant organs. Due to the fact that they are a large group of bioactive chemicals, they were diverse biological functions [53]. Polyphenols are the most numerous and widespread group of bioactive molecules. They have two general classes, the first one is flavonoids and the other is phenolic acids [54]. The flavonoids are phenolic substances widespread in all vascular plants. They constitute a diverse group of phytonutrients, present in many fruits and vegetables and medicinal plants in which they occur as free forms, glycosides, and also methylated derivatives [55]. Research on this compounds began in 1936, when Hungarian scientist Albert Szent - Gyorgi was discovering the synergy between pure vitamin C and as yet unidentified co-factors from lemon skins [55]. The decades of subsequent research have shown that these compounds have a broad spectrum of pharmacological activity, including anti-cancer one [56]. They were reported to be disturbing in initiation, promotion and progression cancer by modulation of various enzymes and receptors in signal transduction pathways associated with cell proliferation, differentiation, apoptosis, inflammation, angiogenesis, metastasis and reversal multi-drug resistance [57, 58]. The flavonoids have a great influence on the cascade immune events related to cancer development and progression. Additionally, polyphenols show pro-oxidative properties, which counteracts the metabolic process of the cell. This may also include block cell propagation and apoptosis. [59, 60]. Studies have also shown that many

other effects of polyphenols have been observed, like reduction of enzymes such as lipoxygenase and telomerase. Moreover, one of the greatest advantage of these compounds is their extreme ease and availability. Many fruits and vegetables contain phenolic acids as key polyphenols [61, 62, 63] (Tab. 2).

Table 2. *Examples of flavonoids sources in fruits and vegetables.*

Examples of flavonoids	Food source
Quercetin, kaempferol	Onion, olive oil, apples, cherries, red wine
Apigenin, rutin, luteolin	Fruit skins, tomato, red pepper
Naringin, taxifolin	Citrus fruits, lemons, oranges
Apigenidin, pelargonidin	Cherries, strawberry

1.5. [Circular economy as a new trend in medicine](#)

Analyzing the potential sources of obtaining BACs, scientists started to think very broadly about the current problems and trends, not only in medicine. The latest data indicate a significant increase in the world's human population from 7.7 billion (2019) to even 9.7 billion people in 2050 [64]. Faced with these numbers, humanity must be prepared for a colossal increase in waste production, which according to the current trend, will increase by 70% in the next 40 years [65]. These premises constitute a challenge to strive for more sustainable development of each area of science, technology and medicine.

Scientists can no longer focus only on one-way thinking and in addition to a strong trend towards the development of potential healing properties, a promising direction is now the economic growth model known as the circular economy (CE) (Fig. 5). As described by Homrich et al., circular economy is a concept that aims to provide mechanisms to minimize the generation of waste and find solutions for its re-use [66].

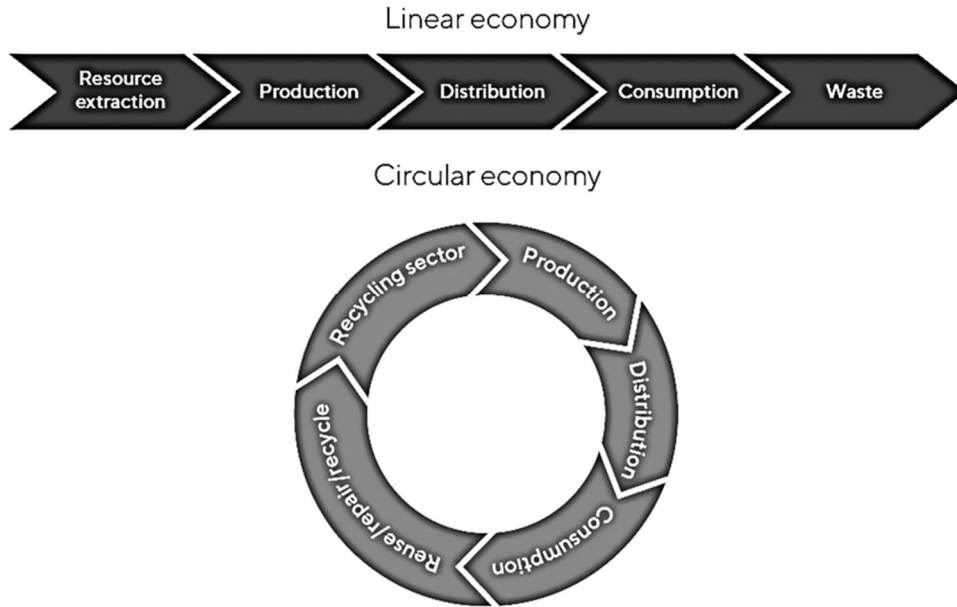


Figure 5. The linear economy and the circular economy model Source: AkzoNobel (2015).

Considering the potential greatest threats to the future of mankind, scientists joined themes about the enormous problem of food waste and the strong trend of returning to natural medicine. It is an undeniable fact that each year about a third of all food produced is wasted, and in the fruit and vegetable sector 45% of total production is lost in post-harvest, processing, distribution and consumption chains [67]. Due to the fact that fruits such as apples, grapes, pomegranates and plums are a very rich source of polyphenols and flavonoids [68], solutions have been created to use their food waste and extract valuable ingredients from them.

These observations prompted scientific world to analyse other areas of life where huge amounts of bio-waste are produced.

1.6. Norway spruce extract *Picea abies* (L.)

The Christmas period inspired to broadly observe the amount of waste related to the use of Christmas trees and use fallen bio-waste needles. Each year, around 50 to 60 million Christmas trees are produced in Europe [69] and before Christmas most of them are thrown on the trash can as wastes. It can be estimate that there are 15.000 growers in the United States who produce approximately 33 million trees each year [70]. Many species are grown as Christmas trees, but the most popular of them is Norway spruce [71]. Due to their excellent post-harvest needle retention and moisture retention properties, the demand for Norway spruce Christmas

trees has increased rapidly. In Europe, the leaders in the production of Christmas trees are Germany - about 19 million trees, followed by France with 9.2 million trees, Denmark 8.5 million trees, Belgium 5.2 million trees and the United Kingdom 4.4 million trees (72).

Picea abies (L.) waste has already been used to extract antioxidants, incl. bark as waste from the carpentry industry [73]. Extensive analysis of bioactive phenolic compounds from Norway spruce, was performed by Metsämuuronen et al. [74]. It has been shown, that the phenolic compounds of Norway spruce exhibit antibacterial activity against several bacteria. Most phenolic compounds are stilbenes, flavonoids, phenolic acids and lignans, which are biosynthesized in wood via the phenylpropanoid pathway [74] and may be a potentially rich source of bioactive compounds.

1.7. Ciprofloxacin

In recent years, a lot of scientific research has been devoted to ciprofloxacin, which turns out to have enormous potential for its use in the treatment of cancers of the genitourinary system. It is an organic compound, included in the second generation of fluoroquinolones, which is characterized by good tissue penetration and favorable pharmacokinetic parameters [77]. For a long time it was believed that ciprofloxacin only affects bacterial cells. It is now known that this drug may significantly affect the viability of eukaryotic cells, including human cancer cells.

The biological effects of ciprofloxacin confirm that this drug can serve as a cytostatic in the treatment of many types of cancer, incl. lung cancer, due to its topoisomerase II inhibitory properties. It is one of the enzymes responsible for changes in the DNA structure during replication, transcription and chromatin condensation [78]. This enzyme is necessary for the most important life processes of eukaryotic cells. It is responsible for the relaxation of the DNA superhelix, which leads to the formation of transient doublestrand [79]. Inhibition of growth of cells treated with ciprofloxacin is usually achieved in the G2/M phase, which suggests a mechanism related to the ability to inhibit topoisomerase II (DNA gyrase) and topoisomerase IV, which are necessary for bacterial DNA replication, transcription, repair or recombination [80].

Many studies have demonstrated the cytotoxic effect of ciprofloxacin on bladder cancer cell lines [81]. It has been shown that this drug may also be a potential chemotherapeutic agent in the treatment of cancers of the genitourinary system, because its doses in the range of 25-800 µg/ml inhibit the proliferation of cells of this tumor at various stages of advancement (Tab. 3).

Table 3. *The effect of ciprofloxacin on the inhibition of proliferation of bladder cancer cell lines [82, 83].*

Cell Line	Drug Concentration (mg/ml)	Incubation (h)	Inhibition of Proliferation (%)
HTB-5	25 - 800	24 - 120	8.1 – 96.6
T24	25 - 800	24 - 120	8.0 – 98.2
HTB-1	25 - 800	24 - 120	20.8 – 97.1
MBT-2	50 - 800	24	50.0 – 90.0
HTB-5	400	96	93.2
HTB-9	400	96	95.4

HTB - 1 (stage I bladder cancer), HTB - 5 (stage IV bladder cancer), HTB - 9 (stage II bladder cancer), MTB - 2 (mouse bladder cancer), T24 - (bladder cancer of the from the transitional covering epithelium)

1.8. Levofloxacin

Levofloxacin (LEV) is an oral fluoroquinolone, the L-isomer of ofloxacin [84] (Fig. 6). It is known as a broad-spectrum antimicrobial agent, and numerous clinical studies confirm its excellent clinical and bacteriological efficacy [85]. The drug has a long half-life, which allows the frequency of its administration to be reduced [86], and its tolerability is assessed as very good. The drug was introduced into clinical use already in the 90s of the last century, and in recent years it has been used more and more often for potential use in many therapeutic areas due to its unique pharmacokinetic (PK) and pharmacodynamic (PD) profile, wide spectrum of action and the previously mentioned satisfactory tolerability [87].

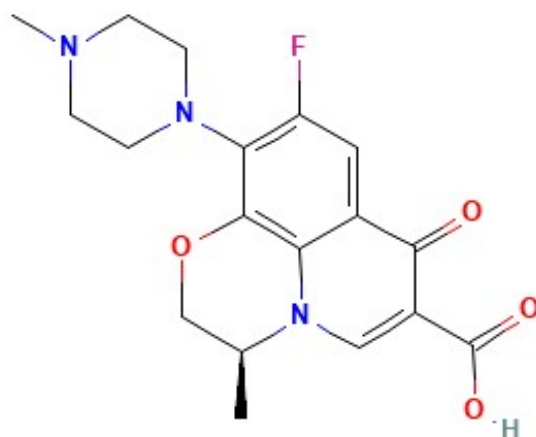


Figure 6. Levofloxacin structure (source: <https://pubchem.ncbi.nlm.nih.gov/compound/Levofloxacin>)

1.9. *In vitro* studies - barriers and opportunities for development

There is a constant need for new *in vitro* test models that will better represent the real world conditions for biotechnology research. The study of drugs combined with biomaterials in two-dimensional (2D) culture does not reflect the conditions prevailing in the *in vivo* environment [88]. Over the last few decades, the most popular platform to perform cancer research has been monolayer cell culture [89]. It is well known that such monolayer cultures do not have the characteristics of three-dimensional solid tumors. Multicellular spheroidal model of tumor has an intermediate complexity between tumors *in vivo* and monolayer cultures *in vitro* and

would be more appropriate for drug screening and preclinical research [90]. Monolayer cell cultures are easy to maintain and monitor. However, no living multicellular organisms exist solely in two-dimensional space. In recent years, three-dimensional systems of cultures have become an increasingly effective tool for biological research [91]. Therefore, 3D cultures are more similar to cells grown in a tissue environment *in vivo* [92]. However, replacing 2D cell culture with 3D neoplastic spheroids is not an easy task, but has a lot of advantages and pushes forward cancer researches [93].

Multicellular spheroids are a known form of 3D cell culture that allows better penetration assessment of drugs in a multicellular structure, imitating a tumor [94]. Spheroids are 3D cultures that mimic organ characteristics and offer a novel approach to diagnostic and therapeutic evaluation [95]. Cells grown in 3D system better mimic the physiological environment of living organisms compared to conventional single layer culture systems [96]. Spherical aggregates of malignant cells, or multicellular neoplastic spheroids, can serve as *in vitro* tumor models. Similarities between the primary tumor and the spheroids include volume growth kinetics and cell heterogeneity [97]. By mimicking the three-dimensional network of cell-matrix and cell-cell interactions, neoplastic spheroids resemble many aspects of the pathophysiological environment in human tumor tissue [98]. Multicellular spheroids also mimic tumor-like patterns of tumor avascular nodule development *in vivo* in terms of morphology and growth kinetic properties [99]. Relative to two-dimensional cultures, spheroids also provide better target cells for drug testing and are appropriate *in vitro* models for studies of drug penetration [100]. Therefore, optimization and simplification methods for creating cancer spheroids are essential for biological research, especially for the development of cancer therapy. Perhaps this will allow the replacement of adherent cell cultures in the future.

Despite the extensive treatment of above mentioned cancers and many modern therapies already used, it is highly desirable to develop new drug delivery systems that can efficiently deliver drug to the bladder tumor and prostate in a specific manner and control drug release [101]. Currently used 2D cell models do not, in any way, reflect the specific microenvironment and do not allow the assessment of parameters such as drug penetration or its release from biomaterials [102]. There are many studies carried out on cell lines representing these tumors, but scientists are looking for the best model to study these cells *in vitro* [103].

The last years of research in a new anticancer biomaterials medicine has highlighted the lack of simple and reliable model methods for analyzing the effectiveness of new anticancer drugs. New drug modifications are widely studied [104, 105]. Unfortunately, currently *in vitro* studies mostly rely on 2D cell models, which do not reliably reflect *in vivo* conditions [106, 107]. One of the thesis goal was to optimize a simple and reproducible method of creating spheroids that would allow the creation of 3D cell models in a basic tissue engineering laboratory. Magnetically bioprinting is a highly reproducible and flexible method using three-dimensional multicellular tumor spheroids. It will easily increase the value of research into new therapies, biomaterials, and drug-modified-based research. The secondary goal was to compare 2D and 3D models of cultures of human prostate and bladder cancer cells, as well as to present their advantages and disadvantages as well as perspectives for further research.

This presented PhD thesis is a step towards increasing the effectiveness of treating some of the most common cancers. The use of the latest discoveries and trends in modern medicine allows for the approach to problems in which uro-oncology is struggling. It also seems necessary to assess whether the chosen directions of development and the hopes associated with them are actually right and promising.

2. Aim of the study

- 2.1. Confirmation of the efficacy of ciprofloxacin and levofloxacin in the treatment of cancers of the genitourinary system.
- 2.2. Assessment of natural extracts from *Picea abies* tree on cancer cells and comparison of the cytotoxic effect of selected drugs combined with the extract.
- 2.3. Assessment of the effect of chitosan biopolymer on cancer cells and comparison of the cytotoxic effect of selected drugs combined with the biopolymer.
- 2.4. Optimization of the method of creating cellular spheroids.
- 2.5. Comparison of 2D and 3D cell models and their sensitivity in basic cytotoxic studies.

3. Material and methods

3.1. Cell culture

3.1.1. T24 cell line

To ensure sterility and safety, all procedures regarding cell culture were carried out using a class II laminar flow cabinet (Bio II Advance – Telstar, Spain). Human bladder carcinoma cell line - T24 (CLS Cell Lines Service) was cultured using DMEM/Ham's F-12 (Corning, USA). Above medium was supplemented with 10% FBS (Corning, USA), 5 µg/ml amphotericin B, 100 U/ml penicillin and 100 µg/ml streptomycin (Corning, USA). Cells were cultured at 37°C in a humidified incubator under 5% CO₂.

3.1.2. DU145 cell line

The human prostate carcinoma cell line DU145 (American Type Culture Collection) was cultured using RPMI1640 (Corning, USA). Medium was supplemented with 10% FBS (Corning, USA), 5 µg/ml amphotericin B, 100 U/ml penicillin and 100 µg/ml streptomycin (Corning, USA). Cells were cultured at 37°C in a humidified incubator under 5% CO₂.

3.2. Cell passage

Cell passage was performed under sterile conditions in a type II laminar chamber. It was carried out after the cells achieved approx. 60-80% coverage of the culturing area. In the first step, the medium was removed and the cell growth surface was washed with PBS without Ca²⁺ and Mg²⁺ ions (PBS - Phosphate Buffered Saline, Corning, USA). The next step was to trypsinization of the cells. For this purpose, 1.5 ml of a 0.05% trypsin solution was added per 25 cm² culture bottle (in the case of T24 cells) and 1.5 ml of 0.25% trypsin solution with EDTA (POCh, Poland) in the case of the DU145 line and incubated for about 2-5 min. at 37 ° C to detach the cells. The cell detachment process was monitored under a microscope with reversed optics (Nikon, Japan). An equal volume of the culture medium for a given cell line was then added to the culture flask to inactivate trypsin. The cell suspension was transferred to a sterile tube and centrifuged for 5 min. at 2500 rpm. After centrifugation, the supernatant was decanted and the cell pellet was resuspended in an appropriate culture medium. The

number of viable cells was calculated using a Neubauer chamber using trypan blue (Corning, USA). To 25 µl of the cell suspension 0.4% filtered trypan blue solution (Sigma, Germany) was added. The cell suspension and trypan blue solution was applied to the Neubauer chamber. Cells were counted using an inverted optics microscope. Viable cells were counted from the 4 squares of the chamber and their total number was calculated by the formula:

$$L=A/4*2*10^4*B$$

Where:

L – total number of cells

A – number of live cells counted from four squares

B – volume of medium [ml]

3.3. Preparation of multicellular tumor spheroids

A method of magnetic 3D printing using magnetic nanoparticles NanoShuttle™ (Greiner Bio-One, Austria) was used to create spheroids. Those nanoparticles were biocompatible, with no effect on metabolism and proliferation. The cells were seeded in a 24-well plate at a density of 10.000, 12.000, 14.000 and 16.000 cells/well. After achieving the state of 60% confluence, magnetic particles were added (Fig 7). The following day a passage was made and the cells were counted and seeded on 3D plates [NanoCluture 96-well Plate® (NCP-LH-96); SCIVAX, Kanagawa, Japan] at a density of 5.000, 10.000 and 15.000 cells/well to optimize the cell number needed to create spheroids.

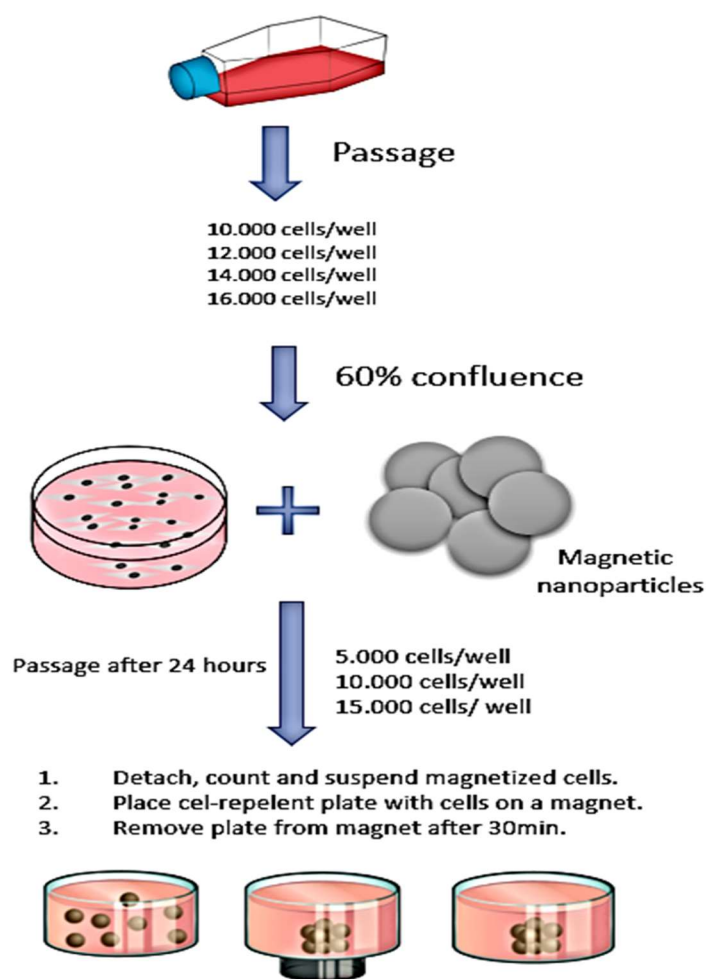


Figure 7. Cells grown to 60% confluence in 2D were incubated overnight with magnetic nanoparticles (NanoShuttle, NS). After resuspending the cells for a few hours, the cells were distributed into the wells of low attachment 96-well microplate. The cells were then printed for 20 min by putting the plate atop a 96-well magnetic drive. After printing, the magnet was removed.

3.4. Assessment of cell viability in a microscope with inverted optics

Morphological evaluation of cells was performed with the use of an inverted, phase contrast microscope (CKX53-FL, Olympus, Japan) and a dedicated 4K colour camera (UC90, Olympus, Japan). Image analysis was carried out at intervals - at the start of the experiment, after 24 hours, after 48 and 72 hours from the start of the experiment. At each of the stages, photos of the examined cells were taken, assessing their morphology and the percentage share of the growth of the culture surface.

3.5. Drugs solutions

In order to obtain the concentrated solution of ciprofloxacin (CIP), the powdered drug (Sigma-Aldrich, Saint Louis, MO, USA) was dissolved in slightly acidic solution (pH 4.7) to increase solubility. The PBS was titrated with HCl, then filtered using a 0.22 syringe filter (Merck Millipore, Burlington, MA, USA). Stock solutions of powdered levofloxacin (LEV) (Cayman Chemical, USA) was prepared in PBS (pH 7.4). The drugs were diluted in fresh media before each experiment, with final concentrations at the range of 10–1000 μM . The concentrations have been established on the basis of previous studies (Tab. 4).

Table 4. List of abbreviations of solutions of chemotherapeutic agents and concentrations used during the studies.

Abbreviation	Chemotherapeutic agent	Concentration [μM]
CONTROL CHITOSAN	Chitosan	0.1 (%w) chitosan
CIP10	Ciprofloxacin	10
CIP100	Ciprofloxacin	100
CIP500	Ciprofloxacin	500
CIP1000	Ciprofloxacin	1000
CIP10 CHIT	Ciprofloxacin	Drug 10 μM with 0.1 (%w) chitosan
CIP100 CHIT	Ciprofloxacin	Drug 100 μM with 0.1 (%w) chitosan
CIP500 CHIT	Ciprofloxacin	Drug 500 μM with 0.1 (%w) chitosan
CIP1000 CHIT	Ciprofloxacin	Drug 1000 μM with 0.1 (%w) chitosan
LEV10	Levofloxacin	10
LEV100	Levofloxacin	100
LEV500	Levofloxacin	500
LEV1000	Levofloxacin	1000
LEV10 CHIT	Levofloxacin	Drug 10 μM with 0.1 (%w) chitosan
LEV100 CHIT	Levofloxacin	Drug 100 μM with 0.1 (%w) chitosan
LEV500 CHIT	Levofloxacin	Drug 500 μM with 0.1 (%w) chitosan
LEV1000 CHIT	Levofloxacin	Drug 1000 μM with 0.1 (%w) chitosan

3.6. Chitosan solution preparation and characterization

Following the protocol suggested by Sigma Aldrich to prepare the chitosan nanoparticle using a crosslinker, the following system was prepared. The first trial consisted of preparing a solution of 0.1%w/v chitosan in 3% v/v acetic acid and once the chitosan is dissolved the pH of the solution was adjusted to 4.7 using a solution of 1M NaOH. After that, of 0.5% TPP was prepared to have a 1mM solution of the drug. To allow the ionic gelation to take place, over 3mL of the chitosan solution, a 1mL mixture consisting of 0.1mL of the drug and 0.9mL of the TPP was added dropwise (Fig. 8). The final suspension was prepared under stirring at 350 rpm for 30 min. Then, sample was taken to be analyzed using TEM (Transmission Electron Microscopy). To collect the nanoparticles the solution can be centrifuged at 13.000g at 4°C for 30 min. after which the supernatant has been removed, and the precipitate was either dried or suspended in a solution. The morphology of the nanoparticles was checked using the TEM model JEOL JEM1011 (JEOL USA, Inc, Peabody, MA).

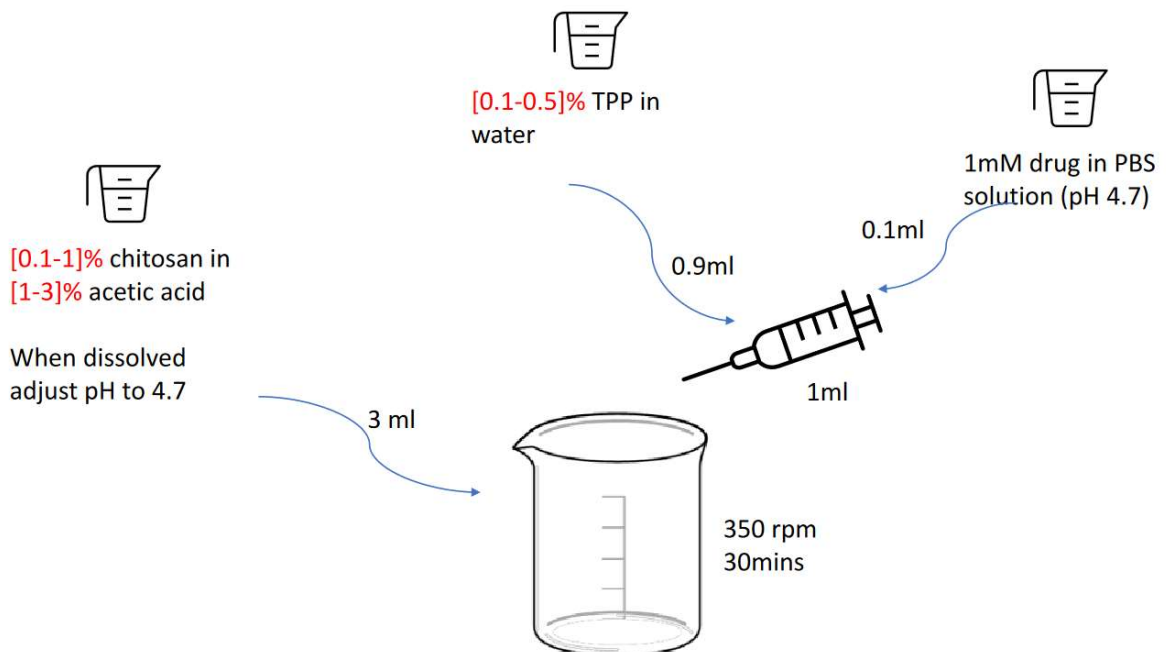


Figure 8. Simplified flow chart of the drug-chitosan combination process.

3.7. Transmission Electron Microscope (TEM)

The morphology of the nanoparticles was checked using the Transmission Electron Microscope (TEM) JEOL JEM1011 (JEOL USA, Inc, Peabody, MA). After solution removed from stirring for 30 min. one drop of the solution was taken and added over a copper grid. Then it was left to air dry at room temperature to be able to analyze it. The real average size of the nanocapsules was calculated using a “ImageJ” software and the TEM micrographs.

3.8. Natural compounds extracts preparation

The dropped needles were collected under European Spruce *Picea abies* (L.) tree, which is recognized as the one of the most popular Christmas trees in East-Central Europe. The needles were collected during 2021 Christmas period. After the collection, samples of the biomass were dried in an oven at 30 °C, approx. 4 weeks, until a constant weight was observed. The final fineness of the needles were < 300 µm, this size were achieved using a knife mill Retsch GRINDOMIX GM. For BACs extraction, freshly ground and full needles were used.

Four types of extraction were used:

- 1) main solid=liquid,
- 2) additional performed with water,
- 3) water at pH 4.75,
- 4) methanol.

All about were carried out for 1h. All solutions and experiments were prepared using ultrapure water quality Milli-Q system (conductivity = 0.055 µS). In solid-liquid extractions 1g of biomass material with 20 mL of Phosphate-Buffered Saline (PBS) at pH 4.75 for 5 min, 15 min, 30 min, 1 h, 2 h, 6 h and 24 h at room temperature (22 ± 2 °C) were used.

All extractions with ground samples were carried out by magnetic stirring at 750 rpm, while the extraction of uncrushed needles was performed using the Orbital Shaker-Incubator ES 80 set up at 250 rpm. After all the extractions, the mixtures were filtered using sterile Syringe

Filters containing polyether sulfone membrane with 0.22 μm pore size (VWR International, USA).

3.9. Biologically active compounds characterization

The total phenolic content (TPC) was determined by using the Folin-Ciocalteu's method. The following protocol was applied: in the first step 0.5 mL of extract was added to the 25.0 mL volumetric flask containing 7.5 mL of ultrapure water and 3.0 mL of 20 % Na_2CO_3 . After that, 2.0 mL of the Folin-Ciocalteu's reagent was added and volume was made up with ultrapure water to 25.0 mL. The absorbance was measured at 765 nm after 2 h using UV-vis Spectrometer. PBS (Corning, USA) at pH 4.75 was used as a blank solution. TPC was reported as Gallic acid (3,4,5-Trihydroxybenzoic acid) equivalent calculated by following the equation $C = 2.1009 \times \text{Abs}$, $R^2 = 0.9881$. Sodium carbonate, Gallic acid as well as Folin-Ciocalteu's phenolic reagent were supplied by Merck, Germany.

The total flavonoids content (TFC) was characterized by using the method involving aluminium chloride complex formation. First of all, 0.5 mL of 5 % AlCl_3 was added to the 25.0 mL volumetric flask containing 10.0 mL of methanol. Then, 1.0 mL of the test solution was added to the flask and the volume was made up with methanol to 25.0 mL. The absorbance was measured at 300 nm after 30 min with the UV-vis Spectrometer (iMark™ Microplate Reader BIO-RAD, USA). As above, PBS pH 4.75 was used as a blank solution. TFC is reported as Quercetin (3,3',4',5,7-Pentahydroxyflavone) equivalent, calculated by following the equation $C = 2.5022 \times \text{Abs}$, $R^2 = 0.9875$. Aluminium chloride anhydrous Quercetin and methanol were provided by Merck Germany.

3.10. Spheroids kinetics growth

Spheroids were observed with live imaging system for 6 days after initial cell seeding (day 0). A series of bright field images were recorded on days 0–6 using a BZ-X710® inverted microscope (Keyence, Osaka, Japan). Morphometric analysis of spheroids and measuring their area was performed using EPview 1.3 software (Olympus, Tokyo, Japan). Growth kinetics were analyzed using two technologies: kinetic imaging without the use of dyes (real-time, stain-free live-imaging) and image analysis using a pixel classifier based on a dedicated U-NET neural network. It was essential to create an effective classification system prior creation of

a dedicated neural network that is able to distinguish between objects, namely: cells and background.

3.11. Imaging technique and training a neural network

In order to guarantee the correct operation of the classifier, it was necessary to ensure identical imaging conditions when preparing the training database (Ground Truth), as well as the proper study of growth kinetics. A motorized one was used for imaging inverted microscope IX83 (Olympus, Japan) adapted to this type of acquisition, equipped with a monochrome camera (Hamamatsu Orca Spark). Imaging was performed in 96-well plates with a plastic flat bottom. Featured photos participation in network training and analysis was carried out using the High Contrast Brightfield Technique, which secured no shading artifacts that are present when using the contrast technique phase with this type of culture vessel. Obtained photos without permanent changes were saved in the .vsi format, which was compatible with the software to be performed training a neural network. For data obtained from kinetic analysis for a single imaging site, a series of photos were taken, which over time formed the t-axis. The neural network-based classifier was trained using the Cellsens Dimensions package with the addition of AI. The training database contained over 100 photos of cells made at different stages of proliferation. In the photos, pixels belonging to three classes of objects were manually marked with high accuracy: background, cells and cells in the process of division (having a circular morphology). Then, training of a neural network based on U-NET has begun. Network training was performed using hardware acceleration (GPU Quadro p2200) and took at least 100.000 network iterations until over 97% success was achieved. The generated classifier was then validated for accuracy on a new pool of images on which it was not trained. The finally obtained neural network was saved in the form of a .nn file and used in the further stages of the study as a classifier.

3.12. Live/Dead Assay

Fluorescence-based LIVE/DEAD™ Cell Imaging Kit (Thermo Fisher Scientific, USA) assay was used to examine cells viability. It is a two-color assay to determine viability of cells based on plasma membrane integrity and esterase activity. Green-fluorescent Calcein-AM (ex/em 488nm/515nm) and red-fluorescent DNA stain (ex/em 570nm/602nm) allows for precise determination of live and dead cells in a population. Live cells bright green, whereas dead cells

with compromised membranes fluoresce red. Cells were seeded on 96-well plates at a density of 2.000 cells/cm². After 24 h incubation, drugs and compounds were added to wells, and cells were cultured for the next 72 h. Cell staining was performed in accordance to manufacturer protocol. Labelled cells were viewed under a fluorescence microscope (IX83, Olympus, Japan). Microscopic images were used for subsequent quantitative analysis (Cell Sens Dimension, Olympus, Japan). Image analysis was performed in the Count and Measure module dedicated Cellsens Dimenison software (Olympus, Japan) and it consisted on detecting objects using the "manual threshold" method and counting the detected ones objects with which apoptotic cells were stained. The exported results contained the number of detected objects that meet the given parameters in the .xls format.

3.13. Cell viability assessment by thiazolyl blue tetrazolium bromide assay (MTT)

Thiazolyl blue tetrazolium bromide (MTT, Sigma-Aldrich, St. Louis, MO, USA) was used to measure cell viability as a function of redox potential according to the ISO 10993-5:2009.

Cells (100 µl medium/well) were plated (day 0) in 2D plates [Falcon 96-well Tissue Culture Plate[®] (353072); Corning Inc., NY, USA]. The numbers of cells seeded per well were as follows: T24: 2.000 (2D) and DU145: 2.000 (2D). For spheroids culture: mature spheroids grown from 5.000 cells (T24 and DU145) on 3D plates [NanoCulture 96-well Plate[®] (NCP-LH-96); SCIVAX, Kanagawa, Japan] were incubated with drugs for 24, 48 and 72h.

Drugs were added on day 1. After 72 hours of incubation, the media were replaced with MTT reagent (1 mg/ml, Sigma-Aldrich, St. Louis, MO, USA). The cells were incubated with the reagent for at least 2 hours at 37 °C. Following incubation, the media were aspirated and the remaining formazan was dissolved in DMSO (Fig. 9). The absorbance of the solution was then read at 570 nm in a spectrophotometer with background subtraction at 690 nm. Each experiment was performed at least in triplicate. After all replicates were performed, the results were used to calculate the half maximal inhibitory concentration causing 50% cell death - IC₅₀. Based on the obtained results, the curve equation was generated, which allowed for the appropriate calculation of the IC value.

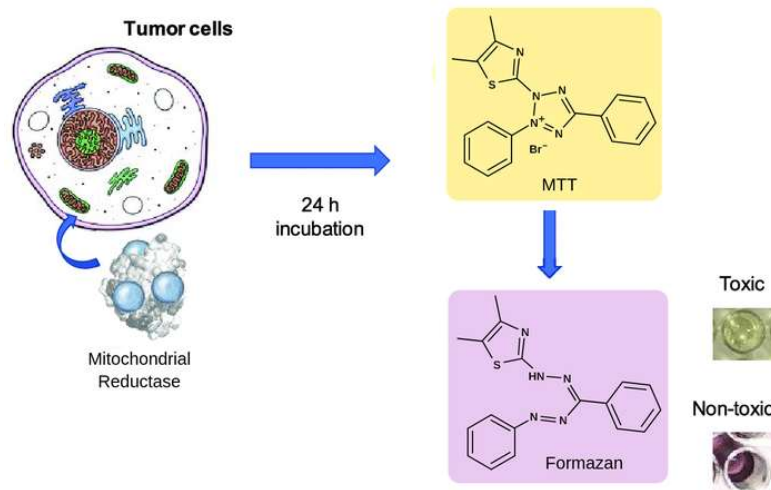


Figure 9. Diagram of the procedure for assessing cell viability using the MTT test. The diagram shows the reduction of 3-(4,5-dimethylthiazol-2-yl)-2,5-diphenyltetrazolium bromide (MTT) reagent to purple formazan by living cells. Wells with unreacted dead cells remain yellow.

3.14. Cell viability assessment by WST8 assay

WST-8 cell proliferation assay is based on the extracellular reduction of WST-8 by NADH produced in the mitochondria resulting in a water-soluble formazan which dissolves directly into the culture medium.

WST-8 Cell Proliferation Assay Kit (Cayman Chemical Company, USA) was used. Cells were seeded in a 96-well plate at a density of 2,000 cells/well in 100 μ L of culture medium and then incubated at 37 $^{\circ}$ C for 48h. WST-8 mixture was added to each well. 2D adherent cell culture was incubated for 2 hours, spheroids for 4 hours. The absorbance of the solution was then read at 450 nm in a spectrophotometer.

3.15. Assessment of apoptosis - identification of caspase 3 and 7 activity

Caspase-3 is one of the key effector caspases in the apoptotic signal cascade. Its homologue is caspase-7. Identification of active enzymes indicates apoptosis death in the cell. Two fluorochromes were used in the fluorescence reaction: FITC (Fluorescein Isothiocyanate) and DAPI (4',6-diamidin-2-phenylindole). CellEvent [™] Caspase-3/7 Green Detection Reagent (Invitrogen by Thermo Fisher Scientific, USA) is a peptide (DEVD) conjugated to a nucleic acid-

binding dye. The DEVD peptide sequence is a caspase-3/7 cleavage site, and the conjugated dye is non-fluorescent until cleaved from the peptide and bound to DNA.

Both 24 and 72 hour incubation samples were prepared for analysis exposure to test compounds, a separate one was used for each time replicate plate. Cells were seeded at density 2.000/well in a 96-well plate. From each well containing the appropriate concentrations of test compounds, 50 μ L of medium was removed and 5 μ L of CellEvent™ Caspase-3/7 Green Detection Reagent (Invitrogen by Thermo Fisher Scientific, USA) was added. Then incubated 45 min. After the incubation time, 20 μ l of DEVD reagent was added per well and incubation continued for another one hour. Aqueous DAPI solution was added at a concentration of 0.2 μ g/ml (Sigma, Germany) with an incubation of 10 min. Cells were then fixed for 10 min. with the addition of 50 μ L of 6% formaldehyde for each well. After fixation, the wells were rinsed with PBS, which was also left to read. Apoptosis was visualized with a fluorescence microscope (CKX53 FN Olympus, Japan) and a camera (VC90 4K Olympus, Japan) using the CellSens program (Olympus, Japan). In order to ensure identical reading conditions, the same reading parameters for all test wells were used. The photos were taken under 20x magnification. Green fluorescence of the FITC fluorochrome was observed in apoptotic cells, and identification of the nuclei was achieved by staining them with DAPI blue. Image analysis was performed in the Count and Measure module dedicated Cellsens Dimension software (Olympus, Japan) and it consisted on detecting objects using the "manual threshold" method and counting the detected ones objects with which apoptotic cells were stained. The exported results contained the number of detected objects that meet the given parameters were stored in the .xls format.

3.16. Cell proliferation by thymidine analogue 5-Bromo-2'-deoxyuridine method

The analysis was performed with a thymidine analogue 5-Bromo-2'-deoxyuridine (BrdU) (Merck Millipore, USA). It is based on the quantitative measurement of DNA synthesis. Bromodeoxyuridine (BrdU - Bromodeoxyuridine, 5-bromo-2-deoxyuridine) is a synthetic analogue of thymidine nucleoside and is used to identify proliferating cells. It incorporates into DNA during cell division, during the S phase.

Detection of incorporated molecules is possible with the use of antibodies directed against BrdU. This allows for a colorimetric analysis of the cell proliferative capacity. A positive BrdU result proves the viability of a given cell line and is proportional to their proliferation. Cells were seeded at 2.000/well in a 96-well plate. To each well containing the appropriate concentrations of test compounds, 20 µl of BrdU solution was added, followed by incubation for 24 hours at 37 ° C. After this time, the medium was removed and 100 µl of Fixing Solution was added for an incubation time of 30 min. at room temperature. Next, the wells were washed 3 times with the use of Wash Buffer. 100 µl of the primary antibody (anti BrdU Monoclonal Detector Antibody) was added and incubated for 1 hour. The wells were washed 3 times with the washing buffer again. After washing, 100 µl of secondary antibody (Peroxidase Goat Ani-Mause Igb Conjugate) was added. The final wash also includes washing the wells 3 times with the washing buffer. After drainage, 100 µl of TMB Peroxidase Substrate was added with 30 min incubation in the dark. After this time, 100 µL of Stop Solution was added. Absorbance was read at wavelength 450/595nm with a spectrophotometer (iMark™ Microplate Reader BIO-RAD, USA).

3.17. pH of the cell culture medium measurement

The negative logarithm of the hydrogen ion concentration was measured with a pH meter (Mettler Toledo, Switzerland) fitted with a combined electrode (Hydromet, type ERH-12-6 no. 2162, Poland). The pH value was assessed after 24, 48 and 72 hours of cell culture. The medium from the culture wells, both the control and the test compounds, was transferred to Eppendorf tubes in the amount of 500 µl, and then the pH value was measured 3 times.

3.18. Statistical analysis

Statistical analysis was performed by GraphPad Software 8.4 serial no. JPZP602E256505AR-D (GraphPad Software, San Diego, CA, USA). Each experiment was performed at least in triplicate. The average cell viability was expressed as a percentage relative to the control. All data were presented as means \pm SD. Normal distribution of data was analysed using the Shapiro–Wilk test. Parametric analysis was performed with one-way ANOVA with Tukey post hoc (for cell viability) or two-way ANOVA with Sidak post hoc (for grouped analysis). For Non-parametric analysis the t-test with the Mann-Withey post-test was used. The analysis assumed that the p value, i.e. the test probability, must be less than 0.05 for the difference to be considered statistically significant.

4. Results

4.1. Chitosan drugs' modification

The surface morphological characterization and size conformation of the nanoparticles were determined by using TEM and it is shown in Fig. 10. It was shown that the capsules obtained have a regular and spherical shape having an average diameter of 40 ± 9 nm. The sizes of nanocapsules containing drug were measured and the encapsulation efficiency was considered as 100%. The nanocapsules appeared separated, well-formed and globe-shaped. Furthermore, the smaller particles had larger surface area to volume ratios, thus it could have a significant impact on drug loading capacity and a slow drug release/diffusion rate.

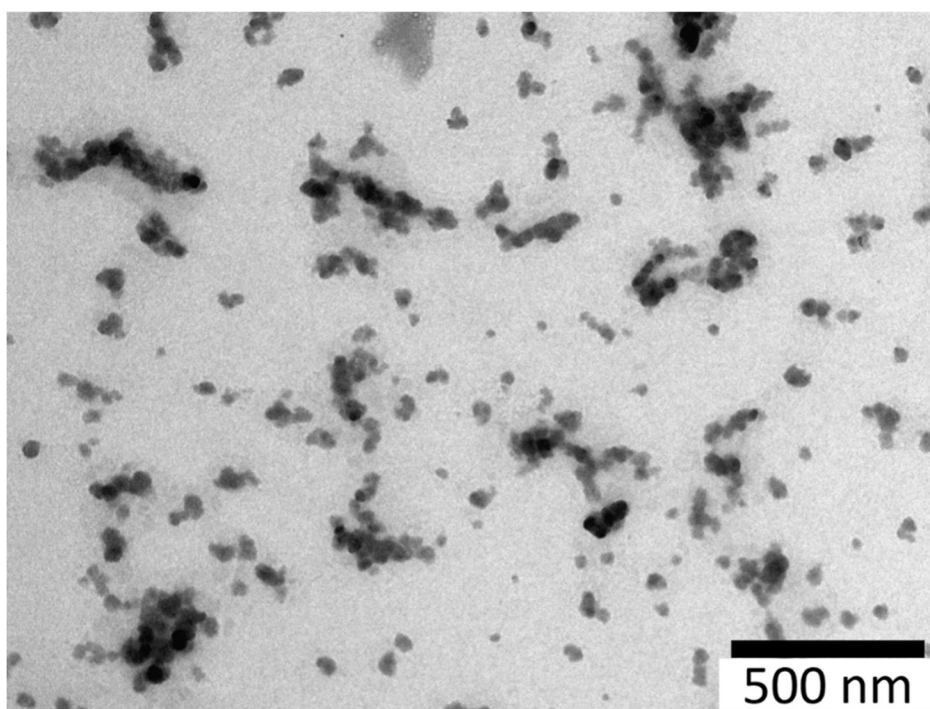


Figure 10. TEM micrograph of chitosan nanoparticles prepared with ciprofloxacin.

4.2. Chitosan drugs' modification – adherent cell culture

4.2.1. Assessment of cell viability in a microscope with inverted optics

Morphology analysis is the basic method by which the appearance and changes in the morphology of cells over time can be evaluated. T24 and DU145 cells were observed over a 72 hour period, both on the basis of live-imaging and point observation (24, 48 and 72 hour time points). The results for the last time point are shown below, i.e. after 72 hours.

Morphological changes in the bladder cell lines including cell shrinkage, rounding, and detachment were visible after ciprofloxacin treatment, especially in higher concentrations (Fig. 11). Seventy-two hour incubation of T24 with a low concentration of ciprofloxacin (100 μM) led to cell shrinkage and their detachment. In higher ciprofloxacin concentrations (500 and 1000 μM), only a small number of cells remained attached. Crystals of ciprofloxacin appeared in culture in 500 μM and in higher concentration 1000 μM for ciprofloxacin with chitosan. Morphometric analysis showed, in most cases, a lack of changes in the cells' area in lower drug concentrations compared to control for both drugs. Cells area reduction was observed in higher (500 and 1000 μM) drug concentrations for modified and unmodified drug.

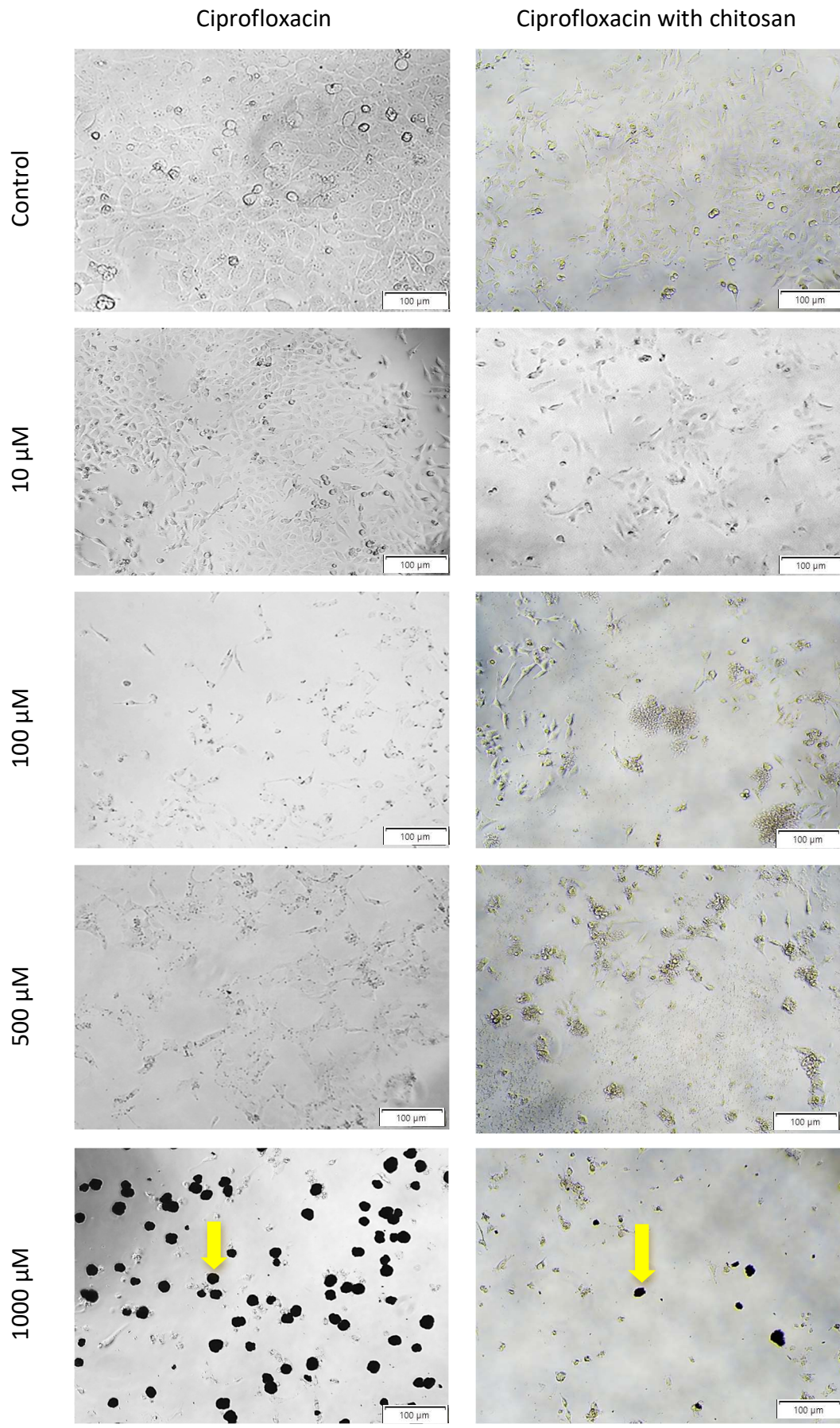


Figure 11. T24 cells at 72 hours of cultivation in the presence of: culture medium, ciprofloxacin and ciprofloxacin modified with chitosan at concentrations of 10, 100, 500, 1000 μM . Arrows mark visible particles of ciprofloxacin crystals.

All cells in the control had a regular shape and size (Fig. 12). Cells have grown in clusters and had regular hexagonal shape. After incubation with levofloxacin and modified levofloxacin, the cells lost their regular shape and size, they lost their cell-cell contact. Many cells lost their adhesion properties to surface of culture wells, a majority of cells were rounded in appearance. The chitosan-control cells did not show any changes after incubation.

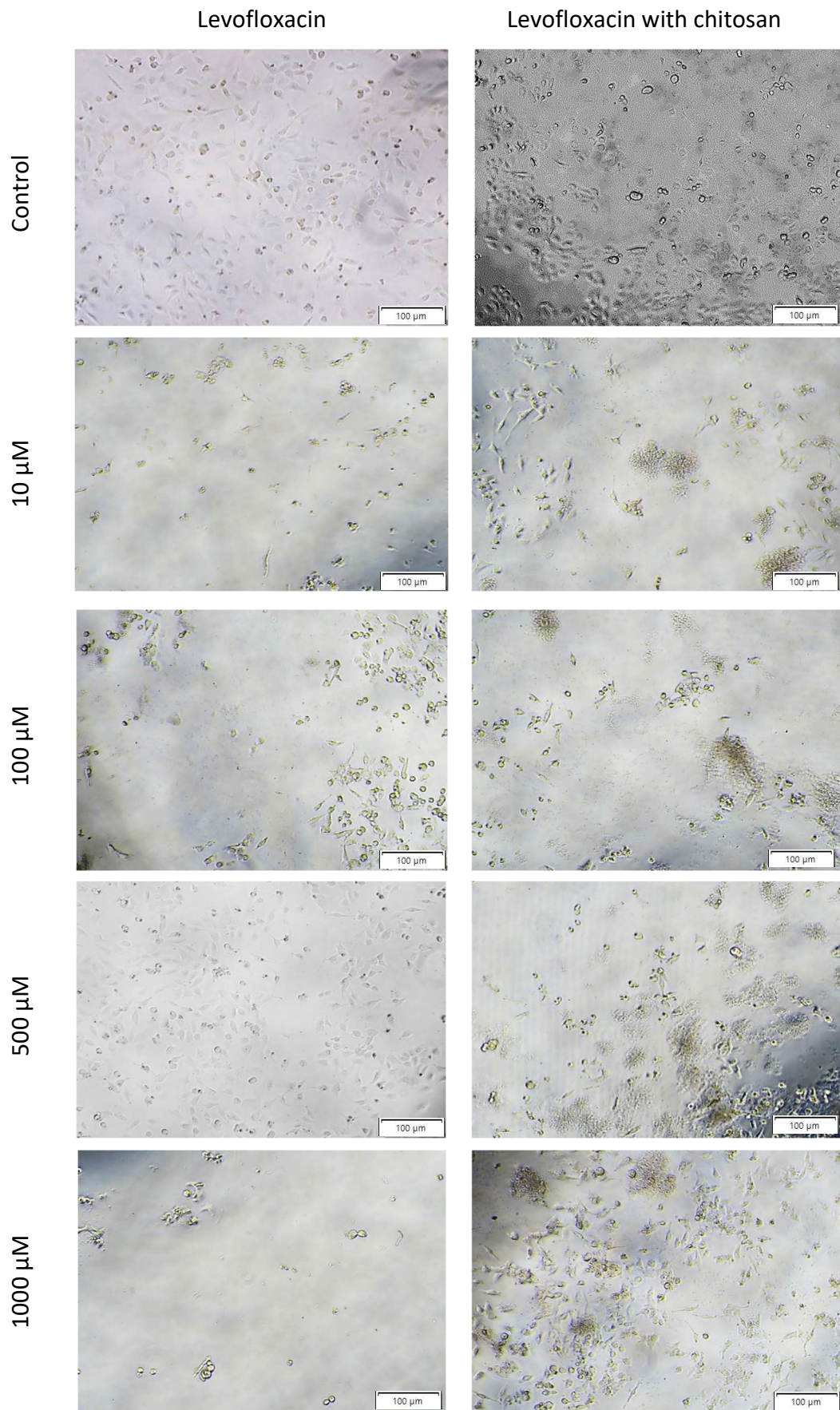


Figure 12. T24 cells at 72 hours of cultivation in the presence of: culture medium, levofloxacin and levofloxacin modified with chitosan at concentrations of 10, 100, 500, 1000 μM .

Morphological changes of prostate cell line (DU-145) were also observed after ciprofloxacin treatment, especially in higher concentrations (Fig. 13). Cell shrinking, rounding, and detachment that led to a decrease in cell number with increasing drug concentration were visible. Changes in cell morphology were more visible in the case of cancer DU-145 cells, in which detachment and shape changed, into a more rounded shape. It was observed even in 100 μM concentration, especially for ciprofloxacin with chitosan. Morphometric analysis showed a lack of changes in the cells' area in lower drug concentrations compared to control. The cell area reduction was observed in higher (500 and 1000 μM) drug concentrations.

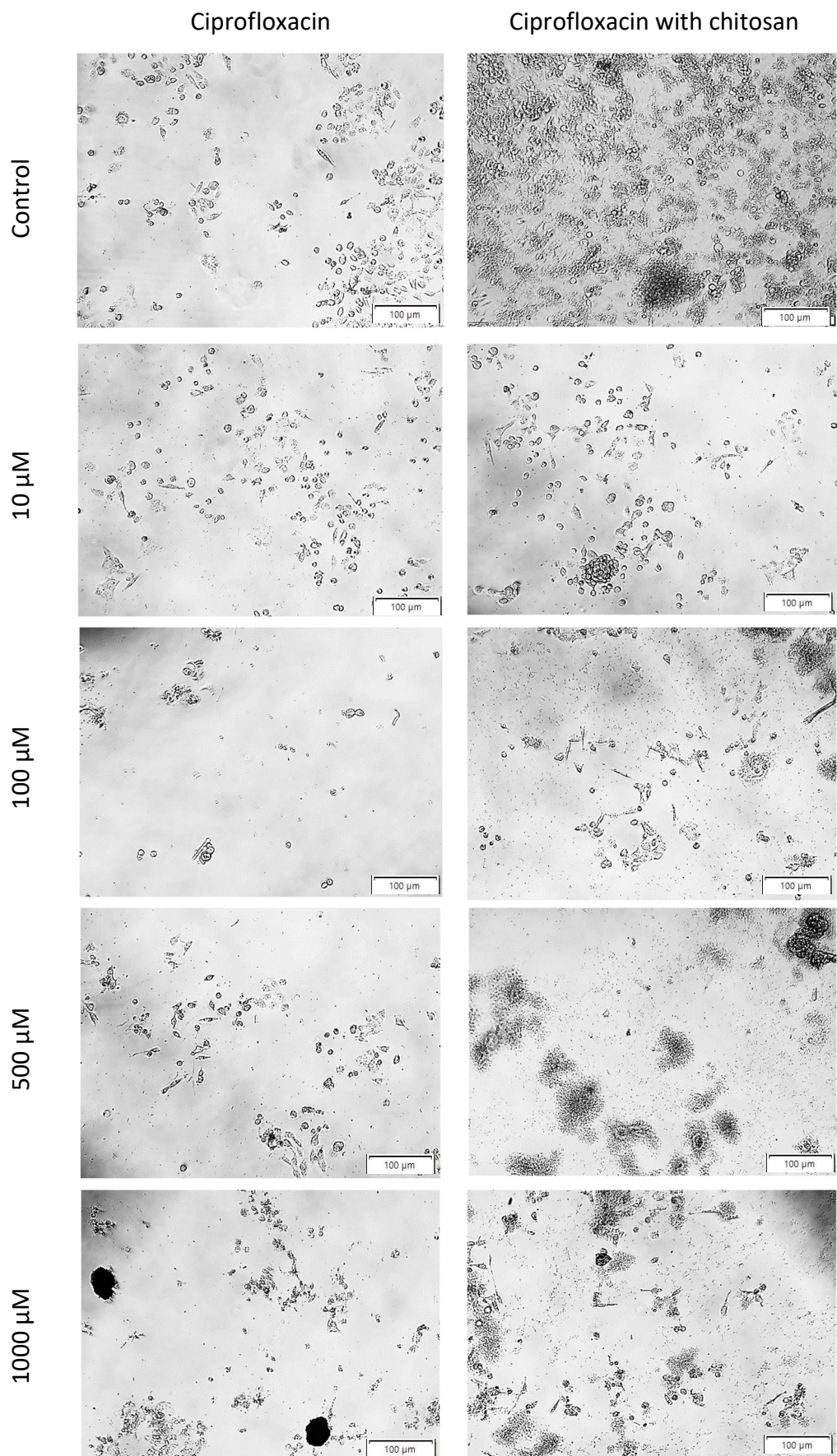


Figure 13. DU145 cells at 72 hours of cultivation in the presence of: culture medium, ciprofloxacin and ciprofloxacin modified with chitosan at concentrations of 10, 100, 500, 1000 μM .

DU145 cells were elongated and spindle-shaped. Tightly covered wells area with numerous cytoplasmic lamellipodia. After incubation with levofloxacin, many cells lost their attachment to surface of culture wells, a majority of cells were rounded in appearance (Fig. 14). Morphometric analysis showed in most cases a lack of changes in the cells' area in lower drug concentrations compared to control. Cells area reduction was observed in higher (500 and 1000 μ M) drug concentrations.

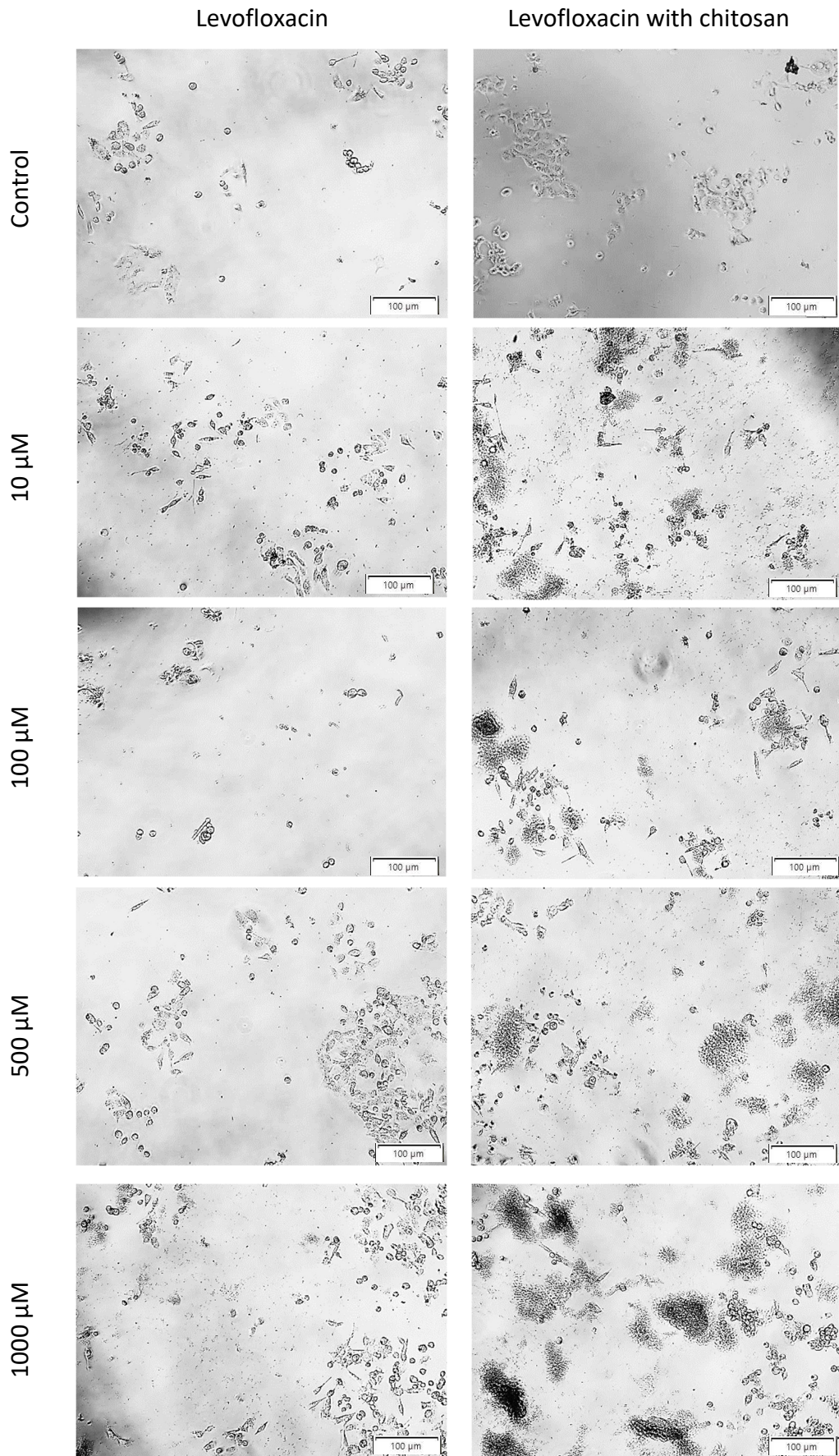


Figure 14. DU145 cells at 72 hours of cultivation in the presence of: culture medium, levofloxacin and levofloxacin modified with chitosan at concentrations of 10, 100, 500, 1000 μM .

4.2.2. Live/Dead Assay

Assessment of cell viability is an important study for estimation of the drug's effect, physical or chemical stimulants. In this test, Live or Dead™ cell viability two fluorogenic indicators were determined: calcein AM for viable cells and propidium iodide a cell-impermeable DNA-binding dye for the cells with compromised membranes, propidium iodide.

Live/dead test results for bladder cancer cell line showed an increasing number of dead cells with increasing concentration of the test drug. After 24 hours of cell incubation with the tested drugs, for a concentration of 10 μM , the percentage of dead cells was 10.52% for levofloxacin and 4.28% for modified ciprofloxacin. The most similar values were observed for a concentration of 500 μM , followed by 22.36% and 23.00%. The highest differences in the percentage of dead cells were observed for the concentration of 1000 μM , and was calculated as 37.5% after incubation with modified levofloxacin (Fig. 15, 16).

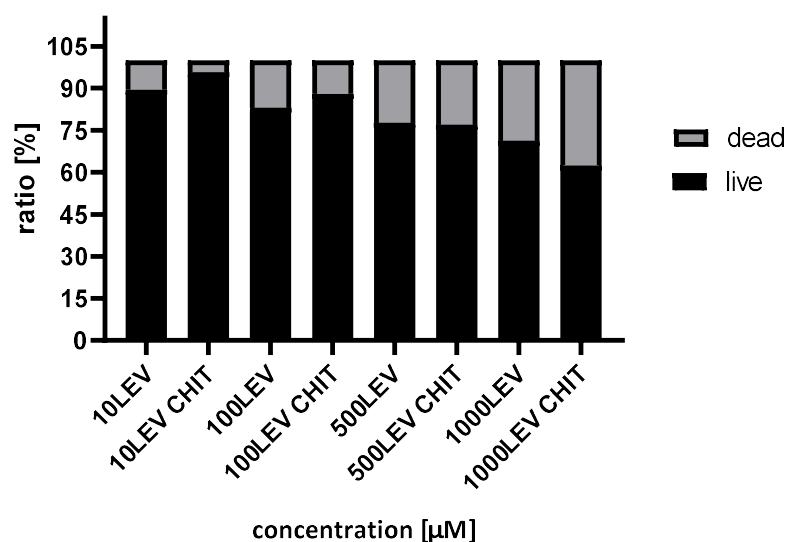


Figure 15. The graph shows the ratio of live to dead cells at individual drug concentrations for the T24 cell line. Cell viability was assessed after 24 hours incubation with drugs. Each concentration was assessed at least in triplicate, and the cells were counted from 6 images taken in each well tested. "#" - statistically significant difference between the corresponding concentrations of levofloxacin and modified levofloxacin was showed ($p < 0.05$).

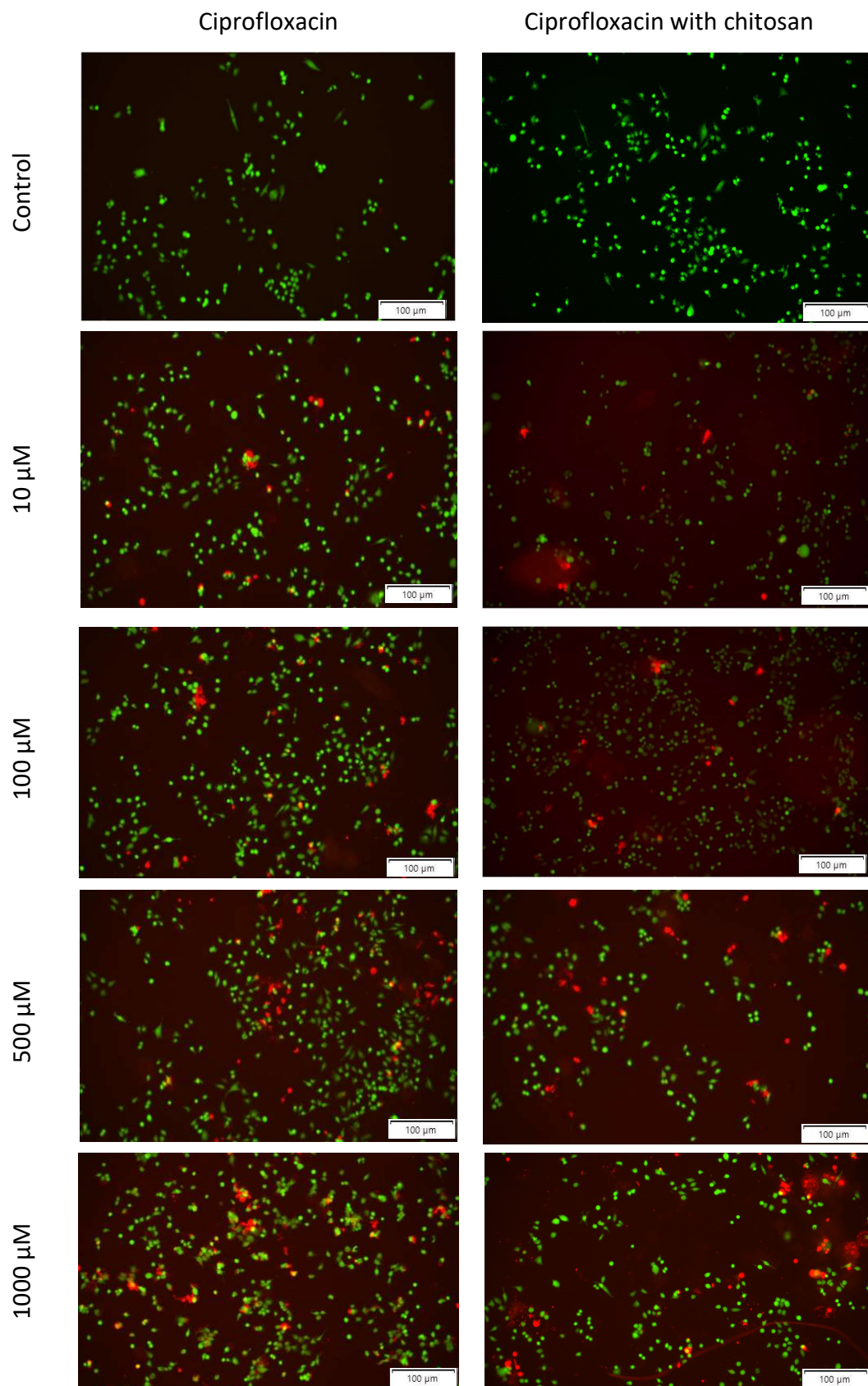


Figure 16. Microscopic images demonstrating how T24 culture conditions influence the visibility of dead cells detected using the fluorescent live/dead assay kit. Cell death was induced by chemotherapeutic agent - levofloxacin and levofloxacin with chitosan. Imaging Assay of Live or Dead™ Cell Viability. Live cells, dead cells and the mixture of two cells (Live/Dead) were analysed with Live or Dead™ Cell Viability Assay Kit, and imaged in channels mCh (red) and AlexaFluor488 (green) with fluorescence microscope.

For ciprofloxacin, the percentage of dead cells after 24 hours of incubation with modified drug was higher for each tested, respectively: for concentration 10 μM (CIP - 9.58% and CIP CHIT - 18.24%), 100 μM (CIP - 14.03% and CIP CHIT - 26.75%), 500 μM (CIP - 29.39% and CIP CHIT - 35.33%). What is more, at the highest concentration, statistical analysis showed a statistically significant difference between modified and unmodified ciprofloxacin of 21.63%, in favor of a modified drug (Fig. 17, 18).

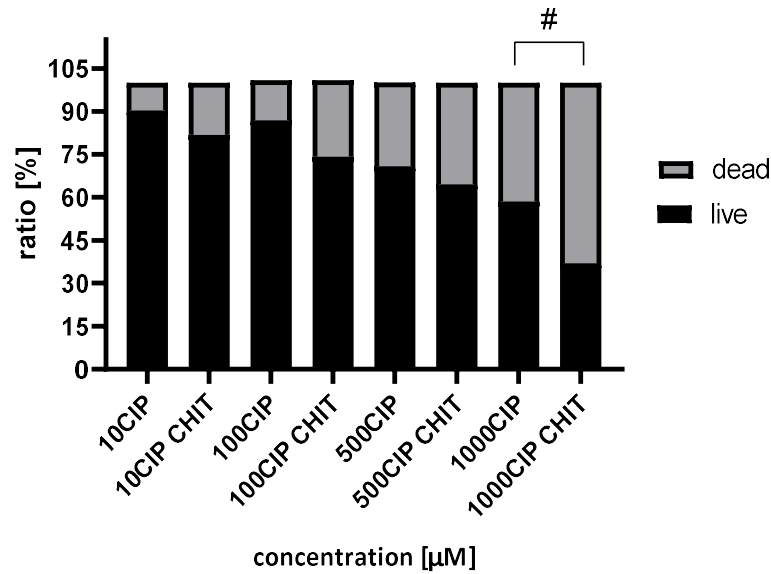


Figure 17. The graph shows the ratio of live to dead cells at individual drug concentrations for the T24 cell line. Cell viability was assessed after 24 hours incubation with drugs. Each concentration was assessed at least in triplicate, and the cells were counted from 6 images taken in each well tested. "#" - statistically significant difference between the corresponding concentrations of ciprofloxacin and modified ciprofloxacin was showed ($p < 0.05$).

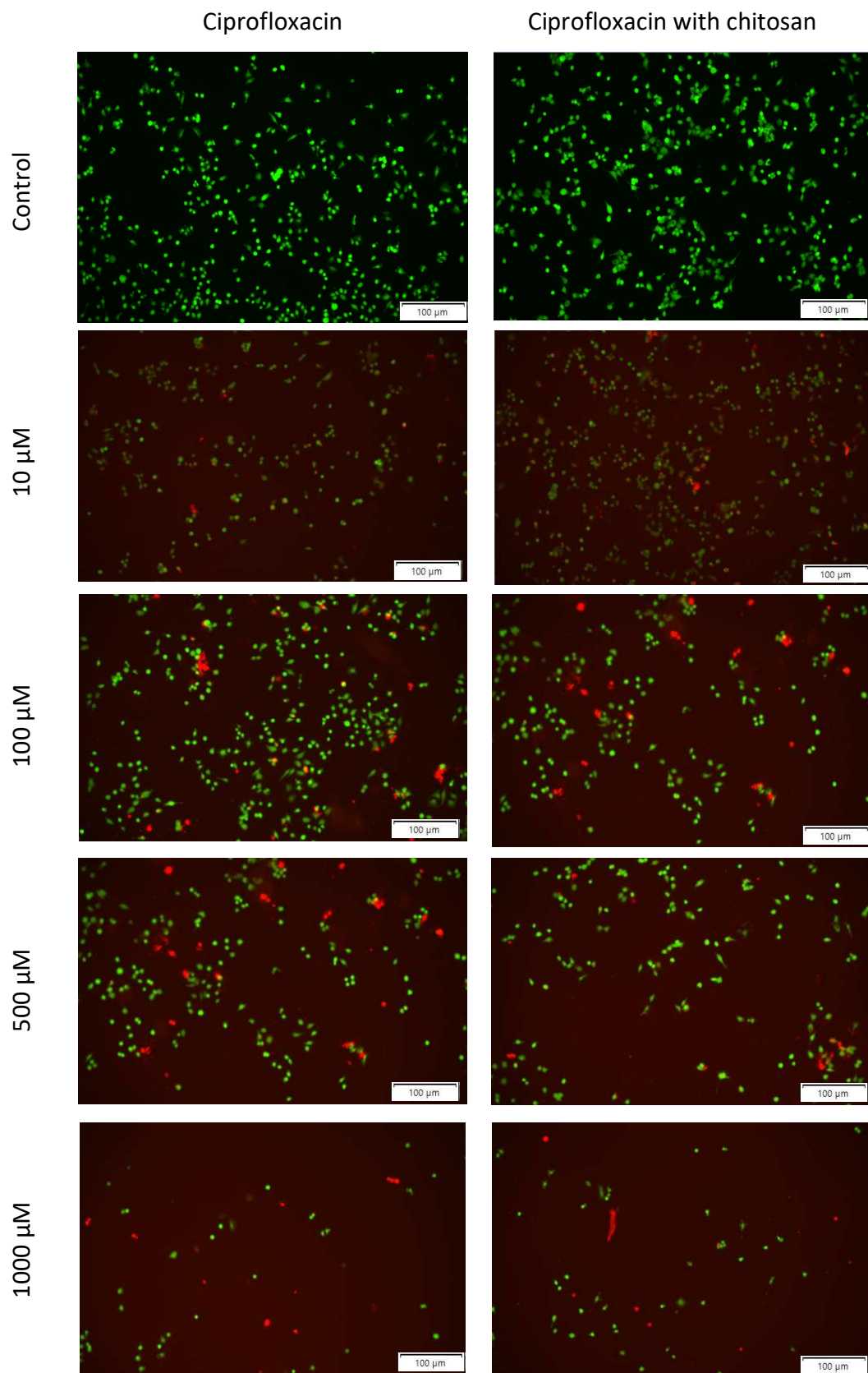


Figure 18. Microscopic images demonstrating how T24 culture conditions influence the visibility of dead cells detected using the fluorescent live/dead assay kit. Cell death was induced by chemotherapeutic agent - levofloxacin and levofloxacin with chitosan. Imaging Assay of Live or Dead™ Cell Viability. Live cells, dead cells and the mixture of two cells (Live/Dead) were analysed with Live or Dead™ Cell Viability Assay Kit, and imaged in FITC and Alexa Fluor channels with fluorescence microscope.

In the case of prostate cancer cell line, for levofloxacin, the percentage of dead cells after 24 hours of incubation with modified drug was also higher for each concentration tested. For 10 μM (LEV - 1.6% and LEV CHIT - 8.01%), 500 μM (LEV - 21.787% and LEV CHIT - 24.64%) and for 1000 μM (LEV - 25.39% and LEV CHIT - 29.86%) For 100 μM percentage quantity of dead cells were almost the same for both forms of drug – 23.56% and 23.25% (Fig. 19, 20). Despite these observations, these differences were not assessed as statistically significant.

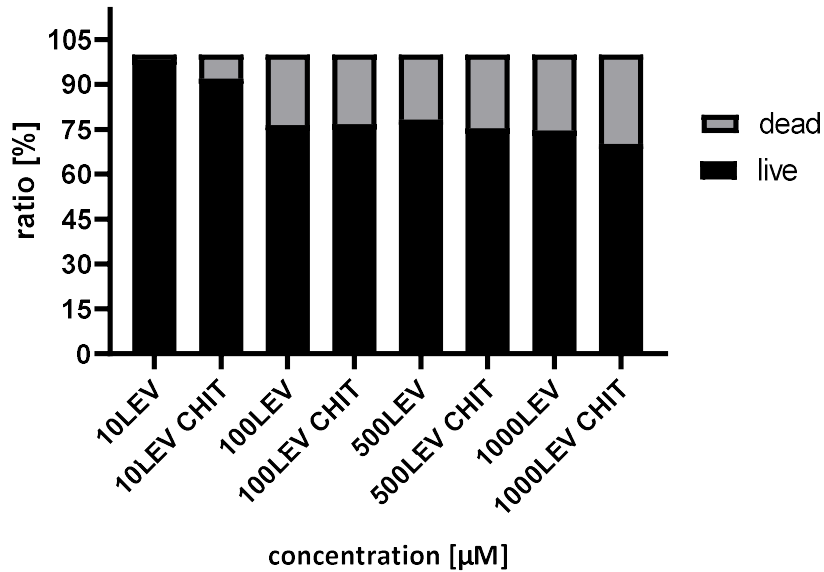


Figure 19. The graph shows the ratio of live to dead cells at individual drug concentrations for the DU145 cell line. Cell viability was assessed after 24 hours incubation with drugs. Each concentration was assessed at least in triplicate, and the cells were counted from 6 images taken in each well tested. "#" - statistically significant difference between the corresponding concentrations of levofloxacin and modified levofloxacin was showed ($p < 0.05$).

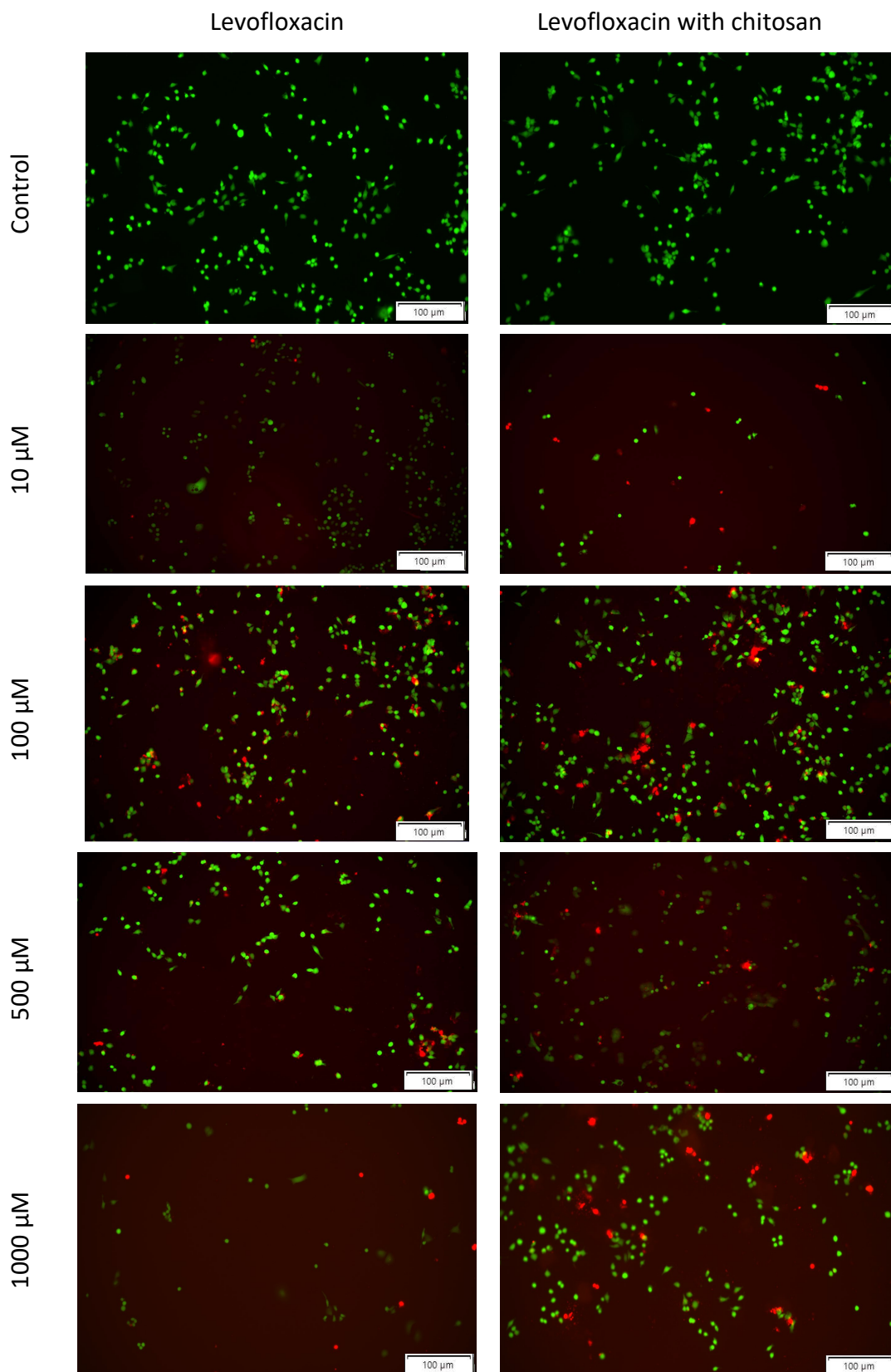


Figure 20. Microscopic images demonstrating how DU145 culture conditions influence the visibility of dead cells detected using the fluorescent live/dead assay kit. Cell death was induced by chemotherapeutic agent - levofloxacin and levofloxacin with chitosan. Imaging Assay of Live or Dead™ Cell Viability. Live cells, dead cells and the mixture of two cells (Live/Dead) were analysed with Live or Dead™ Cell Viability Assay Kit, and imaged in FITC and Alexa Fluor channels with fluorescence microscope.

For ciprofloxacin, the percentage of dead cells after 24 hours of incubation with modified drug was higher for each concentration tested 10 μM (CIP - 7.58% and CIP CHIT - 15.24%), 100 μM (CIP- 16.03% and CIP CHIT - 20.75%). A statistically significant difference between the two forms of the drug was observed in the case of the highest concentrations of the drug 500 μM (CIP - 20.39% and CIP CHIT - 33.33%) and 1000 μM (CIP - 39.43% and CIP CHIT 62.06%) (Fig. 21, 22).

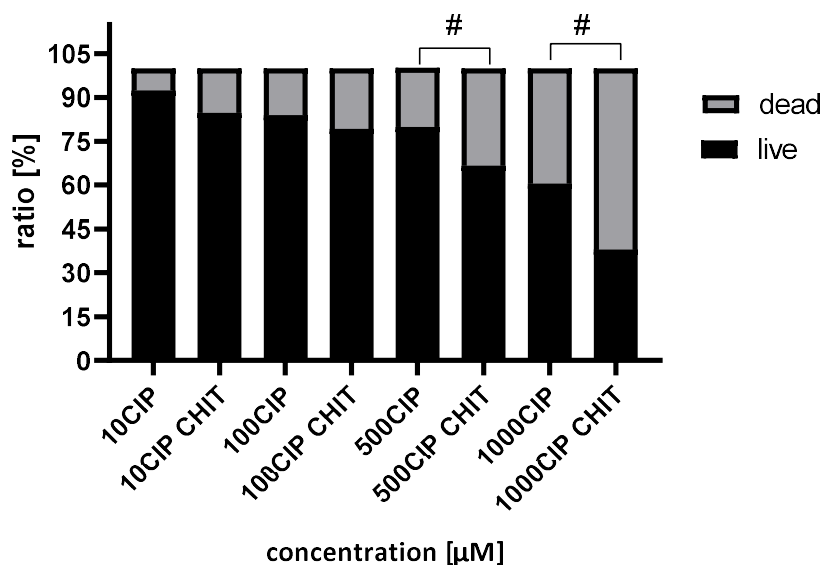


Figure 21. The graph shows the ratio of live to dead cells at individual drug concentrations for the T24 cell line. Cell viability was assessed after 24 hours incubation with drugs. Each concentration was assessed at least in triplicate, and the cells were counted from 6 images taken in each well tested. "#" - statistically significant difference between the corresponding concentrations of ciprofloxacin and modified ciprofloxacin was showed ($p < 0.05$).

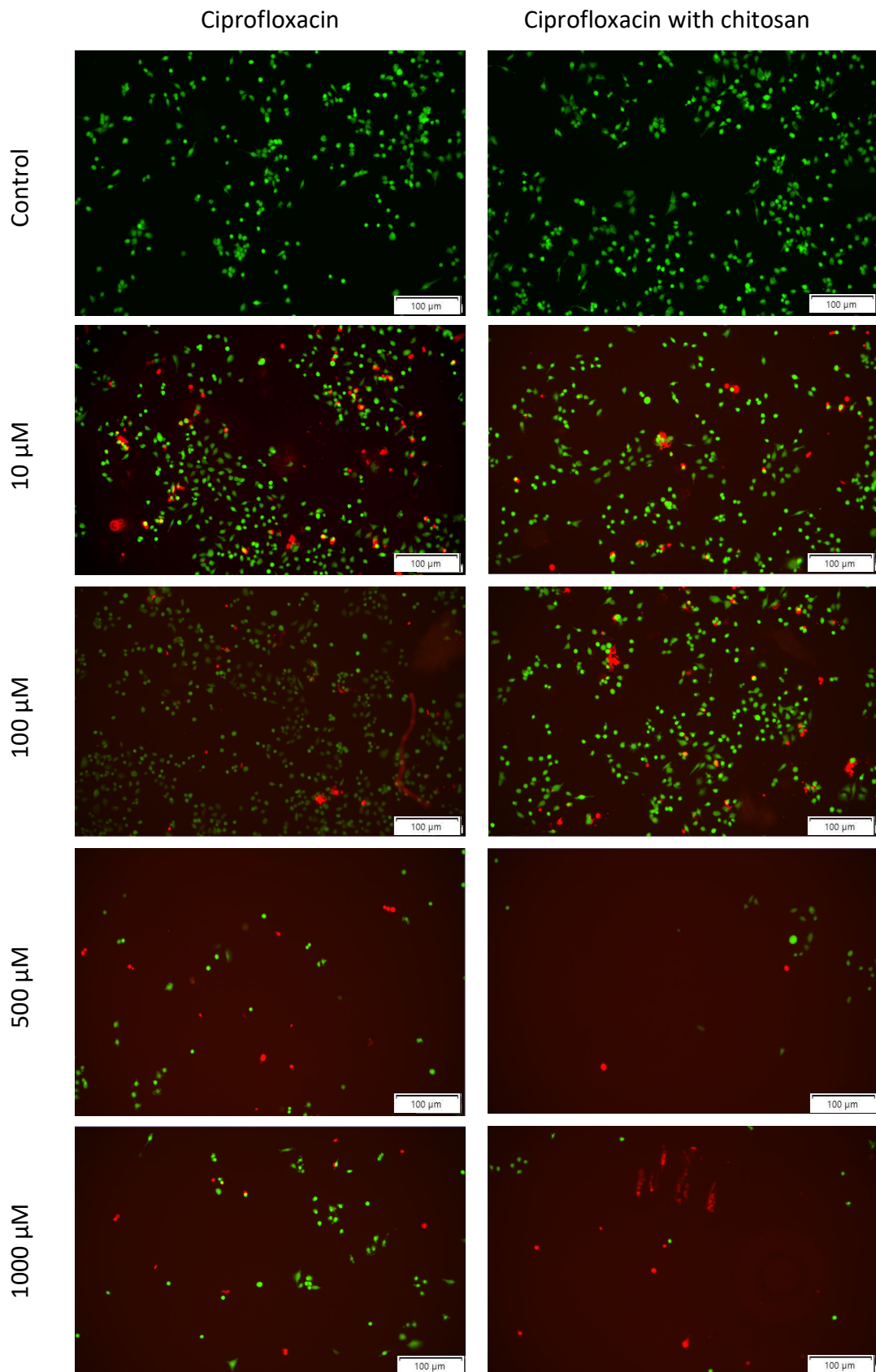


Figure 22. Microscopic images demonstrating how DU145 culture conditions influence the visibility of dead cells detected using the fluorescent live/dead assay kit. Cell death was induced by chemotherapeutic agent - ciprofloxacin and ciprofloxacin with chitosan. Imaging Assay of Live or Dead™ Cell Viability. Live cells, dead cells and the mixture of two cells (Live/Dead) were analysed with Live or Dead™ Cell Viability Assay Kit, and imaged in FITC and Alexa Fluor channels with fluorescence microscope.

4.2.3. Cell viability assessment by thiazolyl blue tetrazolium bromide assay (MTT)

The cytotoxicity of ciprofloxacin and ciprofloxacin modified with chitosan was analysed using the MTT test. Both of these substances significantly reduced the metabolic activity of T24 cells, and increasing concentrations resulted in a gradual decrease in survival (Fig. 23). The results of the analysis were also performed using an additional control that contained the used solvents of the test compounds, i.e., deionized water and PBS at the concentrations used at the 1000 μ M dilution.

In the case of the T24 line, the results of the experiment showed a very strong cytotoxic effect of both ciprofloxacin and modified ciprofloxacin. Each of the concentrations caused a statistically significant decrease in cell viability compared to the control (Fig. 23).

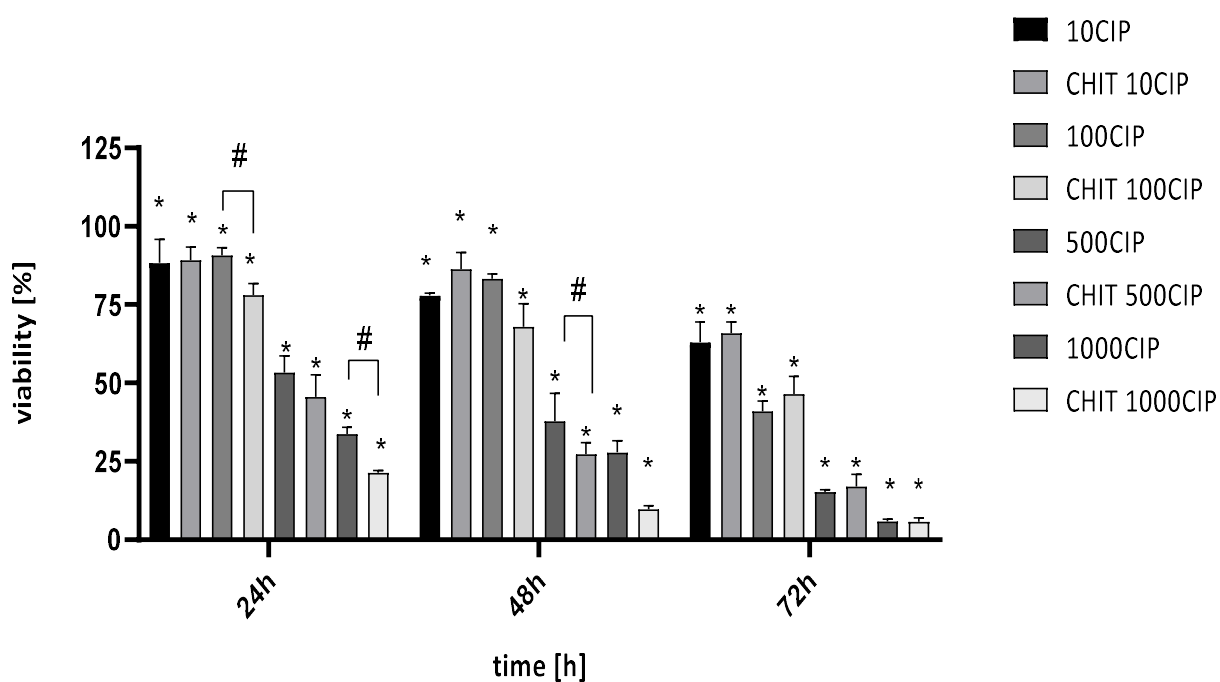


Figure 23. MTT test results for the T24 line in the following days from the start of incubation with the addition of ciprofloxacin and modified ciprofloxacin in the concentration range of 10-1000 μ M. "*" - statistical significance in relation to the control; "#" - statistically significant difference between the corresponding concentrations of ciprofloxacin and modified ciprofloxacin ($p < 0.05$).

The smallest differences in cell viability with time were noted for modified ciprofloxacin at the concentration of 10 μM . Higher cell mortality was observed for the modified ciprofloxacin in concentrations of 100-1000 μM . However, a statistically significant difference between the tested compounds was observed for the concentration of 10, 500 and 1000 μM in the 24 hour of the experiment. The highest death rate of T24 cells was caused by the use of ciprofloxacin modified with chitosan at a concentration of 1000 μM , after 72 hours of incubation with a cytostatics (5.79 % of viability).

With regard to levofloxacin, statistically significant differences can be seen at 48 and 72 hours of the experiment for the highest concentration of both forms of the drug. For 48 hours, was noticed a difference in viability of 13.65% in favor of levofloxacin with chitosan (22.45% viability) (Fig. 24).

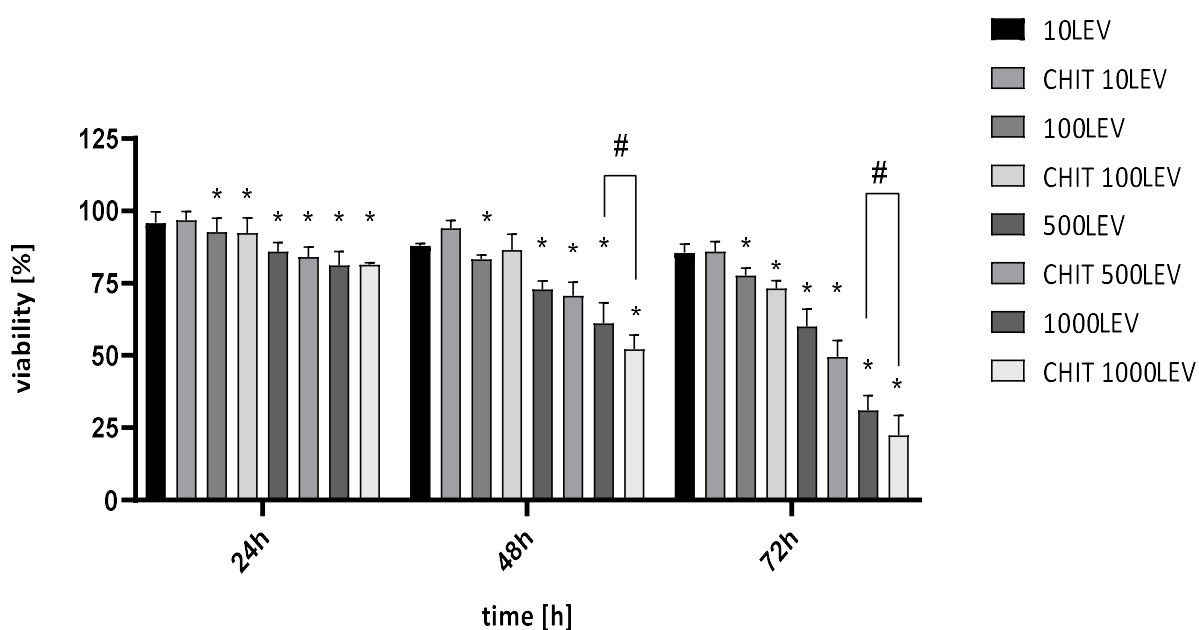


Figure 24. MTT test results for the T24 line in the following days from the start of incubation with the addition of levofloxacin and modified levofloxacin in the concentration range of 10-1000 μM . "*" - statistical significance in relation to the control; "#" - statistically significant difference between the corresponding concentrations of levofloxacin and modified levofloxacin ($p < 0.05$).

Viability evaluation of DU145 cells showed that ciprofloxacin and modified ciprofloxacin induce cell death that was dependent on the duration of exposure to the compound. Statistically significant mortality, compared to controls, was caused by the concentration of ciprofloxacin 10-1000 μM during 24, 48 and 72 hours and ciprofloxacin modified in the range of 100-1000 μM during 24 and 48 and 10-1000 μM in the last 72 hours. Modified ciprofloxacin was more effective at concentrations 500 μM in 24 and 48 hours of the experiment and 500 and 1000 μM in 72 hours of the experiment (Fig. 25).

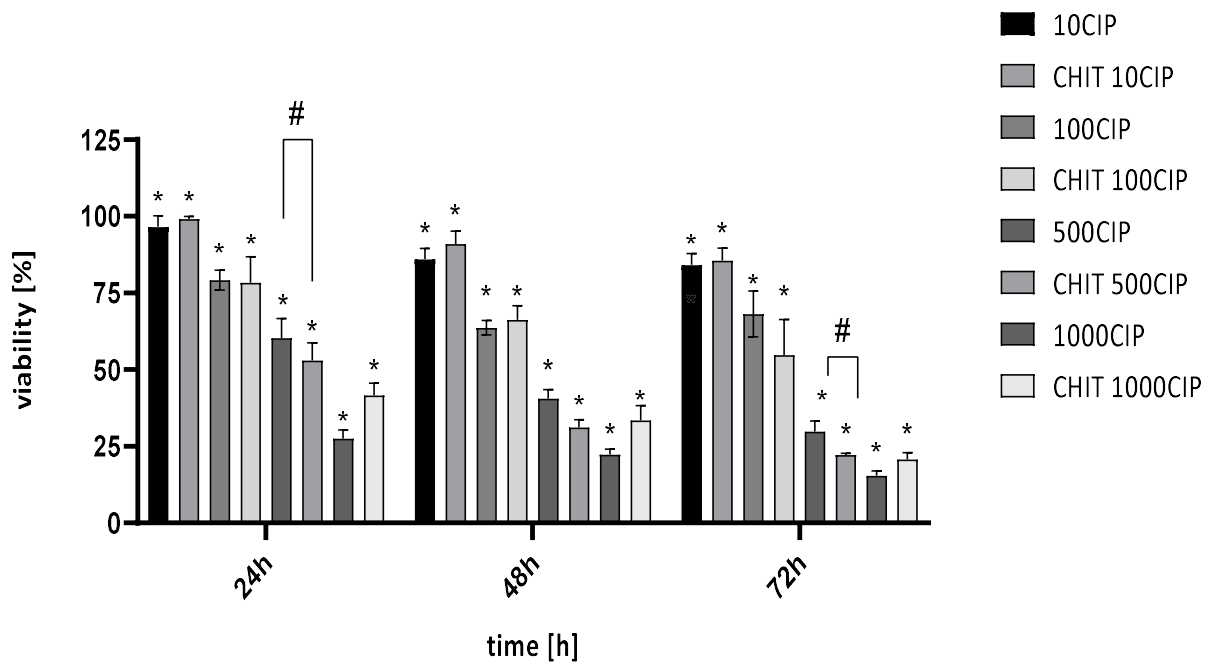


Figure 25. MTT test results for the DU145 line in the following days from the start of incubation with the addition of ciprofloxacin and modified ciprofloxacin in the concentration range of 10-1000 μM . "*" - statistical significance in relation to the control; "#" - statistically significant difference between the corresponding concentrations of ciprofloxacin and modified ciprofloxacin ($p < 0.05$).

Viability evaluation of DU145 cells showed that levofloxacin and modified levofloxacin initiate cell death that is dependent on the duration of exposure to the compound. Statistically significant mortality, compared to controls, was caused by the concentration of levofloxacin at any concentration except 72 hours for concentration 10 μM of both forms of levofloxacin (Fig. 26). Statistically significant differences in cell viability after incubation with both forms of the drug were observed in the concentration 1000 μM at 48 and 72 hours of the experiment. The IC50 for levofloxacin was 509.9 μM and for modified levofloxacin was 488.4 μM .

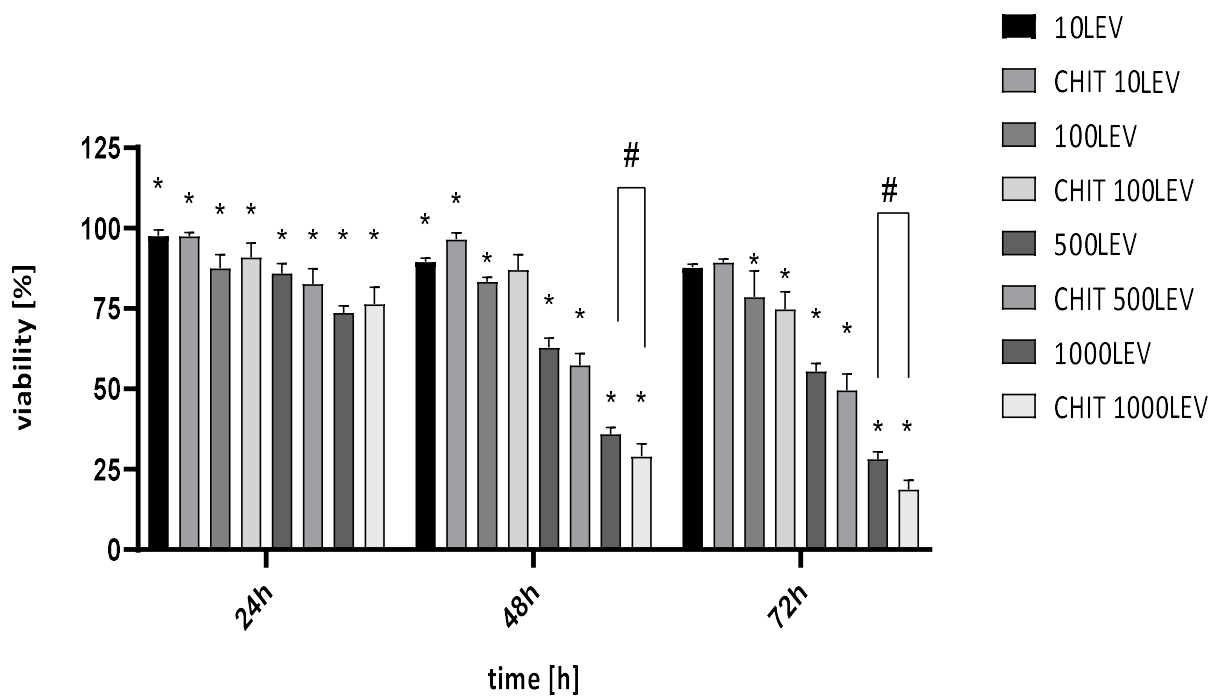


Figure 26. MTT test results for the DU145 line in the following days from the start of incubation with the addition of levofloxacin and modified levofloxacin in the concentration range of 10-1000 μM . "*" - statistical significance in relation to the control; "#" - statistically significant difference between the corresponding concentrations of levofloxacin and modified levofloxacin ($p < 0.05$).

Using the result of the MTT test, the IC50 value was determined (Tab. 5), i.e. the inhibitor concentration, which inhibits 50% of the biological functions of cells in 72 hours of exposure to the tested concentrations of cytostatics.

Table 5. The IC50 value for tested chemotherapeutic agents. The R² value for both compounds was over 0.95, which means a very good fit of the trend line.

	T24		DU145	
	IC50	R²	IC50	R²
CIP	117.8 μ M	0.9924	214.9 μ M	0.9826
CIP CHIT	136.6 μ M	0.9726	153.12 μ M	0.9587
LEV	422.6 μ M	0.9697	509.9 μ M	0.9791
LEV CHIT	613.6 μ M	0.9726	488.4 μ M	0.9769

4.2.4. Cell viability assessment by WST8 assay

This test was made primarily for the high sensitivity of the results. The detection sensitivity is higher than with other tetrazolium salt-based assays such as MTT, XTT or MTS. This assay kit is based on the cellular reduction of the tetrazolium salt WST-8 into a highly water-soluble, orange-colored formazan dye upon reduction in the presence of an electron carrier. As opposed to MTT assay, no solubilization process is required since this formazan does not require solvation, because the WST-8 is soluble in the tissue culture medium.

The assessment of viability using the WST-8 assay showed that in the case of bladder cancer cells, they are of particular interest at the highest concentration of both forms of the drug. For 24 hours, cell viability was 42.98% (CIP) and 38.40% (CIP CHIT), respectively. For 48 hours, where the difference between the viability of both forms of the drug was statistically significant, the viability of 37.87% (CIP) and 25.75% (CIP CHIT) can be noted. At 72 hours of the experiment it was noticed, that the viability level for both forms in the concentration 1000 μ M was very similar, at 16.14% (CIP) and 15.78% (CIP CHIT) (Fig. 27).

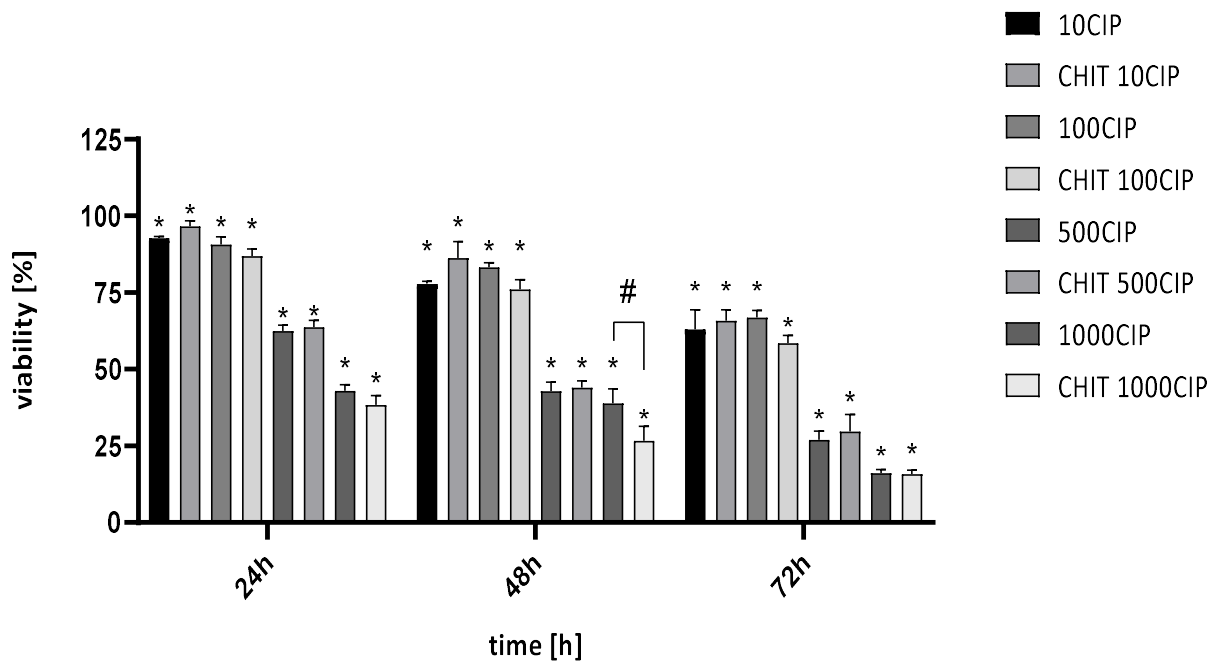


Figure 27. WST8 test results for the T24 line in the following days from the start of incubation with the addition of ciprofloxacin and modified ciprofloxacin in the concentration range of 10-1000 μM . "*" - statistical significance in relation to the control; "#" - statistically significant difference between the corresponding concentrations of ciprofloxacin and modified ciprofloxacin ($p < 0.05$).

When evaluating levofloxacin, the greatest decrease in viability was observed at 48 and 72 hours of the experiment. Statistically significant differences in viability were detected for concentration 1000 μM . At 48 hours was calculated as 58.20% (LEV) and 43.41% (LEV CHIT) and for 72 hours as 24.14% (LEV) and 15.16% (LEV CHIT) (Fig. 28).

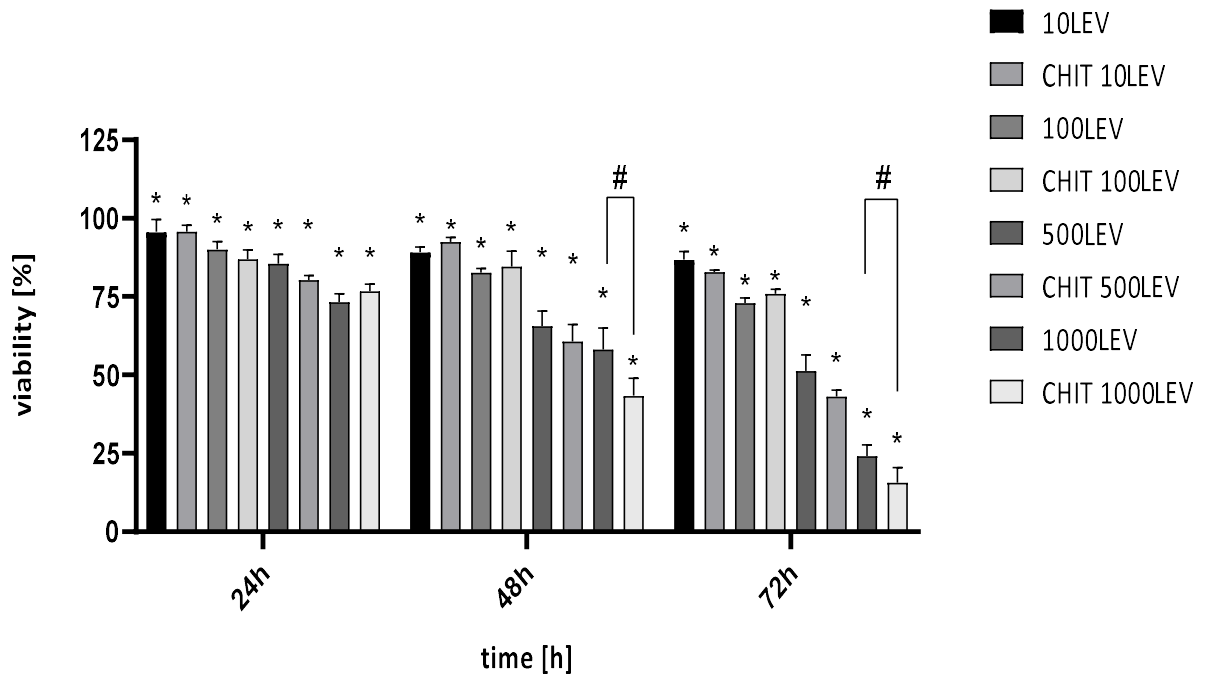


Figure 28. WST8 test results for the T24 line in the following days from the start of incubation with the addition of levofloxacin and modified levofloxacin in the concentration range of 10-1000 μM . "*" - statistical significance in relation to the control; "#" - statistically significant difference between the corresponding concentrations of levofloxacin and modified levofloxacin ($p < 0.05$).

In the case of the DU145 line, the study showed that statistically significant differences in viability for both forms of the drug appear for the concentration of 500 μM at 24 and 72 hours of the experiment. For the initial hours, these differences were 64.82% (CIP) and 56.33% (CIP CHIT). In the final hours of the experiment, it was a viability of 37.87% (CIP) and 31.09% (CIP CHIT) (Fig. 29).

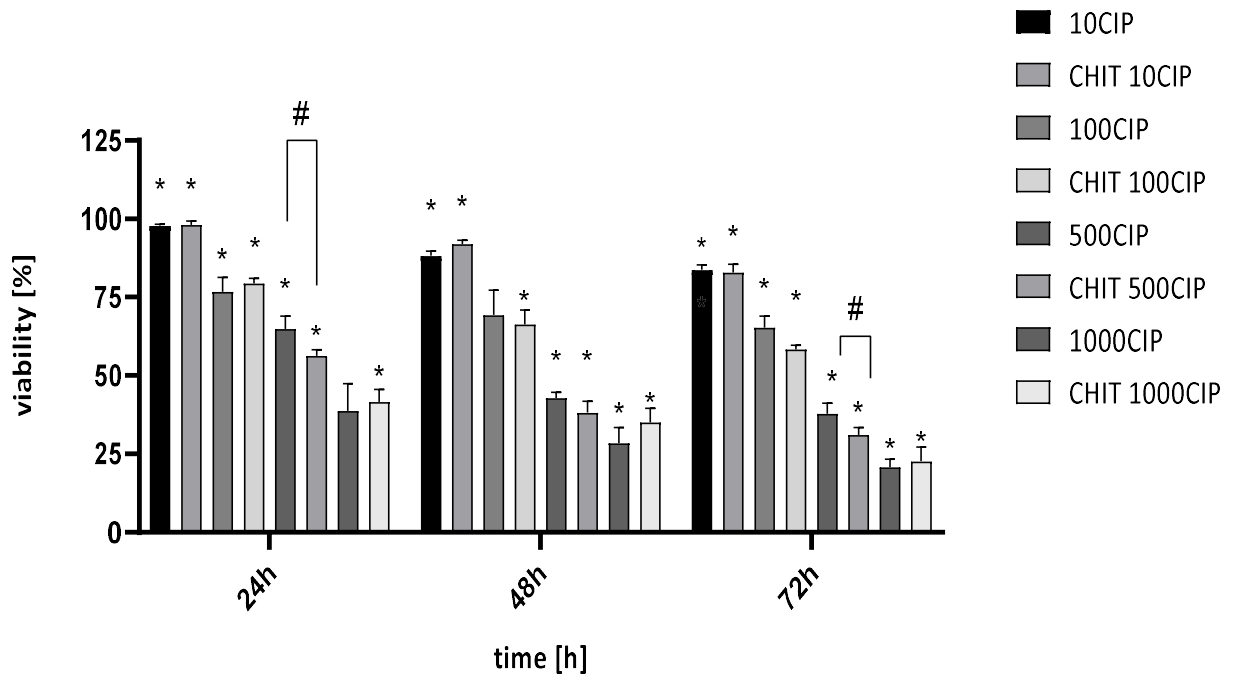


Figure 29. WST8 test results for the DU145 line in the following days from the start of incubation with the addition of ciprofloxacin and modified ciprofloxacin in the concentration range of 10-1000 μM . "*" - statistical significance in relation to the control; "#" - statistically significant difference between the corresponding concentrations of ciprofloxacin and modified ciprofloxacin ($p < 0.05$).

Prostate cancer cells treated with levofloxacin and levofloxacin with chitosan showed a statistically significant difference in viability at 72 hours of the experiment - for LEV 29.54% and for LEV CHIT 18.32% (Fig. 30).

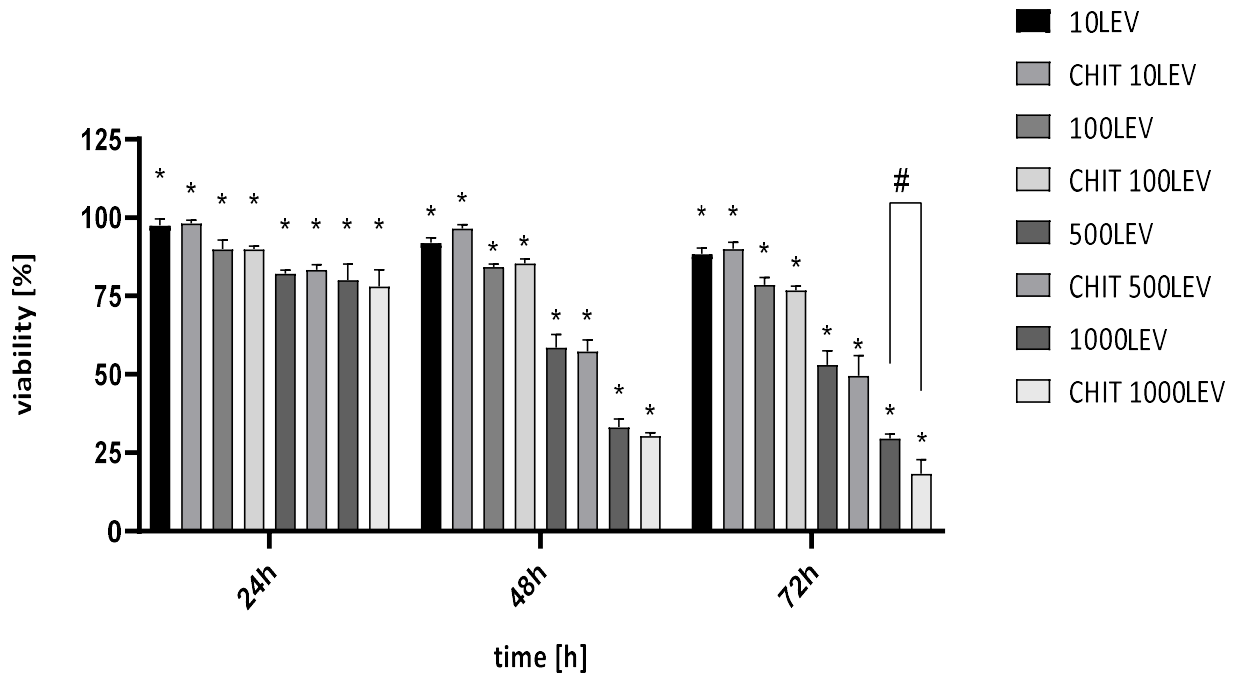


Figure 30. WST8 test results for the DU145 line in the following days from the start of incubation with the addition of levofloxacin and modified levofloxacin in the concentration range of 10-1000 μM . "*" - statistical significance in relation to the control; "#" - statistically significant difference between the corresponding concentrations of levofloxacin and modified levofloxacin ($p < 0.05$).

4.2.5. Assessment of apoptosis - identification of caspase 3 and 7 activity

The results of the test for the presence of active caspase 3/7 allowed for the assessment of the type of cell death that was caused by the action of ciprofloxacin and ciprofloxacin modified. Control tests were performed with the use of cisplatin and doxorubicin at concentrations of 10 μM .

Cell death by apoptosis is manifested by the green light of the FITC fluorochrome. The greatest concentration of apoptotic cells were observed at ciprofloxacin concentrations of 500-1000 μM (Fig. 31). To assess the events induced by chitosan treatment, the activity of tumor cells cultured with the detection of caspase-3 and -7 was examined. In chitosan-treated cultures, the number of cells increased after 3 days of culture, but the total number of treated cells was lower than in control cells. After 3 days of incubation, the caspase-3 activity of chitosan-treated cells increased several times compared to control cells. The trigger cell death mode by ciprofloxacin on T24 human prostate cancer cells was detected as the apoptosis. Control images were shown with the FITC channel and phase contrast overlay to visualize the number of cells. At concentrations above 500 μM , a lot of cells with apoptotic nature were visible - this applies to both: single cells and cell aggregates. Visual examination showed a higher number of apoptotic cells in the chitosan samples. The results for bladder cancer cells treated with levofloxacin showed the late apoptotic signals for concentrations ranging from 10-500 μM (Fig. 32).

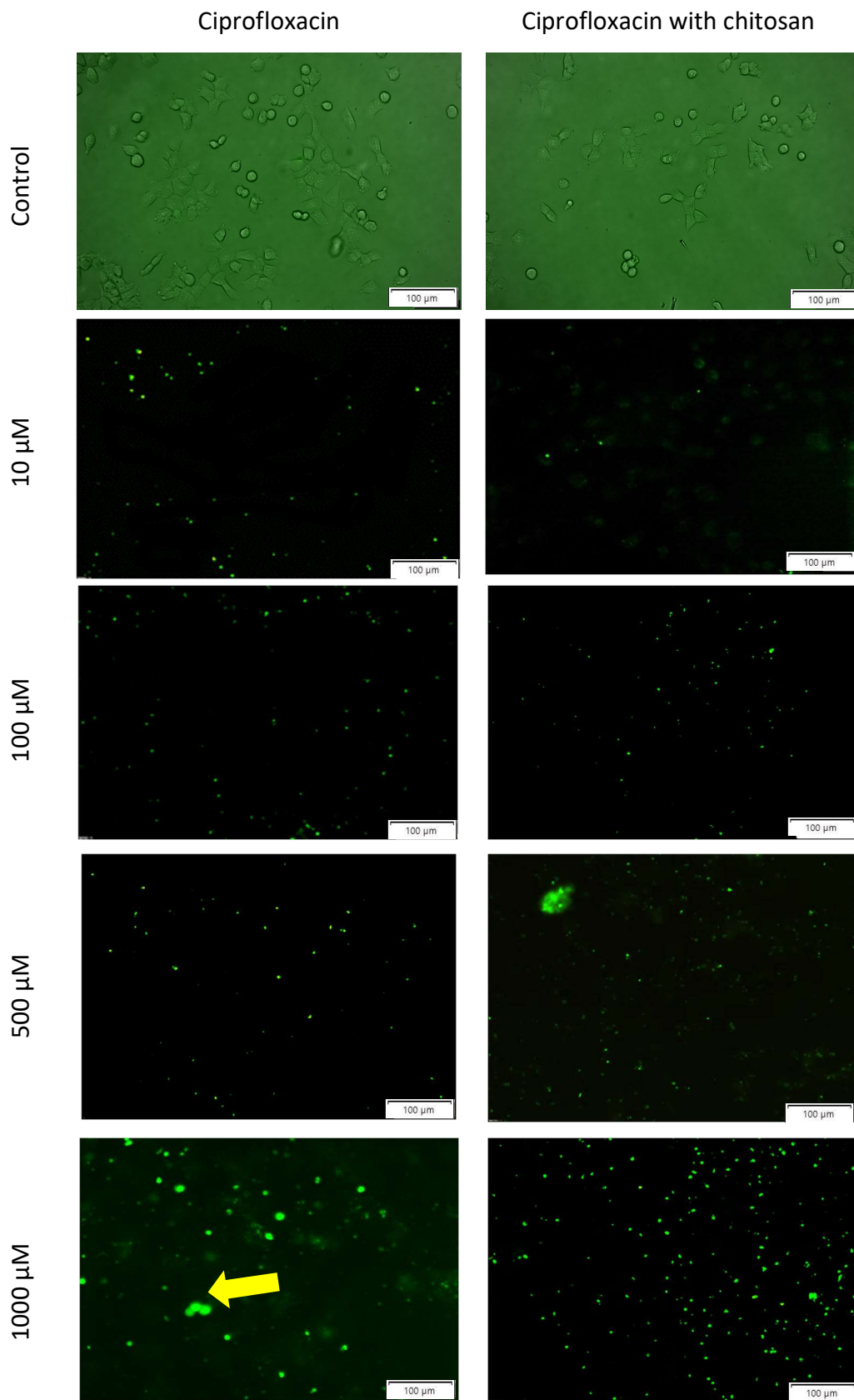


Figure 31. Bladder cancer cells – T24 after 72 hours with chitosan capsules with ciprofloxacin - FITC - cells that promote apoptosis. Arrow marks visible apoptotic cells. Pictures were taken with a fluorescence microscope CKX53 FN Olympus, Japan and a VC90 4K Olympus camera, Japan.

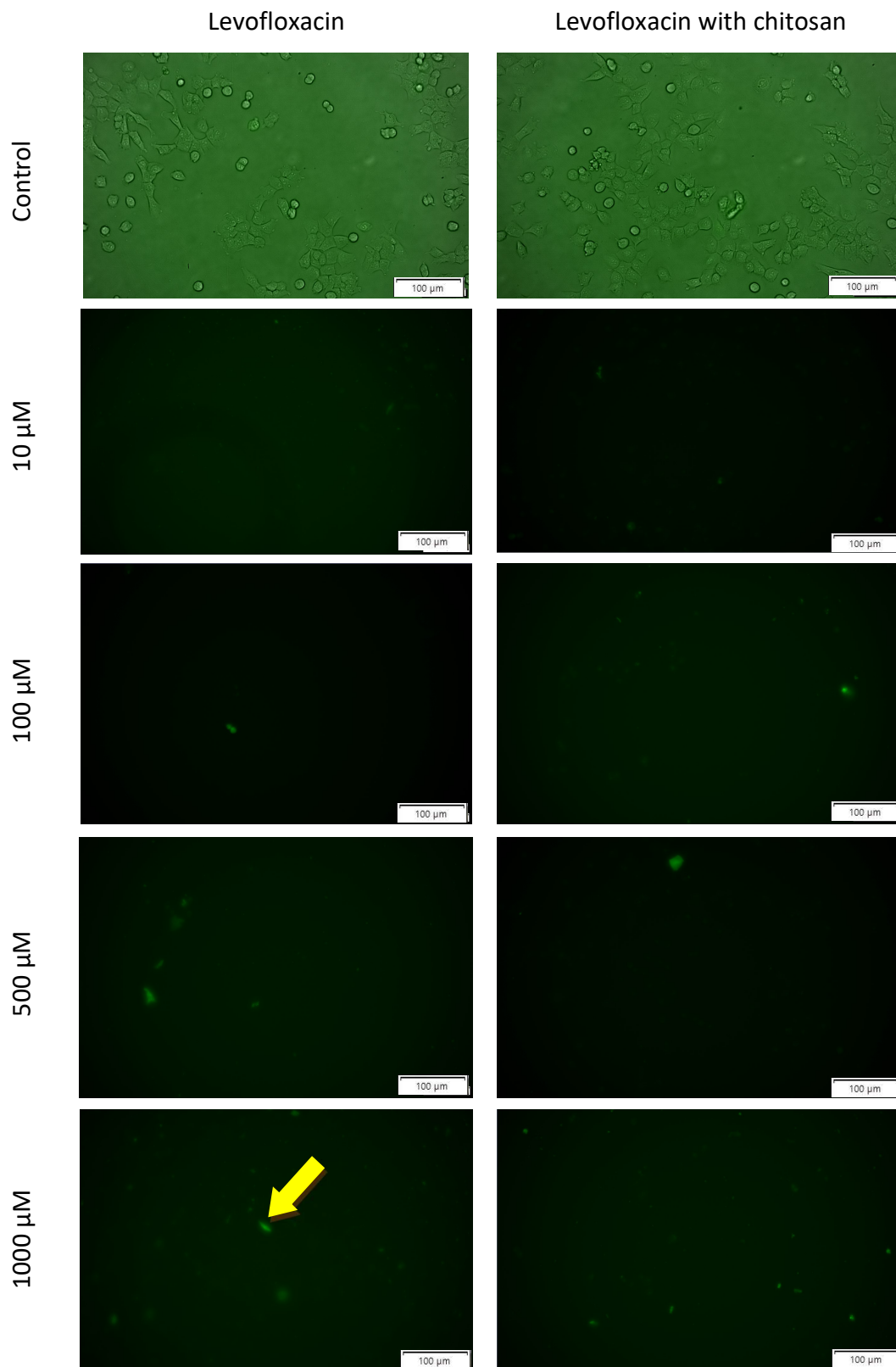


Figure 32. Bladder cancer cells – T24 after 24h with chitosan capsules with levofloxacin - FITC - cells that promote apoptosis. Arrow marks visible apoptotic cells. Pictures were taken with a fluorescence microscope CKX53 FN Olympus, Japan and a VC90 4K Olympus camera, Japan. Control images are shown with the FITC channel and phase contrast overlay to visualize the number of cells.

In relation to the DU145 line, numerous apoptotic cells were visible only at the highest concentration. At lower concentrations, these cells were single. Numerous aggregates of apoptotic cells at a concentration of 1000 μ M of the chitosan-modified drug were visible (Fig. 33). After reaching the desired observation time point (72 hours), it was observed that the activity of caspase-3 and -7 cells treated with the drug combined with chitosan increased several times more compared to control cells and compared to cells treated with the drug without additional components.

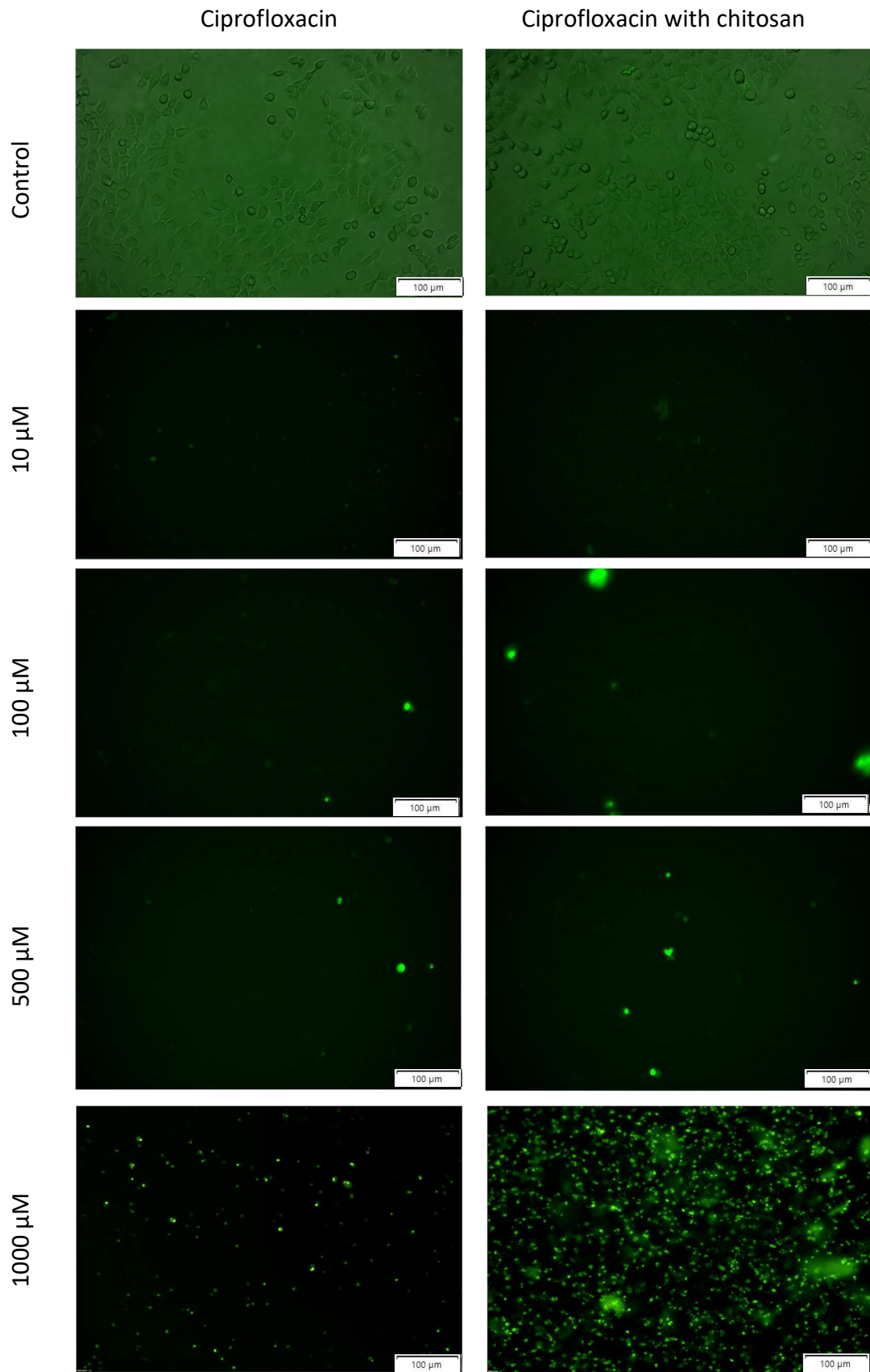


Figure 33. Prostate cancer – DU145 after 24h with chitosan capsules with ciprofloxacin - FITC - cells that promote apoptosis. Pictures were taken with a fluorescence microscope CKX53 FN Olympus, Japan and a VC90 4K Olympus camera, Japan. The trigger cell death mode by ciprofloxacin on DU-145 human prostate cancer cells was detected to be apoptosis. Control images are shown with the FITC channel and phase contrast overlay to visualize the number of cells.

Considering DU145 cells, only single cells undergoing death by apoptosis can be observed. The single apoptotic cells were observed at concentrations of levofloxacin 500 μM and 1000 μM (Fig. 34). In the case of levofloxacin modified at a concentration of 1000 μM , aggregates of several cells undergoing apoptosis were observed.

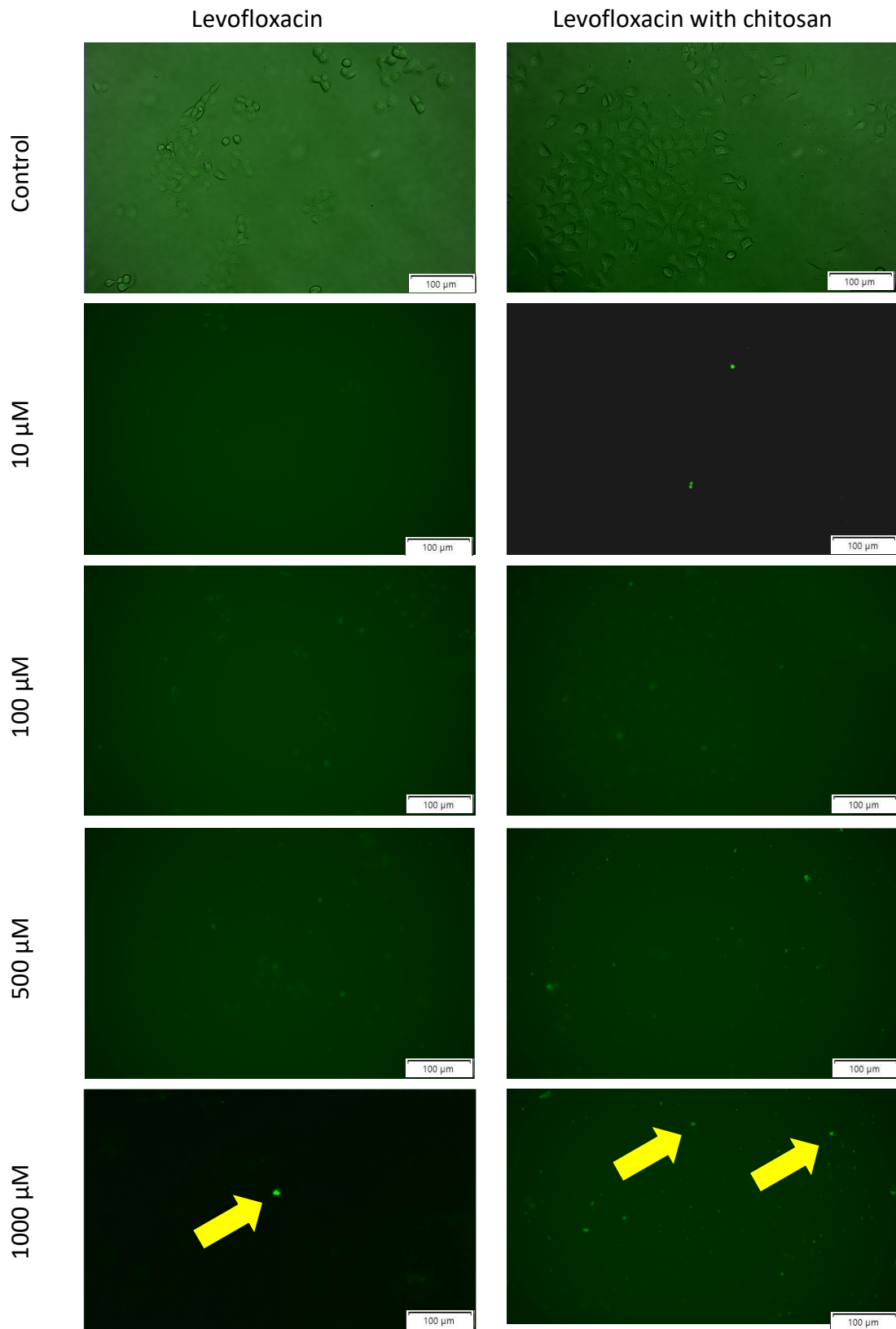


Figure 34. Prostate cancer – DU145 after 24h with chitosan capsules with levofloxacin - FITC - cells that promote apoptosis. Arrows mark visible apoptotic cells. Pictures were taken with a fluorescence microscope CKX53 FN Olympus, Japan and a VC90 4K Olympus camera, Japan. Control images are shown with the FITC channel and phase contrast overlay to visualize the number of cells.

4.2.6. Cell proliferation by thymidine analogue 5-Bromo-2'-deoxyuridine method

Ciprofloxacin at concentrations of 10-1000 μM inhibited the proliferation of T24 cells. The most effective action of ciprofloxacin was observed in 72 hours of the experiment, for a concentration of 1000 μM . In the first 24 hours, a statistically significant inhibition of cell proliferation was caused by ciprofloxacin at a concentration of 500 μM . Comparing ciprofloxacin and modified ciprofloxacin, statistically significant differences in their activity were visible only in 24 hours for the concentration of 100 μM , 500 μM and 1000 μM . At 72 hours, each concentration of both tested compounds caused a significant inhibition of the proliferation rate of the T24 line compared to the control (Fig. 35).

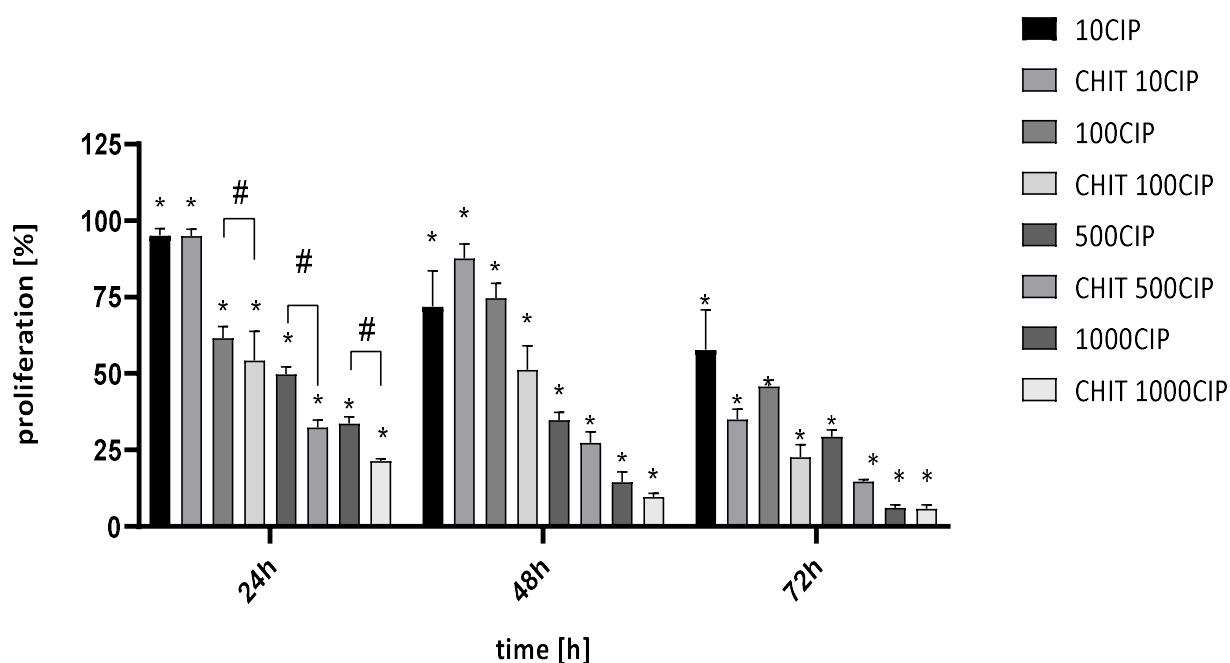


Figure 35. Proliferation of the T24 line in the following days from the start of incubation with the addition of ciprofloxacin and modified ciprofloxacin in the concentration range of 10-1000 μM . "*" - statistical significance in relation to the control; "#" - statistically significant difference between the corresponding concentrations of ciprofloxacin and modified ciprofloxacin ($p < 0.05$).

Moving on to levofloxacin, it was observed that the modification of the drug did not favorably inhibit the proliferation of cancer cells (Fig. 36). The graph shows differences in the case of 72 hours of the experiment for the concentration of 500 μM . It was 41.65% for the drug in the basic form and 54.82% proliferating cells for the drug combined with chitosan. Similar observations, have been seen for concentration 1000 μM , sequentially 26.36% for levofloxacin and 32.46% of proliferation for modified levofloxacin.

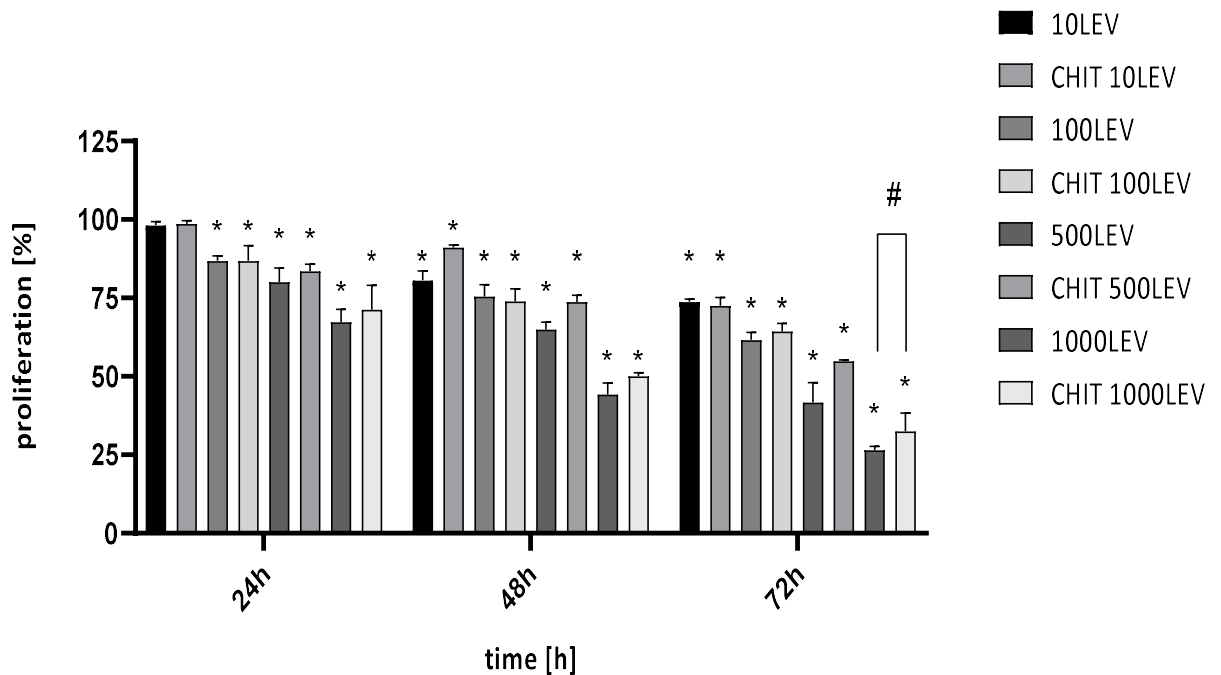


Figure 36. Proliferation of the T24 line in the following days from the start of incubation with the addition of levofloxacin and modified levofloxacin in the concentration range of 10-1000 μM . "*" - statistical significance in relation to the control; "#" - statistically significant difference between the corresponding concentrations of ciprofloxacin and modified ciprofloxacin ($p < 0.05$).

The results of the BrdU test indicated that ciprofloxacin at a concentration of 100-1000 μM reduced the potential of cells to proliferate (Fig. 37). A statistically significant difference in the effect of both chemotherapeutics was observed at 24 hours for a concentration of 100 μM and 1000 μM , where ciprofloxacin was definitely more effective in inhibiting cell proliferation (74.67% and 34.72% of cells' proliferation).

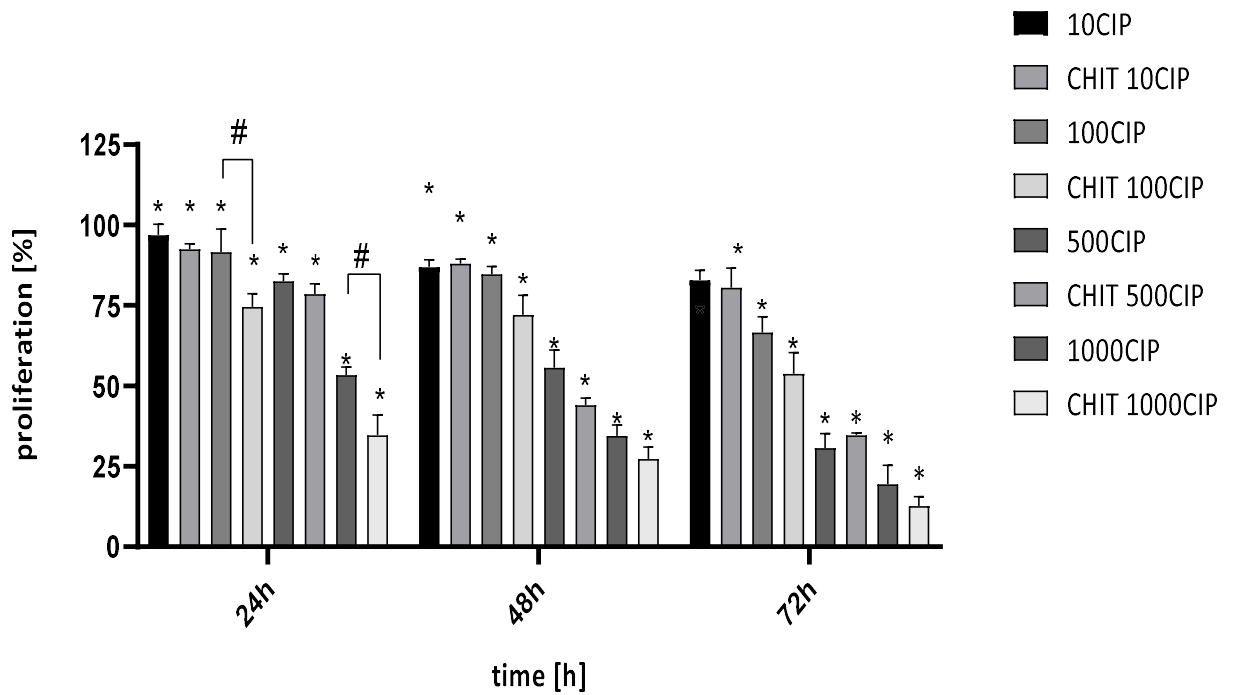


Figure 37. Proliferation of the DU145 line in the following days from the start of incubation with the addition of ciprofloxacin and modified ciprofloxacin in the concentration range of 10-1000 μM . "*" - statistical significance in relation to the control; "#" - statistically significant difference between the corresponding concentrations of ciprofloxacin and modified ciprofloxacin ($p < 0.05$).

The mechanism underlying the antiproliferative activity of LEV has not been elucidated, but the results of the BrdU test indicated that levofloxacin concentrations reduce the potential of cells to proliferate. Statistically significant differences were observed for both forms of levofloxacin at concentrations from 100 to 1000 μM for 72 hours of the study. Despite the differences in the inhibition of proliferation, the differences for individual concentrations were not statistically significant between the two forms of the drug (Fig. 38).

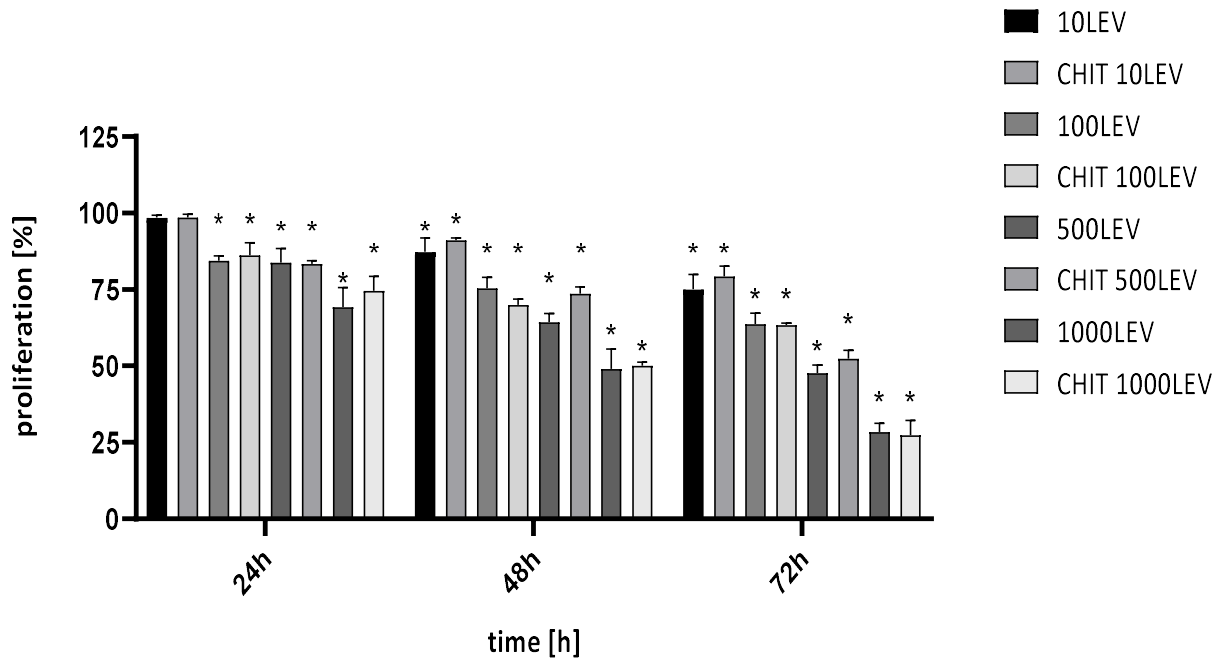


Figure 38. Proliferation of the DU145 line in the following days from the start of incubation with the addition of levofloxacin and modified levofloxacin in the concentration range of 10-1000 μM . "*" - statistical significance in relation to the control; "#" - statistically significant difference between the corresponding concentrations of levofloxacin and modified levofloxacin ($p < 0.05$).

4.2.7. pH of the cell culture medium measurement

Yellowing of phenol red in culture media was pronounced in control wells cells. Chronically CIP-exposed T24 cells alkalized the surrounding culture media in a dose-dependent manner (Tab. 6). At 24 hours no significant difference was observed for the lowest concentrations of ciprofloxacin and modified ciprofloxacin.

Table 6. Ciprofloxacin and modified ciprofloxacin-induced media pH shifts following 3-days exposure, in T24 cells. pH shifts recorded in CIP-supplemented (0–1000 μ M) culture media, following overnight exposure, subsequent to 3-day treatment; mean \pm SD., n=3.

	pH	24h	48h	72h
control		7.84 \pm 0.0173	7.83 \pm 0.0374	7.79 \pm 0.0093
10 μ M CIP		8.03 \pm 0.0783	8.02 \pm 0.0536	8.02 \pm 0.0312
100 μ M CIP		8.16 \pm 0.0057	8.17 \pm 0.0019	8.17 \pm 0.0792
500 μ M CIP		8.37 \pm 0.0503	8.36 \pm 0.0098	8.36 \pm 0.0028
1000 μ M CIP		8.46 \pm 0.0124	8.45 \pm 0.0797	8.44 \pm 0.0678

	pH	24h	48h	72h
Control CHIT		7.96 \pm 0.0659	7.92 \pm 0.0830	7.98 \pm 0.0389
10 μ M CIP CHIT		7.83 \pm 0.0384	7.82 \pm 0.0029	7.82 \pm 0.0087
100 μ M CIP CHIT		8.03 \pm 0.0930	8.02 \pm 0.0638	8.01 \pm 0.0038
500 μ M CIP CHIT		8.33 \pm 0.0083	8.34 \pm 0.0830	8.34 \pm 0.0949
1000 μ M CIP CHIT		8.47 \pm 0.0039	8.46 \pm 0.0928	8.46 \pm 0.0837

An increase in the pH value of the medium depending on time and the concentration of the tested drug was detected. For samples with the content of chitosan, greater alkalinity of the culture medium was observed (Tab. 7).

Table 7. Levofloxacin and modified levofloxacin-induced media pH shifts following 3-days exposure, in T24 cells. pH shifts recorded in LEV-supplemented (0–1000 μ M) culture media, following overnight exposure, subsequent to 3-day treatment; mean \pm SD., n=3.

	pH	24h	48h	72h
Control		7.83 \pm 0.0028	7.82 \pm 0.0328	7.80 \pm 0.0304
10 μ M LEV		7.59 \pm 0.0054	7.58 \pm 0.0289	7.57 \pm 0.0292
100 μ M LEV		7.69 \pm 0.0837	7.68 \pm 0.0029	7.65 \pm 0.0294
500 μ M LEV		8.08 \pm 0.0249	8.07 \pm 0.0024	8.08 \pm 0.0029
1000 μ M LEV		8.37 \pm 0.0503	8.36 \pm 0.0098	8.36 \pm 0.0028

	pH	24h	48h	72h
Control CHIT		7.57 \pm 0.0839	7.53 \pm 0.0394	7.60 \pm 0.0029
10 μ M LEV CHIT		7.96 \pm 0.0659	7.92 \pm 0.0830	7.94 \pm 0.0389
100 μ M LEV CHIT		8.03 \pm 0.0239	8.05 \pm 0.0632	8.06 \pm 0.0384
500 μ M LEV CHIT		8.01 \pm 0.0033	8.03 \pm 0.0304	8.05 \pm 0.0029
1000 μ M LEV CHIT		8.35 \pm 0.0193	8.40 \pm 0.0892	8.41 \pm 0.0084

By observing the changes in the DU145 line, an increase in the pH value was also observed for samples containing chitosan for both ciprofloxacin and levofloxacin. The increase in pH was greater with ciprofloxacin than levofloxacin compared to the control (Tab. 8, 9).

Table 8. Ciprofloxacin and modified ciprofloxacin-induced media pH shifts following 3-days exposure, in DU-145 cells. pH shifts recorded in CIP-supplemented (0–1000 μ M) culture media, following overnight exposure, subsequent to 3-day treatment; mean \pm SD., n=3.

	pH	24h	48h	72h
Control		7.95 \pm 0.0374	7.94 \pm 0.0320	7.92 \pm 0.0340
10 μ M CIP		7.94 \pm 0.0493	7.89 \pm 0.0029	7.88 \pm 0.0029
100 μ M CIP		7.95 \pm 0.0394	7.97 \pm 0.0235	7.98 \pm 0.0534
500 μ M CIP		7.66 \pm 0.0093	7.65 \pm 0.0038	7.60 \pm 0.0094
1000 μ M CIP		8.01 \pm 0.0034	8.00 \pm 0.0739	8.05 \pm 0.0649

	pH	24h	48h	72h
Control CHIT		7.95 \pm 0.9359	7.96 \pm 0.0833	7.97 \pm 0.0435
10 μ M CIP CHIT		7.59 \pm 0.0384	7.58 \pm 0.0022	7.91 \pm 0.0098
100 μ M CIP CHIT		7.93 \pm 0.0029	7.95 \pm 0.0695	7.97 \pm 0.0038
500 μ M CIP CHIT		7.90 \pm 0.0339	7.93 \pm 0.0948	7.94 \pm 0.0534
1000 μ M CIP CHIT		7.64 \pm 0.0209	7.63 \pm 0.0890	7.60 \pm 0.0859

Table 9. Levofloxacin and modified levofloxacin-induced media pH shifts following 3-days exposure, in DU-145 cells. pH shifts recorded in LEV-supplemented (0–1000 μ M) culture media, following overnight exposure, subsequent to 3-day treatment; mean \pm SD., n=3.

pH	24h	48h	72h
Control	7.68 \pm 0.0384	7.64 \pm 0.0430	7.71 \pm 0.0782
10 μ M LEV	7.77 \pm 0.0804	7.76 \pm 0.0345	7.75 \pm 0.0284
100 μ M LEV	7.90 \pm 0.0034	7.89 \pm 0.0384	7.88 \pm 0.0084
500 μ M LEV	7.92 \pm 0.0384	7.94 \pm 0.0938	7.96 \pm 0.0022
1000 μ M LEV	8.02 \pm 0.0098	8.05 \pm 0.0039	8.08 \pm 0.0394

pH	24h	48h	72h
Control	7.68 \pm 0.0384	7.64 \pm 0.0430	7.71 \pm 0.0782
10 μ M LEV CHIT	7.77 \pm 0.0804	7.76 \pm 0.0345	7.75 \pm 0.0284
100 μ M LEV CHIT	7.90 \pm 0.0034	7.89 \pm 0.0384	7.88 \pm 0.0084
500 μ M LEV CHIT	7.92 \pm 0.0384	7.94 \pm 0.0938	7.96 \pm 0.0022
1000 μ M LEV CHIT	8.02 \pm 0.0098	8.05 \pm 0.0039	8.08 \pm 0.0394

4.3. *Picea abies* tree extract drugs modification – adherent cell culture

4.3.1. Biologically active compounds characterization

By applying the Folin–Ciocalteu method, it was reported that the average concentrations of total phenolics in the needles of different ages and damage classes were between 58 and 81 mg in 1 g of needles frozen in liquid nitrogen. Moreover, there were no significant differences found in the concentrations of phenolics in needles from trees of different damage classifications. Electrospray mass spectra analysis (ESI-MS) showed that the obtained extracts are mixtures of various types of phenolic compounds. Based on the identification of fragment ions and their corresponding molecular weights, four different phenolic compounds were identified. The dominant one was luteolin, a natural flavonoid compound that has been shown to have anticancer properties against various types of cancer. In addition to it, high content was also shown for Pilloin, o-Vanillin or Quinic acid.

In the evaluation of the effect of the *Picea abies* tree, a series of optimization studies were performed to select the best concentration of drug modification with the spruce extract. Tests were performed on both tumor cell lines (T24 and DU145) and normal SV-HUC-1 epithelial cells line. Concentrations in the range of 0.1%, 0.5%, 1%, 5%, 10%, 15%, 20%, 30%, 40%, 50% were tested. After the analysis of the results, the concentration of 5% was selected for further studies.

4.3.1. Assessment of cell viability in a microscope with inverted optics

Morphological changes in bladder cell lines, including shrinkage, rounding and detachment of cells, were evident after treatment with ciprofloxacin, especially at higher concentrations (Fig. 39). Seventy-two-hour incubation of T24 with a low concentration of ciprofloxacin (100 μM) led to cell shrinkage and separation. At higher concentrations of ciprofloxacin, also with the addition of plant extract (500 μM and 1000 μM), only a small number of cells remained attached. In the case of the addition of the extract, numerous granules were visible in the morphology of the cells, which were not visible in the basic form of the drug.

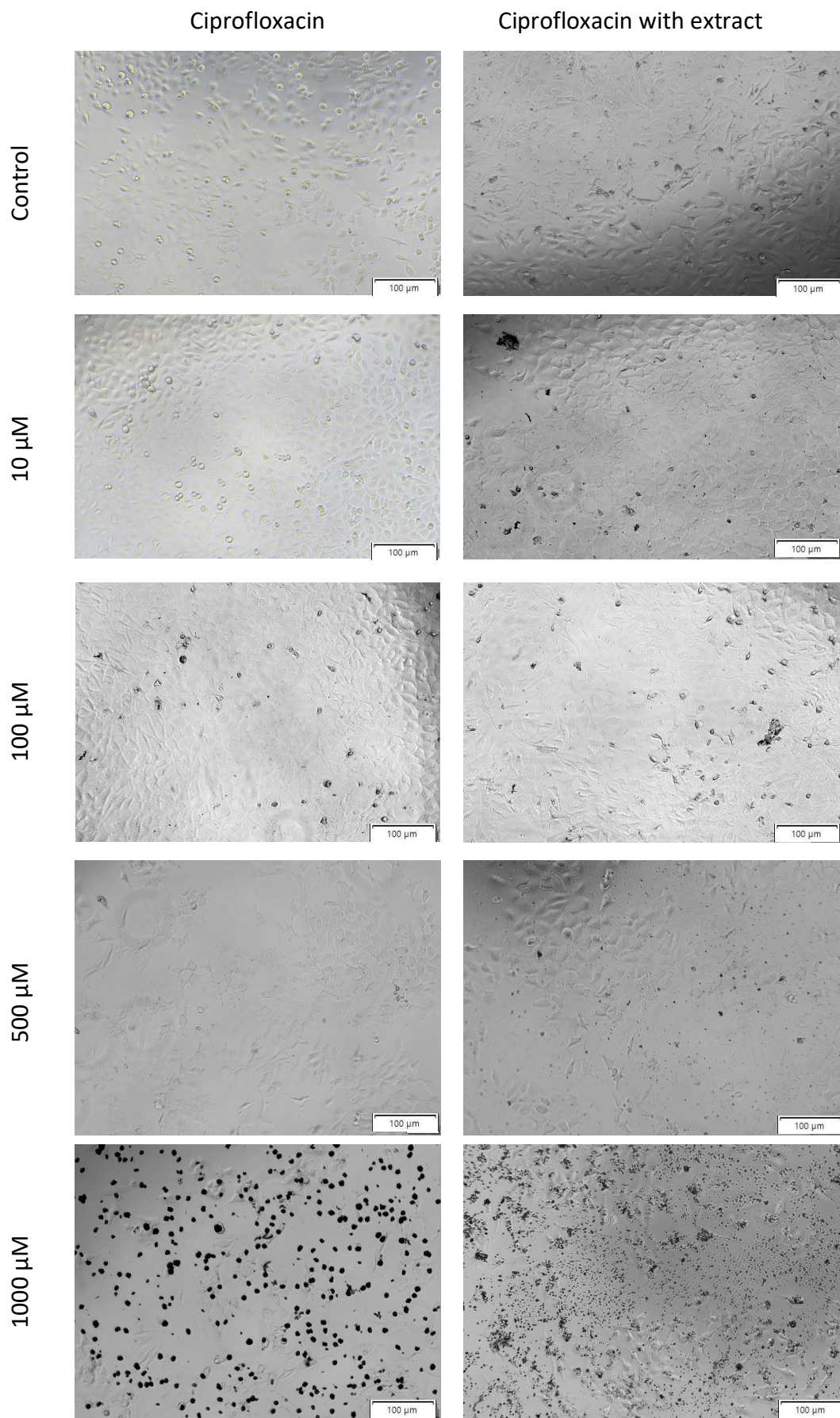


Figure 39. T24 cells at 72 hours of cultivation in the presence of: culture medium, ciprofloxacin and ciprofloxacin modified with natural extract at concentrations of 10, 100, 500, 1000 μM .

Morphological changes in the bladder cancer cell line were also observed after treatment with levofloxacin (Fig. 40), especially at higher concentrations. Shrinking, rounding and separating of the cells was seen, leading to a decrease in the number of cells as the concentration of the drug increased. Changes in cell morphology were visible in the case of T24 tumor cells, in which detachment and a change in shape to a more rounded one was observed already at a concentration of 100 μ M, especially after 72 h of incubation. Morphometric analysis showed no changes in the cell area at lower drug concentrations compared to the control. A reduction in cell surface area was observed at higher drug concentrations.

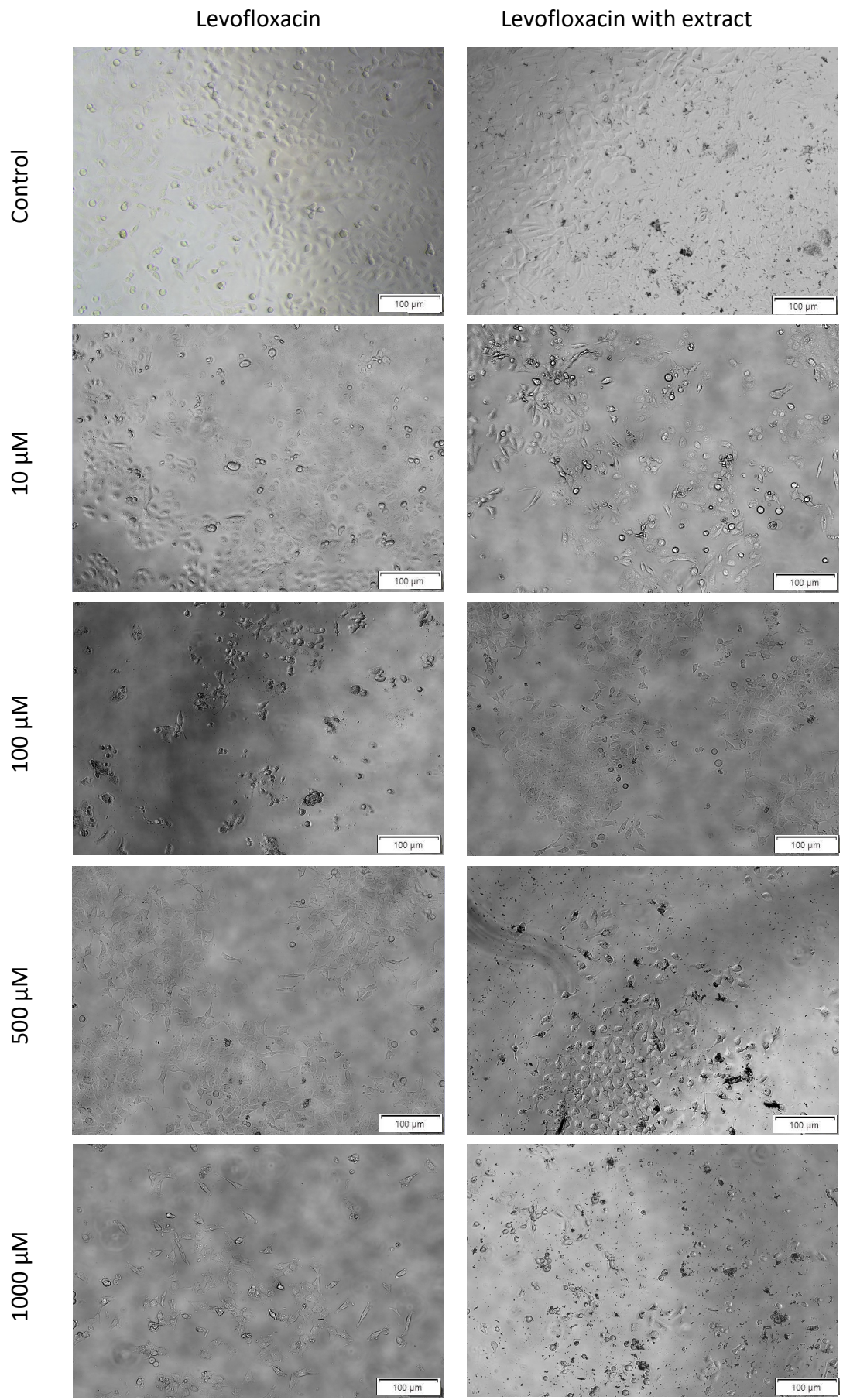


Figure 40. T24 cells at 72 hours of cultivation in the presence of: culture medium, levofloxacin and levofloxacin modified with natural extract at concentrations of 10, 100, 500, 1000 μM .

Single crystals of ciprofloxacin began to appear in the culture at the concentration of 500 μM and more abundant at the highest concentration (1000 μM). Morphometric analysis showed no changes in the cell area in most cases at lower drug concentrations compared to the control. A reduction in cell surface area was observed at higher drug concentrations (Fig. 41).

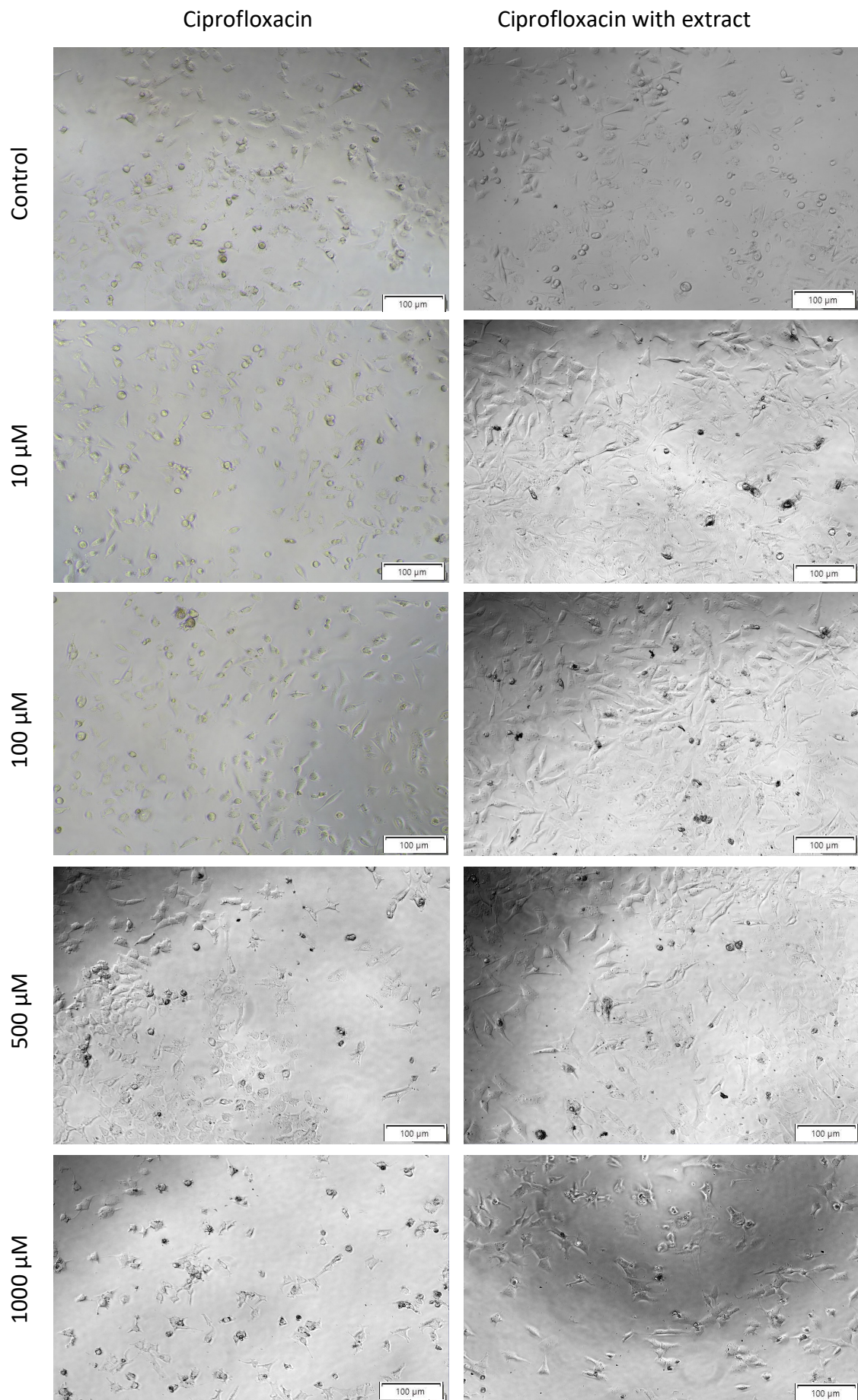


Figure 41. DU145 cells at 72 hours of cultivation in the presence of: culture medium, ciprofloxacin and ciprofloxacin modified with natural extract at concentrations of 10, 100, 500, 1000 μM .

Prostate cell lines after treatment with ciprofloxacin were characterized by significant elongation, change in shape, loss of integrity with the culture medium. Morphometric analysis showed no changes in the cell area in most cases at lower drug concentrations compared to the control. A reduction in cell surface area was observed at higher drug concentrations (Fig. 42).

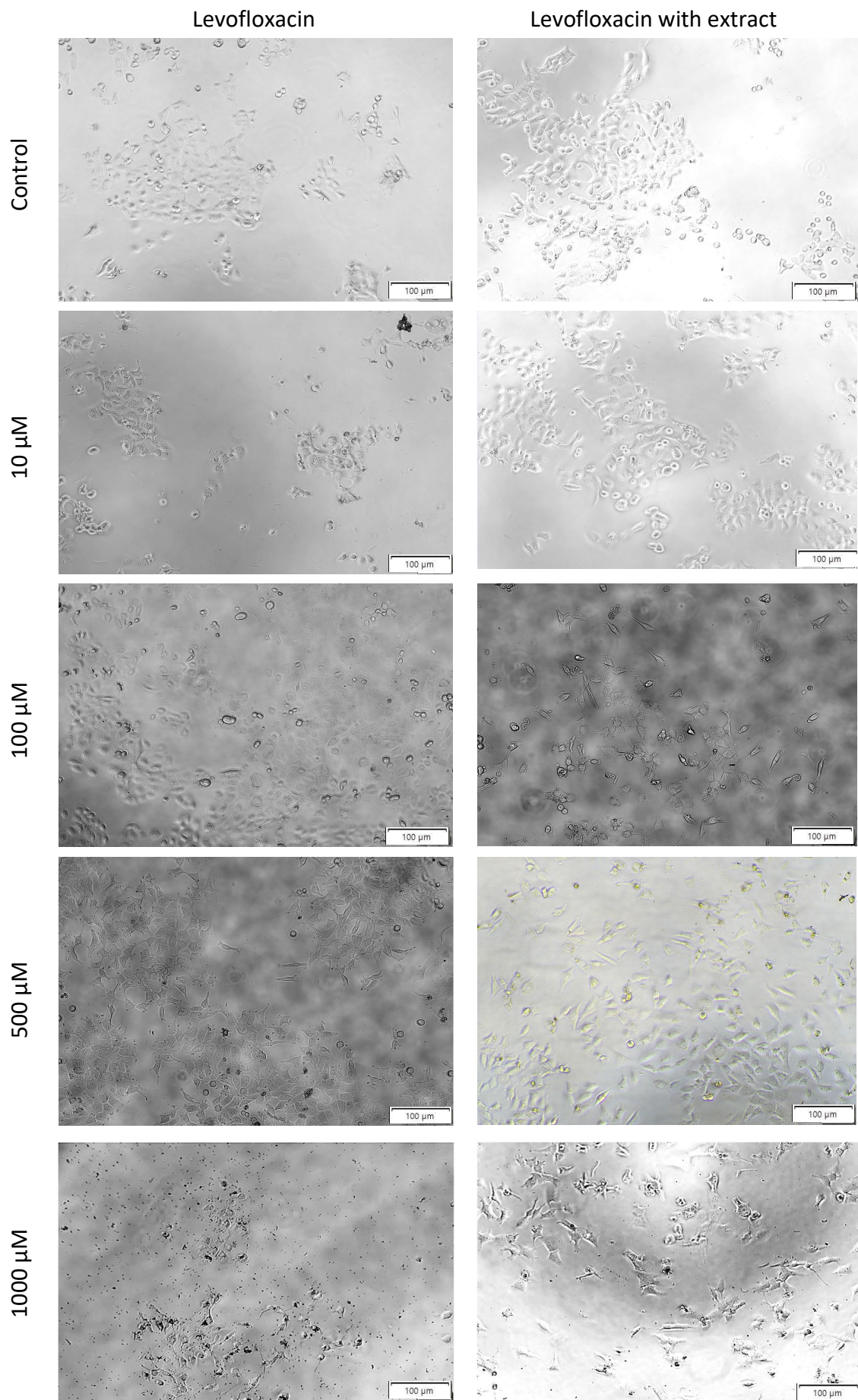


Figure 42. DU145 cells at 72 hours of cultivation in the presence of: culture medium, levofloxacin and levofloxacin modified with natural extract at concentrations of 10, 100, 500, 1000 μM .

4.4.2. Live/Dead Assay

The LIVE/DEAD Cell Imaging Assay distinguishes viable commercial T24 cells by the presence of ubiquitous intracellular esterase activity as determined by the enzymatic conversion of the virtually non-fluorescent cell permeable calcein AM to intensely fluorescent calcein which was well retained in viable cells. Propidium iodide (stained red) was impermeable to cells and therefore enters cells only with damaged membranes. In dying and dead cells, bright red fluorescence is generated when bound to DNA. Background fluorescence levels are inherently low in this test technique as the dyes hardly fluoresce before interacting with cells.

By assessing the percentage ratio of live and dead cells in the tested samples of bladder cancer cells (Fig. 43A) statistically significant differences in the case of incubation of cells with ciprofloxacin and the drug with the addition of the extract were noticeable. The percentage of dead cells was 30.52%, while after adding 5% of the extract, this number increased by more than 25%. This is clearly noticeable in the visualization of the cells, where large aggregates of red-stained cells were visible at the highest concentration (Fig. 44). In the case of levofloxacin, no significant differences in the ratio of live to dead cells after the use of an additional extract was noticed (Fig. 43B, Fig. 45).

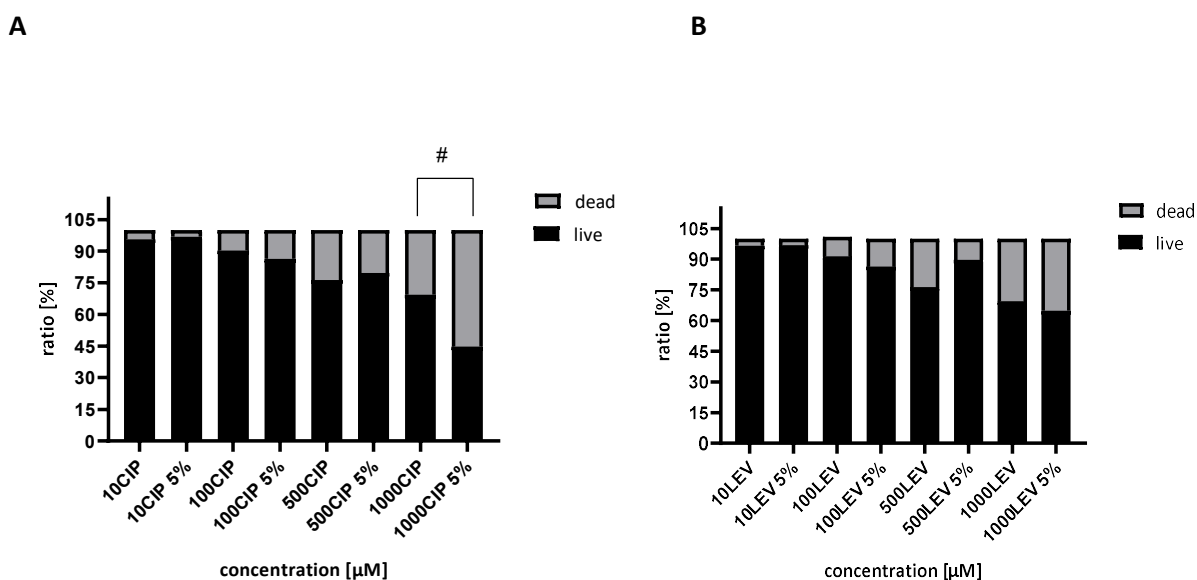


Figure 43. Percentage of live and dead cells T24 cell line cultured in medium containing test drugs ciprofloxacin (A) and levofloxacin (B). Viable and dead cell concentrations were determined using calcein-AM and PI dyes. A minimum of three samples and were counted for each condition percentage of cells is reported as mean \pm SD.

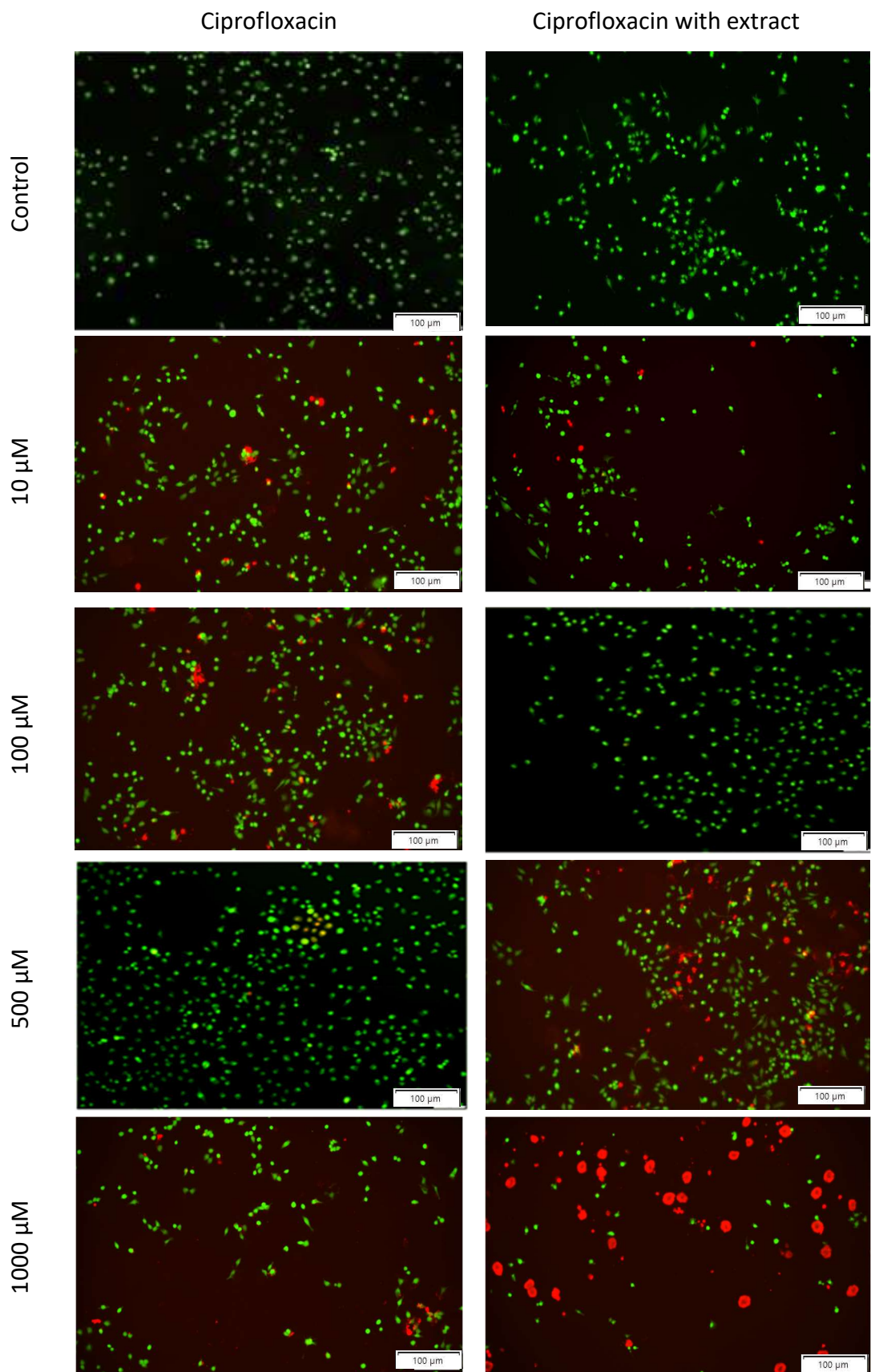


Figure 44. Microscopic images demonstrating how T24 culture conditions influence the visibility of dead cells detected using the fluorescent live/dead assay kit. Cell death was induced by chemotherapeutic agent - ciprofloxacin and ciprofloxacin with natural extract.

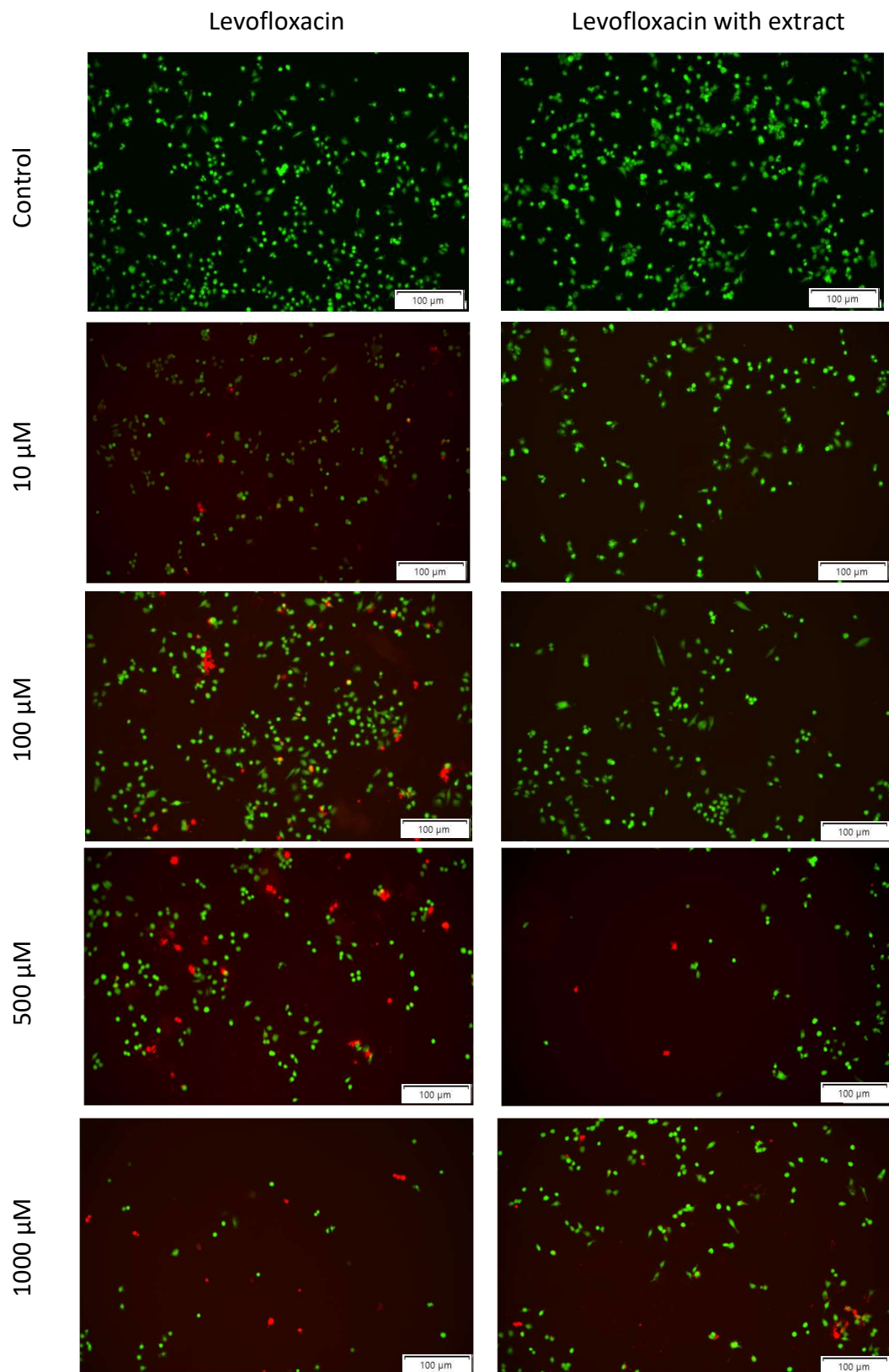


Figure 45. Microscopic images demonstrating how T24 culture conditions influence the visibility of dead cells detected using the fluorescent live/dead assay kit after incubation with levofloxacin.

In the case of DU145 cell lines, the addition of tree extract significantly affected the highest concentration of ciprofloxacin (Fig. 46A), which was also clearly noticeable in the microscopic image (Fig. 47). It was also seen that all ciprofloxacin concentrations tested led to a significant effect changes in the ratio of live/dead cells after 24 hours of incubation, and this ratio changed with increasing drug concentration. However, in the case of levofloxacin, these differences were not noticeable even for the highest concentration of the drug (Fig. 46B, Fig. 48), and the mixture with the extract did not significantly increased the percentage of dead cells.

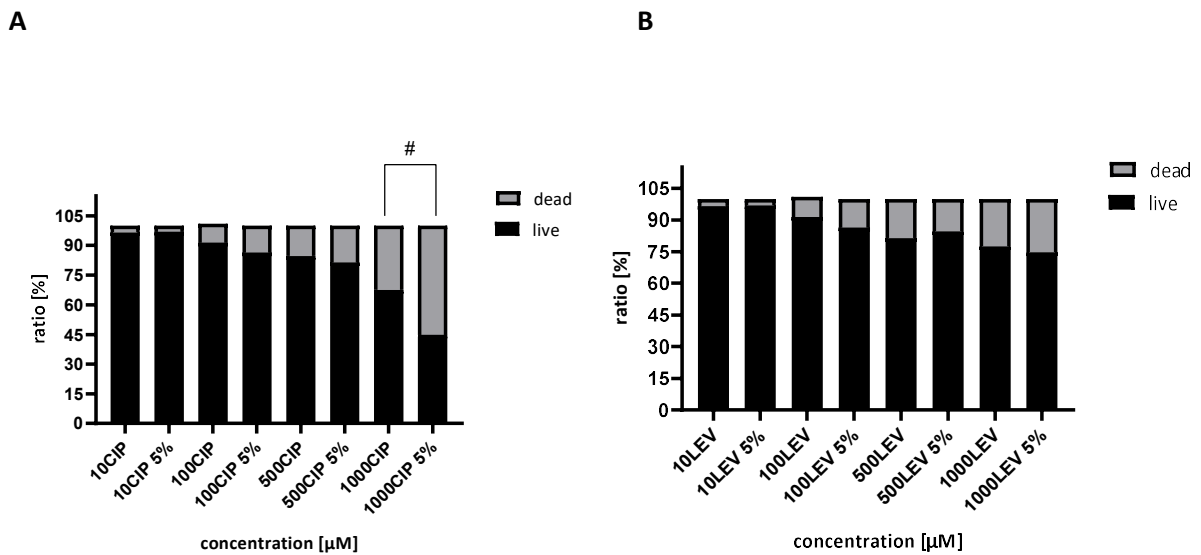


Figure 46. Percentage of live and dead cells DU145 cell line cultured in medium containing test drugs ciprofloxacin (A) and levofloxacin (B). A minimum of three samples and were counted for each condition percentage of cells is reported as mean \pm SD.

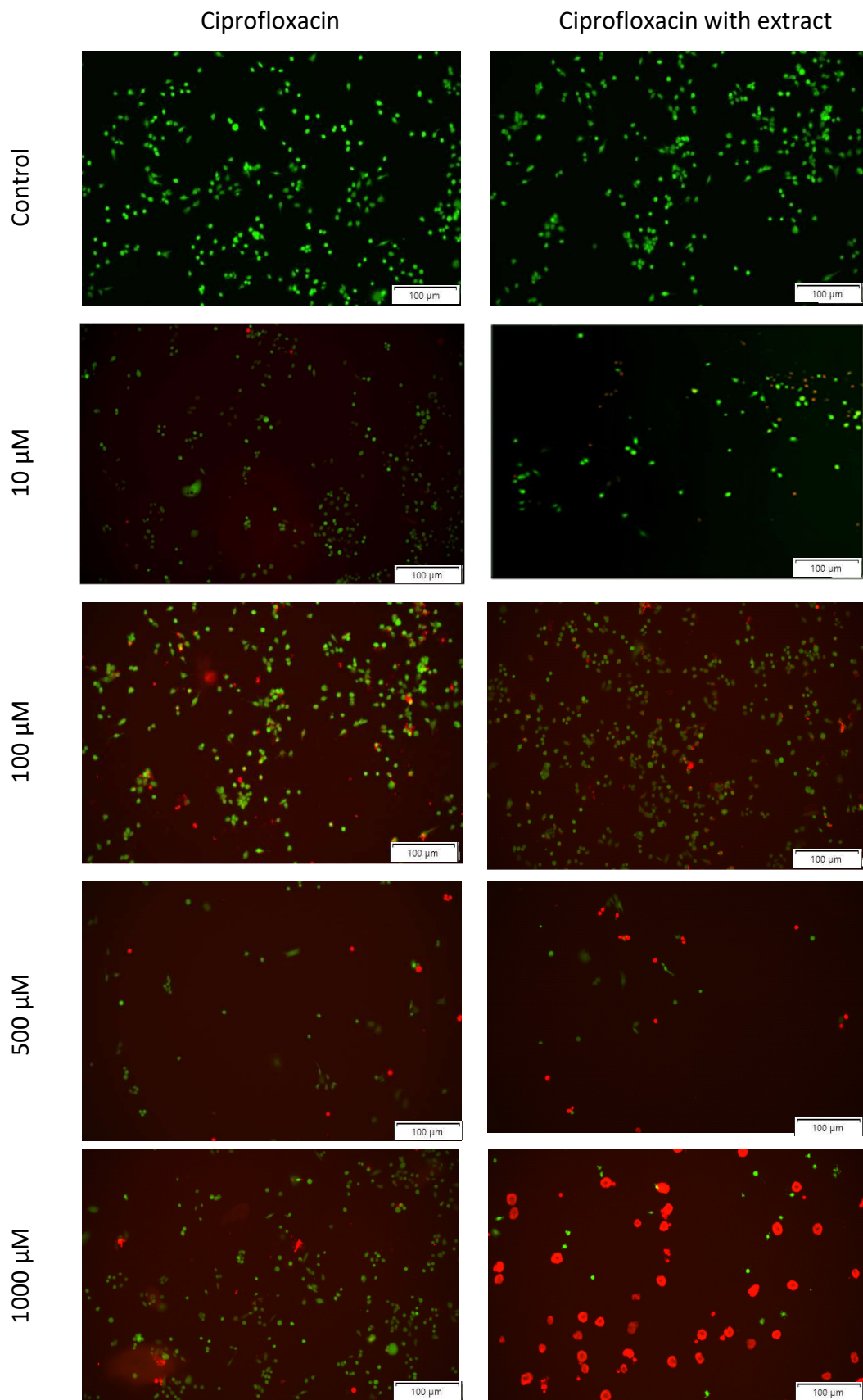


Figure 47. Microscopic images demonstrating how DU145 culture conditions influence the visibility of dead cells detected using the fluorescent live/dead assay kit after incubation with ciprofloxacin.

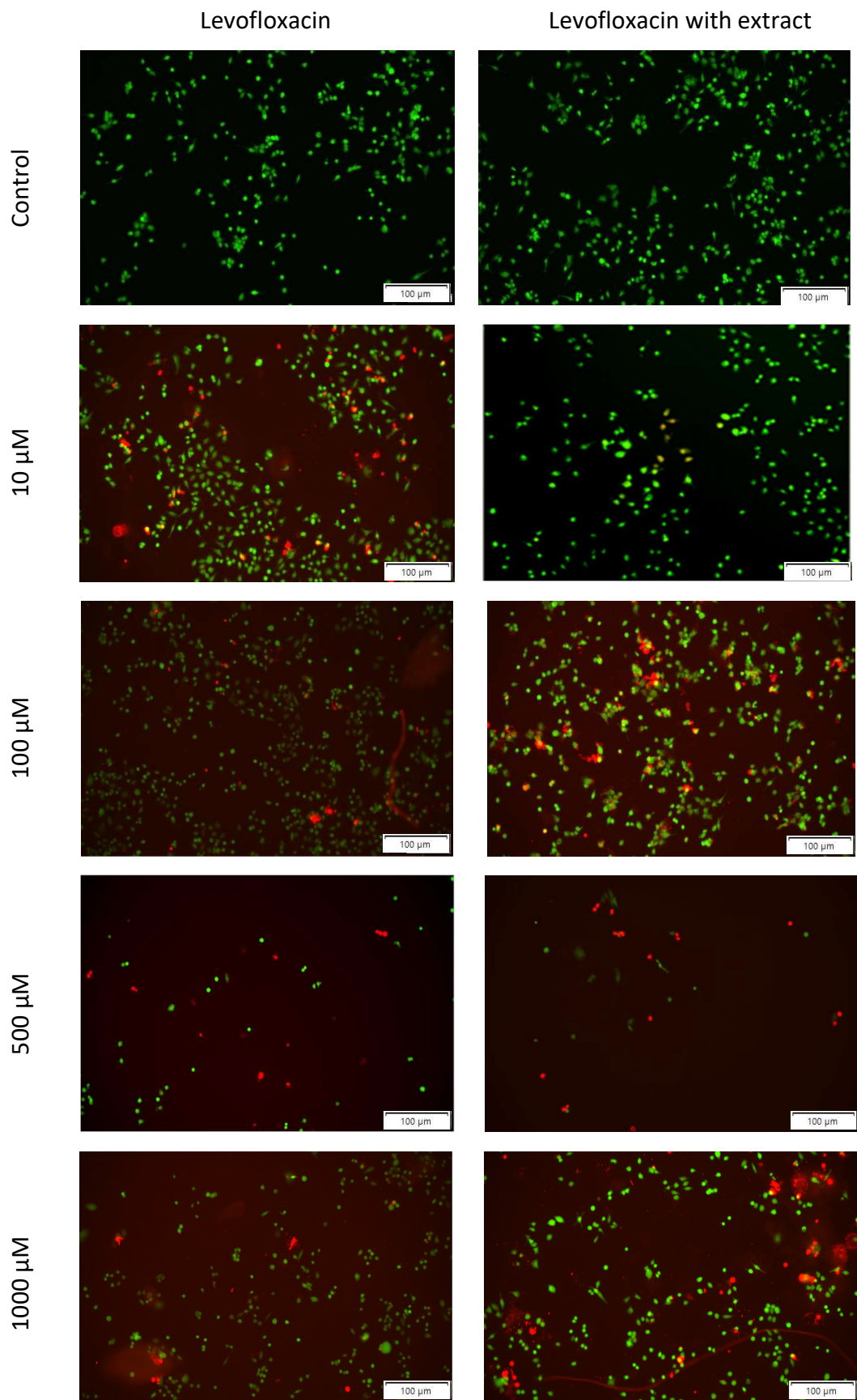


Figure 48. Microscopic images demonstrating how DU145 culture conditions influence the visibility of dead cells detected using the fluorescent live/dead assay kit after incubation with levofloxacin.

4.4.3. Cell viability assessment by thiazolyl blue tetrazolium bromide assay (MTT)

Statistically significant ($p < 0.05$) changes in the metabolic activity of T24 cells after 24 hours with ciprofloxacin and ciprofloxacin modified with 5% extract, comparing the same drug concentrations, were noticeable for following concentrations: 500 μM ciprofloxacin - 52.09% and 500 μM with extract - 29.03%, and 1000 μM - 33.68% and 1000 μM with extract - 29.39% viability. After 48 h, statistically significant changes between the studied groups were observed for 1000 μM ciprofloxacin - 27.87% CIP and 1000 μM with extract - 9.76% of viability (Fig. 49). In relation to the T24 line, the results of the experiment showed a very strong cytotoxic effect of both ciprofloxacin and the modified ciprofloxacin. Each concentration caused a statistically significant decrease in cell viability compared to controls.

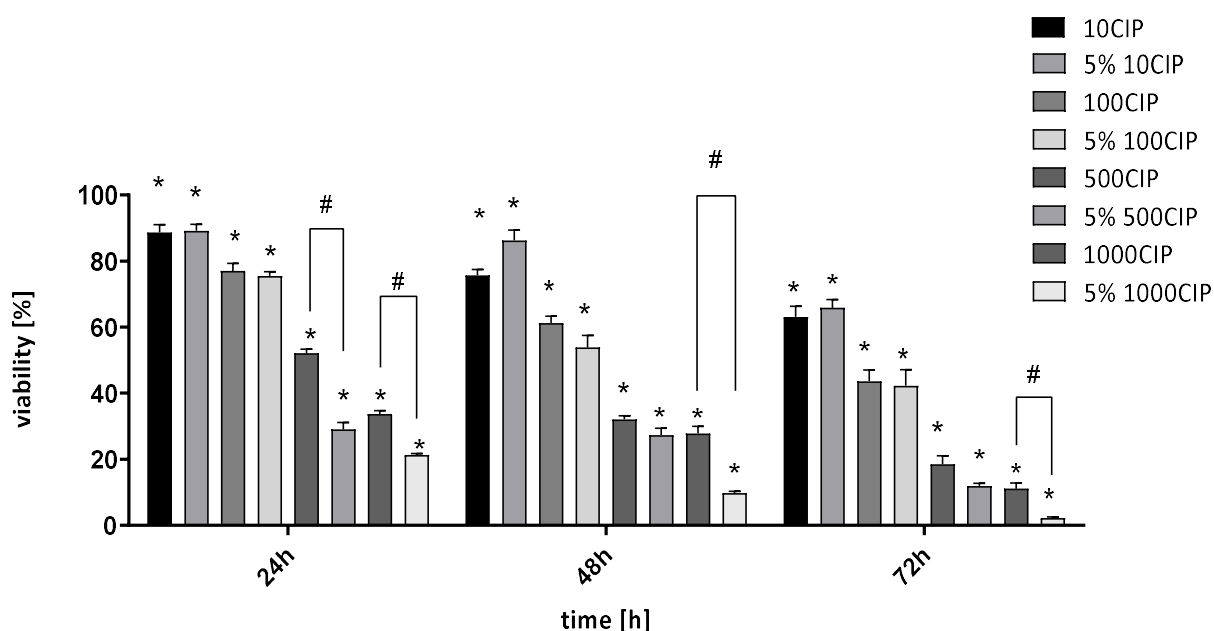


Figure 49. The results of the MTT test for the T24 line on the following days from the start of incubation with the addition of ciprofloxacin and ciprofloxacin modified natural extract from the 10-1000 μM concentration range. "*" - statistical significance in relation to the control; "#" - a statistically significant difference between the corresponding concentrations of ciprofloxacin and modified ciprofloxacin ($p < 0.05$). Bars represent standard deviation.

The metabolic activity of T24 cells was significantly changed by incubation with the levofloxacin solutions tested (Fig. 50). After only 24 hours of incubation, all samples, except for the lowest concentration, exposed to the drug significantly differed from the control. The lowest survival rate at 72 hours of incubation was observed for the 1000 μ M levofloxacin solution with the addition of 5% plant extract solution (18.56%). For 24 and 48 hours of incubation, a statistically significant difference in the cytotoxic effect of levofloxacin was observed when comparing both forms of the drug.

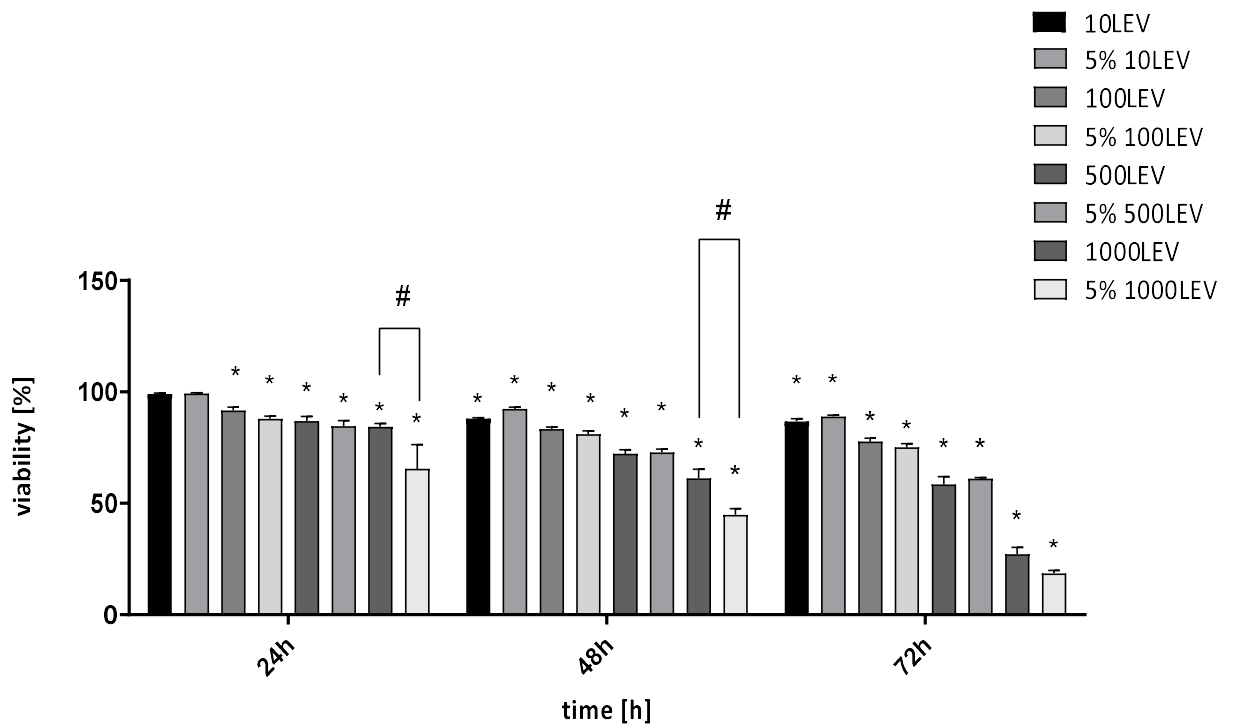


Figure 50. The results of the MTT test for the T24 line on the following days from the start of incubation with the addition of levofloxacin and levofloxacin modified natural extract from the 10-1000 μ M concentration range. "*" - statistical significance in relation to the control; "#" - a statistically significant difference between the corresponding concentrations ($p < 0.05$). Bars represent standard deviation.

Assessment of the effect of ciprofloxacin on the metabolic activity of prostate cancer cells showed significant decrease in cell survival after exposure to the tested solutions (Fig. 51). The 24-hour exposure led to a statistically significant decrease in cell survival for 100 μM (78.3%) and 100 μM EX 5% (78.74%), which showed no significant differences in the effect of the extract for the first hours of incubation. Similar observations can be seen for the concentration of CIP500 (54.98%) CIP500 EX 5% (64.91%) and for the concentration of CIP1000 (27.58%) and CIP1000 EX 5% (26.39%). Interestingly, in the 72nd hour of the experiment, was observed, that the addition of the extract to a lower concentration of ciprofloxacin, results in similar cell survival values for the concentration of 10 μM (62.43%) and 100 μM (62.36%). At 72 hours of incubation, survival of ciprofloxacin-treated cells was still significantly lower than that of the control.

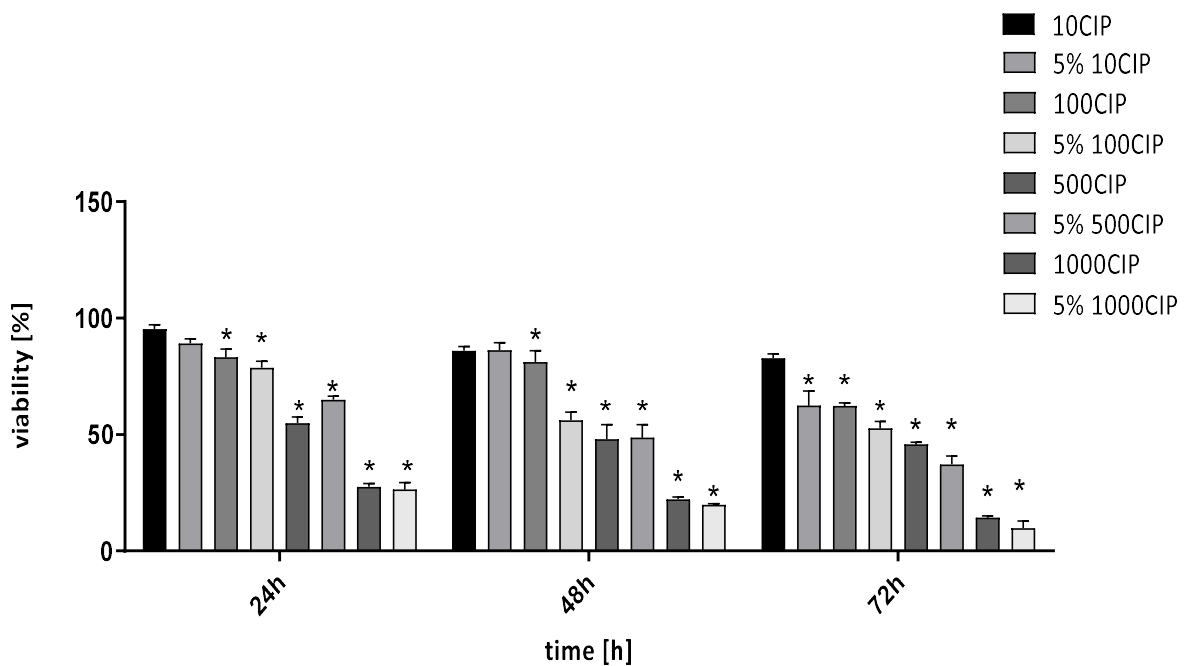


Figure 51. MTT test results for DU145 exposed to the ciprofloxacin concentrations tested. The graph shows the average [%] of survival and the standard deviations based on it on the metabolic activity of the cells relative to the control at a given time. Results significantly statistically different from controls are marked with "*". "#" - a statistically significant difference between the corresponding drugs' concentrations ($p < 0.05$). Bars represent standard deviation.

The study of the metabolic activity of DU145 cells treated with levofloxacin showed a time- and dose-dependent cytotoxic nature of this drug (Fig. 52). The lowest survival rate at 72 hours of incubation was recorded for LEV1000 EX 5% (11.90%) and mortality decreased over time, still maintaining this drug concentration as the most cytotoxic. Differences between levofloxacin and levofloxacin modified for the highest tested concentration were visible at each time point. The greatest differences in the level of survival were observed at 24 hours of incubation, respectively 48.86% for LEV1000 EX 5% and 73.96% for LEV1000. It was also the only statistically significant difference in viability in the tested forms of the drug.

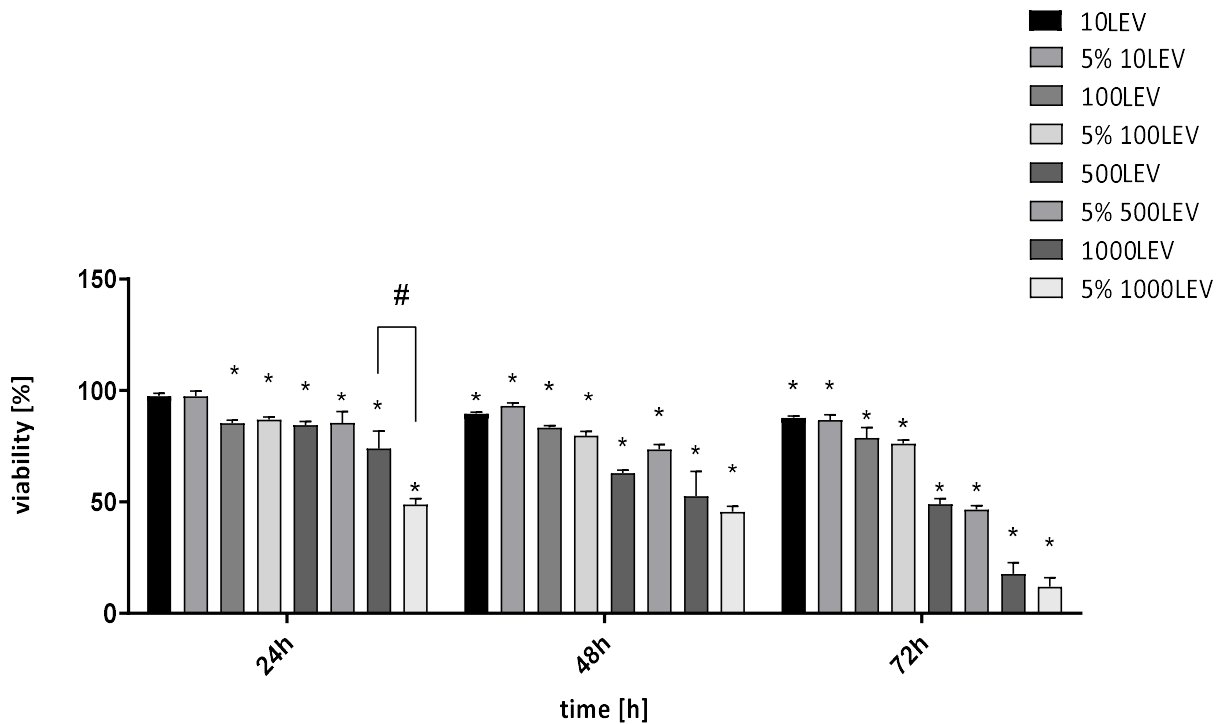


Figure 52. MTT test results for DU145 exposed to the ciprofloxacin concentrations tested. The graph shows the average [%] of survival and the standard deviations based on it on the metabolic activity of the cells relative to the control at a given time. Results significantly statistically different from controls are marked with "*". "#" - a statistically significant difference between the corresponding drugs' concentrations ($p < 0.05$). Bars represent standard deviation.

The IC50 values calculated on the basis of metabolic activity represent theoretical concentrations that should lead to 50% inhibition of the growth of the tested cell lines (Tab. 10). The values show that bladder cancer cells seem to be more sensitive to the effects of both drugs. The lower concentrations of ciprofloxacin and levofloxacin cause a faster inhibition of viability of 50%. It has been observed that the addition of the extract to ciprofloxacin in relation to prostate cancer cells, achieves IC50 at a lower concentration than that of ciprofloxacin.

Table 10. The IC50 value for tested chemotherapeutic agents modified with natural extract. IC50 values calculated on the basis of the nonlinear regression curve for MTT test results, the table also shows the fitting parameter of the theoretical R² curve.

	T24		DU145	
	IC50	R²	IC50	R²
CIP	135.8 μ M	0.9574	246.4 μ M	0.9737
CIP 5% EX	198.4 μ M	0.9600	176.8 μ M	0.9511
LEV	490.0 μ M	0.9685	458.5 μ M	0.9665
LEV 5% EX	539.4 μ M	0.9627	652.9 μ M	0.9875

4.4.4. Cell viability assessment by WST8 assay

The WST8 metabolic activity assay shows [%] survival versus data controls drug concentrations at three different incubation time points (24, 48 and 72h). The analysis of the results showed the cytotoxic nature of all the drugs tested, depending on both the concentration and incubation time. Increasing the incubation time resulted in a decrease in the metabolic activity of the tested cancer cell lines. The lowest cell survival values were achieved with the highest drug doses.

The results of the WST8 assay in assessing cell viability confirmed the previous results developed for the MTT assay (Fig. 53). Additional statistical analysis (t-test, CI=95%) between the groups of drugs showed statistically significant differences, especially in the 72nd hour of the experiment for concentrations in the range of 10 μ M and 500-1000 μ M. A significant change was observed after the use of an additional plant extract at a concentration of 5%. Survivability compared to the control was: 85.24% (10CIP) and 69.75% (10CIP 5% EX); 49.15% (500CIP) and 37.17% (500CIP 5% EX); 18.14% (1000CIP) and 10.11% (1000CIP EX 5%).

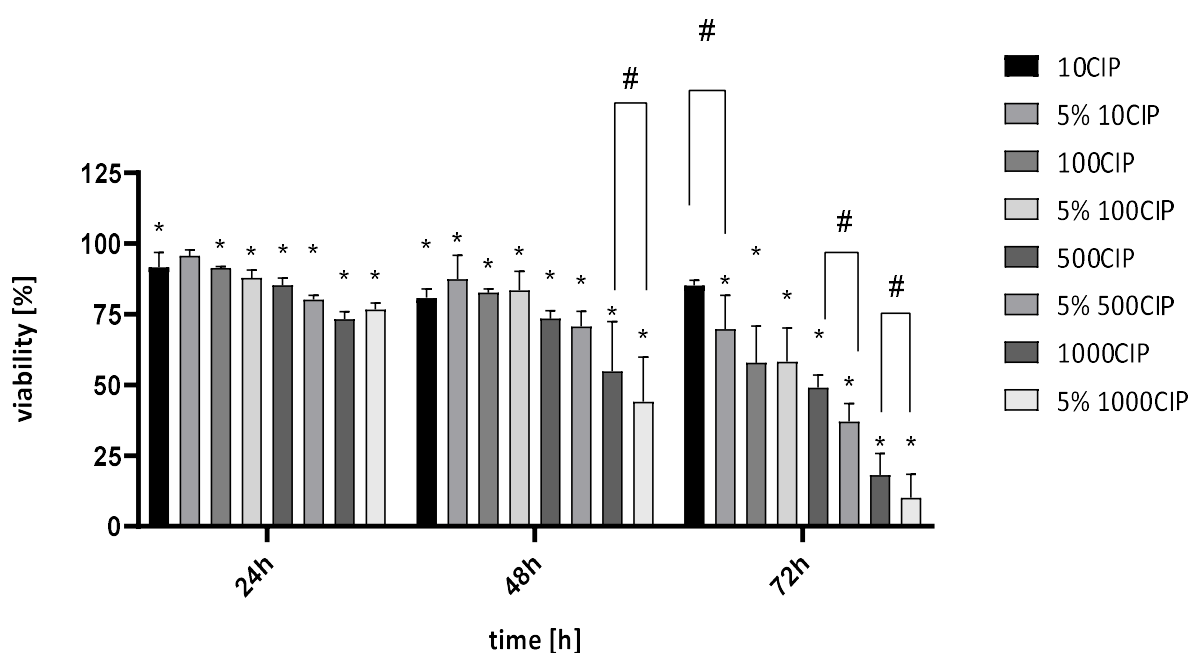


Figure 53. WST8 test results for the T24 line in the following days from the start of incubation with the addition of ciprofloxacin in the concentration range of 10-1000 μ M. "*" - statistical significance in relation to the control; "#" - statistically significant difference between the corresponding concentrations of ciprofloxacin and modified ciprofloxacin ($p < 0.05$).

The results of the WST8 test for levofloxacin at 72 hours of the experiment, showed all tested concentrations of the drug had a significant effect on the metabolic activity of the cells (Fig. 54). The standard deviations of the results increased over time. Differences in cell viability were statistically significant and showed a difference of 18.23% for 24 hours of incubation at 1000 μ M levofloxacin and 8.04% at 48 hours for the same concentration. The results showed that over time, the difference in the cytotoxic effect between the drug in the basic form and with the addition of the extract was getting lower and was most noticeable in the first hours of observation.

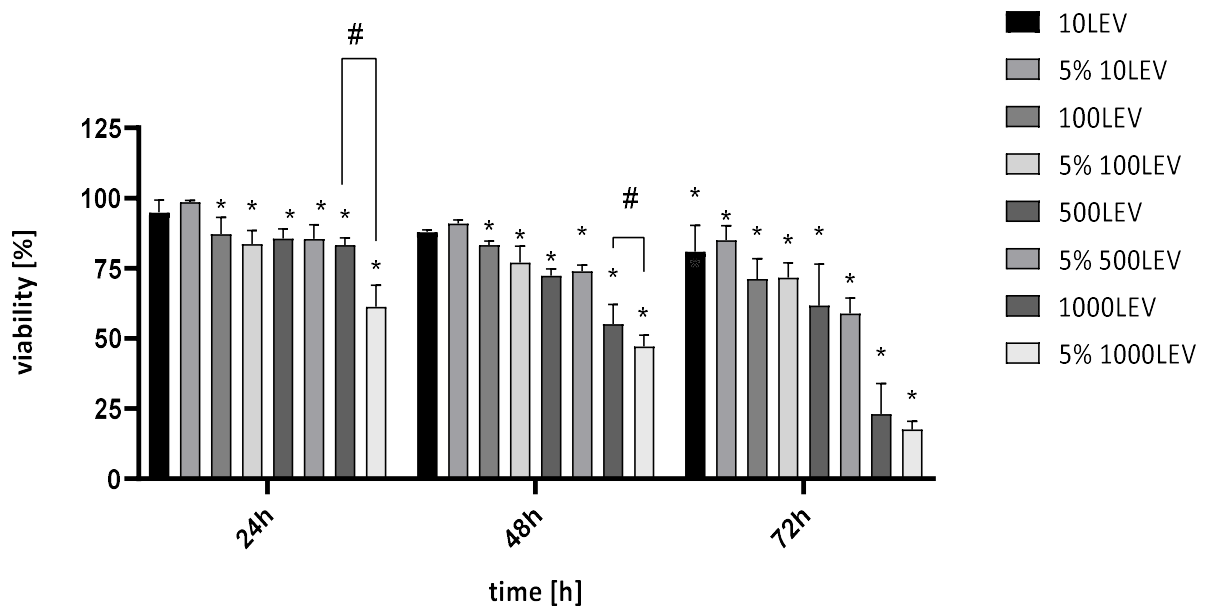


Figure 54. WST8 test results for the T24 line in the following days from the start of incubation with the addition of levofloxacin in the concentration range of 10-1000 μ M. "*" - statistical significance in relation to the control; "#" - statistically significant difference between the corresponding concentrations of levofloxacin and modified levofloxacin ($p < 0.05$).

The metabolic activity of DU145 cells changed significantly after incubation with the tested solutions of ciprofloxacin (Fig. 55). The time point with significantly increases the cytotoxic effect of the tested concentration was the 48 hour of the experiment. At this point, the CIP100 5% EX concentration was 25% more effective than the non-modified form of the drug. Moreover, it was noticeable that when *Picea abies* tree extract was added, a lower concentration (100 μM) produces a very similar cytotoxic effect as a concentration of 500 μM at the same time point (56.12% viability for 100LEV 5% EX and 51.91% viability for 500LEV).

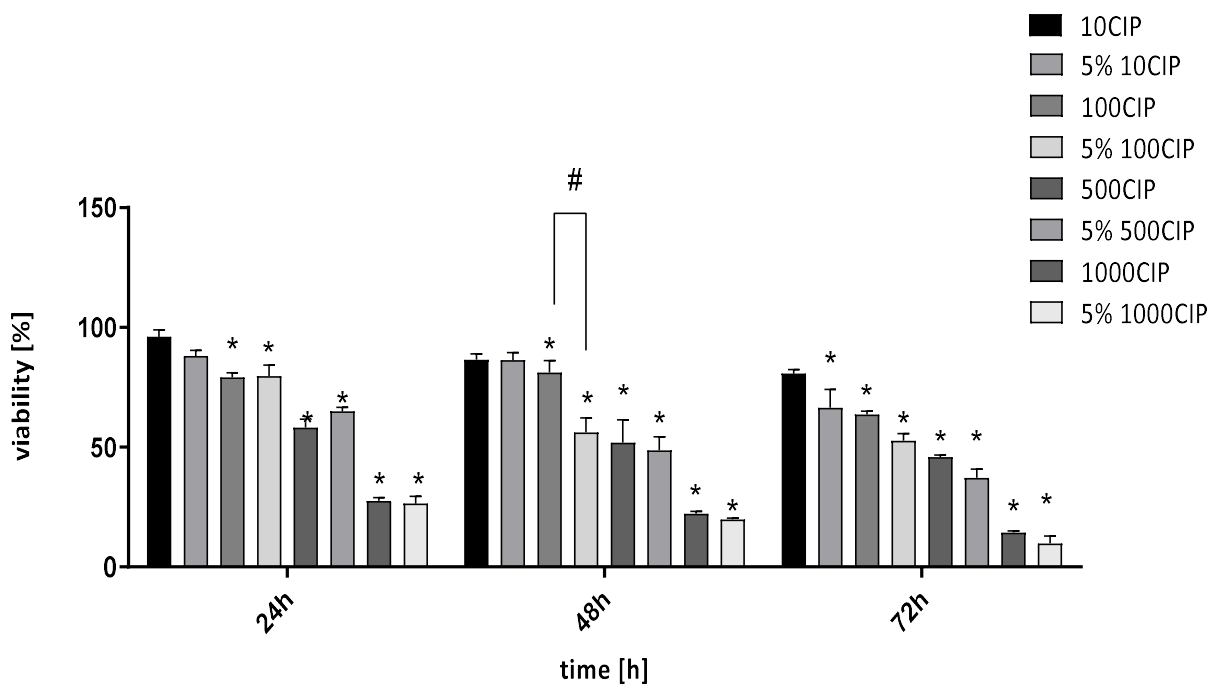


Figure 55. WST8 test results for the DU145 line in the following days from the start of incubation with the addition of ciprofloxacin and modified ciprofloxacin in the concentration range of 10-1000 μM . "*" - statistical significance in relation to the control; "#" - statistically significant difference between the corresponding concentrations of ciprofloxacin and modified ciprofloxacin ($p < 0.05$).

After 24 hours of incubation with levofloxacin, there was a statistically significant reduction in survival for 1000 μ M, 500 μ M and 100 μ M (Fig. 56). Despite a 24-hour incubation, no decrease in survival was observed at the lowest LEV10 concentration. Only 48 and 72-hour incubation showed a decrease in survival for the lowest concentrations of the tested drug. Cell survival in this case was 76.31% (10LEV) and was similar to the effect noted for 10LEV 5% EX (76.88%).

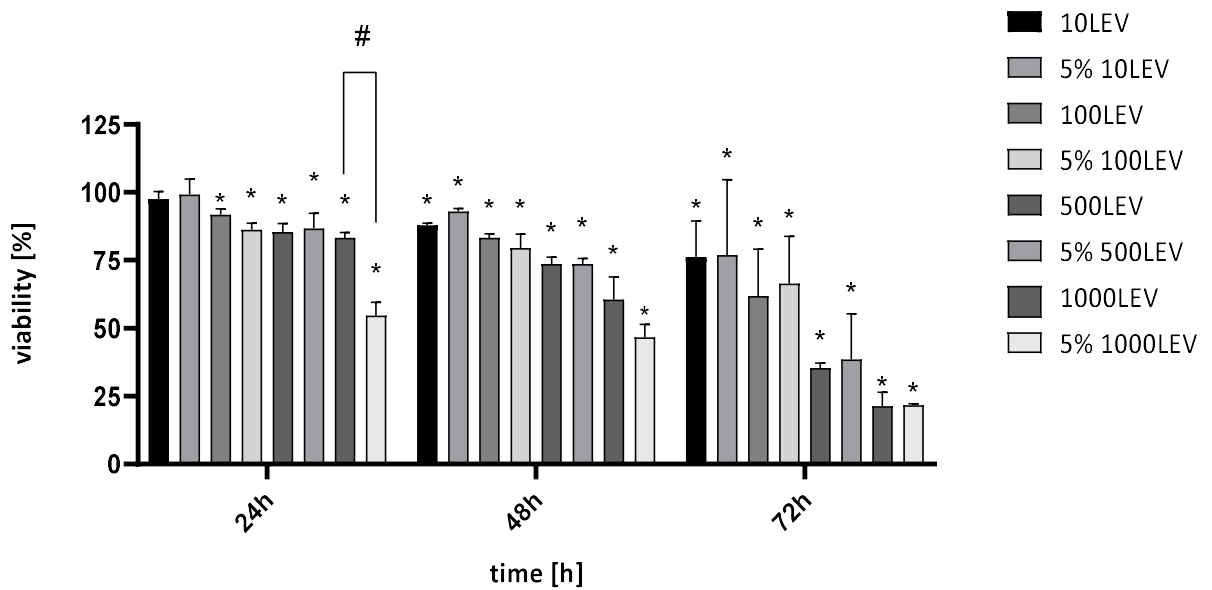


Figure 56. WST8 test results for the DU145 line in the following days from the start of incubation with the addition of levofloxacin and modified levofloxacin in the concentration range of 10-1000 μ M. "*" - statistical significance in relation to the control; "#" - statistically significant difference between the corresponding concentrations of ciprofloxacin and modified ciprofloxacin ($p < 0.05$).

4.4.5. Assessment of apoptosis - identification of caspase 3 and 7 activity

The effect of the applied chemotherapeutic agents on the level of cellular apoptosis assessed by the DEVD FLICA method showed a progression of apoptosis depending on both dose and time for all tested drugs. However, a significant difference in the number of apoptotic cells was visible in the case of incubation of tumor cells with plant extract. The 100 μ M concentration of ciprofloxacin led to significant differences in the number of apoptotic cells compared to the control. After 72 hours, differences were evident for all tested ciprofloxacin concentrations. With respect to cells incubated with the extract, a very slight increase in the percentage of apoptotic cells with increasing concentration of the modified drug was observed (Fig. 57).

Evaluating the effects of levofloxacin and levofloxacin with the addition of a plant extract, images were taken with phase contrast, visualized the number of cells present (Fig. 58). It was observed that, compared to ciprofloxacin, incubation of cells with levofloxacin resulted in a significantly lower increase in apoptotic cells with increasing concentration and incubation time. In addition, as with the previous showed drug, it was also noticed that the *Picea abies* tree extract did not lead to an increase in the number of apoptotic cells in any of the tested solutions.

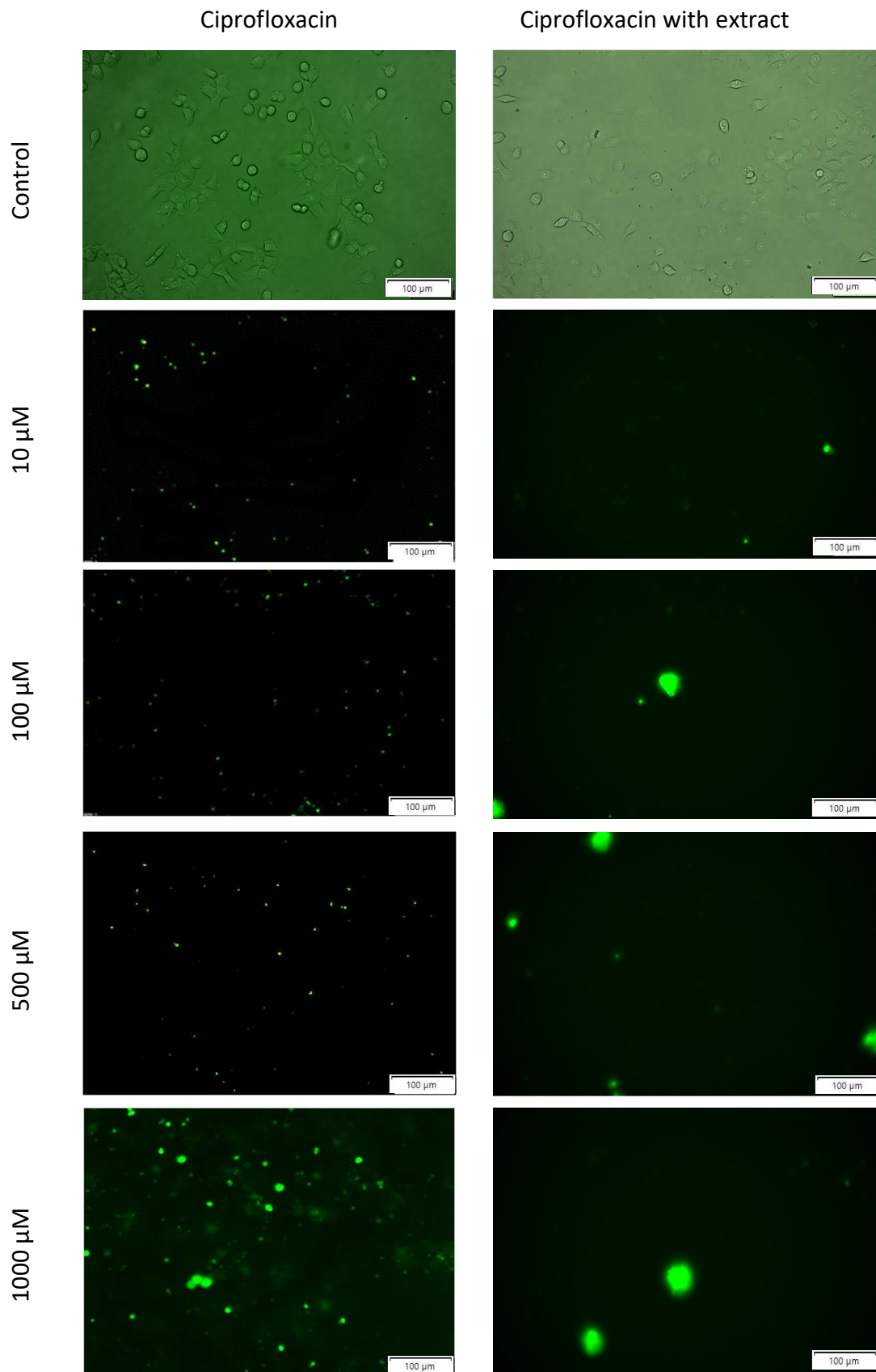


Figure 57. Bladder cancer after 24h with *Picea abies* tree extract and ciprofloxacin - FITC - cells that promote apoptosis. Pictures were taken with a fluorescence microscope CKX53 FN Olympus, Japan and a VC90 4K Olympus camera, Japan. Control images are shown with the FITC channel and phase contrast overlay to visualize the number of cells.

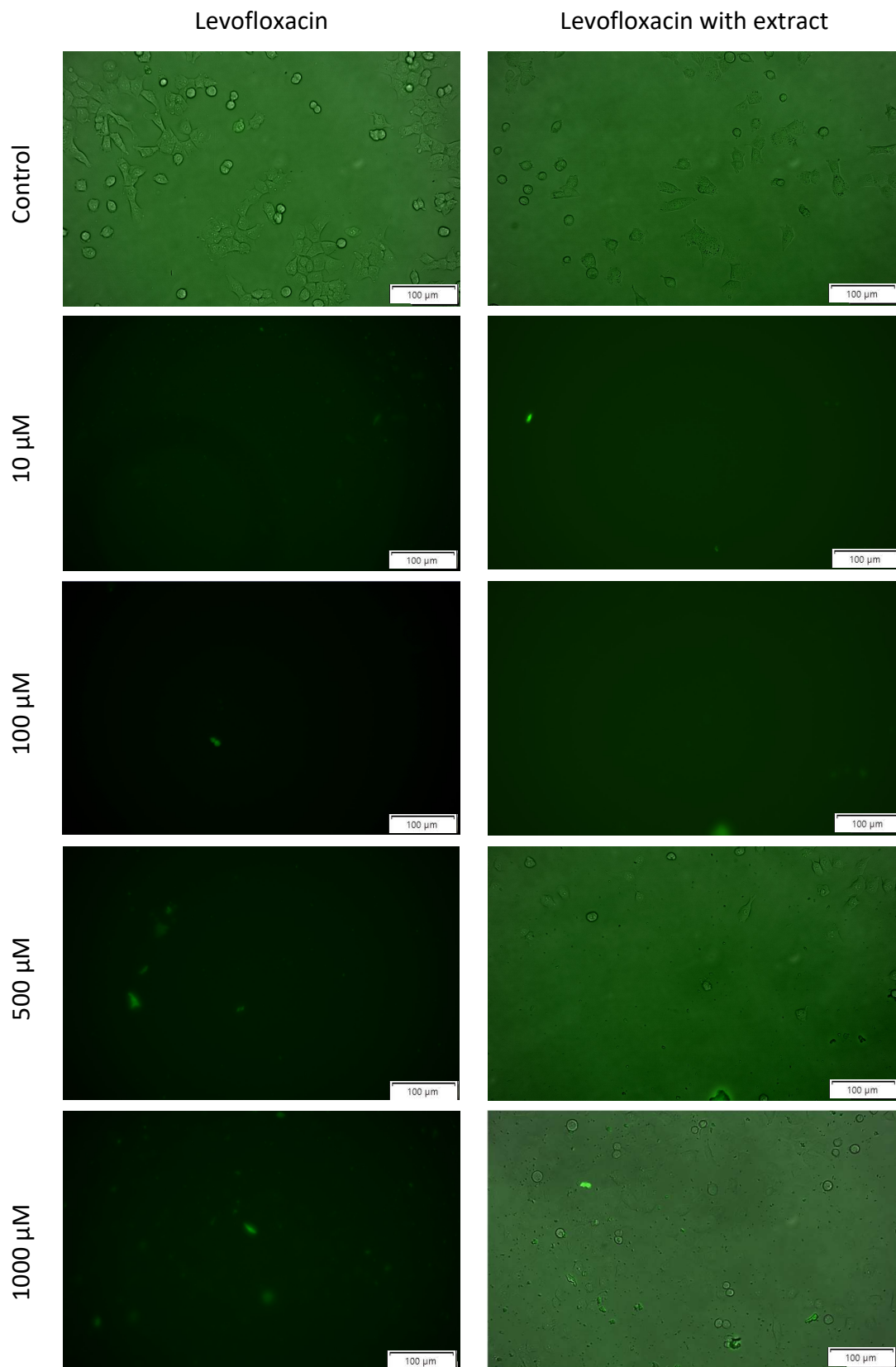


Figure 58. Bladder cancer after 24h with *Picea abies* tree extract and levofloxacin - FITC - cells that promote apoptosis. Pictures were taken with a fluorescence microscope CKX53 FN Olympus, Japan and a VC90 4K Olympus camera, Japan.

In assessing the activity of caspase-3 and -7 in the metabolism of prostate cancer tumor cells, strong signals of apoptotic cells were also observed with ciprofloxacin (Fig. 59). In the case of a drug with an extract, these signals were noticeably weaker, identifiable only in single cells or groups of cells (marked with yellow arrows). For visualization of cells incubated with the addition of 5% *Picea abies* tree extract, phase contrast microscopy was used. It showed decreased number of cells with no significant increase in the apoptosis signal.

The obtained results also showed that levofloxacin induces much weaker signal of apoptosis and significantly noticeable only for concentrations in the range 100 – 1000 μ M (Fig. 60). In the case of corresponding concentrations for levofloxacin with the addition of plant extract, was also considered a suppression of the apoptosis signal even in the case of the highest concentrations of the drug. Phase contrast photos showed that even cells morphologically considered as dead (round, detached) marked with a red circle do not induce apoptosis signal at a concentration of 1000LEV 5% EX.

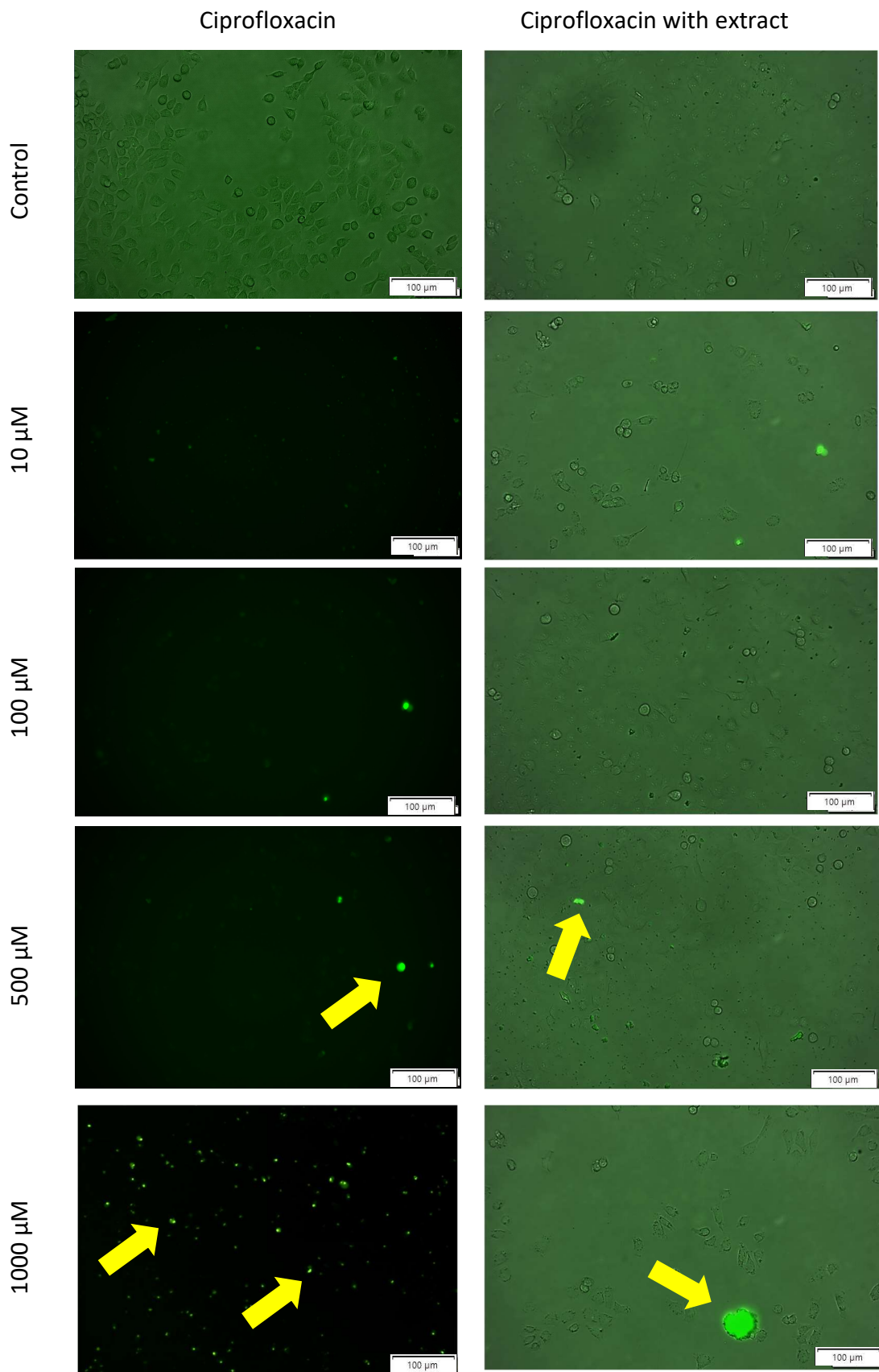


Figure 59. Prostate cancer cell line after 24h with *Picea abies* tree extract and ciprofloxacin - FITC - cells that promote apoptosis. Arrows indicate apoptotic cells. Pictures were taken with a fluorescence microscope CKX53 FN Olympus, Japan and a VC90 4K Olympus camera, Japan.

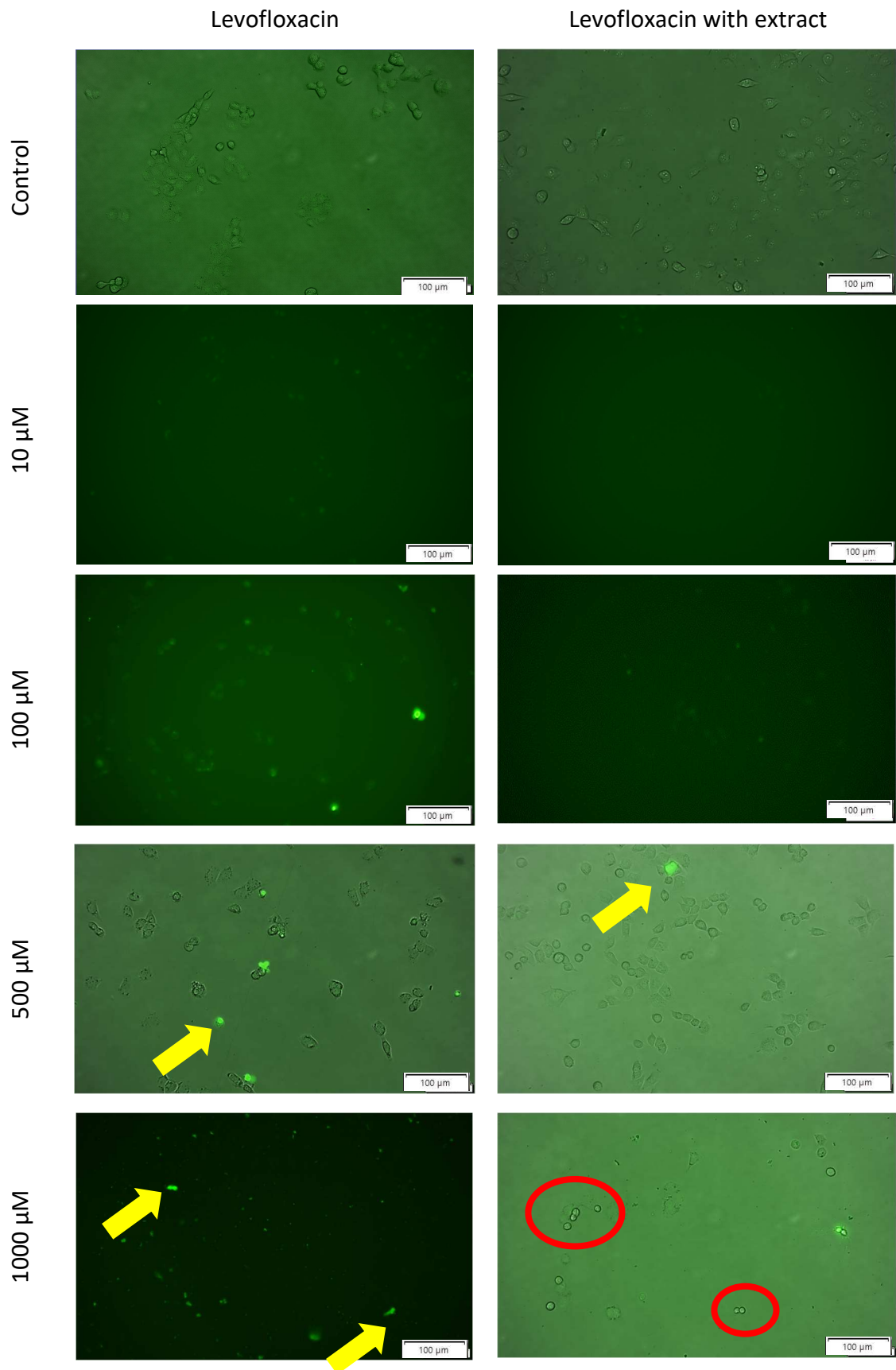


Figure 60. Prostate cancer cell line after 24h with *Picea abies* tree extract and levofloxacin - FITC - cells that promote apoptosis. Arrows indicate apoptotic cells. The red circles mark dead non apoptotic cells.

4.4.6. Cell proliferation by thymidine analogue 5-Bromo-2'-deoxyuridine method

Ciprofloxacin led to a statistically significant decrease in the level of T24 proliferation after 24 hours of incubation at all concentrations tested (Fig. 61). Concentration at this time CIP1000 and CIP1000 EX 5% led to a high level of proliferation inhibition of 53.03% and 37.97% respectively compared to the control. A decrease in T24 proliferation was also observed with increasing incubation time with the drug. The concentration at the level of 500 μ M for both tested forms of the drug allowed the observation of significant differences in the percentage of proliferation at the level of 27.44% (CIP500) and 18.15% (CIP500 5% EX). Both at 24 and 72 hours of incubation, a relationship was observed between the concentration of the drug used and the decrease in the proliferation level of the tested cells.

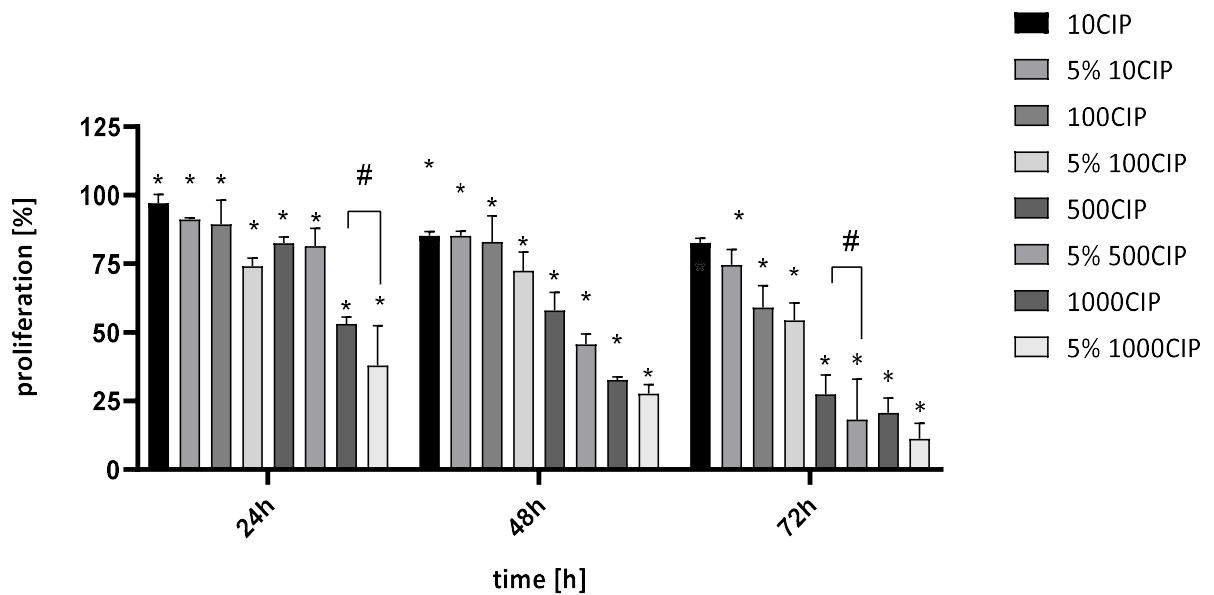


Figure 61. Proliferation of the T24 line in the following days from the start of incubation with the addition of ciprofloxacin and modified ciprofloxacin in the concentration range of 10-1000 μ M. "*" - statistical significance in relation to the control; "#" - statistically significant difference between the corresponding concentrations of ciprofloxacin and modified ciprofloxacin ($p < 0.05$).

No significant decrease in the level of proliferation with levofloxacin was observed (Fig. 62). At 24 hours of incubation the smallest effect on the decrease in the level of proliferation was shown by the concentrations of 10LEV and 10LEV 5% EX, which did not significantly affect the decrease in the rate of proliferation. It was not until 48 hours that this decrease was statistically significant, and the proliferation was respectively 87.37% and 89.52%. In the 72 hour of the experiment, that the addition of 5% of the extract significantly reduced the level of cell proliferation for the concentration of 1000LEV, which resulted in the inhibition of the rate of cell proliferation at the level of 25.04% (1000LEV) and 17.14% (1000LEV 5% EX).

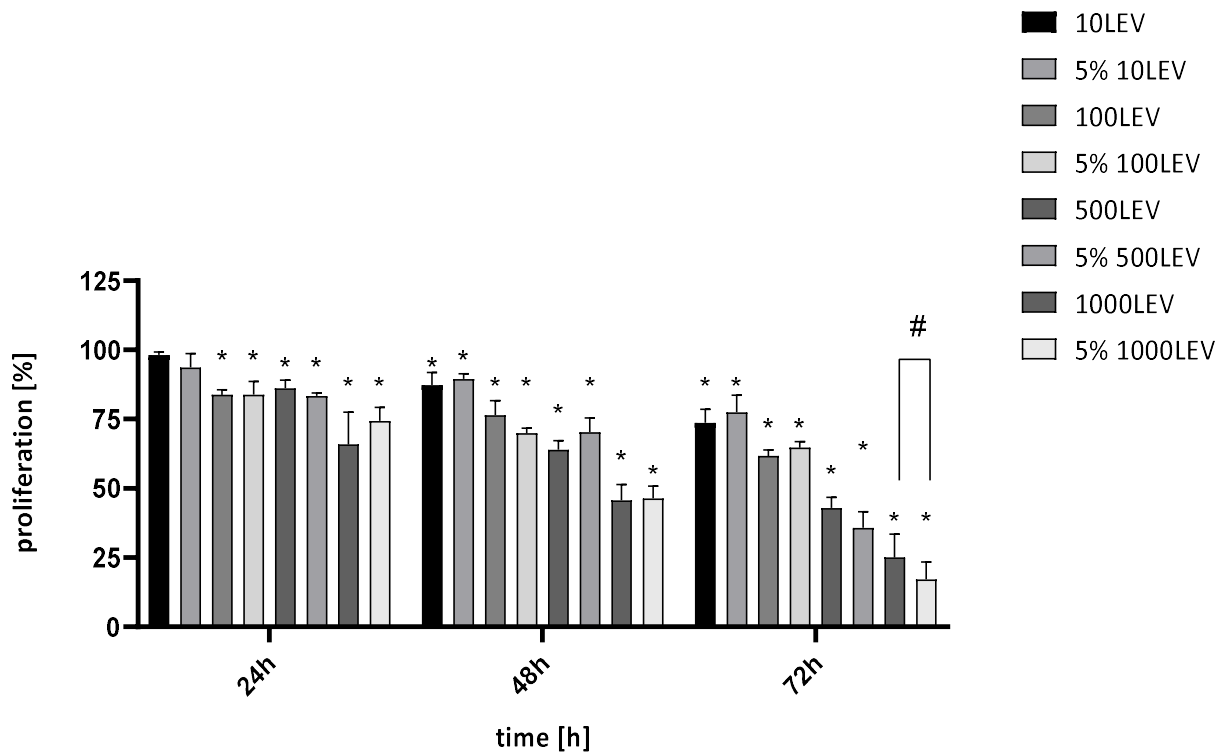


Figure 62. Proliferation of the T24 line in the following days from the start of incubation with the addition of ciprofloxacin and modified ciprofloxacin in the concentration range of 10-1000 μ M. "*" - statistical significance in relation to the control; "#" - statistically significant difference between the corresponding concentrations of levofloxacin and modified levofloxacin ($p < 0.05$).

The results of prostate cancer cells using the BrdU method indicated significant differences between the proliferative potential of control cells and cells exposed to chemotherapeutic drugs (Fig. 63). After 24 hours of incubation, the higher differences in the observed proliferation rate were noted for 500 μ M, 78.94% (500CIP) and 54.31% (500CIP 5% EX) of the control values. It was observed that the addition of 5% plant extract caused a similar decrease in the rate of proliferation at 100CIP (81.81%) as at 500 μ M (78.94%) without the addition of the extract. After 72 hours, the concentration of 1000 μ M resulted in a high level of proliferation inhibition of 9.66% (1000CIP) and 5.78% (CIP1000 EX 5%) compared to the control.

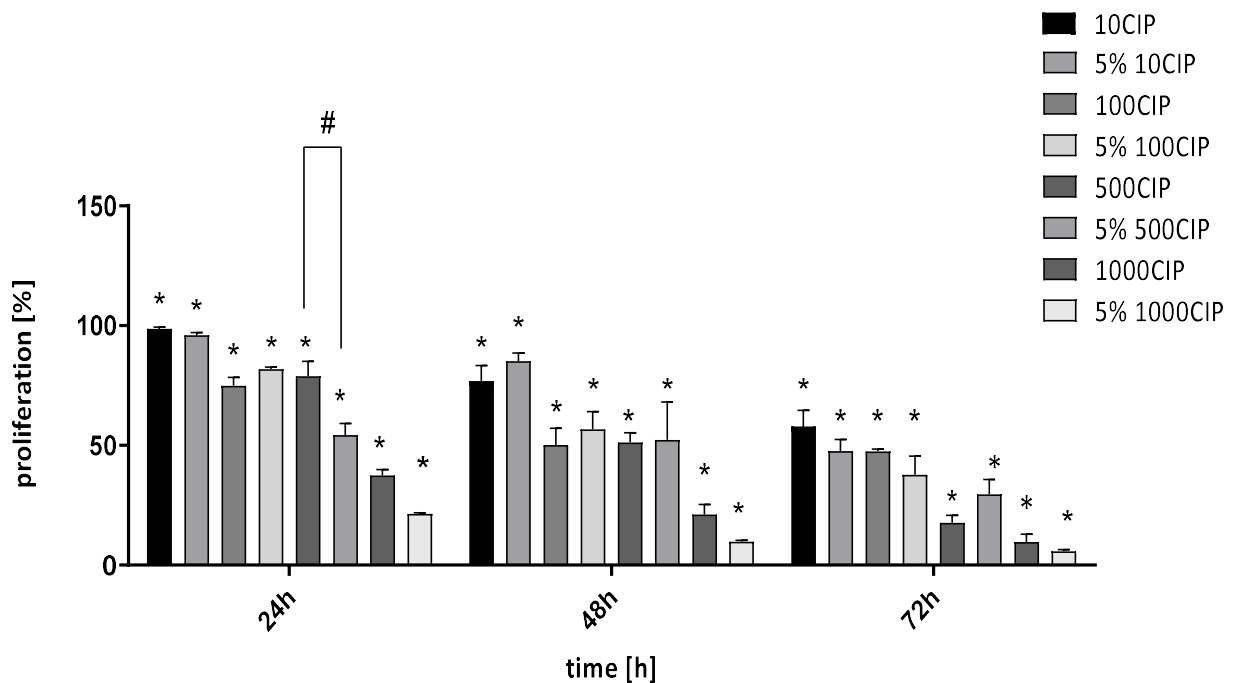


Figure 63. Proliferation of the DU145 line in the following days from the start of incubation with the addition of ciprofloxacin and modified ciprofloxacin in the concentration range of 10-1000 μ M. "*" - statistical significance in relation to the control; "#" - statistically significant difference between the corresponding concentrations of ciprofloxacin and modified ciprofloxacin ($p < 0.05$).

In the case of levofloxacin, addition of the extract to the lowest concentration also did not result in a decrease in the rate of proliferation compared to the control (Fig. 64). At 24 hours of incubation the smallest effect on the decrease in the level of proliferation was shown by the concentration of 10 μM levofloxacin and amounted to 2.1% compared to the control. With the increase of the incubation time, a further decrease in the level of proliferation was difficult to observe, as it was very low already after 24 hours of incubation. After 72 hours of incubation, a decrease in the level of proliferation DU145 cells was observed. For the concentration of 10LEV 5% EX, it decreased by 5% from the previous evaluation. No statistically significant differences in the effect of levofloxacin on cell proliferation were observed when levofloxacin *Picea abies* tree extract was added to different concentrations.

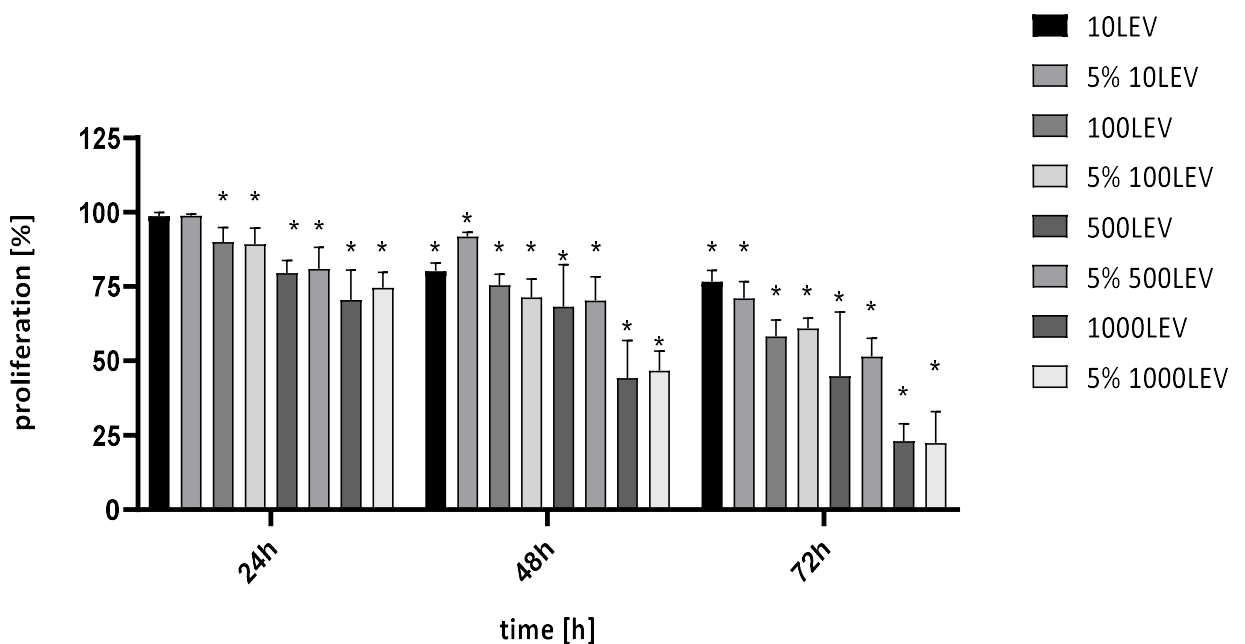


Figure 64. Proliferation of the T24 line in the following days from the start of incubation with the addition of ciprofloxacin and modified ciprofloxacin in the concentration range of 10-1000 μM . "*" - statistical significance in relation to the control; "#" - statistically significant difference between the corresponding concentrations of levofloxacin and modified levofloxacin ($p < 0.05$).

4.4.7. pH of the cell culture medium measurement

An increase in the pH value of the medium depending on time and the concentration of the tested drug was observed. For samples with the content of natural extract, higher alkalinity of the culture medium was noted (Tab. 11).

Table 11. Ciprofloxacin and *Picea abies* tree modified ciprofloxacin-induced media pH shifts following 3-days exposure, in T24 cells. pH shifts recorded in CIP-supplemented (0–1000 μ M) culture media, following overnight exposure, subsequent to 3-day treatment; mean \pm SD., n=3.

pH	24h	48h	72h
control	8.37 \pm 0.0503	8.36 \pm 0.0098	8.36 \pm 0.0028
10 μ M CIP	7.84 \pm 0.0173	7.83 \pm 0.0374	7.82 \pm 0.0093
100 μ M CIP	8.16 \pm 0.0057	8.17 \pm 0.0019	8.17 \pm 0.0792
500 μ M CIP	8.03 \pm 0.0783	8.02 \pm 0.0536	8.02 \pm 0.0312
1000 μ M CIP	8.46 \pm 0.0124	8.45 \pm 0.0797	8.44 \pm 0.0678

pH	24h	48h	72h
control	7.96 \pm 0.0659	7.92 \pm 0.0830	7.94 \pm 0.0389
10 μ M CIP 5% EX	7.52 \pm 0.0384	7.82 \pm 0.0029	7.82 \pm 0.0087
100 μ M CIP 5% EX	8.11 \pm 0.0930	8.02 \pm 0.0638	8.21 \pm 0.0038
500 μ M CIP 5% EX	8.34 \pm 0.0083	8.30 \pm 0.0830	8.30 \pm 0.0949
1000 μ M CIP 5% EX	8.20 \pm 0.0039	8.51 \pm 0.0930	8.52 \pm 0.0384

In the case of evaluating the medium of cells cultured in the presence of levofloxacin, the pH meter indicated significantly higher pH values in the case of the drug with the extract. For the highest concentrations on the last day of incubation, this difference was 0.45 (Tab. 12).

Table 12. Levofloxacin and Picea abies tree modified levofloxacin -induced media pH shifts following 3-days exposure, in T24 cells. pH shifts recorded in LEV-supplemented (0–1000 µM) culture media, following overnight exposure, subsequent to 3-day treatment; mean ± SD., n=3.

pH	24h	48h	72h
control	8.37 ±0.0503	8.36 ±0.0098	8.36 ±0.0028
10 µM LEV	7.83 ±0.0028	7.82 ±0.0328	7.83 ±0.0304
100 µM LEV	7.59 ±0.0054	7.58 ±0.0289	7.57 ±0.0292
500 µM LEV	7.69 ±0.0837	7.68 ±0.0029	7.65 ±0.0294
1000 µM LEV	8.08 ±0.0249	8.07 ±0.0024	8.08 ±0.0029

pH	24h	48h	72h
control	8.27 ±0.0659	8.21 ±0.0830	8.12 ±0.0389
10 µM LEV 5% EX	8.13 ±0.0839	7.53 ±0.0394	7.52 ±0.0029
100 µM LEV 5% EX	8.01 ±0.0239	8.15 ±0.0632	8.26 ±0.0384
500 µM LEV 5% EX	8.01 ±0.0033	8.03 ±0.0304	8.45 ±0.0029
1000 µM LEV 5% EX	8.48 ±0.0193	8.40 ±0.0892	8.53 ±0.0084

Similar observations were read from the results for the DU145 cell line, where the addition of the extract significantly increased the pH value towards alkaline for both tested drugs (Tab. 13, 14).

Table 13. Ciprofloxacin and *Picea abies* tree modified ciprofloxacin-induced media pH shifts following 3-days exposure, in DU145 cells. pH shifts recorded in CIP-supplemented (0–1000 μ M) culture media, following overnight exposure, subsequent to 3-day treatment; mean \pm SD., n=3.

pH	24h	48h	72h
control	7.95 \pm 0.0374	7.94 \pm 0.0320	7.92 \pm 0.0340
10 μ M CIP	7.94 \pm 0.0493	7.89 \pm 0.0029	7.88 \pm 0.0029
100 μ M CIP	7.95 \pm 0.0394	7.97 \pm 0.0235	7.98 \pm 0.0534
500 μ M CIP	7.66 \pm 0.0093	7.65 \pm 0.0038	7.60 \pm 0.0094
1000 μ M CIP	8.01 \pm 0.0034	8.00 \pm 0.0739	8.05 \pm 0.0649

pH	24h	48h	72h
control	8.03 \pm 0.9359	8.05 \pm 0.0833	8.04 \pm 0.0435
10 μ M CIP 5% EX	8.11 \pm 0.0384	8.11 \pm 0.0022	8.15 \pm 0.0098
100 μ M CIP 5% EX	8.21 \pm 0.0029	8.25 \pm 0.0695	8.30 \pm 0.0038
500 μ M CIP 5% EX	8.23 \pm 0.0339	8.35 \pm 0.0948	8.30 \pm 0.0534
1000 μ M CIP 5% EX	8.12 \pm 0.0209	8.24 \pm 0.0890	8.34 \pm 0.0859

Table 14. Levofloxacin and *Picea abies* tree modified levofloxacin -induced media pH shifts following 3-days exposure, in DU145 cells. pH shifts recorded in LEV-supplemented (0–1000 μ M) culture media, following overnight exposure, subsequent to 3-day treatment; mean \pm SD., n=3.

pH	24h	48h	72h
control	8.37 \pm 0.0503	8.36 \pm 0.0098	8.36 \pm 0.0028
10 μ M LEV	7.90 \pm 0.0029	7.89 \pm 0.0083	7.90 \pm 0.0534
100 μ M LEV	7.94 \pm 0.0456	7.93 \pm 0.0229	7.95 \pm 0.0039
500 μ M LEV	7.68 \pm 0.0837	7.67 \pm 0.0480	7.66 \pm 0.0578
1000 μ M LEV	7.86 \pm 0.0739	7.85 \pm 0.0284	7.84 \pm 0.0035

pH	24h	48h	72h
control	7.96 \pm 0.0659	7.92 \pm 0.0830	7.94 \pm 0.0389
10 μ M LEV 5% EX	7.90 \pm 0.0804	7.89 \pm 0.0345	7.98 \pm 0.0284
100 μ M LEV 5% EX	8.01 \pm 0.0034	8.04 \pm 0.0384	8.09 \pm 0.0084
500 μ M LEV 5% EX	8.25 \pm 0.0384	8.28 \pm 0.0938	8.28 \pm 0.0022
1000 μ M LEV 5% EX	8.28 \pm 0.0098	8.28 \pm 0.0039	8.29 \pm 0.0394

4.5. Multicellular tumor spheroids – cell culture optimization

4.5.1. Preparation of multicellular tumor spheroids

During the seeding and spheroid formation procedure, the main goal was to optimize the number of spheroid-forming cells, assess their viability and the time needed for the spheroid for further study.

After seeding the cells and adding magnetic nanoparticles to them, a cell viability assay was performed after incubation times of 24, 48 and 72 hours to assess the toxicity of nanoparticles and their impact on cell survival. In addition, the conducted research showed, that nanoparticles did not affect cell viability of both the T24 and DU145 lines (Fig. 65).

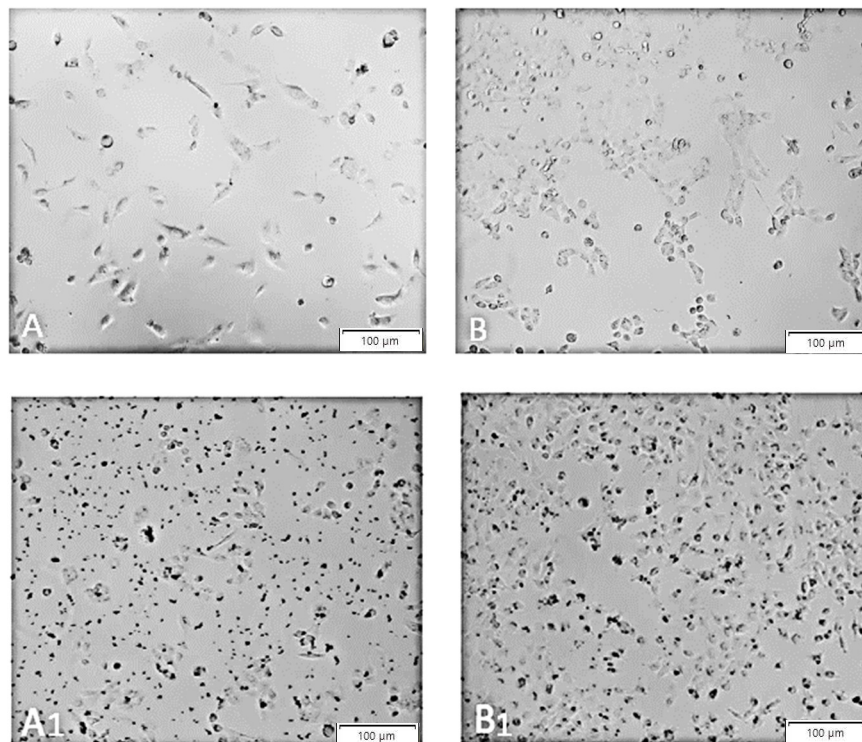


Figure 65. DU145 (A) and T24 (B) cells after 24 hours with nanomagnetic particles (A1 and B1). The nanoparticles penetrated the cells without damaging cells' structure.

Prostate cancer cells (Fig. 66) do not always form optimal spheroids, these cells were more sensitive to the action of nanoparticles. The predisposition to form spheroids depends on the size, cell morphology, propensity for migration or adhesion [109]. The results showed that the optimal density of cells per well was estimated at a level of 5.000 cells. Thanks to this, spheroids assumed a regular shape. Bladder cancer cells (Fig. 67) are highly predisposed to the formation of spheroids.

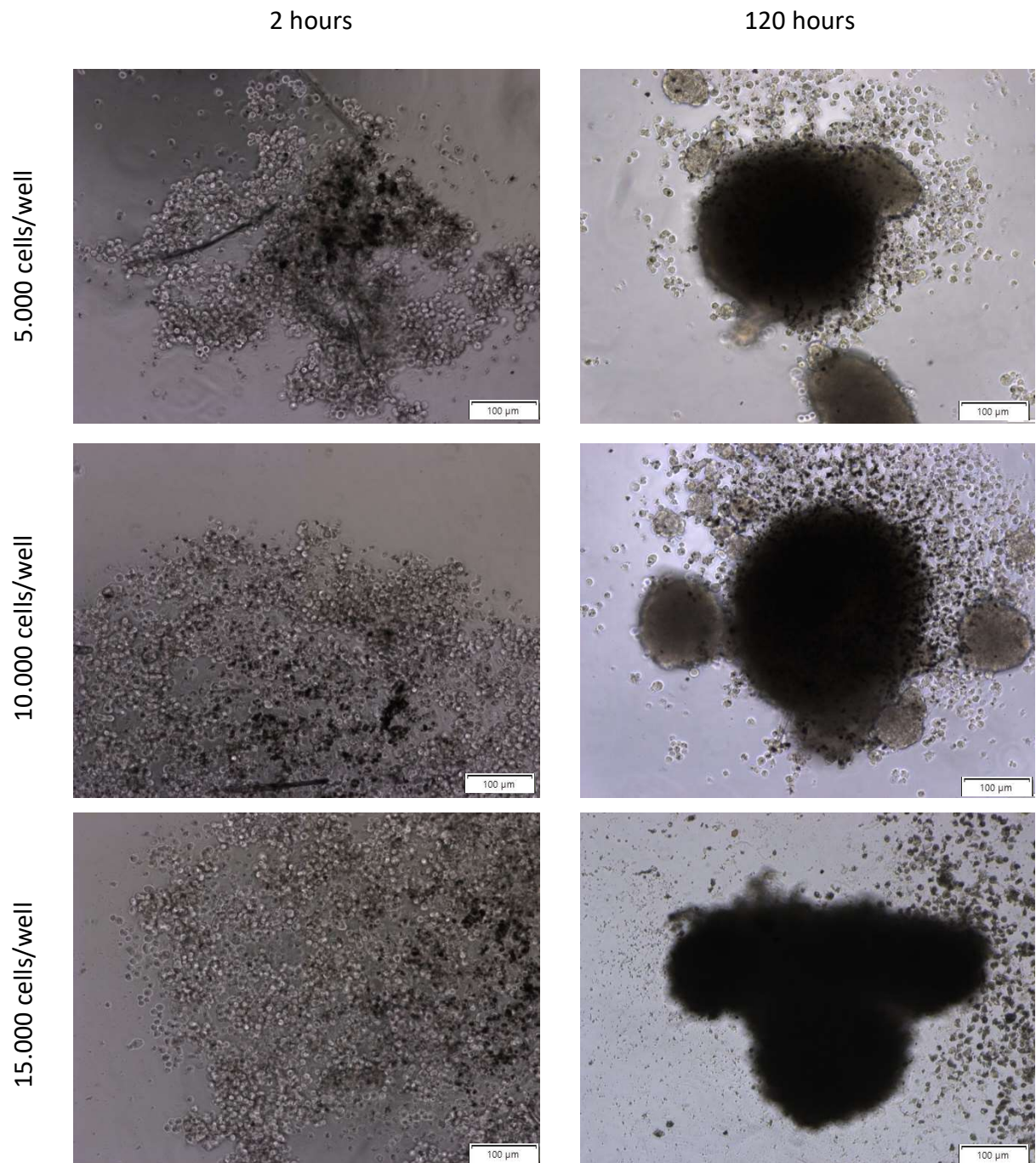


Figure 66. Multicellular spheroids DU145 cells 24 hours and 120 hours after bioprinting process.

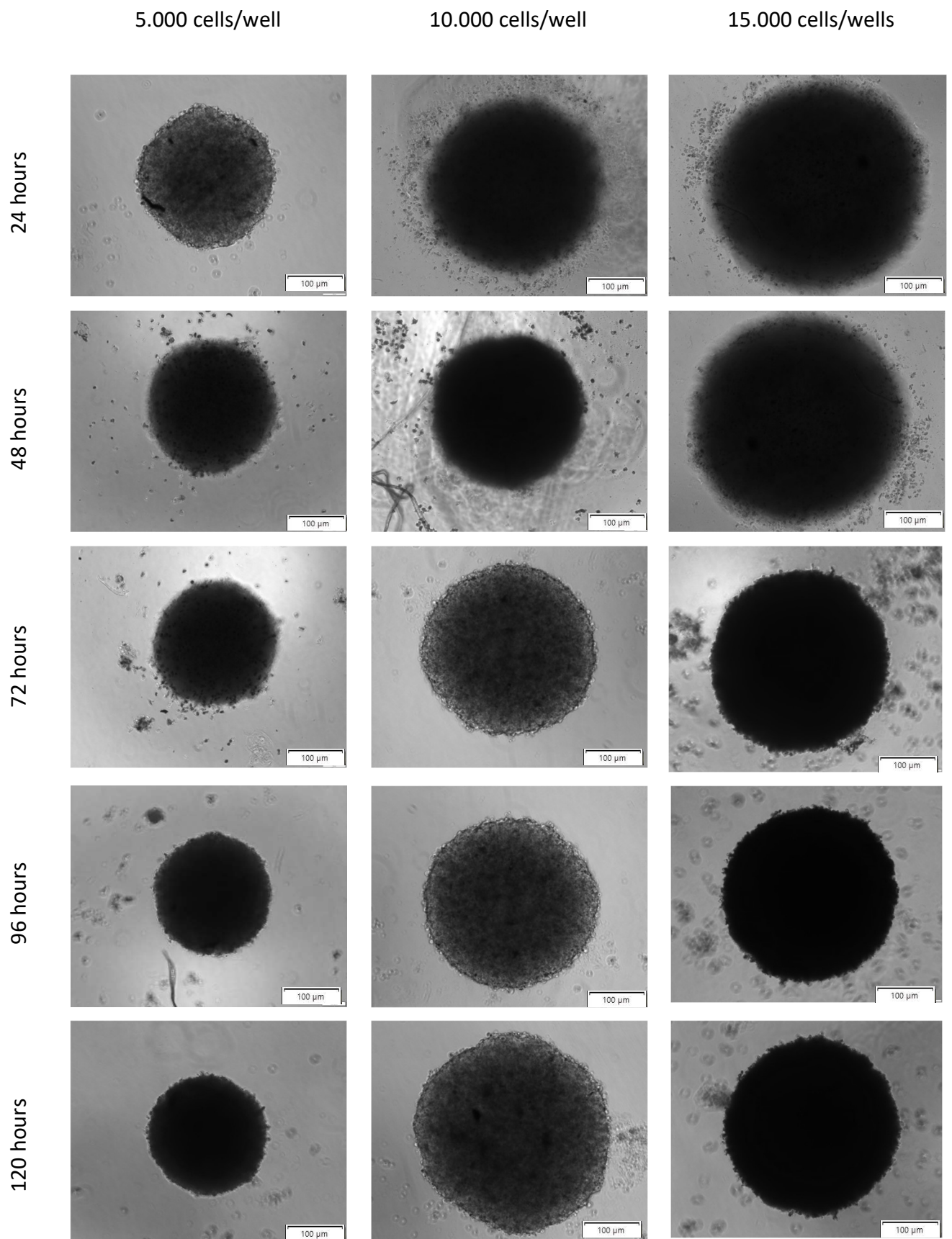


Figure 67. Multicellular spheroids T24 cells after 25 – 120 hours after bioprinting process. Spheroids ranging from 1.000 to 4.000 cells per spheroids were also produced (data not showed), however the results showed that the bioprinting process was significantly lower than 5.000 – 15.000 cells/well.

4.5.2. Spheroids kinetics growth.

Spheroids generated by magnetically bioprinting, even when seeded at different densities, had similar growth trends measured by spheroid diameter (Fig. 68). Spheroids were imaged at regular time intervals, and their growth kinetics. Comparing adherent and non-adherent cells cultures with the same seeding densities, cell growth was much slower. The growth curves showed that the spheroid doubling time was longer than that of monolayer cells. A doubling of the growth time of spheroids corresponds to a doubling of the *in vivo* time of solid tumors, demonstrating that multicellular spheroids mimic the kinetic properties of tumor growth *in vivo* [110]. Characteristic for the growth kinetics of spheroids is the initial expansion of the sphere, while after a few days the spheroid shrinks. The model can be used for further research after stabilization of the spheroid size.

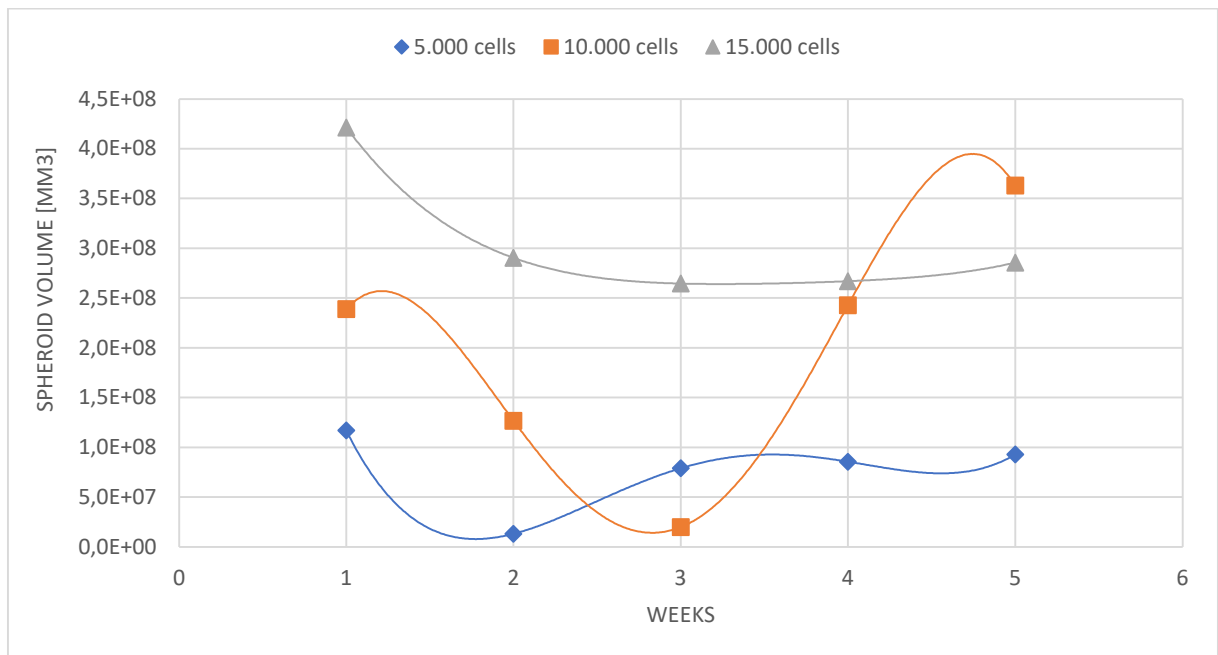


Figure 66. Graph showing growth of multicellular spheroids from T24 cell line over 5 weeks. The growth of only the T24 line spheroids was calculated as they formed regular spheroids.

4.5.3. Live/Dead Assay of Cellular Spheroids.

After 120 hours, when the spheroids had reached a stable size, the viability of the cells forming the spheroids was assessed using the Live/Dead assay (Fig. 69). Phase-contrast images showed that the cells that made up the spheroids had high viability, manifested by the green FITC fluorochrome.

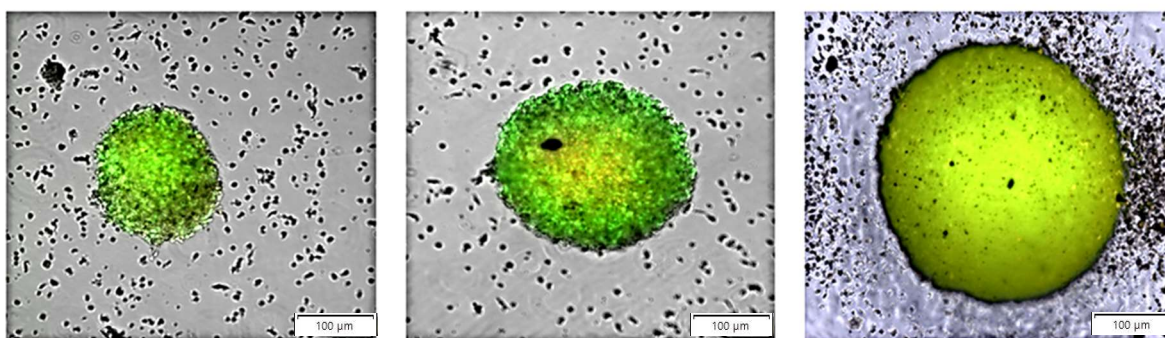


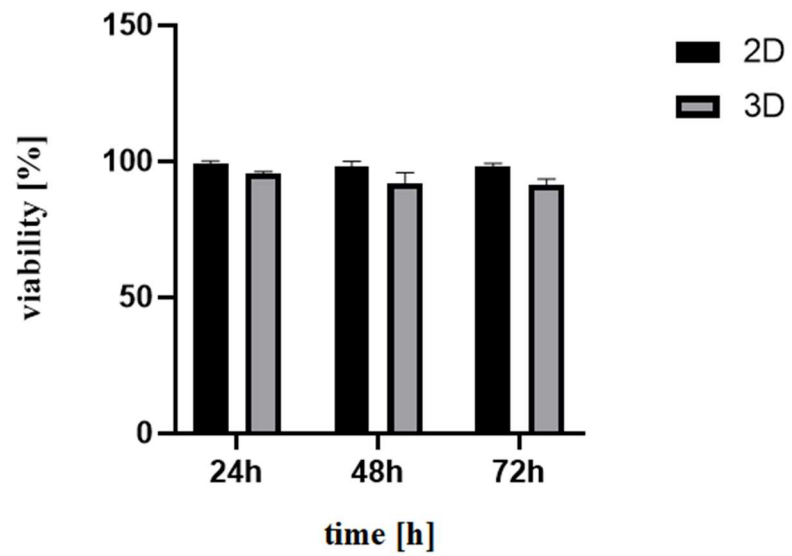
Figure 67. T24 cell spheroids 120 hours after spheroid formation procedure (seeded from 5.000; 10.000; 15.000 cells), stained with Live/Dead assay. The photos were taken with the CKX53 FN Olympus fluorescence microscope, Japan and the VC90 4K Olympus camera, Japan.

4.5.4. Live spheroids assessment - WST8 and MTT assay

The 2D model (100 % viability) was a reference model to which the viability of cells grown in 3D culture was compared. 3D culture cell viability of 98.73 (24h); 96.34 (48h) and 95.39 (72h) [%] was not statistically significant. In the case of the DU145 cell line, the viability of the spheroids compared to the control, i.e. adherent cells, was 16.84 % less, and this decrease was statistically significant (Fig. 70A, B). Based on these results, it was decided to use only spheroids made from the T24 cell line for further research.

On the basis of the tests, spheroids performed with 5.000 T24 (bladder cancer) cells were selected for further research. These spheroids showed high viability compared to cells grown on an adherent medium.

A



B

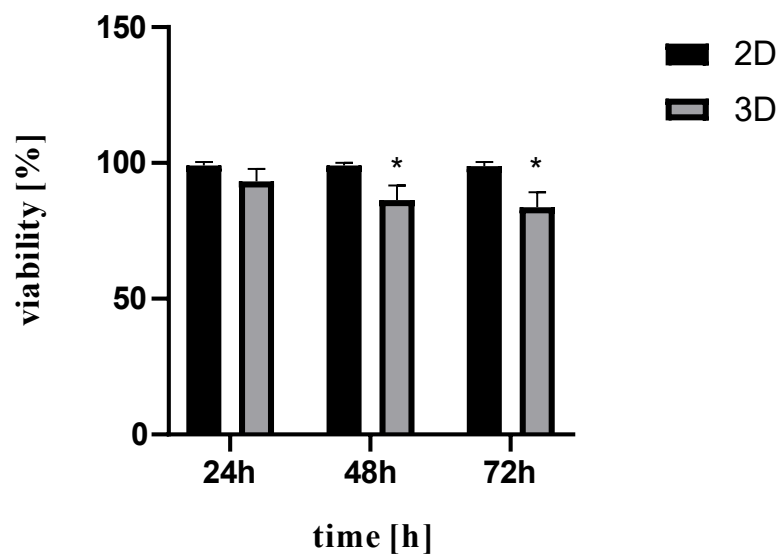


Figure 68. Comparison of viability 2D and 3D model incubated in media T24 (A) and DU145 (B). “*” indicate a statistically significant decrease in viability compared to the control.

4.6. Multicellular spheroids - chitosan drugs' modification

Due to the highest efficiency of the magnetic bioprinting method in the case of creating spheroids of T24 cells (bladder cancer), a model of spheroids from the commercial T24 line was used for further research.

4.6.1. Assessment of cell viability in a microscope with inverted optics

Comparing the appearance of spheroids in microscopic observation, spheroids of similar sizes were selected for testing and comparing the corresponding concentrations of the tested drugs. In the microscopic observation of spheroids incubated with chemotherapeutic agents, it was noticed that the highest concentrations of ciprofloxacin caused disintegration of spheroid cells. Moreover, differences in the shapes of the precipitating ciprofloxacin crystals were detected. In the case of the drug in its basic form, a lump-shaped crystal was noticed, which was also observed in the monolayer culture. In the case of a drug with the addition of chitosan, the crystals took the shape of needles (Fig. 71).

By comparing the corresponding concentrations of both forms of levofloxacin (with and without chitosan), spheroids of similar sizes were selected. For example - control spheroid size 127.18 μm , control spheroid with chitosan size – 122.88 μm (Fig. 72). At a 1000 μM levofloxacin concentration disintegration and degradation of the spheroids has been seen, compared to the control.

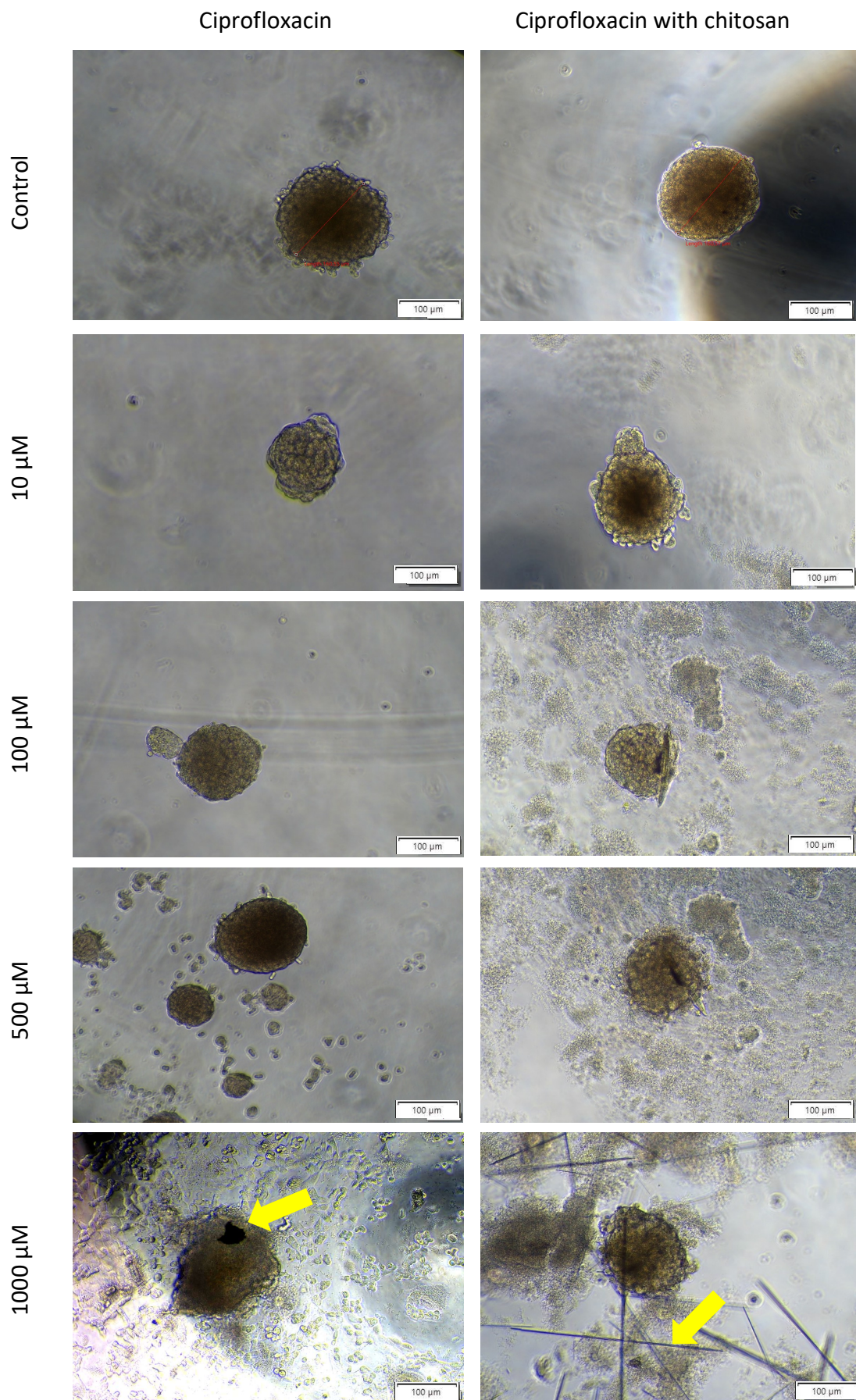


Figure 69. Effect of chemotherapeutic drug ciprofloxacin on the cell growth 3D-cultured bladder (T24) cancer. Cell line was seeded on day 0 and cultured in 3D-conditions through day 6. Brightfield images of each cell line were captured on day 1 (not shown) and 3 (after 72 hours incubation with drugs). Arrows indicate ciprofloxacin crystals precipitate at the highest drug concentration tested.

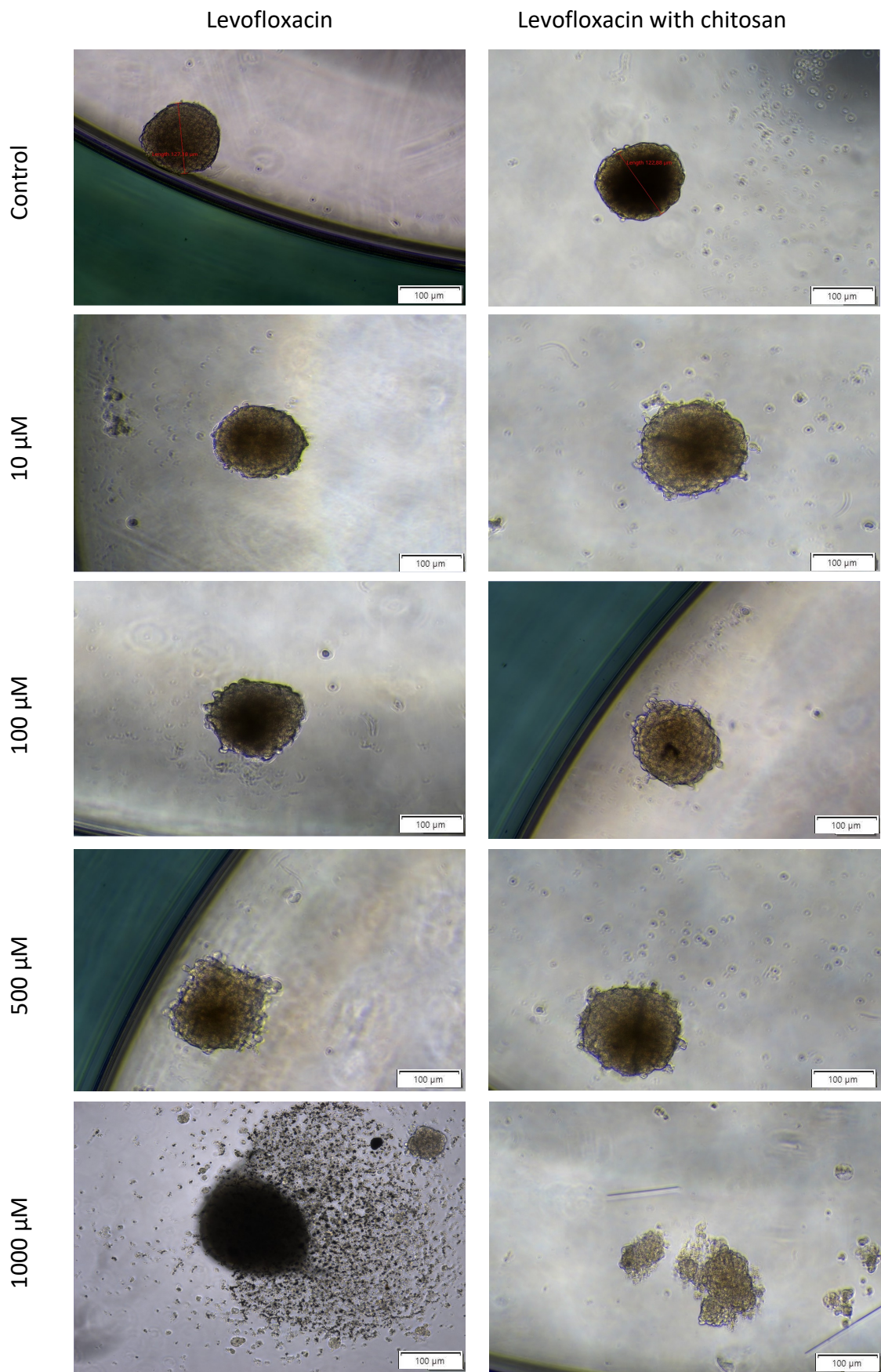


Figure 70. Effect of chemotherapeutic drug levofloxacin on the cell growth 3D-cultured bladder (T24) cancer. Brightfield images of each cell line were captured on day 1 (not shown) and 3 (after 72 hours incubation with drugs).

4.6.2. Live/Dead Assay

There was no significant change of the cytotoxic effect of both frugs, ciprofloxacin alone and modified with chitosan. However, it was detected that the percentage of dead cells in the sample was the highest for the concentration of CIP1000 CHIT and amounts to 87.59% (Fig. 73). The assessment of the ratio of live and dead cells building multicellular spheroids after the action of cytostatic drugs was made using a fluorescence microscope and by measuring the sum fluorescence intensity value for cells stained with calcein AM (green channel) and propidium iodide (red channel) (Fig. 74). The learned neural network detected cells marked as "live" as a yellow field and "dead" as a green field (Fig. 75). Image analysis was performed in the Count and Measure module dedicated Cellsens Dimension software (Olympus, Japan) and it consisted on detecting objects using the "manual threshold" method and counting the detected ones objects with which cells were stained.

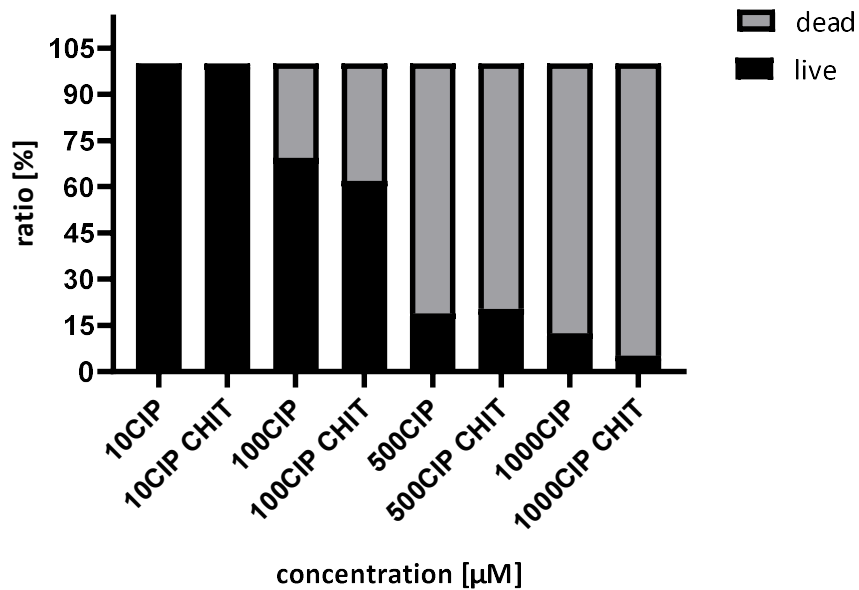


Figure 71. Percentage of live and dead cells T24 cell line cultured in medium containing test drugs ciprofloxacin and ciprofloxacin with chitosan. The evaluation value was measuring the sum fluorescence intensity value.

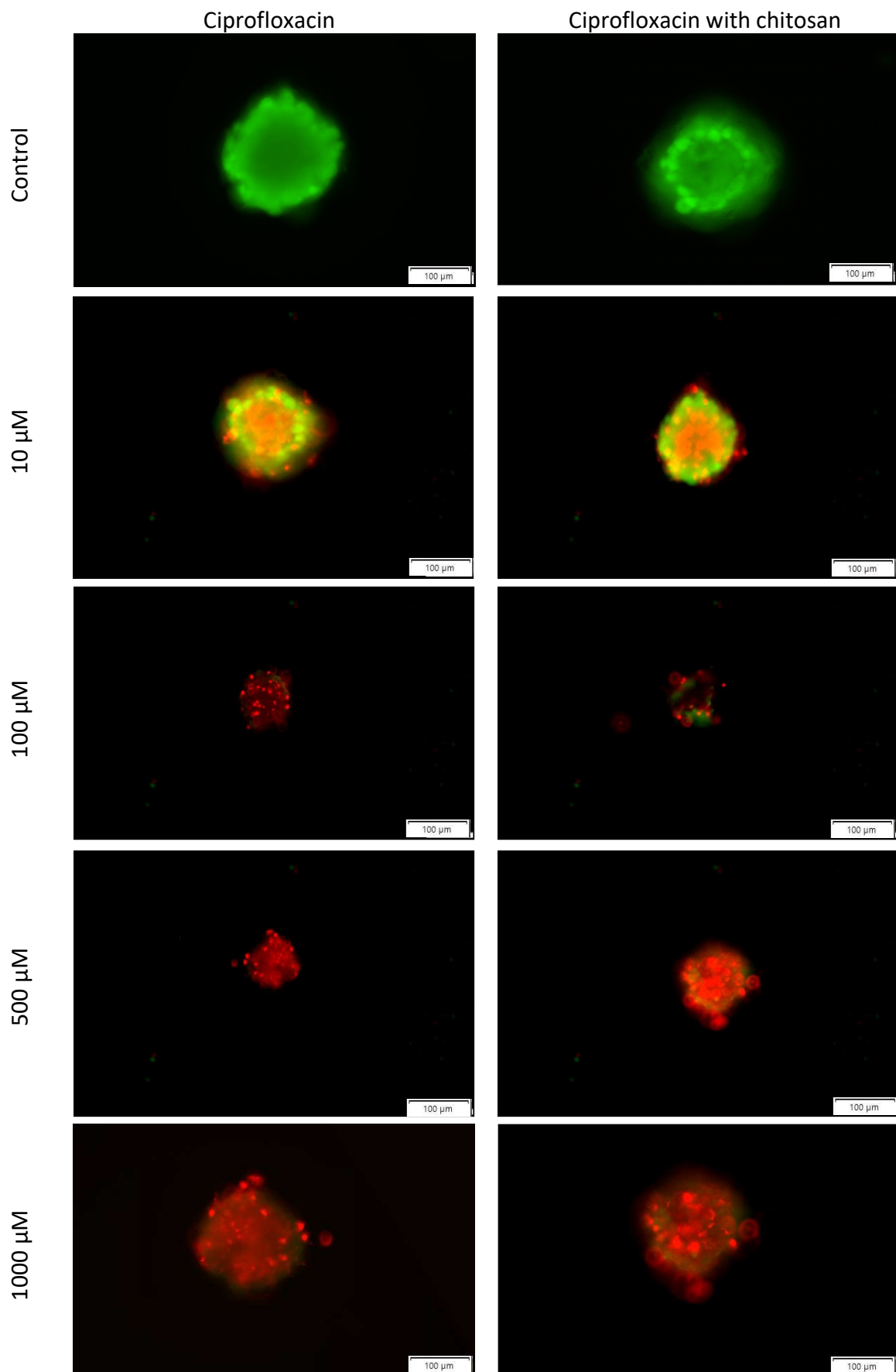


Figure 72. Microscopic images demonstrating how spheroids T24 cell culture conditions influence the visibility of dead cells detected using the fluorescent live/dead assay kit. Cell death was induced by chemotherapeutic agent - ciprofloxacin and ciprofloxacin with chitosan. Imaging Assay of Live or Dead™ Cell Viability.

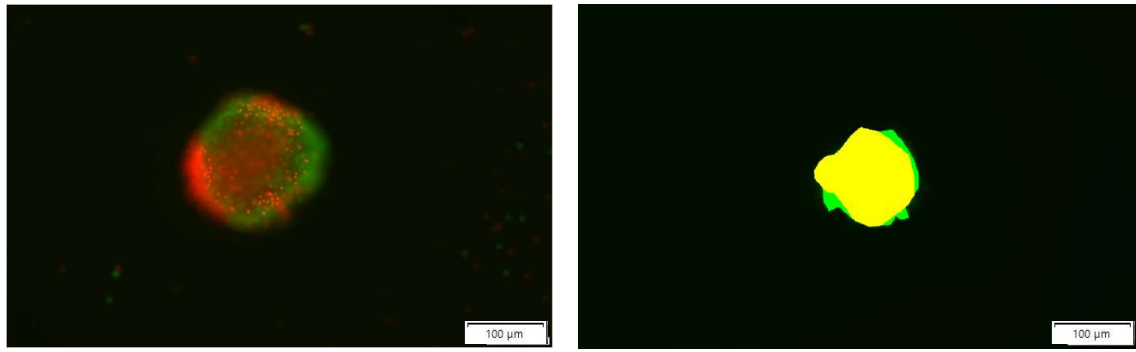


Figure 73. An example of spheroid's microscopic image analysis after incubation in chemotherapeutic agents .
The learned neural network detects cells marked as "live" as a yellow field and "dead" as a green field.

When assessing levofloxacin, it was not found statistically significant differences in the percentage ratio of live and dead cells between the drug combined with chitosan and in its basic form. The lowest level of percentage of viable cells was observed with levofloxacin without modification and this value was 36.64% (Fig. 76). The visualization of these values could be observed in fluorescence microscope images showing photos of stained spheroids (Fig. 77).

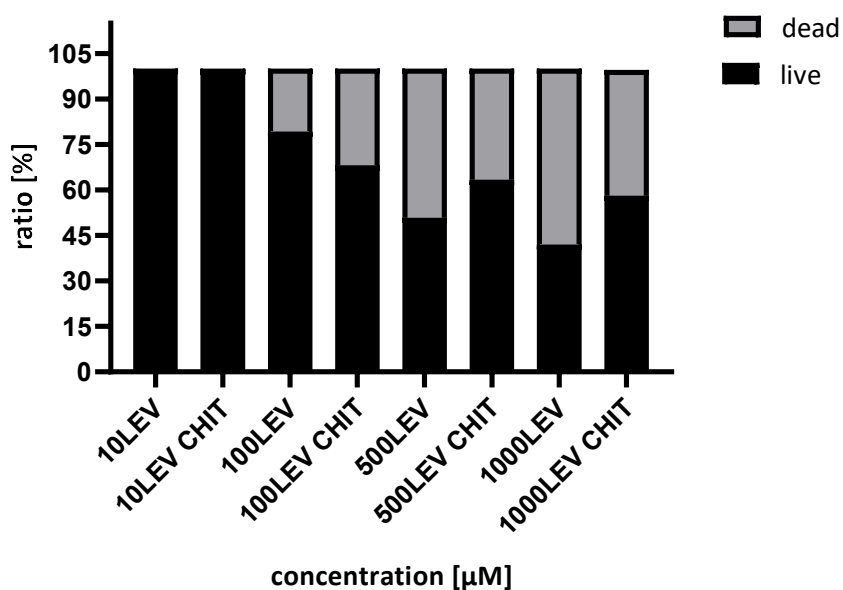


Figure 74. Percentage of live and dead cells T24 cell line cultured in medium containing test drugs levofloxacin and levofloxacin with chitosan. The evaluation value was measuring the sum fluorescence intensity value.

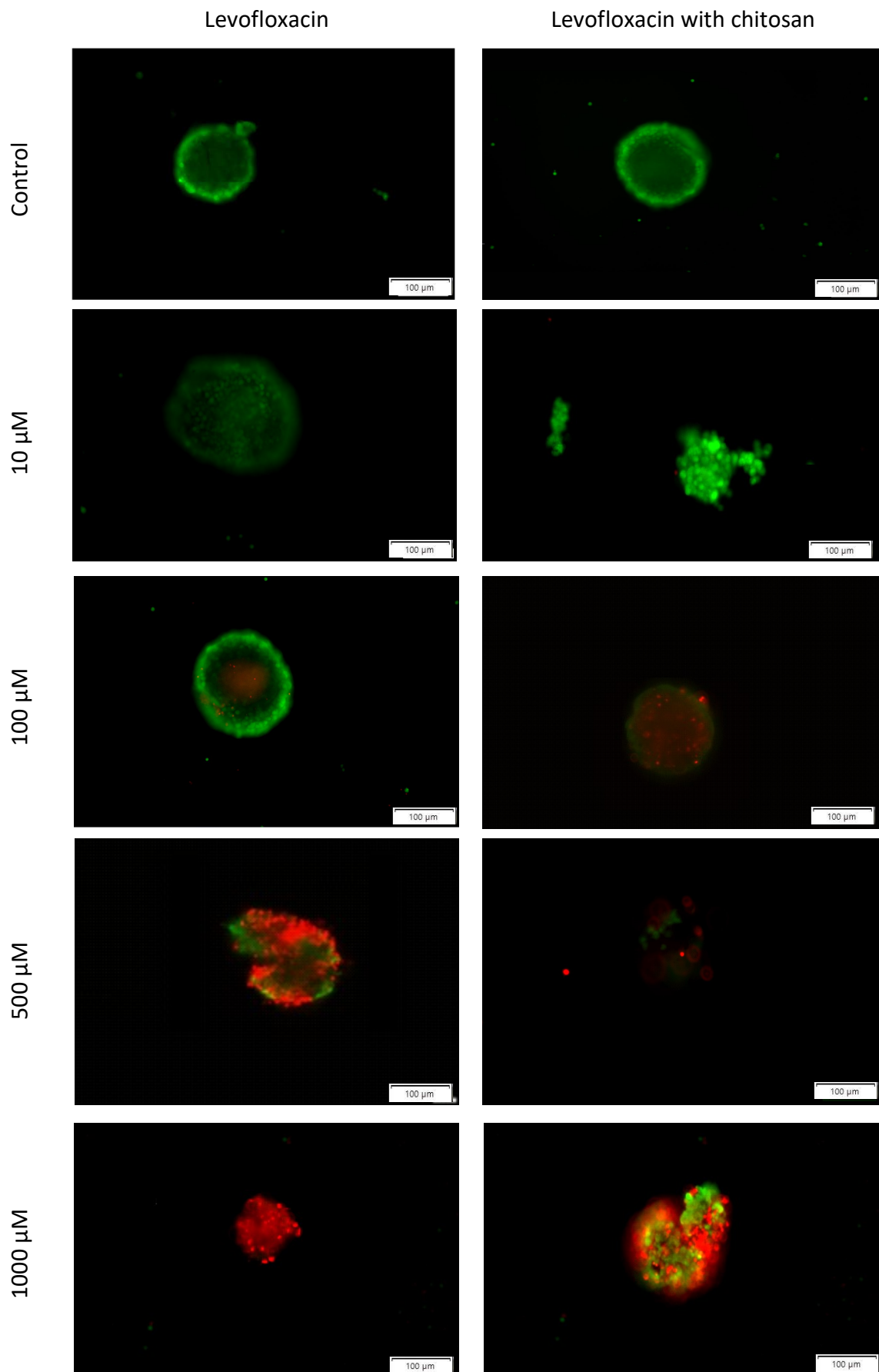


Figure 75. Microscopic images demonstrating how spheroids T24 cell culture conditions influence the visibility of dead cells detected using the fluorescent live/dead assay kit. Cell death was induced by chemotherapeutic agent - levofloxacin and levofloxacin with chitosan. Imaging Assay of Live or Dead™ Cell Viability.

4.6.3. Cell viability assessment by thiazolyl blue tetrazolium bromide assay (MTT)

The results of the experiment on T24 cell line spheroids culture indicated the cytotoxic effect of both ciprofloxacin and modified ciprofloxacin. It was marked a decrease in cell viability increasing with time and concentration.

Statistically significant differences between the drug in the basic form and the modified form were reported in the 24th hour of the experiment for the concentration of 1000 μ M. The difference of spheroids viability was 20.76%. In the 48th-hour of incubation, for the concentration of 500 μ M, a difference in the viability of the spheroids was 14.7% (Fig. 78).

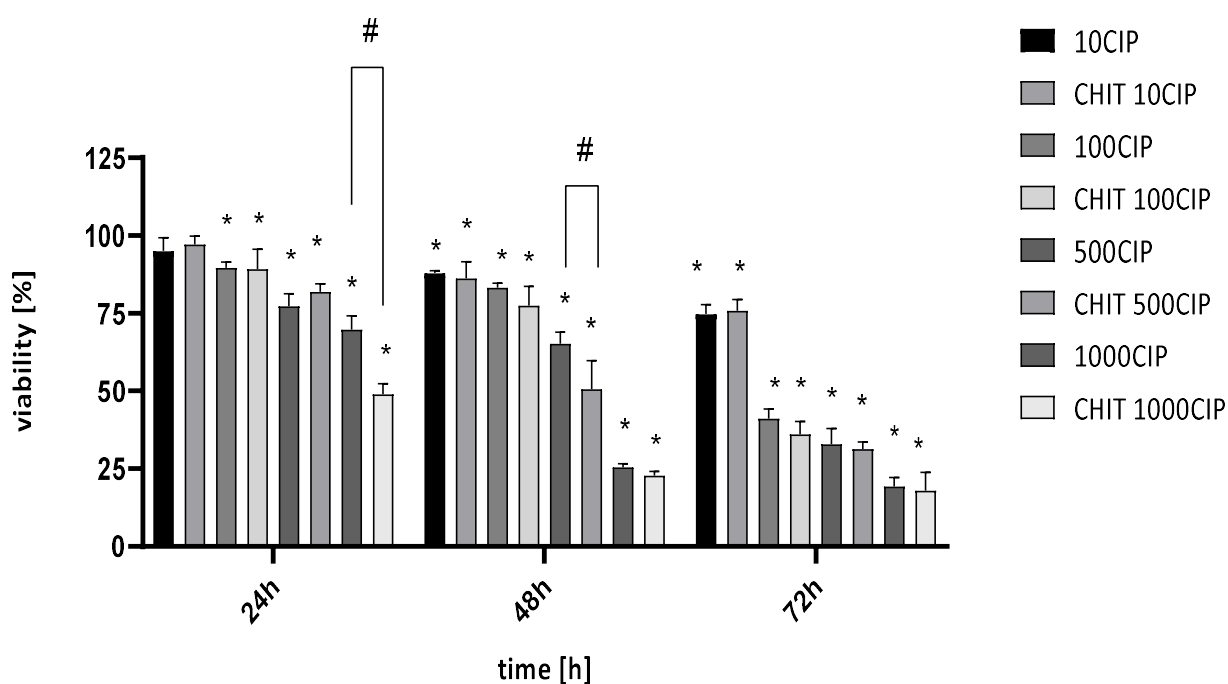


Figure 76. MTT test results for the spheroids of T24 cell line in the following days from the start of incubation with the addition of ciprofloxacin and modified ciprofloxacin in the concentration range of 10-1000 μ M. "*" - statistical significance in relation to the control; "#" - statistically significant difference between the corresponding concentrations of ciprofloxacin and modified ciprofloxacin ($p < 0.05$).

When assessing the viability of multicellular spheroids during cell incubation with both forms of levofloxacin, no statistically significant differences were observed between the tested forms of the drug. Both drugs were cytotoxic, causing a time- and concentration-dependent decrease in viability, but there were no noticeable differences depending on the form of the drug (Fig. 79).

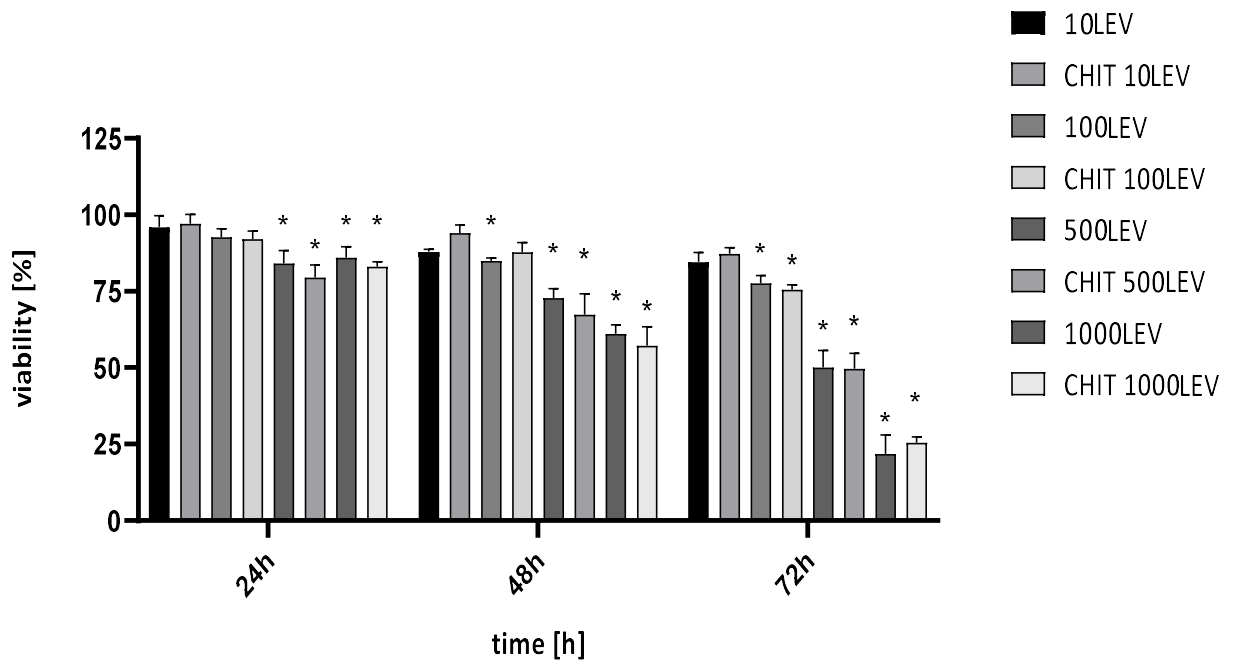


Figure 77. MTT test results for the spheroids T24 cell line in the following days from the start of incubation with the addition of levofloxacin and modified levofloxacin in the concentration range of 10-1000 μM . "*" - statistical significance in relation to the control; no statistically significant difference between the corresponding concentrations of levofloxacin and modified levofloxacin ($p < 0.05$).

As with adherent cultures, using the result of the MTT test, the IC50 value was determined, i.e. the inhibitor concentration, which inhibits 50% of the biological functions of cells in 72 hours of exposure to the tested concentrations of cytostatics. (Tab. 15).

Table 15. IC50 values calculated from non-linear regression curve for test results MTT, the table also shows the fit parameter of the theoretical curve R^2

	2D		3D	
	IC50	R²	IC50	R²
CIP	117.8 μ M	0.9924	131.8 μ M	0.9533
CIP CHIT	136.6 μ M	0.9726	116.9 μ M	0.9548
LEV	422.6 μ M	0.9697	423.6 μ M	0.9776
LEV CHIT	613.6 μ M	0.9726	532.01 μ M	0.9871

4.6.4. Multicellular spheroids growth kinetics analysis

The analysis of the growth kinetics of multicellular spheroids T24 commercial line was carried out using the vital imaging method, without the use of dyes. This method was designed without disadvantages present in other methods, such as: the limit of the tested volume, sensitivity to the initial calibration and the lack of quality control after the end of the experiment.

On the basis of live-imaging observations, the kinetics of spheroid growth depending on time and concentration of the test drug was determined (Fig. 80). Area was calculated every minute of the experiment on the basis of a trained neural network. At concentrations in the range 10-500 μM , a slower growth of spheroids compared to the (red line control) was observed (Fig. 80). The collected data indicated a rapid reduction in the size of the spheroid for 1000 μM , which, combined with the microscopic image (Fig. 81), can be assessed as the disintegration of the multicellular spheroids.

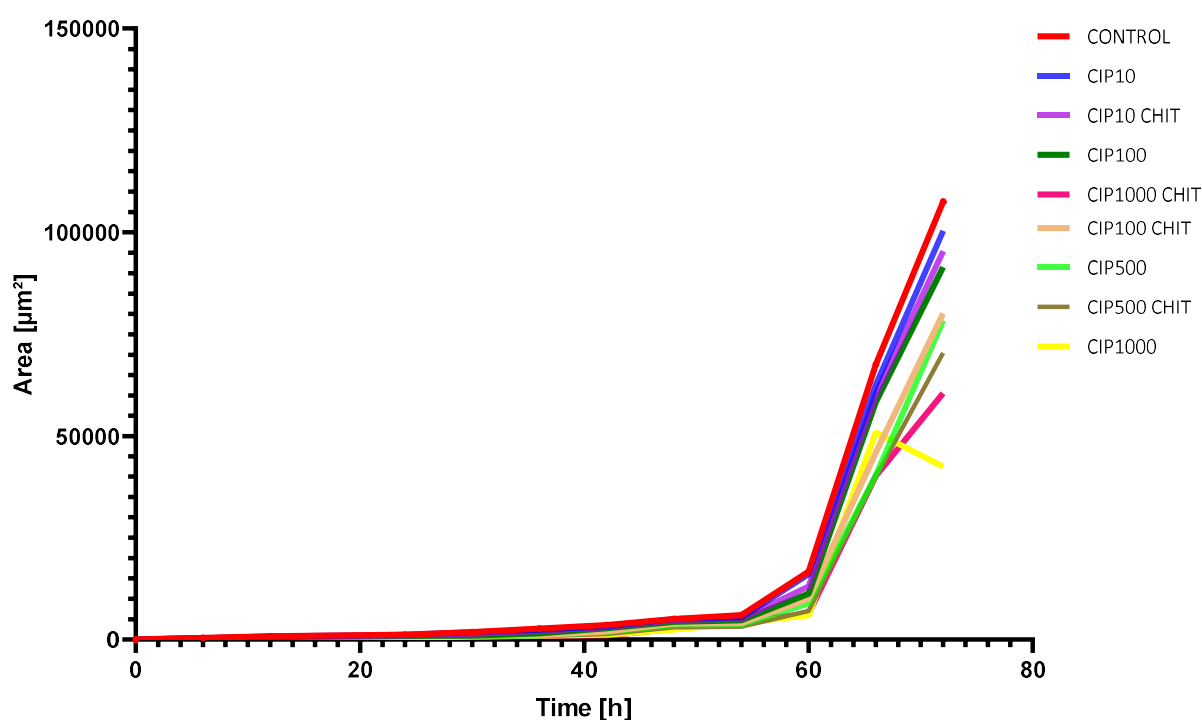


Figure 78. Kinetics of spheroid growth depending on time and concentration of the test drug was determined. The graph shows the data: changing area of the spheroid [μm^2] incubated in ciprofloxacin and chitosan-modified ciprofloxacin in time [h].

During the kinetic imaging without the use of dyes (real-time, stain-free live-imaging), the observation of each spheroid was recorded in the form of a video (Fig. 81). The photos showed single frames from sample videos.

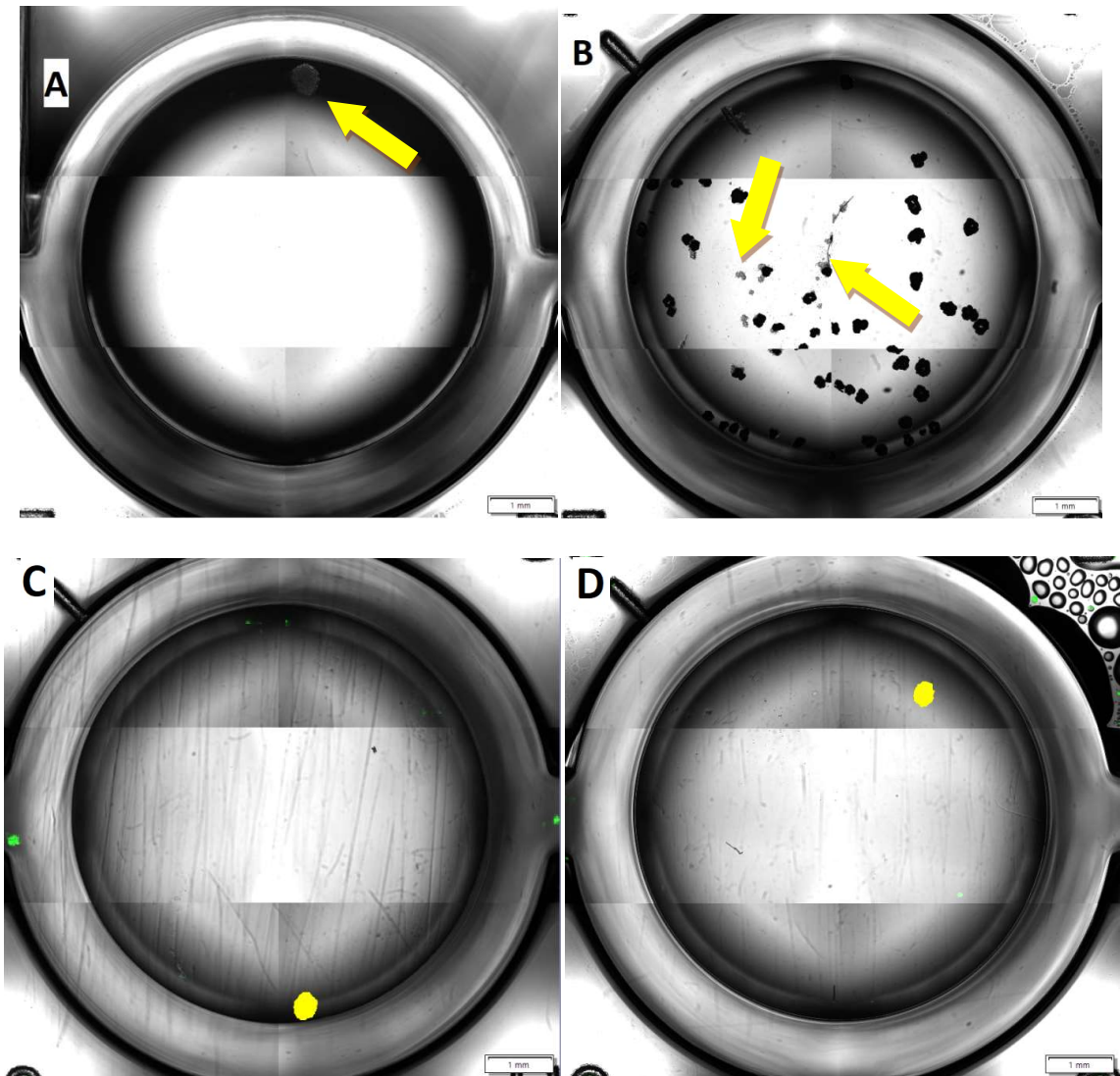


Figure 79. Arrows indicate spheroids (A) – control without drug, (B) - disintegrating spheroid after 72 hours incubation in the highest concentration of ciprofloxacin. A trained neural network detected spheroids and marking the cell fields with yellow color (C and D).

Considering the levofloxacin supplemented spheroids culture, the kinetics of spheroid growth depending on time and concentration of the test drug was determined. Spheroids' surface was calculated every minute of the experiment on the basis of a trained neural network and it was noticed that concentrations in the range 10-500 μM did not have significant influence. The collected data indicated a rapid reduction in the size of the spheroid for 1000 μM , which, combined with the microscopic image (Fig. 82), can be assessed as the disintegration of the multicellular spheroids what was confirmed with microscope images (Fig. 83).

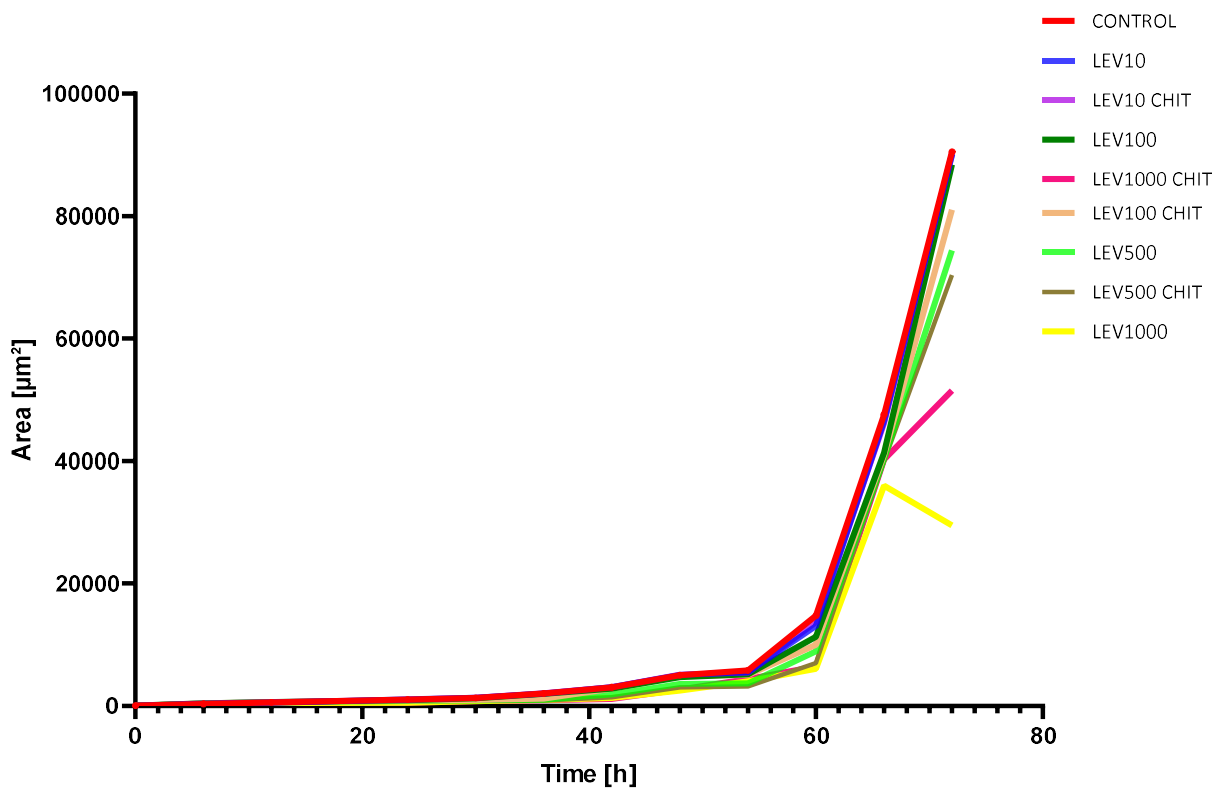


Figure 80. On the basis of live-imaging observations, the kinetics of spheroid growth depending on time and concentration of the test drug was determined. The graph shows the data: changing area of the spheroid [μm^2] incubated in levofloxacin and chitosan-modified levofloxacin in time [h]. Area was calculated every minute of the experiment on the basis of a trained neural network.

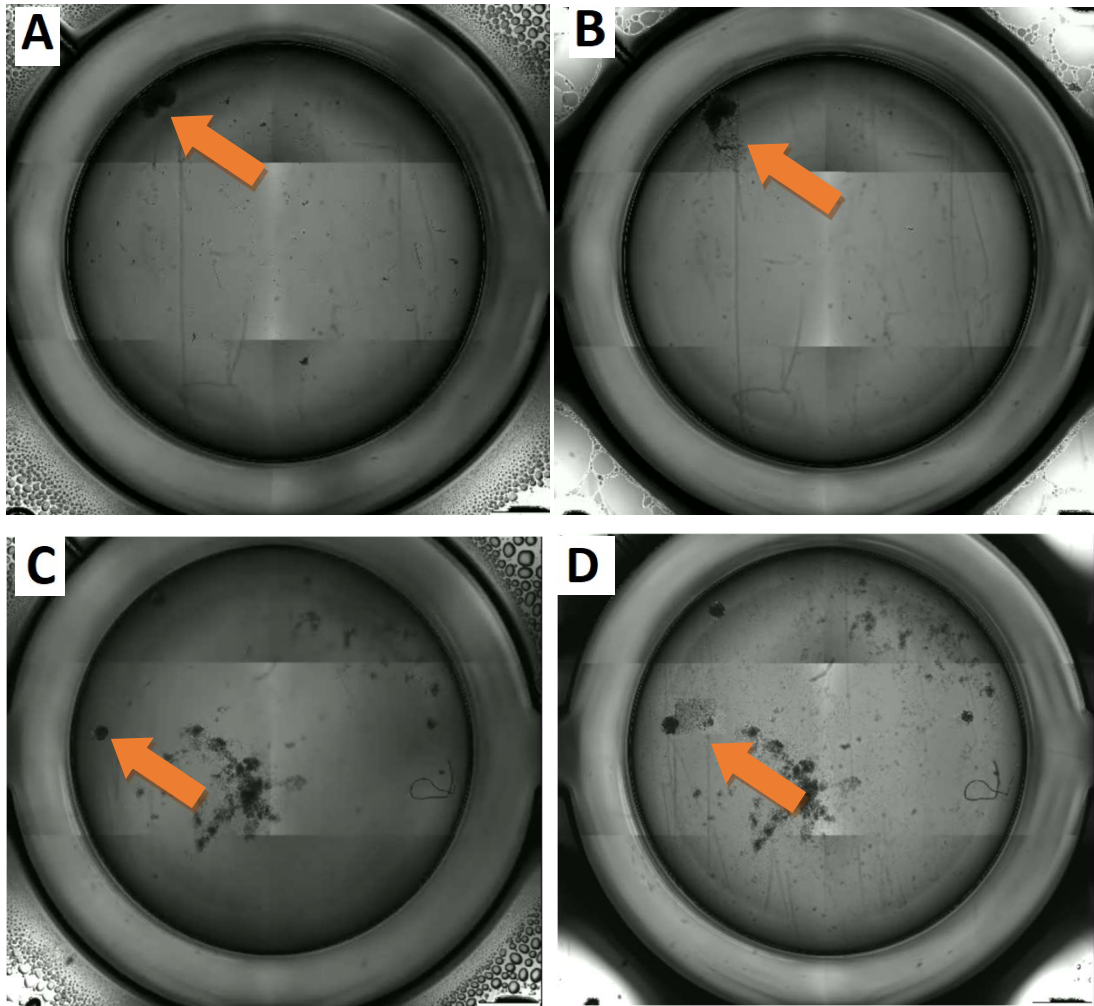


Figure 81. During the kinetic imaging without the use of dyes (real-time, stain-free live-imaging), the observation of each spheroid was recorded in the form of a video. The photos show single frames from sample videos. Arrows indicate spheroids (A) – 1000 μM levofloxacin after 1 hour, (B) - disintegrating spheroid after 72 hours incubation in the highest concentration of levofloxacin. (C) - 1000 μM levofloxacin with chitosan after 1 hour, (D) - disintegrating spheroid after 72 hours incubation in the highest concentration of levofloxacin with chitosan.

4.7. Multicellular spheroids - *Picea abies* tree extract drugs modification

4.7.1. Assessment of cell viability in a microscope with inverted optics

When evaluating spheroids grown from T24 cells, regular shapes of spheroids in the culture even after 72 hours were reported. In the case of increasing concentrations of both ciprofloxacin (Fig. 84) and levofloxacin (Fig. 85), a loss of spheroid structure integrity in the range of 100-500 μM was observed, while at the highest concentration of 1000 μM , complete breakdown of the cellular structure. The lowest tested concentration, 10 μM , did not cause structural and morphological changes visible under the microscope.

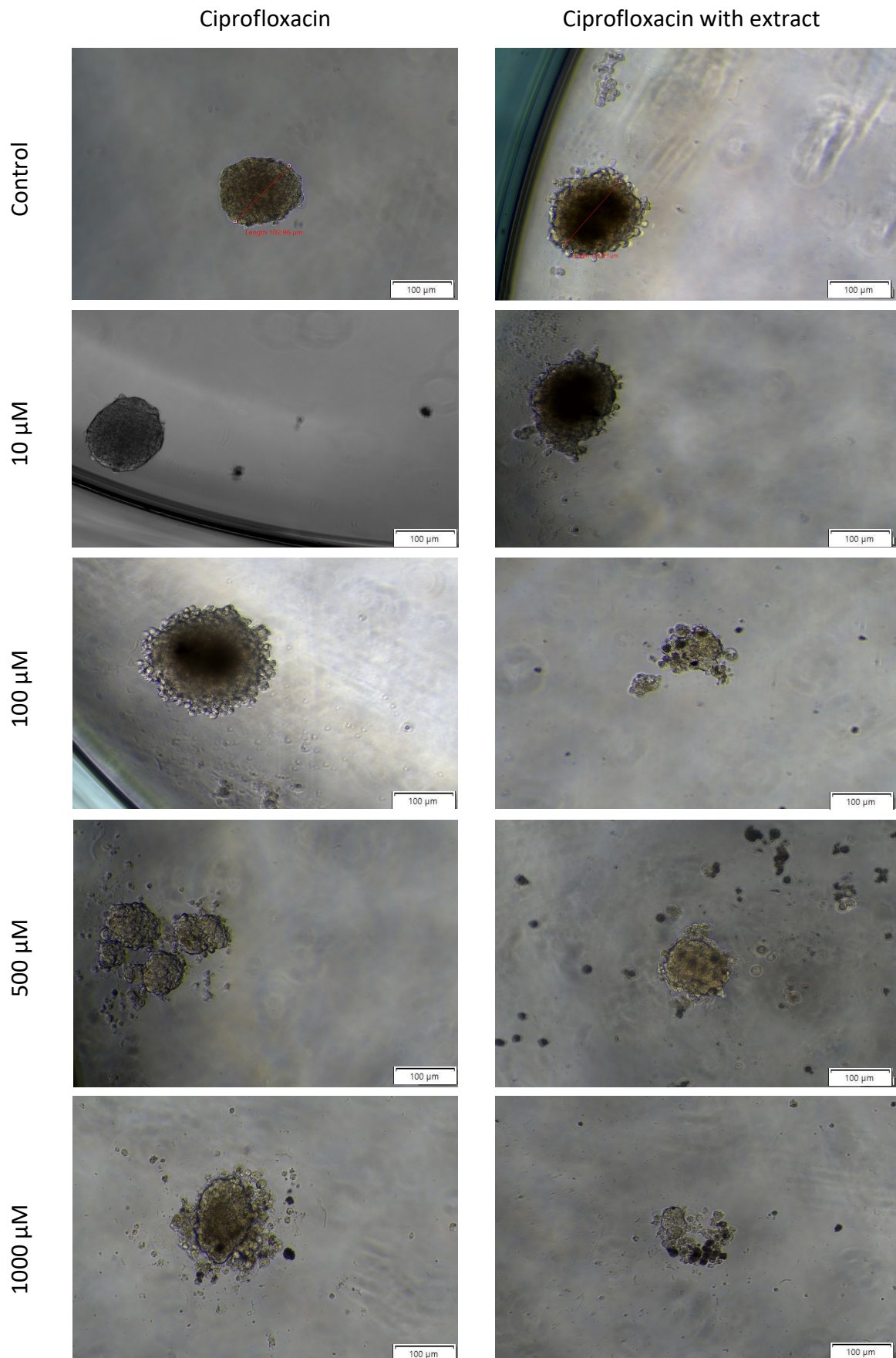


Figure 82. Effect of chemotherapeutic drug ciprofloxacin on the cell growth 3D-cultured bladder (T24) cancer. Brightfield images of each cell line were captured on day 1 (not shown) and 3 (after 72 hours incubation with drugs).

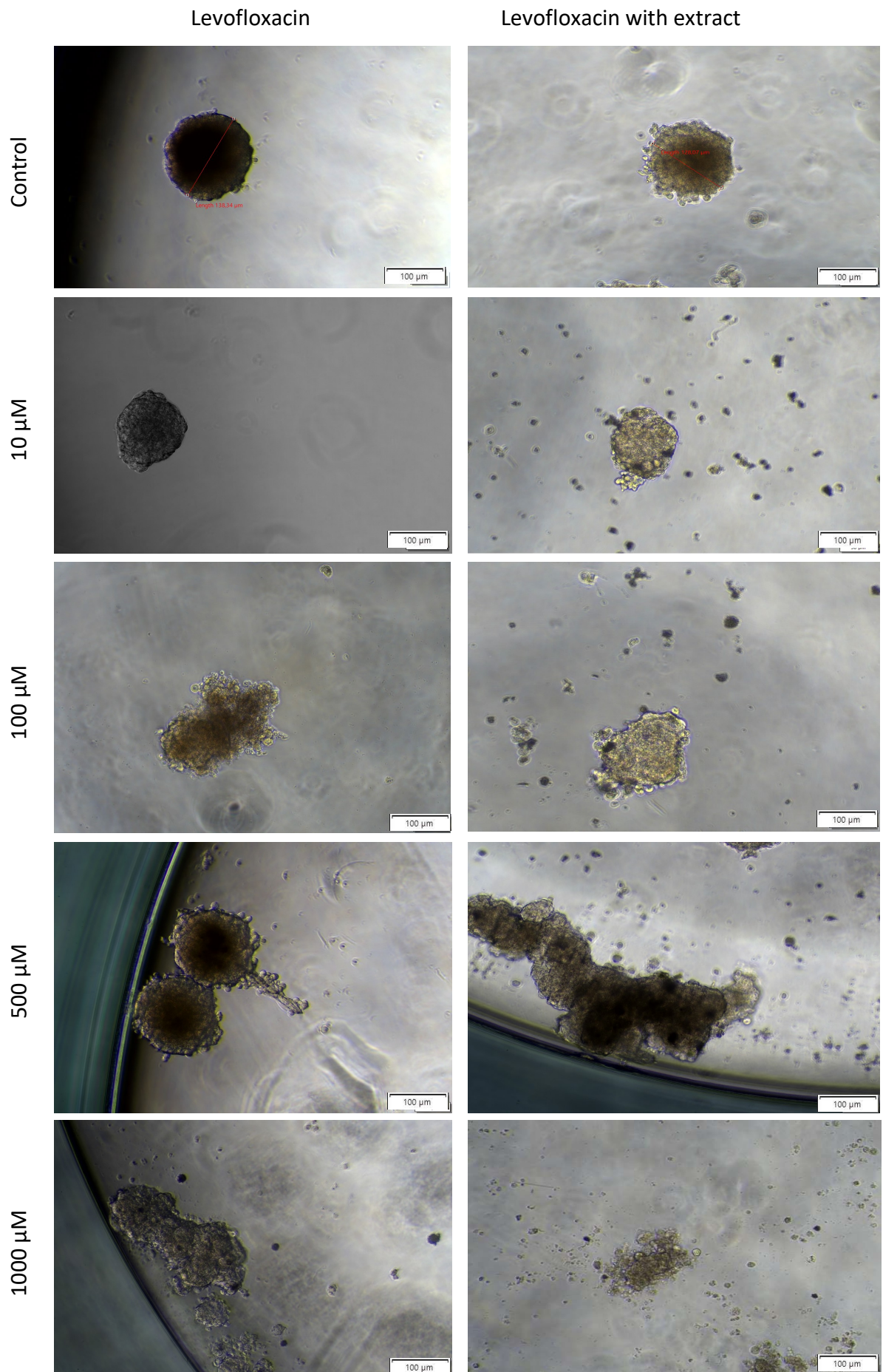


Figure 83. Effect of chemotherapeutic drug levofloxacin on the cell growth 3D-cultured bladder (T24) cancer. Brightfield images of each cell line were captured on day 1 (not shown) and 3 (after 72 hours incubation with drugs).

4.7.2. Live/Dead Assay

Comparing the intensity of cell radiance in the case of incubation of spheroids with ciprofloxacin, it was noticed that the addition of plant extract causes a statistically significant difference in the percentage of dead cells in the sample for the highest concentration of the drug, and for the concentration of 1000CIP 5% EX it was 5.34% (Fig. 86), where in the case of 1000CIP it was 18.52%. However, interestingly, when added to the 500CIP concentration of 5% of the extract, it gave similar results as the use of 1000CIP. The ratio of live and dead cells forming multicellular spheroids after the treatment of cytostatics was assessed using a fluorescence microscope and by measuring the total fluorescence intensity for cells stained with calcein AM (green channel) and propidium iodide (red channel) (Fig. 87).

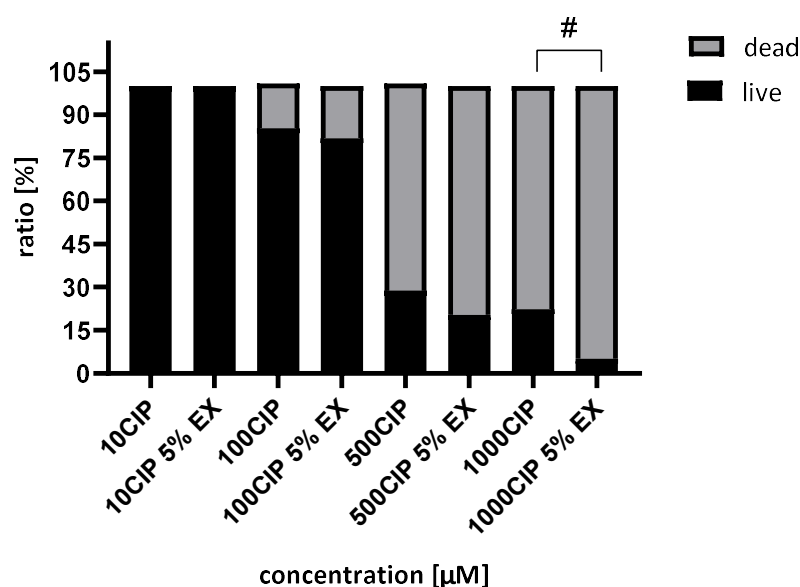


Figure 84. Percentage of live and dead cells T24 cell line cultured in medium containing test drugs ciprofloxacin and ciprofloxacin with extract. The evaluation value was measuring the sum fluorescence intensity value.

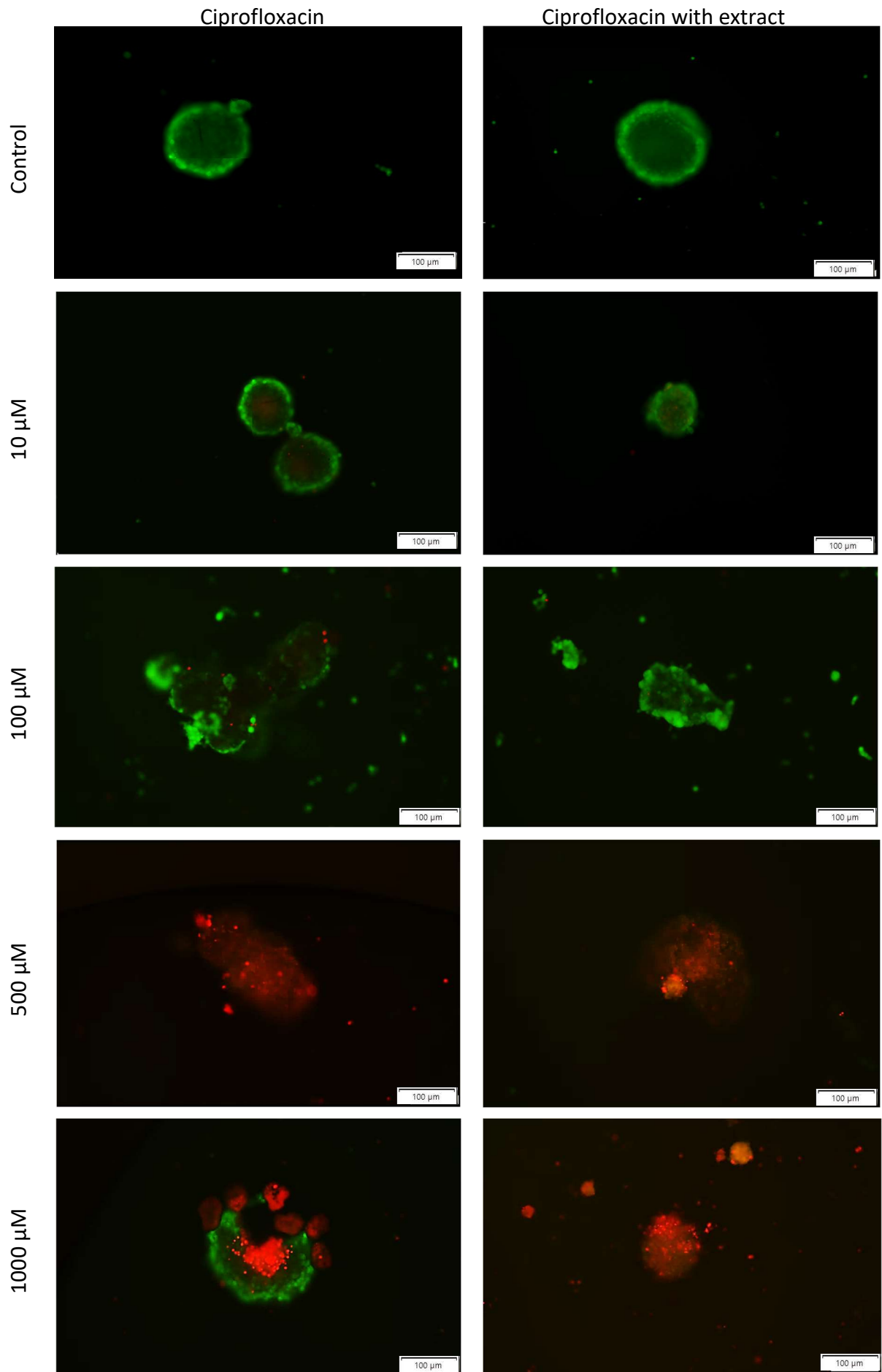


Figure 85. Microscopic images demonstrating how spheroids T24 cell culture conditions influence the visibility of dead cells detected using the fluorescent live/dead assay kit.

When evaluating the effect of levofloxacin, it was observed that the addition of plant extract causes a statistically significant difference in the percentage of dead cells in the sample for the highest concentration of the drug, and for the concentration of 1000LEV 5% EX it was 17.26% (Fig. 88). For the remaining concentrations, the values for the modified and unmodified drug did not show significant differences. The ratio of live and dead cells forming multicellular spheroids after the treatment of cytostatics was assessed using a fluorescence microscope and by measuring the total fluorescence intensity for cells stained with calcein AM (green channel) and propidium iodide (red channel) (Fig. 89).

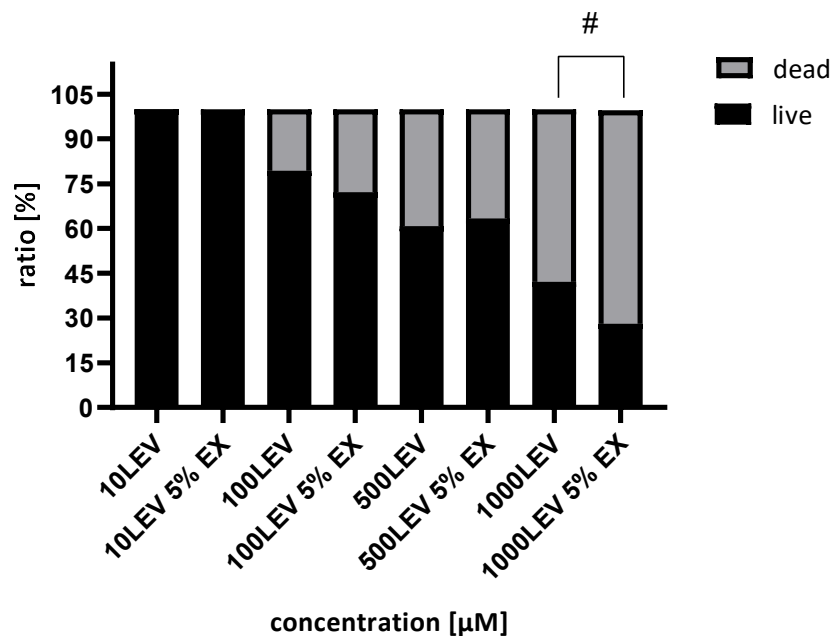


Figure 86. Percentage of live and dead cells T24 cell line cultured in medium containing test drugs levofloxacin and levofloxacin with chitosan. The evaluation value was measuring the sum fluorescence intensity value.

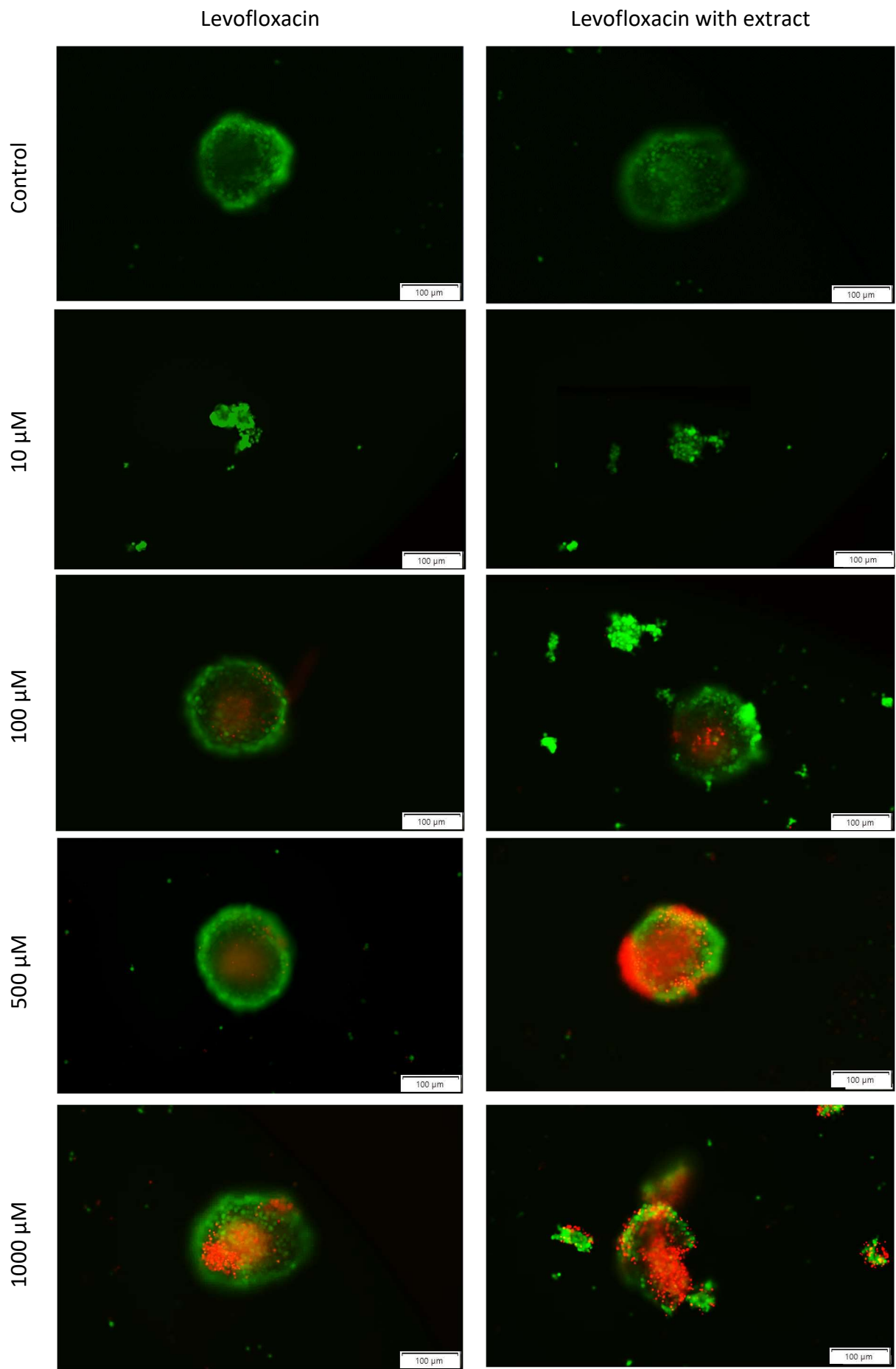


Figure 87. Microscopic images demonstrating how spheroids T24 cell culture conditions influence the visibility of dead cells detected using the fluorescent live/dead assay kit.

4.7.3. Cell viability assessment by thiazolyl blue tetrazolium bromide assay (MTT)

Tetrazole-based assays were optimized for the assessment of adherent cell toxicity, however, the use of these assays to assess spheroids brings challenges, such as the even distribution of tetrazole. However, numerous scientific reports have shown that the MTT test is non-toxic and shows the highest sensitivity in assessing spheroids toxicity among known tetrazole-based tests and can be successfully used in the evaluation of spheroids [111].

The ciprofloxacin-treated spheroids showed statistically significant differences in the level of viability at 24 hours of the experiment for the highest concentration of the tested drug. The difference in viability of cells treated with ciprofloxacin and ciprofloxacin with chitosan was 14.09 % (Fig. 90). This difference persisted up to 48 hours of the experiment, while at the last observation point, the differences between the highest concentrations of ciprofloxacin in both forms of the drug were lower and no longer statistically significant.

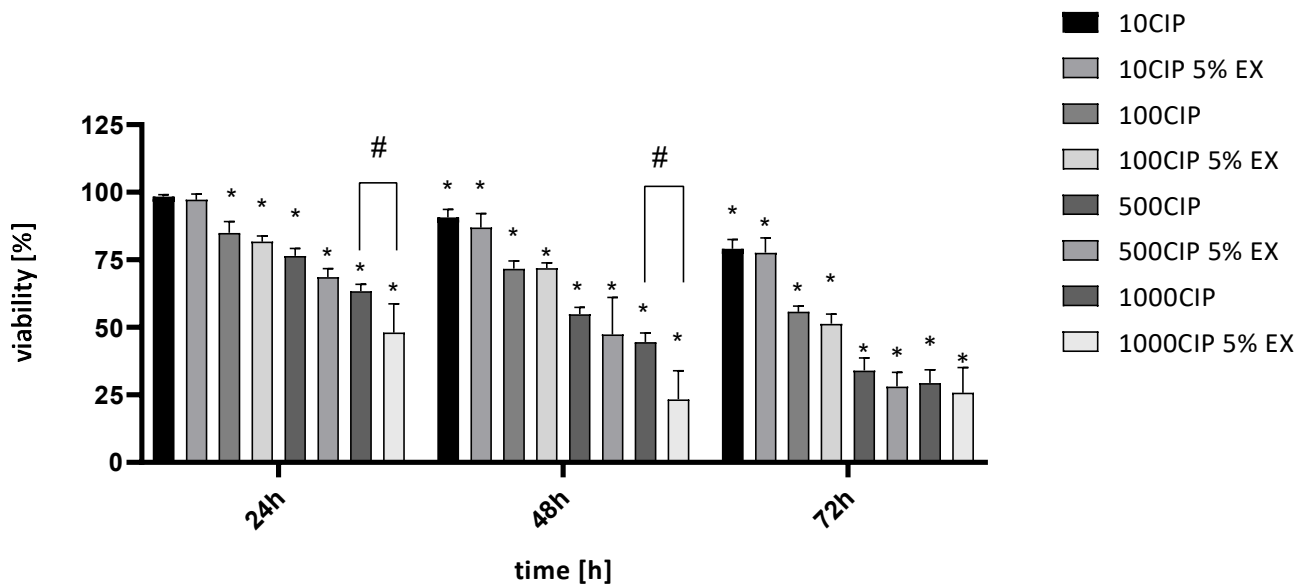


Figure 88. Viability of the spheroids of T24 cell line in the following days from the start of incubation with the addition of ciprofloxacin and modified ciprofloxacin in the concentration range of 10-1000 μ M. "*" - statistical significance in relation to the control; "#" - statistically significant difference between the corresponding concentrations of ciprofloxacin and modified ciprofloxacin ($p < 0.05$).

In assessing the viability of bladder cancer cell spheroids using the MTT method, any statistically significant difference during the experiment was noted (Fig. 91). The highest decrease in viability was caused by the highest concentrations of levofloxacin, reaching the lowest value of 19.35%.

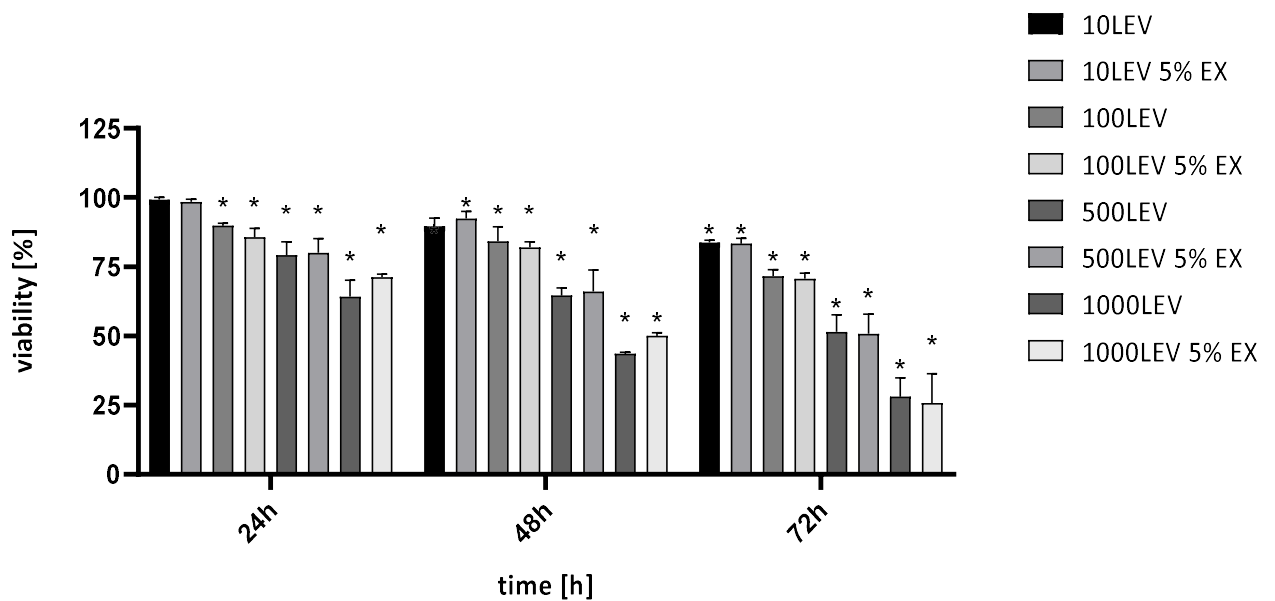


Figure 89. Viability of the spheroids of T24 cell line in the following days from the start of incubation with the addition of levofloxacin and modified levofloxacin in the concentration range of 10-1000 μ M. "*" - statistical significance in relation to the control; no statistically significant difference between the corresponding concentrations of levofloxacin and modified levofloxacin ($p < 0.05$).

Determination of regression curves based on the results of the MTT test, the IC50 values inhibiting 50% of the viability of cells building the multicellular spheroid were estimated (Tab. 16). The table compares the concentration values determined for the T24 cell line in the adherent culture (2D) and the culture of multicellular spheroids 3D. It could be observed that the cells grown in the spheroids seem to be more sensitive to the drugs because the achieved IC50 values were slightly lower. It was also observed that the addition of plant extract reduces the concentration of equine ciprofloxacin to IC50 in the case of spheroid cultures.

Table 16. IC50 values calculated from the results of the MTT assay for the T24 cell line in 2D and 3D culture.

	2D		3D	
	IC50	R²	IC50	R²
CIP	187.5 μ M	0.9574	131.8 μ M	0.9583
CIP 5% EX	198.4 μ M	0.9600	190.9 μ M	0.9678
LEV	490.0 μ M	0.9685	423.6 μ M	0.9976
LEV 5% EX	539.4 μ M	0.9627	602.04 μ M	0.9791

4.7.4. Multicellular spheroids growth kinetics analysis

Analyzing the growth kinetics of spheroids of T24 cells incubated in dilutions of ciprofloxacin with supplemented plant extract (Fig. 92), the graph indicates a clear break in the growth line, suggesting the disintegration of spheroid structures at the 60th hour of incubation. After this time, a clear decrease in the size of the spheroids was noticeable for concentrations ranging from 100-1000 μM drugs with the addition of extract.

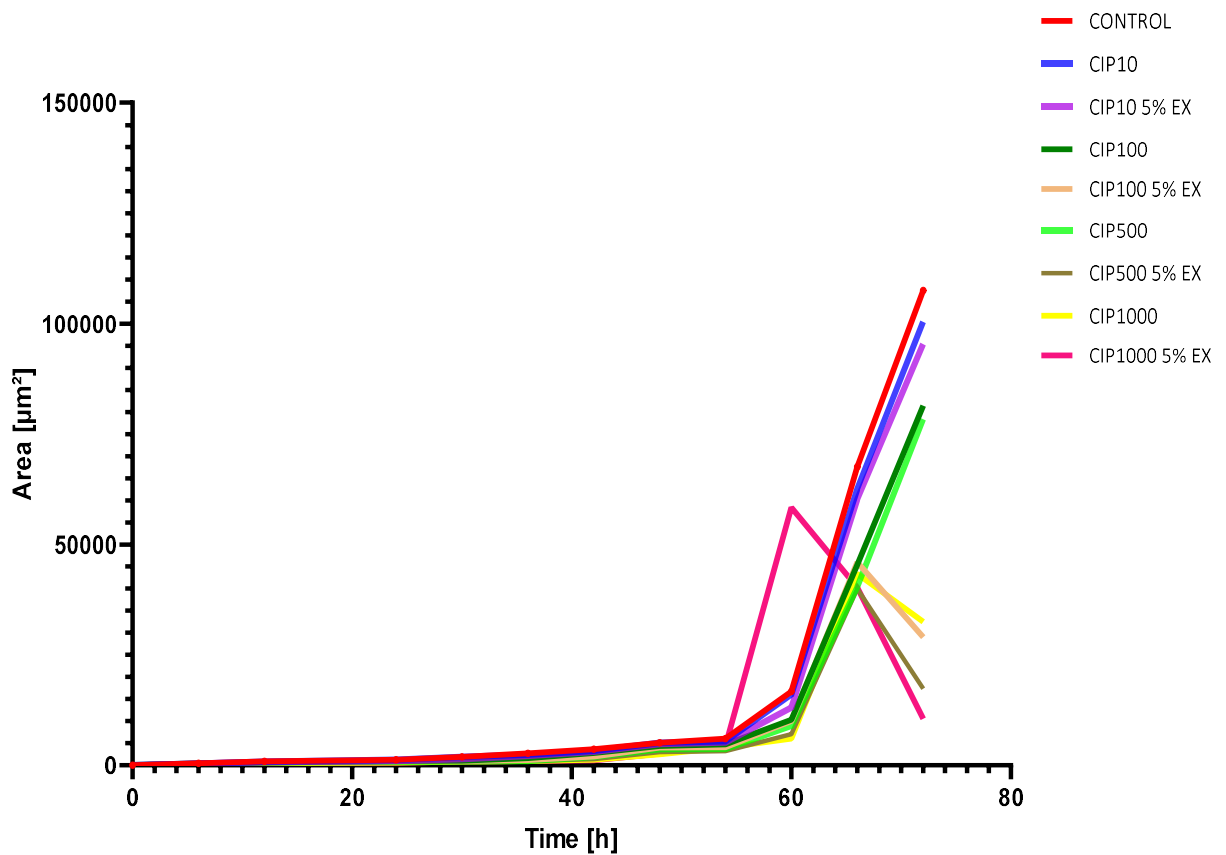


Figure 90. Graph illustrated the kinetics of spheroid growth depending on time and concentration of the test drug was determined. The graph shows the data: changing area of the spheroid [μm^2] incubated in ciprofloxacin and extract-modified ciprofloxacin in time [h].

The observation of the line determined on the basis of the growth of spheroids incubated with levofloxacin revealed a slower growth for concentration in the range of 10-500 μM , compared to the control (red line) (Fig. 93). The 1000 μM drug concentration, caused the spheroids eradication in the 70th hour of the experiment. After this time, the spheroids broke down into smaller and smaller fragments. This decay was also clearly noticeable in the photos taken during the observation of the kinetics of growth (Fig. 94).

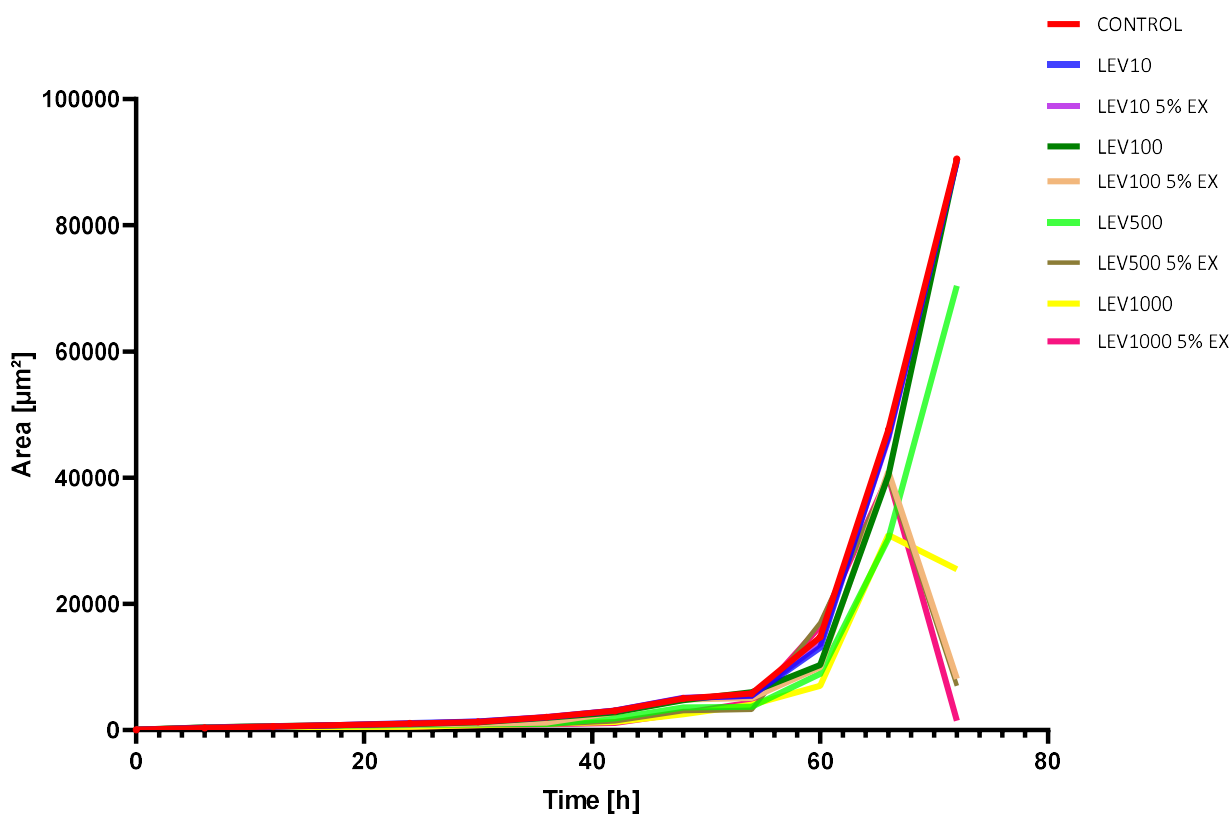


Figure 93. Graph illustrated the kinetics of spheroid growth depending on time and concentration of the test drug was determined. The graph shows the data: changing area of the spheroid [μm^2] incubated in levofloxacin and extract-modified levofloxacin in time [h].

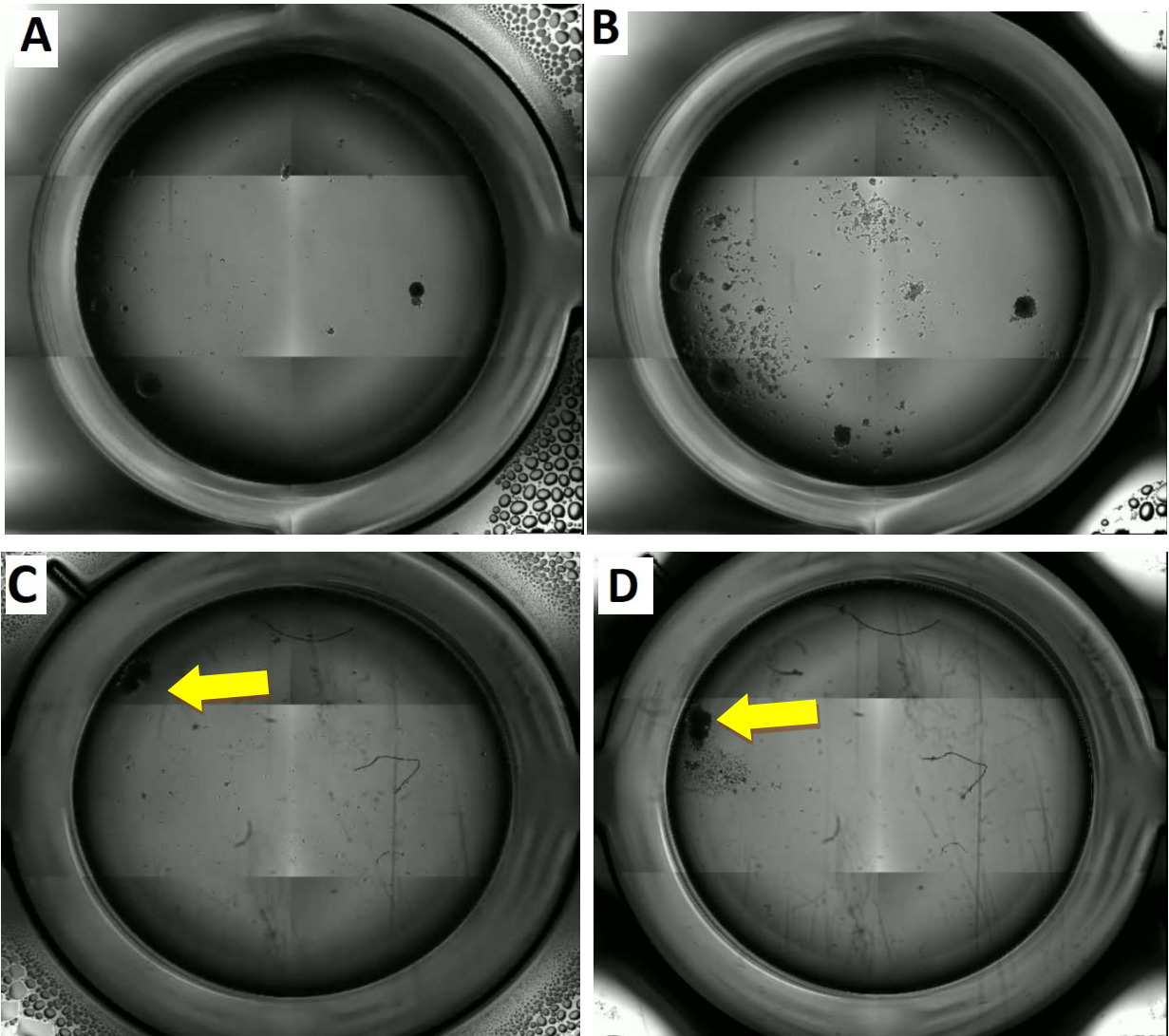


Figure 94. Arrows indicate spheroids (A) – spheroids after 24 hours incubation levofloxacin, (B) - disintegrating spheroid after 80 hours incubation in the highest concentration of levofloxacin, (C) - spheroids after 24 hours incubation levofloxacin with natural extract and (D) - disintegrating spheroid after 80 hours incubation in the highest concentration of levofloxacin with extract.

5. Discussion

The studies conducted during PhD research confirmed the cytotoxic effect of second generation (ciprofloxacin) and third generation (levofloxacin) fluoroquinolones on urogenital cancer cell lines. The tests also showed that the modification of these drugs in combination with chitosan and a European Spruce *Picea abies* extract needles can significantly increase the cytotoxic potential of the tested drugs.

In order to proper characterization of tested drugs on prostate and bladder cancer cell lines, all performed analyzes had a screening nature. As part of the presented doctoral dissertation, it was necessary to collect information on the key parameters of the subjects, such as: metabolic activity, proliferative potential, growth kinetics, apoptosis analysis and morphology assessment. The concentrations of chemotherapeutic agents were selected in order to find the so-called biological effect, i.e. the result observable in the applied biological tests. All substances were analyzed in concentrations achievable in the patient's blood, which may be important from the clinical application point of view [108]. The physicochemical properties of the tested compounds, in particular their solubility, were also very important. That is way all drugs were dissolved in PBS. Worth to note that the ciprofloxacin used in the *in vitro* study differs from that used clinically. The form of ciprofloxacin administrated orally, contains additional components such as HCl and lactic acid [109]. As a result, it is better absorbed in the body and has better solubility. Unfortunately, if these components were used in *in vitro* studies, the mortality of cancer cells could be mainly due to a significant decrease in pH. Therefore, it was necessary to use a different solvent, which was rebuffered PBS at pH 4.7. Unfortunately, lower solubility was obtained, which was associated with the precipitation of ciprofloxacin crystals. This problem was avoided with levofloxacin due to satisfied solubility in the neutral medium.

5.1. Chitosan as a biopolymer in drug modification

All of the tests performed as a part of presented PhD thesis confirms the trend of nano and biotechnology as a promising field in development of new drug delivery systems [110]. Small and even large molecules can be transported with such target-specific drug delivery systems and can be useful for diagnosis and treatment of cancer. In this light, chitosan as

a potential drug carrier, turned out to be a very promising agent for the development of new anti-cancer drugs [111].

Bladder and prostate cancer cell survival was the basic parameter studied with the use of MTT and WST8 assays. It was shown that statistically significant differences in the viability of bladder cancer cells were observed after 24 hours incubation with 100 μM and 1000 μM ciprofloxacin. It also indicated that encapsulation of ciprofloxacin together with chitosan can be a reasonable choice. This effectiveness was also confirmed by WST8 assay after 48 hours of incubation. For levofloxacin, it was also confirmed that higher cytotoxic effect was reported after 72 hours of incubation with the highest concentration of the drug. Research conducted by Sharma P.C. et al. [112] showed that main problem with local, intracervical application of fluoroquinolones is the blood-urine barrier. It limits the penetration of cytostatic into the deeper layers of the urinary tract epithelium. However, it also was proved, that helps in overcoming systemic side effects. Interestingly, in research conducted in presented PhD thesis, it was noted that the use of drugs encapsulated with chitosan causes similar cytotoxic effect, even with lower dose of ciprofloxacin (500 μM). The viability of cancer cells was reduced at similar level as the twice higher dose of the drugs without modification. It may suggest better drug stabilization with the similar cytotoxic effects. In further studies, it will be possible to focus on optimization of drugs doses, so that with the minimum applied encapsulated dose, the highest cytotoxic effects can be achieved.

Cytotoxic analysis, determined on the basis of MTT, revealed that ciprofloxacin modified with chitosan possessed cytotoxic effect against DU145 (prostate cancer) with IC₅₀ value 153.12 μM . In other cases, IC₅₀ is achieved at higher concentrations which may indicate slower action of drugs over time caused their gradual release. Similar studies were conducted by Al-Musawi and his team, they used 5-Fluorouracil modified with chitosan on T24 cell line. It significantly inhibited proliferation of cancer cells in time and dose dependent manner in comparison to the bare nanoparticle and free 5-Fluorouracil [113].

Aforementioned results suggest that modification with chitosan enhances the cytotoxic effect of different drugs with anti-cancer potential. It is consistent with observation made in presented PhD thesis.

An equally important parameter was the ability to proliferate, i.e. to conduct cell division, assessed on the basis of the BrdU assay. The results of proliferation tests correlate to a greater extent with the assessment of viability. Also noticed significant differences between the modified drug and the basic form in the highest concentrations of the tested drugs. These results are confirmed by reports of other scientists [114, 115].

Literature reports show that while chitosan reduces the adhesion and proliferation of the primary melanoma tumor line, it also shows a strong pro-apoptotic effect [116]. In the studied cells, inhibition of specific caspases confirmed that apoptosis occurred via the mitochondrial pathway. More interestingly, exposure to chitosan induced expression of CD95 receptors on the surface of cancer cells, making them more susceptible to apoptosis. The studies carried out also show high levels of cells in the apoptotic phase in samples treated with modified drugs, both ciprofloxacin and levofloxacin. The level of apoptotic cells is apparently much higher than in the case of the basic forms of the drug. These results are confirmed by numerous scientific reports that show DNA fragmentation, which is characteristic of apoptosis, and elevated caspase-3-like activity in chitosan-treated cancer cells [117, 118].

As shown by the research of other scientists in the assessment of biomaterials, the live/dead test plays an important role [119]. Such analysis combined with other methods assessing proliferation and viability, can be correlated with the cell survival rate [120]. Results performed on the bladder carcinoma cell lines, revealed significant differences in the ratio of live/dead cells when comparing the highest doses of the ciprofloxacin. No major differences were observed for levofloxacin. However, as indicated in the literature reports on research conducted on bacterial cells with the low content of live microorganisms in the samples coated with chitosan confirmed the similar survival results [121]. Further studies are definitely needed to determine the viability reducing effect of not only chitosan but also other similar agents in a concentration-dependent manner. Presented results may also influence on the development of the microcapsules formula (size, amount) and the dose which can be used in clinical application.

Described by Ahmadi Nasab [122], modifications with chitosan give many opportunities for evaluating new drug characteristics, for example, releasing it in the appropriate pH of the environment. The performed studies showed that chitosan as a carrier

may increase the solubility of the drug and may allow for controlling its release, depending on pH, where the release of the drug substance was slow and maintained at a low pH compared to the pH of the environment. These modifications provide, above all, the possibility to change the stability or release of the drug, using e.g. stimulating nanocapsules to release at different pH values. The initial assessment of changes in the pH value of the culture medium of cells exposed to drugs in the presence of chitosan was a pilot study showing basic information on the possible direction in further modification of drugs. Observations of pH changes clearly show an increase in pH with higher concentrations, especially in the case of medium containing chitosan. This may indicate a slowdown in cell metabolism as control cells are known to cause instant acidification of the medium due to their rapid metabolism and consumption of the nutrients contained in the culture medium [123].

As the summary of all tests, analysis in real time for observation of cells was performed. Evaluation of the morphology confirmed all previous observations, while paying attention to the importance of the size of the created nanocapsules. Microscopic images after 72 hours of the experiment allowed for the observation of ciprofloxacin crystals releasing from chitosan structures in the highest concentrations of the tested chemotherapeutic agent. These crystals were especially visible in the case of the T24 line, which may be related with a faster metabolic rate of these cells compared to the DU145 line [124].

The provided research showed that more promising results are obtained at all events modification of ciprofloxacin with chitosan. All these results were compared with published data, which indicate that modifications of levofloxacin are used primarily in the treatment of eye diseases [125]. Importantly, the sustained release of levofloxacin from chitosan microspheres was achieved using different modification methods than those used in the PhD thesis. The most often cite modifications are with the use of a spray-drying technique, which showed significantly higher levels of sustained drug release compared to non-crosslinked microspheres [126]. These microspheres showed high encapsulation efficiency and were uniformly spherical with a wrinkled surface. *In vitro* release profiles showed sustained drug release significantly influenced by the cross-linking process [127]. In further considerations, it is definitely worth taking into account the process of optimization and selection of the method of drug modification depending on their chemical structure. Due to the aim of the doctoral thesis, it focused on the biological and cellular aspects of the modification of fluoroquinolones

using chitosan. However, another aspect of the analysis of the obtained research should be the broad chemical characteristics of the obtained nanocapsules. TEM micrographs provides an actual diameter of the size of nanocapsules in dry state. Recompenses of small size particles as a carrier system include high cellular uptake, good suspensibility, which could facilitate penetration into walls of the cells [127]. It should be marked, that the analysis of the results of cell vitality parameters took into account the theoretical 100% efficiency of encapsulation. In further considerations, however, it is necessary to carefully analyze the chemical parameters and determine the drug dose loaded.

Chitosan offers many opportunities for the development and further modification of drugs. In addition to controlled release, increasing drug stability or reducing its side effects, a promising trend is also the use of chitosan in the development of theranostics drugs [128]. It is a combination of a therapeutic drug and a diagnostic agent in one preparation using nanomaterials. Although a variety of biomaterials can be used in cancer theranostics, chitosan, having easy modification sites with excellent biocompatibility and biodegradability, shows great potential [129].

5.2. Polyphenols and flavonoids in cancer therapy

The main goal of ongoing research efforts is largely devoted to the discovery of natural and synthetic compounds that may be useful as anti-cancer therapy [130]. Among other pro-health biological activities, products rich in flavonoids have a strong immunopotential and anticancer effect [131]. The concentration of flavonoids, which constitute the majority of bioactive phenolic molecules in plants, depends on various factors, including but not limited to the plant species used, plant health, season, environmental factors and geographic origin [132].

Many studies indicate the effectiveness of *Picea abies* extract against hormone-dependent cancers, such as breast, endometrial and ovarian cancer [133]. This also indicates potential in the treatment of another hormone-dependent cancer, the prostate, used in the doctoral thesis [134]. Chronic oral consumption of polyphenols from the needles of *Picea abies* L. and *Pinus sylvestris* L. (12.5 mg/kg daily) significantly inhibited development of cancer cells induced by a mixture of testosterone esters in male Wistar rats [135]. In the light of

aforementioned results and those obtained in the presented PhD thesis, it can be said that polyphenols may be tested as chemopreventive agent, also in prostate cancer.

The basic assessment was the observation of changes in cell morphology and in survival rate. Tetrazole-based assays are optimized for the evaluation of adherent cell toxicity, such as MTT or WST8. However, scientific report has shown that the WST-8 test is non-toxic and shows the highest sensitivity than MTT [136]. This assay, is the newest, most evolved form of viability testing, so consequently it was used in presented experiments. Ciprofloxacin in 500 μM concentration influenced the cell viability in moderate manner (52.09%), while in concentration with *Picea abies* extract, this effect was stronger (29.03%).

What is the most interesting, ciprofloxacin modified with natural extract had the same cytotoxic effect, irrespectively from the concentration used. 500 μM mixture of ciprofloxacin and extract demonstrated the 29.03% of living cells, while in 1000 μM concentration it was similar 29.39%. It proves that modification can lead to decrease in chemotherapeutics agents concentration with the same cytotoxic effect.

All this observation were confirmed by WST8 test, where the most promising results were noted for a concentration of 1000 μM with the addition of 5% extract in 72 hours of incubation. Similar observations are noticeable in the studies of other scientists, who indicated the cytotoxicity of polyphenols [137, 138]. However, it is also emphasized that there is a need to confront these results with other, more sensitive methods of assessing viability, such as WST8 or the CellTiter-Glo test. Both, the MTT and the CellTiter-Glo showed the highest decrease in cell viability at the maximum concentration of each compound tested [139]. It can therefore be concluded that, similarly to the WST8 test, it is characterized by greater measurement sensitivity, which has been confirmed in the literature [140, 141]. Almost identical observations were made for the live/dead test, where, over time, an increasing percentage of dead cells of the T24 and DU145 lines was observed in the sample treated with the extract.

The assessment of cell proliferation using the BrdU test pointed out that the biologically active compounds contained in the extracts can induce a decrease in the proliferation of cancer cells in *in vitro* studies. These results can be confirmed with numerous literature reports, where the inhibition of proliferation of prostate (PC-3), liver (LI -90), breast

(T47D and MDA-MB-231) and colon (HT-29 and Caco-2) cancer cells was indicated [142, 143, 144, 145].

Evaluation of pH changes showed that the yellowing of phenol red in the culture media was pronounced in the cells of the control wells, while T24 and DU145 cells chronically exposed to ciprofloxacin and levofloxacin alkalized the surrounding culture medium in a dose-dependent manner. As in the case of modifying drugs with chitosan, it is probably related to the slower metabolism of cells grown in the presence of plant extract [146].

Unlike the results showing the modification of fluoroquinolones with chitosan, the effect of modifying drugs with spruce extract on the induction of apoptosis is not clear. The conducted studies show that adding a 5% concentration of the natural extract to both ciprofloxacin and levofloxacin reduces the apoptotic signal induced by cells, compared to the basic forms of the drug, however, described the significant influence of polyphenols and flavonoids on the appearance of cell death by apoptosis [147]. It is possible that this assessment may be influenced by the type of extract used in the study or the extraction method [148].

Due to great structural diversity among flavonoids, these profiles differ greatly from one compound to another, so that the most abundant polyphenols in daily diet are not necessarily the ones that reach target tissues. Therefore, careful analysis of flavonoids and their metabolites in biological systems is critical. As the analyzes presented in PhD thesis have shown, the *Picea abies* extract consists of, among others: with Luteolin, Pilloin and o-Vanillin. Interestingly, luteolin-rich plants have been used in traditional eastern medicine to treat various conditions such as high blood pressure, inflammatory diseases, and cancer [146]. The biological effects of luteolin may be functionally related. For example, anti-inflammatory effects may be related to its anti-cancer properties. In addition, luteolin sensitizes cancer cells to therapeutically induced cytotoxicity by inhibiting cell survival pathways such as phosphatidylinositol 3'-kinase (PI3K)/Akt, nuclear factor kappa B (NF- κ B) and X-linked inhibitor of apoptosis protein (XIAP) and stimulating pathways apoptosis, including those that induce p53 tumor suppressor [149, 150]. In further research, an interesting direction will certainly be the use of extracted luteolin and other components for compressive analysis of their role in anti-cancer therapies.

5.3. New cell models for *in vitro* research

Many studies have shown that 2D and 3D cultures respond differently to anti-cancer drugs [151]. Variability drug sensitivity is usually explained by different "microenvironments" and gene expression profiles on nutrient and oxygen gradients and drug diffusion capacity [152, 153]. Pickl et al. recently paid attention to an example of the role of such microenvironments in breast cancer, where trastuzumab was tested in 2D and 3D model [154]. Cells in the 3D spheroids were much more sensitive to antibodies. They are dependent on their physiological human epidermal growth factor 2 signaling receptor in the spheroid formation, which is the antibody target [155]. Therefore, clinical prediction of the response of new agents tested in 2D cell assays is limited [156].

When analyzing the need for drug encapsulation and their modification, the form of drug administration to patients is critical. Fluoroquinolones, as drugs often used in oral administration, have a high potential for modification with chitosan due to the convenient formulation of nanocapsules. As demonstrated by preclinical studies by Khan N. et al. [157] there is a great potential of modern cancer drugs, using chitosan encapsulation of drugs used in the treatment of prostate cancer. There are no significant differences in the pharmacokinetics of levofloxacin administered orally and intravenously, suggesting that the two routes of administration can be used interchangeably [158]. Levofloxacin is characterized by rapid absorption after oral administration, which translates into very high bioavailability: 99-100% [158]. Due to the very good oral bioavailability, the routes of administration of levofloxacin - oral and parenteral - are considered equivalent [159]. Levofloxacin modifications enable to change the way the patient takes the drug without losing its high bioavailability.

Interestingly, in the case of levofloxacin, after performing an initial assessment of spheroid survival, it was noted that levofloxacin presents stronger sensitivity in studies conducted on a 3D cell model than on a 2D model. As the literature describes, result of excellent tissue penetration and rapid, wide distribution, levofloxacin reaches concentrations many times higher in tissues than in blood plasma [160], which can be related to accumulation

in spheroid structures. What is more, the value of concentrations achieved by levofloxacin in tissues and organs (in the bronchi, in the lungs, in the prostate gland) is several times higher compared to ciprofloxacin [159]. The studies carried out on the 3D model showed, above all, greater sensitivity of spheroids compared to adherent cells in the case of some tests, e.g. live/dead. These results indicated a much higher cell content in the spheroid compared to adherent cells. This may be related to the rapid disintegration of spheroids after 60 hours of incubation, also observed in the microscopic image and during growth kinetics. This disintegration is especially noticeable in the case of spheroids grown with the extract. However, this disintegration should be investigated in details, due to reports related to the dependence of spheroid exfoliation on the formation of subsequent tumor clusters [161]. Perhaps it is the inhibition of shedding of cells from the primary tumor that can be used to avoid metastases and delay the progression of the cancer. The difference between exfoliation and disintegration should be explored, and fragments of separated areas of spheroids should also be analyzed.

Research by Lal-Nag et al. provided a very important comparison of 2D and 3D methods as a tool for assessing the cytotoxicity of drugs *in vitro* [162]. The results obtained by the author during studies on various drugs demonstrated large differences in the toxicity of compounds depending on the model used. A very important observation made by the author is also the differentiation of the results depending on the applied 3D test methodology. The obtained results of the presented studies also indicated differences in the results of tests conducted on the 2D and 3D models, however, this has not been observed for all tested drugs. Madhu L. showed that the 3D model is more resistant to the toxic effects of all drugs. However, it is worth to add one of the main limitations, which is a common feature of 2D and 3D cultures. This is their lack of ability to migrate and invade cancer cells [163].

Exploration of spheroid survival, was based on the MTT test, kinetics analysis using vital microscopy with artificial intelligence (AI) analysis. However, the MTT test did not allow for testing the effects of compounds after exceeding 72 hours of incubation. Therefore, for the analysis of longer incubation periods with drugs, intravital imaging was used to observe the growth of the spheroids also in the later hours. In addition to accurate measurements, this method made it possible to track the growth of spheroids during incubation with the tested drugs. In contrast to the MTT test, the method used facilitated the collection of more time

points and was not burdened with the disadvantages and limitations described by Mahshid G. et al. [158], such as the concentration of MTT reagent added to the cells, time of incubating cells with MTT, type of culture media. The greatest advantage of the method used was the lack of the need to add any other substance apart from the study drug. This is especially useful when testing series of biologically active compounds.

Absorption of the drug into spheroid and the contact with cultured cells can be another mechanism reducing the sensitivity of spheroids to drugs. Above mentioned absorption may be slower than in 2D model, where drugs has almost unlimited contact with all cultured cells after its addition. One of the model drugs that was also tested in the presented work was doxorubicin. Another author has described the absorption kinetics of this drug by spheroids because it has fluorescent properties, which makes it easy to track [164]. Total absorption, depending on the size of the spheroid, took about 5 hours, differences in the achievement of IC50 values for individual lines and models used are also noticeable [165, 166].

Approval rates for new anti-cancer drugs are $\leq 5\%$ [166] and one of the strategy to improve the success rate of bringing new anti-cancer drugs into the clinic would be to more closely align the cell models used in early research leading to pre-clinical animal and cancer models. For solid tumors, this will require the development and implementation of 3D *in vitro* tumor models that more accurately reflect the architecture and biology of human solid tumors. Studies on 3D models showed that optimizing the methods used and adapting *in vitro* tests to assess the parameters of survival, proliferation, growth and genetics of spheroids can significantly contribute to accelerating the process of research and approval of new drugs in the clinical phase [167]. Scalability and reproducibility of the 3D cells spheroids is one of the most important challenge pervading the scientists. This is a requirement of pharmaceutical companies dealing with drug screening at the preclinical level evaluation. The method of magnetic bioprinting performed in this PhD thesis ensured the consistency of the size and shape of each batch [168]. Bioprinting, by manipulating the magnetic properties of the cells and then the spheroid, ensures consistency in batch-to-batch production of spheroids and seeding of spheroids while reducing reliance on manual processes [169].

In conclusion, this PhD thesis is a contribution to the extensive scientific research aimed at the development of new drug therapies and optimalization new *in vitro* model. However, despite conducting a wide range of studies on the interaction of two

chemotherapeutic drugs in two modifications on two models of cancer cells, there are still many unexplored parameters that can help to fully understand the impact of the tested substances on the cells of one of the two most common cancers. These studies provide a basis for other scientists to develop their analysis, helpful into further modification of drugs. An interesting way seems to be a combination of both methods used - encapsulation of drugs with the addition of a natural extract into chitosan structures. Perhaps this will allow to accumulate the inferred advantages that were obtained during the analysis. These included a more cytotoxic effect of drugs in a longer incubation time or a reduction in the dose of the drug necessary to achieve the expected cytotoxic effects. Certainly, thanks to the progress of knowledge on the pharmacology of drugs and the assessment of their accumulation, it will be possible to compare the real concentrations of modified drugs with those that are tested *in vitro*.

6. Conclusions

- 6.1. All tested drugs are cytotoxic to prostate and bladder cancer cells. The cytotoxic effect was conditioned both by the time and the concentration of the tested substances.
- 6.2. Fluoroquinolones modified with 5% the *Picea abies* extract show a highest cytotoxic effect. Modification with natural extract permits the drug dose reduction with the same antiproliferative effect.
- 6.3. Fluoroquinolones encapsulated with chitosan show a higher cytotoxic effect for concentration 1000 μM after 72 hours of incubation. The cytotoxicity of the encapsulated drug increased over time.
- 6.4. Magnetic bioprinting is a promising method for multicellular spheroids formation. The most optimal number of cells is 5.000.
- 6.5. Multicellular spheroids are more sensitivity cell model for *in vitro* cytotoxicity studies.

7. Attachments

7.1. Approval of the Bioethics Committee

Uniwersytet Mikołaja Kopernika w Toruniu
Collegium Medicum im L. Rydygiera w Bydgoszczy
KOMISJA BIOETYCZNA

Ul. M. Skłodowskiej-Curie 9, 85-094 Bydgoszcz, tel.(052) 585-35-63, fax.(052) 585-38-11

KB 698/2019

Bydgoszcz, 24.09.2019 r.

Działając na podstawie art.29 Ustawy z dnia 5 grudnia 1996 roku o zawodzie lekarza (Dz.U. z 1997 r. Nr 28 poz. 152 (wraz z późniejszymi zmianami), zarządzenia Ministra Zdrowia i Opieki Społecznej z dnia 11 maja 1999 r. w sprawie szczegółowych zasad powoływania i finansowania oraz trybu działania komisji bioetycznych (Dz.U.Nr 47 poz.480) oraz Zarządzeniem Nr 21 Rektora UMK z dnia 4 marca 2009 r. z późn. zm. w sprawie powołania oraz zasad działania Komisji Bioetycznej Uniwersytetu Mikołaja Kopernika w Toruniu przy Collegium Medicum im Ludwika Rydygiera w Bydgoszczy oraz zgodnie z zasadami zawartymi w ICH – GCP

Komisja Bioetyczna przy UMK w Toruniu, Collegium Medicum w Bydgoszczy

(skład podano w załączeniu), na posiedzeniu w dniu **24.09.2019 r.** przeanalizowała wniosek, który złożyła kierownik badania:

dr hab. n. med. Anna Bajek
Zakład Inżynierii Tkankowej
Collegium Medicum w Bydgoszczy

z zespołem w składzie

- **dr hab. n. med. Anna Bajek, mgr Karolina Matulewicz,**

w sprawie badania:

„Modyfikacja wybranych cytostatyków w leczeniu nowotworów układu moczowo-płciowego.”

Po zapoznaniu się ze złożonym wnioskiem i w wyniku przeprowadzonej dyskusji oraz głosowania Komisja podjęła

Uchwałę o pozytywnym zaopiniowaniu wniosku

w sprawie przeprowadzenia badań w zakresie określonym we wniosku

Zgoda obowiązuje od daty posiedzenia (24.09.2019 r.) do końca 2022 r.

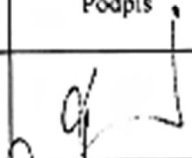
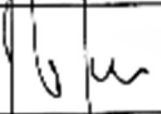
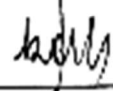
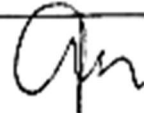
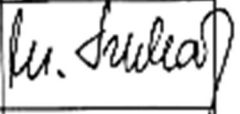
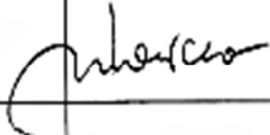
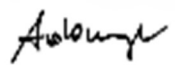
Wydana opinia dotyczy tylko rozpatrywanego wniosku z uwzględnieniem przedstawionego projektu; każda zmiana i modyfikacja wymaga uzyskania odrębnej opinii.

Prof. dr hab. med. Karol Śliwka

Przewodniczący Komisji Bioetycznej

Otrzymuje:
dr hab. n. med. Anna Bajek
Zakład Inżynierii Tkankowej
Collegium Medicum w Bydgoszczy

Lista obecności
na posiedzeniu Komisji Bioetycznej
w dniu 24.09.2019 r.

Lp.	Imię i nazwisko	Funkcja/ Specjalizacja	Podpis
1.	Prof. dr hab. med. Karol Śliwka	Przewodniczący medycyna sądowa	
2.	Mgr prawa Joanna Połetek-Żygas	Z-ca przewodniczącego prawniczka	
3.	Prof. dr hab. med. Mieczysława Czerwionka-Szaflarska	pediatra, alergologia i gastroenterologia dziecięca	
4.	Prof. dr hab. med. Anna Balcar-Boroń	pediatria, nefrologia	
5.	Prof. dr hab. med. Marek Grabiec	położnictwo, ginekologia onkologiczna	
6.	Prof. dr hab. med. Zbigniew Włodarczyk	chirurgia ogólna, transplantologia kliniczna	
7.	Dr hab. n. med. Katarzyna Pawlak-Osińska, prof. UMK	organizacja ochrony zdrowia, otolaryngologia	
8.	Dr hab. n. med. Maria Kłopocka	choroby wewnętrzne, gastroenterologia	
9.	Ks. dr hab. Wojciech Szukalski, prof. UAM	duchowny	
10.	Dr n. med. Radosława Staszak-Kowalska	pediatria, choroby płuc	
11.	Mgr prawa Patrycja Brzezicka	prawniczka	
12.	Mgr farm. Aleksandra Adamczyk	farmaceutka	
13.	Mgr Lidia Iwińska-Tarczykowska	pielęgniarska	

7.2. List of abbreviations

UBC – Urinary bladder cancer

PC – Prostate cancer

CIP – Ciprofloxacin

LEV – Levofloxacin

CHIT - Chitosan

FDA - Food and Drug Administration

DMEM - Dulbecco's Modified Essential Medium

FBS - Fetal Bovine Serum

FITC - Fluorescein isothiocyanate

IC50 - Half Maximal Inhibitory Concentration

MD - Multidrug resistance

MTT - 3-(4,5-dimethylthiazol-2-yl)-2,5-diphenyltetrazolium bromide

p - Probability value

PBS - Phosphate Buffered Saline

R² - Coefficient of Determination

RPMI - Roswell Park Memorial Institute Medium

BACs - Biologically active compounds

CE – Circular economy

PK - Pharmacokinetic

PD – Pharmacodynamic

NNs - Neural networks

BrdU - Bromodeoxyuridine (5-bromo-2'-deoxyuridine)

μM - Micromolar concentration

TEM – Transmission electron microscopy

DLS – Dynamic Light Scattering

ESI-MS - Electrospray mass spectra analysis

WHO - World Health Organization

7.3. List of tables

Table 1. Examples of clinical trials used polyphenols and flavonoids treatment potential.	15
Table 2. Examples of flavonoids sources in fruits and vegetables.....	16
Table 3. The effect of ciprofloxacin on the inhibition of proliferation of bladder cancer cell lines	19
Table 4. List of abbreviations of solutions of chemotherapeutic agents and concentrations used during the studies.....	27
Table 5. The IC ₅₀ value for tested chemotherapeutic agents. The R ² value for both compounds was over 0.95, which means a very good fit of the trend line.	58
Table 6. Ciprofloxacin and modified ciprofloxacin-induced media pH shifts following 3-days exposure, in T24 cells. pH shifts recorded in CIP-supplemented (0–1000 µM) culture media, following overnight exposure, subsequent to 3-day treatment; mean ± SD., n=3.	75
Table 7. Levofloxacin and modified levofloxacin-induced media pH shifts following 3-days exposure, in T24 cells. pH shifts recorded in LEV-supplemented (0–1000 µM) culture media, following overnight exposure, subsequent to 3-day treatment; mean ± SD., n=3.	76
Table 8. Ciprofloxacin and modified ciprofloxacin-induced media pH shifts following 3-days exposure, in DU-145 cells. pH shifts recorded in CIP-supplemented (0–1000 µM) culture media, following overnight exposure, subsequent to 3-day treatment; mean ± SD., n=3.....	77
Table 9. Levofloxacin and modified levofloxacin-induced media pH shifts following 3-days exposure, in DU-145 cells. pH shifts recorded in LEV-supplemented (0–1000 µM) culture media, following overnight exposure, subsequent to 3-day treatment; mean ± SD., n=3.	78
Table 10. The IC ₅₀ value for tested chemotherapeutic agents modified with natural extract.	98
Table 11. Ciprofloxacin and Picea abies tree modified ciprofloxacin-induced media pH shifts following 3-days exposure, in T24 cells.....	113
Table 12. Levofloxacin and Picea abies tree modified levofloxacin -induced media pH shifts following 3-days exposure, in T24 cells. pH shifts recorded in LEV-supplemented (0–1000 µM) culture media, following overnight exposure, subsequent to 3-day treatment; mean ± SD., n=3.....	114
Table 13. Ciprofloxacin and Picea abies tree modified ciprofloxacin-induced media pH shifts following 3-days exposure, in DU145 cells. pH shifts recorded in CIP-supplemented	115
Table 14. Levofloxacin and Picea abies tree modified levofloxacin -induced media pH shifts following 3-days exposure, in DU145 cells. pH shifts recorded in LEV-supplemented	115
Table 15. IC ₅₀ values calculated from non-linear regression curve for test results MTT, the table also shows the fit parameter of the theoretical curve R ²	132
Table 16. IC ₅₀ values calculated from the results of the MTT assay for the T24 cell line in 2D and 3D culture.	146

7.4. List of figures

Figure 1. Ten Leading Cancer Types for the Estimated New Cancer Cases by Sex.....	9
Figure 2. Diagrams show the risk of developing urinary bladder cancer for males (A) and females (B) in the United States of America. Data for 2020.	10
Figure 3. Different types of nanocarriers used as controlled delivery vehicles for cancer treatment	12
Figure 4. Chitosan's structure.	13
Figure 5. The linear economy and the circular economy model	17
Figure 6. Levofloxacin structure.....	20
Figure 7. Cells grown to 60% confluence in 2D were incubated overnight with magnetic nanoparticles (NanoShuttle, NS). After resuspending the cells for a few hours, the cells were distributed into the wells of low attachment 96-well microplate. The cells were then printed for 20 min by putting the plate atop a 96-well magnetic drive. After printing, the magnet was removed.	26
Figure 8. Simplified flow chart of the drug-chitosan combination process.....	28
Figure 9. Diagram of the procedure for assessing cell viability using the MTT test. The diagram shows the reduction of 3-(4,5-dimethylthiazol-2-yl)-2,5-diphenyltetrazolium bromide (MTT) reagent to purple formazan by living cells. Wells with unreacted dead cells remain yellow.....	33
Figure 10. TEM micrograph of chitosan nanoparticles prepared with ciprofloxacin.	37
Figure 11. T24 cells at 72 hours of cultivation in the presence of: culture medium, ciprofloxacin and ciprofloxacin modified with chitosan at concentrations of 10, 100, 500, 1000 μ M. Arrows mark visible particles of ciprofloxacin crystals.	39
Figure 12. T24 cells at 72 hours of cultivation in the presence of: culture medium, levofloxacin and levofloxacin modified with chitosan at concentrations of 10, 100, 500, 1000 μ M.	41
Figure 13. DU145 cells at 72 hours of cultivation in the presence of: culture medium, ciprofloxacin and ciprofloxacin modified with chitosan at concentrations of 10, 100, 500, 1000 μ M.	43
Figure 14. DU145 cells at 72 hours of cultivation in the presence of: culture medium, levofloxacin and levofloxacin modified with chitosan at concentrations of 10, 100, 500, 1000 μ M.	45
Figure 15. The graph shows the ratio of live to dead cells at individual drug concentrations for the T24 cell line. Cell viability was assessed after 24 hours incubation with drugs. Each concentration was assessed at least in triplicate, and the cells were counted from 6 images taken in each well tested.	46
Figure 16. Microscopic images demonstrating how T24 culture conditions influence the visibility of dead cells detected using the fluorescent live/dead assay kit. Cell death was induced by chemotherapeutic agent - levofloxacin and levofloxacin with chitosan.	47
Figure 17. The graph shows the ratio of live to dead cells at individual drug concentrations for the T24 cell line. Cell viability was assessed after 24 hours incubation with drugs.....	48
Figure 18. Microscopic images demonstrating how T24 culture conditions influence the visibility of dead cells detected using the fluorescent live/dead assay kit.....	49
Figure 19. The graph shows the ratio of live to dead cells at individual drug concentrations for the DU145 cell line. Cell viability was assessed after 24 hours incubation with drugs.....	50
Figure 20. Microscopic images demonstrating how DU145 culture conditions influence the visibility of dead cells detected using the fluorescent live/dead assay kit.....	51
Figure 21. The graph shows the ratio of live to dead cells at individual drug concentrations for the T24 cell line. Cell viability was assessed after 24 hours incubation with drugs.....	52

Figure 22. Microscopic images demonstrating how DU145 culture conditions influence the visibility of dead cells detected using the fluorescent live/dead assay kit. Cell death was induced by chemotherapeutic agent - ciprofloxacin and ciprofloxacin with chitosan.....	53
Figure 23. MTT test results for the T24 line in the following days from the start of incubation with the addition of ciprofloxacin and modified ciprofloxacin in the concentration range of 10-1000 μ M.	54
Figure 24. MTT test results for the T24 line in the following days from the start of incubation with the addition of levofloxacin and modified levofloxacin in the concentration range of 10-1000 μ M..	55
Figure 25. MTT test results for the DU145 line in the following days from the start of incubation with the addition of ciprofloxacin and modified ciprofloxacin in the concentration range of 10-1000 μ M.56	
Figure 26. MTT test results for the DU145 line in the following days from the start of incubation with the addition of levofloxacin and modified levofloxacin in the concentration range of 10-1000 μ M... 57	
Figure 27. WST8 test results for the T24 line in the following days from the start of incubation with the addition of ciprofloxacin and modified ciprofloxacin in the concentration range of 10-1000 μ M.	60
Figure 28. WST8 test results for the T24 line in the following days from the start of incubation with the addition of levofloxacin and modified levofloxacin in the concentration range of 10-1000 μ M.	61
Figure 29. WST8 test results for the DU145 line in the following days from the start of incubation with the addition of ciprofloxacin and modified ciprofloxacin in the concentration range of 10-1000 μ M.62	
Figure 30. WST8 test results for the DU145 line in the following days from the start of incubation with the addition of levofloxacin and modified levofloxacin in the concentration range of 10-1000 μ M... 63	
Figure 31. Bladder cancer cells – T24 after 72 hours with chitosan capsules with ciprofloxacin - FITC - cells that promote apoptosis. Arrow marks visible apoptotic cells.	65
Figure 32. Bladder cancer cells – T24 after 24h with chitosan capsules with levofloxacin - FITC - cells that promote apoptosis.	66
Figure 33. Prostate cancer – DU145 after 24h with chitosan capsules with ciprofloxacin - FITC - cells that promote apoptosis.	68
Figure 34. Prostate cancer – DU145 after 24h with chitosan capsules with levofloxacin - FITC - cells that promote apoptosis.	70
Figure 35. Proliferation of the T24 line in the following days from the start of incubation with the addition of ciprofloxacin and modified ciprofloxacin in the concentration range of 10-1000 μ M.	71
Figure 36. Proliferation of the T24 line in the following days from the start of incubation with the addition of levofloxacin and modified levofloxacin in the concentration range of 10-1000 μ M.	72
Figure 37. Proliferation of the DU145 line in the following days from the start of incubation with the addition of ciprofloxacin and modified ciprofloxacin in the concentration range of 10-1000 μ M.	73
Figure 38. Proliferation of the DU145 line in the following days from the start of incubation with the addition of levofloxacin and modified levofloxacin in the concentration range of 10-1000 μ M.	74
Figure 39. T24 cells at 72 hours of cultivation in the presence of: culture medium, ciprofloxacin and ciprofloxacin modified with natural extract at concentrations of 10, 100, 500, 1000 μ M.....	81
Figure 40. T24 cells at 72 hours of cultivation in the presence of: culture medium, levofloxacin and levofloxacin modified with natural extract at concentrations of 10, 100, 500, 1000 μ M.	83
Figure 41. DU145 cells at 72 hours of cultivation in the presence of: culture medium, ciprofloxacin and ciprofloxacin modified with natural extract at concentrations of 10, 100, 500, 1000 μ M.....	85
Figure 42. DU145 cells at 72 hours of cultivation in the presence of: culture medium, levofloxacin and levofloxacin modified with natural extract at concentrations of 10, 100, 500, 1000 μ M.	87
Figure 43. Percentage of live and dead cells T24 cell line cultured in medium containing test drugs ciprofloxacin (A) and levofloxacin (B).....	88

Figure 44. Microscopic images demonstrating how T24 culture conditions influence the visibility of dead cells detected using the fluorescent live/dead assay kit.....	89
Figure 45. Microscopic images demonstrating how T24 culture conditions influence the visibility of dead cells detected using the fluorescent live/dead assay kit after incubation with levofloxacin.	90
Figure 46. Percentage of live and dead cells DU145 cell line cultured in medium containing test drugs ciprofloxacin (A) and levofloxacin (B).....	91
Figure 47. Microscopic images demonstrating how DU145 culture conditions influence the visibility of dead cells detected using the fluorescent live/dead assay kit after incubation with ciprofloxacin.	92
Figure 48. Microscopic images demonstrating how DU145 culture conditions influence the visibility of dead cells detected using the fluorescent live/dead assay kit after incubation with levofloxacin.	93
Figure 49. The results of the MTT test for the T24 line on the following days from the start of incubation with the addition of ciprofloxacin and ciprofloxacin modified natural extract from the 10-1000 μ M concentration range.....	94
Figure 50. The results of the MTT test for the T24 line on the following days from the start of incubation with the addition of levofloxacin and levofloxacin modified natural extract from the 10-1000 μ M concentration range.....	95
Figure 51. MTT test results for DU145 exposed to the ciprofloxacin concentrations tested.....	96
Figure 52. MTT test results for DU145 exposed to the levofloxacin concentrations tested.....	97
Figure 53. WST8 test results for the T24 line in the following days from the start of incubation with the addition of ciprofloxacin in the concentration range of 10-1000 μ M.	99
Figure 54. WST8 test results for the T24 line in the following days from the start of incubation with the addition of levofloxacin in the concentration range of 10-1000 μ M.....	100
Figure 55. WST8 test results for the DU145 line in the following days from the start of incubation with the addition of ciprofloxacin and modified ciprofloxacin in the concentration range of 10-1000 μ M.	101
Figure 56. WST8 test results for the DU145 line in the following days from the start of incubation with the addition of levofloxacin and modified levofloxacin in the concentration range of 10-1000 μ M.	102
Figure 57. Bladder cancer after 24h with Picea abies tree extract and ciprofloxacin - FITC - cells that promote apoptosis.....	104
Figure 58. Bladder cancer after 24h with Picea abies tree extract and levofloxacin - FITC - cells that promote apoptosis.....	105
Figure 59. Prostate cancer cell line after 24h with Picea abies tree extract and ciprofloxacin - FITC - cells that promote apoptosis.	107
Figure 60. Prostate cancer cell line after 24h with Picea abies tree extract and levofloxacin - FITC - cells that promote apoptosis..	108
Figure 61. Proliferation of the T24 line in the following days from the start of incubation with the addition of ciprofloxacin and modified ciprofloxacin in the concentration range of 10-1000 μ M.	109
Figure 62. Proliferation of the T24 line in the following days from the start of incubation with the addition of levofloxacin and modified levofloxacin in the concentration range of 10-1000 μ M.	110
Figure 63. Proliferation of the DU145 line in the following days from the start of incubation with the addition of ciprofloxacin and modified ciprofloxacin in the concentration range of 10-1000 μ M.	111
Figure 64. Proliferation of the DU145 line in the following days from the start of incubation with the addition of levofloxacin and modified levofloxacin in the concentration range of 10-1000 μ M.	112
Figure 65. DU145 (A) and T24 (B) cells after 24 hours with nanomagnetic particles (A1 and B1).	116
Figure 66. Multicellular spheroids T24 cells after 25 – 120 hours after bioprinting process..	118

Figure 67. Multicellular spheroids DU145 cells 24 hours and 120 hours after bioprinting process...	117
Figure 68. Graph showing growth of multicellular spheroids from T24 cell line over 5 weeks.	119
Figure 69. T24 cell spheroids 120 hours after spheroid formation procedure	120
Figure 70. Comparison of viability 2D and 3D model incubated in media T24 (A) and DU145 (B). ...	121
Figure 71. Effect of chemotherapeutic drug ciprofloxacin on the cell growth 3D-cultured bladder (T24) cancer.....	123
Figure 72. Effect of chemotherapeutic drug levofloxacin on the cell growth 3D-cultured bladder (T24) cancer.....	124
Figure 73. Percentage of live and dead cells T24 cell line cultured in medium containing test drugs ciprofloxacin and ciprofloxacin with chitosan. The evaluation value was measuring the sum fluorescence intensity value.	125
Figure 74. Microscopic images demonstrating how spheroids T24 cell culture conditions influence the visibility of dead cells detected using the fluorescent live/dead assay kit. Cell death was induced by chemotherapeutic agent - ciprofloxacin and ciprofloxacin with chitosan. Imaging Assay of Live or Dead™ Cell Viability.....	126
Figure 75. An example of spheroid’s microscopic image analysis after incubation in chemotherapeutic agents . The learned neural network detects cells marked as "live" as a yellow field and "dead" as a green field (B).....	127
Figure 76. Percentage of live and dead cells T24 cell line cultured in medium containing test drugs levofloxacin and levofloxacin with chitosan.	128
Figure 77. Microscopic images demonstrating how spheroids T24 cell culture conditions influence the visibility of dead cells detected using the fluorescent live/dead assay kit.	129
Figure 78. MTT test results for the spheroids of T24 cell line in the following days from the start of incubation with the addition of ciprofloxacin and modified ciprofloxacin in the concentration range of 10-1000 μM	130
Figure 79. MTT test results for the spheroids T24 cell line in the following days from the start of incubation with the addition of levofloxacin and modified levofloxacin in the concentration range of 10-1000 μM	131
Figure 80. Kinetics of spheroid growth depending on time and concentration of the test drug was determined. The graph shows the data: changing area of the spheroid [μm^2] incubated in ciprofloxacin and chitosan-modified ciprofloxacin in time [h].	133
Figure 81. Arrows indicate spheroids (A) – control without drug, (B) - disintegrating spheroid after 72 hours incubation in the highest concentration of ciprofloxacin.....	134
Figure 82. On the basis of live-imaging observations, the kinetics of spheroid growth depending on time and concentration of the test drug was determined.	135
Figure 83. During the kinetic imaging without the use of dyes (real-time, stain-free live-imaging), the observation of each spheroid was recorded in the form of a video.....	136
Figure 84. Effect of chemotherapeutic drug ciprofloxacin on the cell growth 3D-cultured bladder (T24) cancer.	138
Figure 85. Effect of chemotherapeutic drug levofloxacin on the cell growth 3D-cultured bladder (T24) cancer.	139
Figure 86. Percentage of live and dead cells T24 cell line cultured in medium containing test drugs ciprofloxacin and ciprofloxacin with extract.	140
Figure 87. Microscopic images demonstrating how spheroids T24 cell culture conditions influence the visibility of dead cells detected using the fluorescent live/dead assay kit.	141

Figure 88. Percentage of live and dead cells T24 cell line cultured in medium containing test drugs levofloxacin and levofloxacin with chitosan.	142
Figure 89. Microscopic images demonstrating how spheroids T24 cell culture conditions influence the visibility of dead cells detected using the fluorescent live/dead assay kit.	143
Figure 90. Viability of the spheroids of T24 cell line in the following days from the start of incubation with the addition of ciprofloxacin and modified ciprofloxacin in the concentration range of 10-1000 μ M.	144
Figure 91. Viability of the spheroids of T24 cell line in the following days from the start of incubation with the addition of levofloxacin and modified levofloxacin in the concentration range of 10-1000 μ M.	145
Figure 92. Graph illustrated the kinetics of spheroid growth depending on time and concentration of the test drug was determined. The graph shows the data: changing area of the spheroid [μ m ²] incubated in ciprofloxacin and extract-modified ciprofloxacin in time [h].....	147

8. Bibliography

1. Changfa Xia et al, Cancer statistics in China and United States, 2022: profiles, trends, and determinants, *Chin Med J*, Feb 2022
2. Mularczyk-Tomczewska P, Zarnowski A, Gujski M, Jankowski M, Bojar I, Wdowiak A, Krakowiak J. Barriers to accessing health services during the COVID-19 pandemic in Poland: A nationwide cross-sectional survey among 109,928 adults in Poland. *Front Public Health*. 2022 Sep 8;10:986996. doi: 10.3389/fpubh.2022.986996. PMID: 36159267; PMCID: PMC9495711.
3. Religioni U, Cancer incidence and mortality in Poland, *Clinical Epidemiology and Global Health* 2020, ISSN: 2213-3984, Vol: 8, Issue: 2, Page: 329-334
4. Rebecca L. Siegel MPH, Kimberly D. Miller MPH, Hannah E. Fuchs BS, Ahmedin Jemal, Cancer statistics, 2022, Volume 72, Issue 1, January/February 2022, Pages 7-33, <https://doi.org/10.3322/caac.21708>
5. Sohrabi C, Alsafi Z, O'Neill N, Khan M, Kerwan A, Al-Jabir A, Iosifidis C, Agha R. World Health Organization declares global emergency: A review of the 2019 novel coronavirus (COVID-19). *Int J Surg*. 2020 Apr;76:71-76. doi: 10.1016/j.ijsu.2020.02.034. Epub 2020 Feb 26. Erratum in: *Int J Surg*. 2020 May;77:217. PMID: 32112977; PMCID: PMC7105032.
6. Mattiuzzi C, Lippi G. Current Cancer Epidemiology. *J Epidemiol Glob Health*. 2019 Dec;9(4):217-222. doi: 10.2991/jegh.k.191008.001. PMID: 31854162; PMCID: PMC7310786.
7. White MC, Holman DM, Boehm JE, Peipins LA, Grossman M, Henley SJ. Age and cancer risk: a potentially modifiable relationship. *Am J Prev Med*. 2014 Mar;46(3 Suppl 1):S7-15. doi: 10.1016/j.amepre.2013.10.029. PMID: 24512933; PMCID: PMC4544764.
8. Angel Justiz Vaillant, Lyvan Gardiner, Maryam Mohammed et al, Narrative Literature Review on Risk Factors Involved in Lung Cancers, Breast Cancers, Brain Cancers, Gastrointestinal Cancers, Gynecologic Cancers, and Urogenital Cancers *Journal of Cancer and Tumor International* 11(4): 11-28, 2021; Article no. JCTI .70447, ISSN: 2454-7360
9. Richters A, Aben KA, Lambertus A. L., Kiemeney M, The global burden of urinary bladder cancer: an update *World Journal of Urology* (2020) 38:1895–1904 <https://doi.org/10.1007/s00345-019-02984-4>
10. Saginala K, Barsouk A, Aluru JS, Rawla P, Padala SA, Barsouk A. Epidemiology of Bladder Cancer. *Med Sci (Basel)*. 2020 Mar 13;8(1):15. doi: 10.3390/medsci8010015. PMID: 32183076; PMCID: PMC7151633.
11. Bray F., Ferlay J., Soerjomataram I., Siegel R.L., Torre L.A., Jemal A. Global cancer statistics 2018: GLOBOCAN estimates of incidence and mortality worldwide for 36 cancers in 185 countries. *CA Cancer J. Clin*. 2018;68:394–424. doi: 10.3322/caac.21492.
12. Ferlay J., Ervik M., Lam F., Colombet M., Mery L., Piñeros M., Znaor A., Soerjomataram I., Bray F. Global Cancer Observatory: Cancer Today. International Agency for Research on Cancer; Lyon, France: 2018. [(accessed on 10 Jan 2022)]. Available online: <https://gco.iarc.fr/>

13. Mostafa M.H., Sheweita S., O'Connor P.J. Relationship between Schistosomiasis and Bladder Cancer. *Clin. Microbiol. Rev.* 1999;12:97–111. doi: 10.1128/CMR.12.1.97.
14. Richters A, Katja, K.Aben, Lambertus A.L., M.Kiemeney, The global burden of urinary bladder cancer: an update, *World Journal of Urology* (2020) 38:1895–1904, <https://doi.org/10.1007/s00345-019-02984-4>
15. Phillips DE et al (2014) A composite metric for assessing data on mortality and causes of death: the vital statistics performance index. *Popul Health Metr* 12:14
16. Rawla P. Epidemiology of Prostate Cancer. *World J Oncol.* 2019 Apr;10(2):63-89. doi: 10.14740/wjon1191. Epub 2019 Apr 20. PMID: 31068988; PMCID: PMC6497009.
17. Van Booven DJ, Kuchakulla M, Pai R, et al. A Systematic Review of Artificial Intelligence in Prostate Cancer. *Res Rep Urol.* 2021;13:31-39. Published 2021 Jan 22. doi:10.2147/RRU.S268596
18. Ferlay J EM, Lam F, Colombet M, Mery L, Pineros M, Znaor A, Soerjomataram I. et al. Global cancer observatory: cancer tomorrow. Lyon, France: International Agency for Research on Cancer. Available from: <https://gco.iarc.fr/tomorrow>, Accessed 05 May 2022. [Internet]
19. Megumi Hori, Matthew Palmer, Age-specific prostate cancer incidence rate in the world, *Japanese Journal of Clinical Oncology*, Volume 51, Issue 1, January 2021, Pages 164–165, <https://doi.org/10.1093/jjco/hyaa253>
20. Mohs RC, Greig NH. Drug discovery and development: Role of basic biological research. *Alzheimers Dement (N Y)*. 2017 Nov 11;3(4):651-657. doi: 10.1016/j.trci.2017.10.005. PMID: 29255791; PMCID: PMC5725284.
21. Zhong, L., Li, Y., Xiong, L. et al. Small molecules in targeted cancer therapy: advances, challenges, and future perspectives. *Sig Transduct Target Ther* 6, 201 (2021). <https://doi.org/10.1038/s41392-021-00572-w>
22. Bedard, P. L., Hyman, D. M., Davids, M. S. & Siu, L. L. Small molecules, big impact: 20 years of targeted therapy in oncology. *Lancet* 395, 1078–1088 (2020)
23. Wen H, Jung H, Li X. Drug Delivery Approaches in Addressing Clinical Pharmacology-Related Issues: Opportunities and Challenges. *AAPS J.* 2015 Nov;17(6):1327-40. doi: 10.1208/s12248-015-9814-9. Epub 2015 Aug 15. PMID: 26276218; PMCID: PMC4627459.
24. Yoon MS, Lee YJ, Shin HJ, Park CW, Han SB, Jung JK, Kim JS, Shin DH. Recent Advances and Challenges in Controlling the Spatiotemporal Release of Combinatorial Anticancer Drugs from Nanoparticles. *Pharmaceutics.* 2020 Nov 27;12(12):1156. doi: 10.3390/pharmaceutics12121156. PMID: 33261219; PMCID: PMC7759840.
25. El-Aassar, M.R.; Ibrahim, O.M.; Al-Oanzi, Z.H. Biotechnological Applications of Polymeric Nanofiber Platforms Loaded with Diverse Bioactive Materials. *Polymers* 2021, 13, 3734. <https://doi.org/10.3390/polym13213734>
26. Tiwari G, Tiwari R, Sriwastawa B, Bhati L, Pandey S, Pandey P, Bannerjee SK. Drug delivery systems: An updated review. *Int J Pharm Investig.* 2012 Jan;2(1):2-11. doi: 10.4103/2230-973X.96920. PMID: 23071954; PMCID: PMC3465154.

27. Senapati S, Mahanta AK, Kumar S, Maiti P. Controlled drug delivery vehicles for cancer treatment and their performance. *Signal Transduct Target Ther*. 2018 Mar 16;3:7. doi: 10.1038/s41392-017-0004-3. PMID: 29560283; PMCID: PMC5854578.
28. Soppimath KS, Aminabhavi TM, Kulkarni AR, Rudzinski WE. Biodegradable polymeric nanoparticles as drug delivery devices. *J. Control. Release*. 2001;70:1–20. doi: 10.1016/S0168-3659(00)00339-4.
29. Vargason, A.M., Anselmo, A.C. & Mitragotri, S. The evolution of commercial drug delivery technologies. *Nat Biomed Eng* 5, 951–967 (2021). <https://doi.org/10.1038/s41551-021-00698-w>
30. Mitchell, M.J., Billingsley, M.M., Haley, R.M. et al. Engineering precision nanoparticles for drug delivery. *Nat Rev Drug Discov* 20, 101–124 (2021). <https://doi.org/10.1038/s41573-020-0090-8>
31. Blanco, E., Shen, H. & Ferrari, M. Principles of nanoparticle design for overcoming biological barriers to drug delivery. *Nat. Biotechnol.* 33, 941–951 (2015).
32. Gopi, S., Amalraj, A., Sukumaran, N., Haponiuk, J., & Thomas, S. (2018). Biopolymers and Their Composites for Drug Delivery: A Brief Review. *MACROMOLECULAR SYMPOSIA*, 380(1), 1022-1360. <https://doi.org/10.1002/masy.201800114>
33. Samir, A., Ashour, F.H., Hakim, A.A.A. et al. Recent advances in biodegradable polymers for sustainable applications. *npj Mater Degrad* 6, 68 (2022). <https://doi.org/10.1038/s41529-022-00277-7>
34. Senapati, S., Mahanta, A.K., Kumar, S. et al. Controlled drug delivery vehicles for cancer treatment and their performance. *Sig Transduct Target Ther* 3, 7 (2018). <https://doi.org/10.1038/s41392-017-0004-3>
35. Jiménez-Gómez CP, Cecilia JA. Chitosan: A Natural Biopolymer with a Wide and Varied Range of Applications. *Molecules*. 2020 Sep 1;25(17):3981. doi: 10.3390/molecules25173981. PMID: 32882899; PMCID: PMC7504732.
36. Islam S., Bhuiyan M.A.R., Islam M.N. Chitin and Chitosan: Structure, Properties and Applications in Biomedical Engineering. *J. Polym. Environ.* 2017;25:854–866. doi: 10.1007/s10924-016-0865-5.
37. Fernandes, A.I.; Jozala, A.F. Polymers Enhancing Bioavailability in Drug Delivery. *Pharmaceutics* 2022, 14, 2199. <https://doi.org/10.3390/pharmaceutics14102199>
38. Aranaz I, Alcántara AR, Civera MC, Arias C, Elorza B, Heras Caballero A, Acosta N. Chitosan: An Overview of Its Properties and Applications. *Polymers (Basel)*. 2021 Sep 24;13(19):3256. doi: 10.3390/polym13193256. PMID: 34641071; PMCID: PMC8512059.
39. Rinaudo M. Chitin and chitosan: Properties and applications. *Prog. Polym. Sci.* 2006;31:603–632. doi: 10.1016/j.progpolymsci.2006.06.001.
40. Ways T.M.M., Lau W.M., Khutoryanskiy V.V. Chitosan and its derivatives for application in mucoadhesive drug delivery systems. *Polymers*. 2018;10:267. doi: 10.3390/polym10030267.
41. Ke C.L., Deng F.S., Chuang C.Y., Lin C.H. Antimicrobial actions and applications of Chitosan. *Polymers*. 2021;13:904. doi: 10.3390/polym13060904.

42. Bernkop-Schnürch A, Dünnhaupt S. Chitosan-based drug delivery systems. *Eur J Pharm Biopharm.* 2012 Aug;81(3):463-9. doi: 10.1016/j.ejpb.2012.04.007. Epub 2012 Apr 26. PMID: 22561955.
43. Garg U, Chauhan S, Nagaich U, Jain N. Current Advances in Chitosan Nanoparticles Based Drug Delivery and Targeting. *Adv Pharm Bull.* 2019 Jun;9(2):195-204. doi: 10.15171/apb.2019.023. Epub 2019 Jun 1. PMID: 31380245; PMCID: PMC6664124.
44. Lemonnier, Nathanaëla; Zhou, Guang-Biaob; Prasher, Bhavanac; Mukerji, Mitalic,d; Chen, Zhue,f; Brahmachari, Samir K.d; Noble, Denisg; Auffray, Charlesa; Sagner, Michaelh. Traditional Knowledge-based Medicine: A Review of History, Principles, and Relevance in the Present Context of P4 Systems Medicine. *Progress in Preventive Medicine: December 2017 - Volume 2 - Issue 7 - p e0011* doi: 10.1097/pp9.0000000000000011
45. Ekor M. The growing use of herbal medicines: issues relating to adverse reactions and challenges in monitoring safety. *Front Pharmacol.* 2014 Jan 10;4:177. doi: 10.3389/fphar.2013.00177. PMID: 24454289; PMCID: PMC3887317.
46. Zhang Q, Zhao Q, Shen Y, Zhao F and Zhu Y (2022) Allium Vegetables, Garlic Supplements, and Risk of Cancer: A Systematic Review and Meta-Analysis. *Front. Nutr.* 8:746944. doi: 10.3389/fnut.2021.746944
47. Fujiki H, Watanabe T, Sueoka E, Rawangkan A, Suganuma M. Cancer Prevention with Green Tea and Its Principal Constituent, EGCG: from Early Investigations to Current Focus on Human Cancer Stem Cells. *Mol Cells.* 2018 Feb 28;41(2):73-82. doi: 10.14348/molcells.2018.2227. Epub 2018 Jan 31. PMID: 29429153; PMCID: PMC5824026.
48. Bae JM, Lee EJ, Guyatt G. Citrus fruits intake and prostate cancer risk: a quantitative systematic review. *J Prev Med Public Health.* 2008 May;41(3):159-64. doi: 10.3961/jpmph.2008.41.3.159. PMID: 18515992.
49. Lippi G, Targher G. Tomatoes, lycopene-containing foods and cancer risk. *Br J Cancer.* 2011 Mar 29;104(7):1234-5. doi: 10.1038/bjc.2011.59. Epub 2011 Feb 22. PMID: 21343935; PMCID: PMC3068500.
50. Kristo AS, Klimis-Zacas D, Sikalidis AK. Protective Role of Dietary Berries in Cancer. *Antioxidants (Basel).* 2016 Oct 19;5(4):37. doi: 10.3390/antiox5040037. PMID: 27775562; PMCID: PMC5187535.
51. Norleena P. Gullett, A.R.M. Ruhul Amin, Soley Bayraktar, John M. Pezzuto, Dong M. Shin, Fadlo R. Khuri, Bharat B. Aggarwal, Young-Joon Surh, Omer Kucuk, *Cancer Prevention With Natural Compounds, Seminars in Oncology, Volume 37, Issue 3, 2010, Pages 258-281, ISSN 0093-7754, https://doi.org/10.1053/j.seminoncol.2010.06.014.*
52. Jain A, Madu CO, Lu Y. Phytochemicals in Chemoprevention: A Cost-Effective Complementary Approach. *J Cancer.* 2021 Apr 30;12(12):3686-3700. doi: 10.7150/jca.57776. PMID: 33995644; PMCID: PMC8120178.
53. Twaij, B.M.; Hasan, M.N. Bioactive Secondary Metabolites from Plant Sources: Types, Synthesis, and Their Therapeutic Uses. *Int. J. Plant Biol.* 2022, 13, 4-14. <https://doi.org/10.3390/ijpb13010003>
54. Munawar Abbas, Farhan Saeed, Faqir Muhammad Anjum, Muhammad Afzaal, Tabussam Tufail, Muhammad Shakeel Bashir, Adnan Ishtiaq, Shahzad Hussain & Hafiz Ansar, Rasul Suleria (2017) *Natural*

polyphenols: An overview, *International Journal of Food Properties*, 20:8, 1689-1699, DOI: 10.1080/10942912.2016.1220393

55. Panche AN, Diwan AD, Chandra SR. Flavonoids: an overview. *J Nutr Sci*. 2016 Dec 29;5:e47. doi: 10.1017/jns.2016.41. PMID: 28620474; PMCID: PMC5465813.

56. Grzybowski A, Pietrzak K. Albert Szent-Györgyi (1893-1986): the scientist who discovered vitamin C. *Clin Dermatol*. 2013 May-Jun;31(3):327-31. doi: 10.1016/j.clindermatol.2012.08.001. PMID: 23738385.

57. Subramaniam S, Selvaduray KR, Radhakrishnan AK. Bioactive Compounds: Natural Defense Against Cancer? *Biomolecules*. 2019 Nov 21;9(12):758. doi: 10.3390/biom9120758. PMID: 31766399; PMCID: PMC6995630.

58. Vladu, A.F.; Fikai, D.; Ene, A.G.; Fikai, A. Combination Therapy Using Polyphenols: An Efficient Way to Improve Antitumoral Activity and Reduce Resistance. *Int. J. Mol. Sci*. 2022, 23, 10244. <https://doi.org/10.3390/ijms231810244>

59. Khan, H.; Reale, M.; Ullah, H.; Sureda, A.; Tejada, S.; Wang, Y.; Zhang, Z.-J.; Xiao, J. Anti-cancer effects of polyphenols via targeting p53 signaling pathway: Updates and future directions. *Biotechnol. Adv*. 2020, 38, 107385.

60. Mileo AM, Miccadei S. Polyphenols as Modulator of Oxidative Stress in Cancer Disease: New Therapeutic Strategies. *Oxid Med Cell Longev*. 2016;2016:6475624. doi: 10.1155/2016/6475624. Epub 2015 Nov 16. PMID: 26649142; PMCID: PMC4663347.

61. Pandey KB, Rizvi SI. Plant polyphenols as dietary antioxidants in human health and disease. *Oxid Med Cell Longev*. 2009 Nov-Dec;2(5):270-8. doi: 10.4161/oxim.2.5.9498. PMID: 20716914; PMCID: PMC2835915.

62. Waheed Janabi AH, Kamboh AA, Saeed M, Xiaoyu L, BiBi J, Majeed F, Naveed M, Mughal MJ, Korejo NA, Kamboh R, Alagawany M, Lv H. Flavonoid-rich foods (FRF): A promising nutraceutical approach against lifespan-shortening diseases. *Iran J Basic Med Sci*. 2020 Feb;23(2):140-153. doi: 10.22038/IJBMS.2019.35125.8353. PMID: 32405356; PMCID: PMC7211351.

63. Panche AN, Diwan AD, Chandra SR. Flavonoids: an overview. *J Nutr Sci*. 2016 Dec 29;5:e47. doi: 10.1017/jns.2016.41. PMID: 28620474; PMCID: PMC5465813.

64. Leridon H., Population mondiale : vers une explosion ou une implosion?, *Population & Sociétés*, 2020/1 (N° 573), p. 1-4. DOI : 10.3917/popsoc.573.0001. URL : <https://www.cairn.info/revue-population-et-societes-2020-1-page-1.htm>

65. Chiocchio, I.; Mandrone, M.; Tomasi, P.; Marincich, L.; Poli, F. Plant Secondary Metabolites: An Opportunity for Circular Economy. *Molecules* 2021, 26, 495. <https://doi.org/10.3390/molecules26020495>

66. Aline Sacchi Homrich, Graziela Galvão, Lorena Gamboa Abadia, Marly M. Carvalho, The circular economy umbrella: Trends and gaps on integrating pathways, *Journal of Cleaner Production*, Volume 175, 2018, Pages 525-543, ISSN 0959-6526, <https://doi.org/10.1016/j.jclepro.2017.11.064>.

67. Campos, D.A.; Gómez-García, R.; Vilas-Boas, A.A.; Madureira, A.R.; Pintado, M.M. Management of Fruit Industrial By-Products—A Case Study on Circular Economy Approach. *Molecules* 2020, 25, 320. <https://doi.org/10.3390/molecules25020320>
68. Fidelis, M.; de Moura, C.; Kabbas Junior, T.; Pap, N.; Mattila, P.; Mäkinen, S.; Putnik, P.; Bursać Kovačević, D.; Tian, Y.; Yang, B.; Granato, D. Fruit Seeds as Sources of Bioactive Compounds: Sustainable Production of High Value-Added Ingredients from By-Products within Circular Economy. *Molecules* 2019, 24, 3854. <https://doi.org/10.3390/molecules24213854>
69. Blaire S, What's under the Christmas Tree? A Soil Sulfur Amendment Lowers Soil pH and Alters Fir Tree Rhizosphere Bacterial and Eukaryotic Communities, Their Interactions, and Functional Traits; *ASM Journals Microbiology Spectrum* 2021, Vol. 9, No. 1, <https://doi.org/10.1128/Spectrum.00166-21>
70. Gary A. Chastagner and D. Michael Benson, The Christmas Tree: Traditions, Production, and Diseases, *Plant Health Progress* 2000 1:1 DOI:10.1094/PHP-2000-1013-01-RV
71. Martin Pettersson, Venche Talgø, Odd Ragnar Johnskås, Jan-Ole Skage, Torfinn Torp & Inger Sundheim Fløistad (2020) Postharvest needle retention in Norway spruce Christmas trees, *Scandinavian Journal of Forest Research*, 35:8, 456-467, DOI: 10.1080/02827581.2020.1795242
72. Davidson, E. 1999. Ten day visit provides revealing snapshot of Irish tree business. *Christmas Tree Lookout* 32(2):30-32.
73. Spinelli, S.; Costa, C.; Conte, A.; La Porta, N.; Padalino, L.; Del Nobile, M.A. Bioactive Compounds from Norway Spruce Bark: Comparison Among Sustainable Extraction Techniques for Potential Food Applications. *Foods* 2019, 8, 524. <https://doi.org/10.3390/foods8110524>
74. Metsämuuronen, S., Sirén, H. Bioactive phenolic compounds, metabolism and properties: a review on valuable chemical compounds in Scots pine and Norway spruce. *Phytochem Rev* 18, 623–664 (2019). <https://doi.org/10.1007/s11101-019-09630-2>
75. Jyske, T.; Järvenpää, E.; Kunnas, S.; Sarjala, T.; Raitanen, J.-E.; Mäki, M.; Pastell, H.; Korpinen, R.; Kaseva, J.; Tupasela, T. Sprouts and Needles of Norway Spruce (*Picea abies* (L.) Karst.) as Nordic Specialty—Consumer Acceptance, Stability of Nutrients, and Bioactivities during Storage. *Molecules* 2020, 25, 4187. <https://doi.org/10.3390/molecules25184187>
76. Chiocchio, I.; Mandrone, M.; Tomasi, P.; Marincich, L.; Poli, F. Plant Secondary Metabolites: An Opportunity for Circular Economy. *Molecules* 2021, 26, 495. <https://doi.org/10.3390/molecules26020495>
77. Kloskowski T, Frąckowiak S, Adamowicz J, Szeliski K, Rasmus M, Drewa T, Pokrywczyńska M. Quinolones as a Potential Drug in Genitourinary Cancer Treatment-A Literature Review. *Front Oncol.* 2022 Jun 8;12:890337. doi: 10.3389/fonc.2022.890337. PMID: 35756639; PMCID: PMC9213725.
78. Kloskowski T, Gurtowska N, Olkowska J, Nowak JM, Adamowicz J, Tworkiewicz J, Dębski R, Grzanka A, Drewa T. Ciprofloxacin is a potential topoisomerase II inhibitor for the treatment of NSCLC. *Int J Oncol.* 2012 Dec;41(6):1943-9. doi: 10.3892/ijo.2012.1653. Epub 2012 Oct 4. PMID: 23042104; PMCID: PMC3583647.
79. Lee JH, Berger JM. Cell Cycle-Dependent Control and Roles of DNA Topoisomerase II. *Genes (Basel).* 2019 Oct 30;10(11):859. doi: 10.3390/genes10110859. PMID: 31671531; PMCID: PMC6896119.

80. Larsen AK, Skladanowski A, Bojanowski K. The roles of DNA topoisomerase II during the cell cycle. *Prog Cell Cycle Res.* 1996;2:229-39. doi: 10.1007/978-1-4615-5873-6_22. PMID: 9552399.
81. Kloskowski T The Influence Of Ciprofloxacin On Viability Of A549, Hepg2, A375.S2, B16 And C6 Cell Lines In Vitro, *Acta Poloniae Pharmaceutica ñ Drug Research*, Vol. 68 No. 6 pp. 859ñ865, 2011
82. Tomasz Kloskowski, Natalia Gurtowska, Tomasz Drewa, Does ciprofloxacin have an obverse and a reverse?, *Pulmonary Pharmacology & Therapeutics*, Volume 23, Issue 5, 2010, Pages 373-375, ISSN 1094-5539, <https://doi.org/10.1016/j.pupt.2010.02.005>.
83. Gurtowska N, Kloskowski T, Drewa T. Ciprofloxacin criteria in antimicrobial prophylaxis and bladder cancer recurrence. *Medical Science Monitor : International Medical Journal of Experimental and Clinical Research.* 2010 Oct;16(10):RA218-23. PMID: 20885364.
84. Ben Ayed, A.; Akrouf, I.; Albert, Q.; Greff, S.; Simmler, C.; Armengaud, J.; Kielbasa, M.; Turbé-Doan, A.; Chaduli, D.; Navarro, D.; et al. Biotransformation of the Fluoroquinolone, Levofloxacin, by the White-Rot Fungus *Coriolopsis gallica*. *J. Fungi* 2022, 8, 965. <https://doi.org/10.3390/jof8090965>
85. He, Xiaoqiong and Yao, Qian and Song, Zhong Yu and Fan, Dan and You, Yu Tong and Lian, Wen Jing and Zhou, Zhang Ping and Duan, Ling, Levofloxacin Can Greatly Influence Clinical Practice of Cancer Treatment: It Has Broad-Spectrum Anticancer Activity and Synergistically Enhance Conventional Chemotherapy (July 24, 2019). Available at SSRN: <https://ssrn.com/abstract=3426094> or <http://dx.doi.org/10.2139/ssrn.3426094>
86. Numakura K et el, Effect of Levofloxacin on the Efficacy and Adverse Events in Intravesical Bacillus Calmette-Guerin Treatment for Bladder Cancer: Results of a Randomized, Prospective, Multicenter Study, *European Urology Focus*, June 2022, <https://doi.org/10.1016/j.euf.2022.06.002>
87. Davis, R., Bryson, H.M. Levofloxacin. *Drugs* 47, 677–700 (1994). <https://doi.org/10.2165/00003495-199447040-00008>
88. Ma H, Jiang Q, Han S, et al. Multicellular Tumor Spheroids as an in Vivo–Like Tumor Model for Three–Dimensional Imaging of Chemotherapeutic and Nano Material Cellular Penetration. *Molecular Imaging*. November 2012. doi:10.2310/7290.2012.00012
89. Igor Vasyutin, Lillian Zerihun, Cristina Ivan, Anthony Atala; Bladder Organoids and Spheroids: Potential Tools for Normal and Diseased Tissue Modelling 10.21873/anticancer.13219 *Anticancer Research* March 2019 vol. 39 no. 3 1105-1118
90. Mueller-Klieser, W. Multicellular spheroids. *J Cancer Res Clin Oncol* 113, 101–122 (1987). <https://doi.org/10.1007/BF00391431>
91. Franziska Sambale, Antonina Lavrentieva, Frank Stahl, Cornelia Blume, Meike Stiesch, Cornelia Kasper, Detlef Bahnemann, Thomas Scheper; Three dimensional spheroid cell culture for nanoparticle safety testing; *Journal of Biotechnology*, Volume 205, 2015, Pages 120-129, ISSN 0168-1656, <https://doi.org/10.1016/j.jbiotec.2015.01.001>.
92. Comparative Assay of 2D and 3D Cell Culture Models: Proliferation, Gene Expression and Anticancer Drug Response; *Current Pharmaceutical Design*, Volume 24, Number 15, 2018, pp. 1689-1694(6);

93. Baek N, Seo OW, Kim M, Hulme J, An SS. Monitoring the effects of doxorubicin on 3D-spheroid tumor cells in real-time. *Onco Targets Ther.* 2016 Nov 22;9:7207-7218. doi: 10.2147/OTT.S112566. PMID: 27920558; PMCID: PMC5125797.
94. Costa EC, de Melo-Diogo D, Moreira AF, Carvalho MP, Correia IJ. Spheroids Formation on Non-Adhesive Surfaces by Liquid Overlay Technique: Considerations and Practical Approaches. *Biotechnol J.* 2018 Jan;13(1). doi: 10.1002/biot.201700417. Epub 2017 Nov 15. PMID: 29058365.
95. Law AMK, Rodriguez de la Fuente L, Grundy TJ, Fang G, Valdes-Mora F, Gallego-Ortega D. Advancements in 3D Cell Culture Systems for Personalizing Anti-Cancer Therapies. *Front Oncol.* 2021 Nov 30;11:782766. doi: 10.3389/fonc.2021.782766. PMID: 34917509; PMCID: PMC8669727.
96. Edmondson R, Broglie JJ, Adcock AF, Yang L. Three-dimensional cell culture systems and their applications in drug discovery and cell-based biosensors. *Assay Drug Dev Technol.* 2014 May;12(4):207-18. doi: 10.1089/adt.2014.573. PMID: 24831787; PMCID: PMC4026212.
97. Han, S.J., Kwon, S. & Kim, K.S. Challenges of applying multicellular tumor spheroids in preclinical phase. *Cancer Cell Int* 21, 152 (2021). <https://doi.org/10.1186/s12935-021-01853-8>
98. Pinto B, Henriques AC, Silva PMA, Bousbaa H. Three-Dimensional Spheroids as In Vitro Preclinical Models for Cancer Research. *Pharmaceutics.* 2020 Dec 6;12(12):1186. doi: 10.3390/pharmaceutics12121186. PMID: 33291351; PMCID: PMC7762220.
99. Giusti, I.; Poppa, G.; D'Ascenzo, S.; Esposito, L.; Vitale, A.R.; Calvisi, G.; Dolo, V. Cancer Three-Dimensional Spheroids Mimic In Vivo Tumor Features, Displaying "Inner" Extracellular Vesicles and Vasculogenic Mimicry. *Int. J. Mol. Sci.* 2022, 23, 11782. <https://doi.org/10.3390/ijms231911782>
100. Mehta G, Hsiao AY, Ingram M, Luker GD, Takayama S. Opportunities and challenges for use of tumor spheroids as models to test drug delivery and efficacy. *J Control Release.* 2012 Dec 10;164(2):192-204. doi: 10.1016/j.jconrel.2012.04.045. Epub 2012 May 18. PMID: 22613880; PMCID:
101. Yao Y, Zhou Y, Liu L, Xu Y, Chen Q, Wang Y, Wu S, Deng Y, Zhang J, Shao A. Nanoparticle-Based Drug Delivery in Cancer Therapy and Its Role in Overcoming Drug Resistance. *Front Mol Biosci.* 2020 Aug 20;7:193. doi: 10.3389/fmolb.2020.00193. PMID: 32974385; PMCID: PMC7468194.
102. Lv D, Hu Z, Lu L, Lu H, Xu X. Three-dimensional cell culture: A powerful tool in tumor research and drug discovery. *Oncol Lett.* 2017 Dec;14(6):6999-7010. doi: 10.3892/ol.2017.7134. Epub 2017 Oct 3. PMID: 29344128; PMCID: PMC5754907.
103. Mirabelli P, Coppola L, Salvatore M. Cancer Cell Lines Are Useful Model Systems for Medical Research. *Cancers (Basel).* 2019 Aug 1;11(8):1098. doi: 10.3390/cancers11081098. PMID: 31374935; PMCID: PMC6721418.
104. Senapati S, Mahanta AK, Kumar S, Maiti P. Controlled drug delivery vehicles for cancer treatment and their performance. *Signal Transduction and Targeted Therapy.* 2018;3:7. DOI: 10.1038/s41392-017-0004-3. PMID: 29560283; PMCID: PMC5854578.
105. Heng Mei, Shengsheng Cai, Dennis Huang, Huile Gao, Jun Cao, Bin He, Carrier-free nanodrugs with efficient drug delivery and release for cancer therapy: From intrinsic physicochemical properties to external modification, *Bioactive Materials*, Volume 8, 2022, Pages 220-240, ISSN 2452-199X, <https://doi.org/10.1016/j.bioactmat.2021.06.035>.

106. Jensen C and Teng Y (2020) Is It Time to Start Transitioning From 2D to 3D Cell Culture? *Front. Mol. Biosci.* 7:33. doi: 10.3389/fmolb.2020.00033
107. Kloskowski et al., Ciprofloxacin and Levofloxacin as Potential Drugs in Genitourinary Cancer Treatment—The Effect of Dose–Response on 2D and 3D Cell Cultures, *Int. J. Mol. Sci.* 2021, 22(21), 11970; <https://doi.org/10.3390/ijms222111970>
108. Mark H. Gotfried, Larry H. Danziger, Keith A. Rodvold, Steady-State Plasma and Intrapulmonary Concentrations of Levofloxacin and Ciprofloxacin in Healthy Adult Subjects, *Chest*, Volume 119, Issue 4, 2001, Pages 1114-1122, ISSN 0012-3692, <https://doi.org/10.1378/chest.119.4.1114>.
109. Summary of Medicinal Product Ciprofloxacin, 2014, rejestrymedyczne.ezdrowie.gov.pl
110. Bhatia, S.N., Chen, X., Dobrovolskaia, M.A. et al. Cancer nanomedicine. *Nat Rev Cancer* **22**, 550–556 (2022). <https://doi.org/10.1038/s41568-022-00496-9>
111. Afsana Sheikh, Shadab Md, Nabil A. Alhakamy, Prashant Kesharwani, Recent development of aptamer conjugated chitosan nanoparticles as cancer therapeutics, *International Journal of Pharmaceutics*, Volume 620, 2022, 121751, ISSN 0378-5173, <https://doi.org/10.1016/j.ijpharm.2022.121751>.
112. Sharma PC, Jain A, Jain S, Fluoroquinolone antibacterials: a review on chemistry, microbiology and therapeutic prospects *Acta Poloniae Pharmaceutica – Drug Research*, Vol. 66 No. 6 pp. 587604, 2009.
113. Al-Musawi S, Hadi AJ, Suhad Jameel Hadi SJ, Hindi NKK, Preparation and Characterization of Folated Chitosan/Magnetic Nanocarrier for 5-Fluorouracil Drug Delivery and Studying its Effect in Bladder Cancer Therapy *Journal of Global Pharma Technology*, ISSN: 0975 -8542
114. Mohammad Zaki Ahmad, Md. Rizwanullah, Javed Ahmad, Mohammed Yahia Alasmay, Md. Habban Akhter, Basel A. Abdel-Wahab, Musarrat Husain Warsi & Anzarul Haque (2022) Progress in nanomedicine-based drug delivery in designing of chitosan nanoparticles for cancer therapy, *International Journal of Polymeric Materials and Polymeric Biomaterials*, 71:8, 602-623, DOI: 10.1080/00914037.2020.1869737
115. Ysrafil Y, Astuti I. Chitosan nanoparticle-mediated effect of antimRNA-324-5p on decreasing the ovarian cancer cell proliferation by regulation of GLI1 expression. *Bioimpacts*. 2022;12(3):195-202. doi: 10.34172/bi.2021.22119. Epub 2021 Nov 29. PMID: 35677668; PMCID: PMC9124874.
116. Ghazal Hatami Fard, Zeynab Moinipoor, Salzitsa Anastasova-Ivanova, Hafiz M.N. Iqbal, Miriam V. Dwek, StephenJ. Getting, Tajalli Keshavarz, Development of chitosan, pullulan, and alginate based drug-loaded nano-emulsions as a potential malignant melanoma delivery platform, *Carbohydrate Polymer Technologies and Applications*, Volume 4, 2022, 100250, ISSN 2666-8939, <https://doi.org/10.1016/j.carpta.2022.100250>
117. Laure Gibot, Stéphane Chabaud, Sara Bouhout, Stéphane Bolduc, François A. Auger, Véronique J. Moulin, Anticancer properties of chitosan on human melanoma are cell line dependent, *International Journal of Biological Macromolecules*, Volume 72, 2015, Pages 370-379, ISSN 0141-8130, <https://doi.org/10.1016/j.ijbiomac.2014.08.033>.

118. Raquel Rodríguez-González, Elia Bosch-Rué, Leire Díez-Tercero, Luis M. Delgado, Román A. Pérez, Tailorable low temperature silica-gelatin biomaterials for drug delivery, *Ceramics International*, Volume 48, Issue 19, Part A, 2022, Pages 28659-28668, ISSN 0272-8842, <https://doi.org/10.1016/j.ceramint.2022.06.180>.
119. Hu, C., He, S., Lee, Y.J. et al. Live-dead assay on unlabeled cells using phase imaging with computational specificity. *Nat Commun* 13, 713 (2022). <https://doi.org/10.1038/s41467-022-28214-x>
120. T.P. Punarvasu, K.V. Harish Prashanth, Self-assembled chitosan derived microparticles inhibit tumor angiogenesis and induce apoptosis in Ehrlich-ascites-tumor bearing mice, *Carbohydrate Polymers*, Volume 278, 2022, 118941, ISSN 0144-8617, <https://doi.org/10.1016/j.carbpol.2021.118941>.
121. Bünger, C.M., Jahnke, A., Stange, J., De Vos, P. and Hopt, U.T. (2002), MTS Colorimetric Assay in Combination with a Live-Dead Assay for Testing Encapsulated L929 Fibroblasts in Alginate Poly-L-Lysine Microcapsules In Vitro. *Artificial Organs*, 26: 111-116. <https://doi.org/10.1046/j.1525-1594.2002.06853.x>
122. Navid Ahmadi Nasab, Hassan Hassani Kumleh, Mojtaba Beygzadeh, Shahram Teimourian & Mahmood Kazemzad (2018) Delivery of curcumin by a pH-responsive chitosan mesoporous silica nanoparticles for cancer treatment, *Artificial Cells, Nanomedicine, and Biotechnology*, 46:1, 75-81, DOI: 10.1080/21691401.2017.1290648
123. Jun Jie Wang, Zhao Wu Zeng, Ren Zhong Xiao, Tian Xie, Guang Lin Zhou, Xiao Ri Zhan & Shu Ling Wang (2011) Recent advances of chitosan nanoparticles as drug carriers, *International Journal of Nanomedicine*, 6:, 765-774, DOI: 10.2147/IJN.S17296
124. Iztok Turel, Peter Bukovec, Miguel Quirós, Crystal structure of ciprofloxacin hexahydrate and its characterization, *International Journal of Pharmaceutics*, Volume 152, Issue 1, 1997, Pages 59-65, ISSN 0378-5173, [https://doi.org/10.1016/S0378-5173\(97\)04913-2](https://doi.org/10.1016/S0378-5173(97)04913-2).
125. Aameeduzzafar, Syed Sarim Imam, Syed Nasir Abbas Bukhari, Javed Ahmad, Asgar Ali, Formulation and optimization of levofloxacin loaded chitosan nanoparticle for ocular delivery: In-vitro characterization, ocular tolerance and antibacterial activity, *International Journal of Biological Macromolecules*, Volume 108, 2018, Pages 650-659, ISSN 0141-8130, <https://doi.org/10.1016/j.ijbiomac.2017.11.170>.
126. Seyedeh Elham Mousavi Kalajahi, Shadi Ghandiha, Optimization of spray drying parameters for encapsulation of Nettle (*Urtica dioica* L.) extract, *LWT*, Volume 158, 2022, 113149, ISSN 0023-6438, <https://doi.org/10.1016/j.lwt.2022.113149>.
127. N. Bhattarai, H.R. Ramay, S.H. Chou, M. Zhang Chitosan and lactic acid-grafted chitosan nanoparticles as carriers for prolonged drug delivery *Int J Nanomed*, 1 (2006), pp. 181-187.
128. Umme Ruman, Sharida Fakurazi, Mas Jaffri Masarudin & Mohd Zobir Hussein (2020) Nanocarrier-Based Therapeutics and Theranostics Drug Delivery Systems for Next Generation of Liver Cancer Nanodrug Modalities, *International Journal of Nanomedicine*, 15:, 1437-1456, DOI: 10.2147/IJN.S236927

129. Jhaveri, J.; Raichura, Z.; Khan, T.; Momin, M.; Omri, A. Chitosan Nanoparticles-Insight into Properties, Functionalization and Applications in Drug Delivery and Theranostics. *Molecules* 2021, 26, 272. <https://doi.org/10.3390/molecules26020272>
130. Hazafa, A., Iqbal, M.O., Javaid, U. et al. Inhibitory effect of polyphenols (phenolic acids, lignans, and stilbenes) on cancer by regulating signal transduction pathways: a review. *Clin Transl Oncol* 24, 432–445 (2022). <https://doi.org/10.1007/s12094-021-02709-3>
131. Prasain JK, Barnes S. Metabolism and bioavailability of flavonoids in chemoprevention: current analytical strategies and future prospectus. *Mol Pharm.* 2007 Nov-Dec;4(6):846-64. doi: 10.1021/mp700116u. PMID: 18052086.
132. Marie Yayinie, Minaleshewa Atlabachew, Alemu Tesfaye, Woldegiorgis Hilluf, Chaltu Reta & Tessera Alemneh (2022) Polyphenols, flavonoids, and antioxidant content of honey coupled with chemometric method: geographical origin classification from Amhara region, Ethiopia, *International Journal of Food Properties*, 25:1, 76-92, DOI: 10.1080/10942912.2021.2021940
133. Vladu, A.F.; Ficai, D.; Ene, A.G.; Ficai, A. Combination Therapy Using Polyphenols: An Efficient Way to Improve Antitumoral Activity and Reduce Resistance. *Int. J. Mol. Sci.* 2022, 23, 10244. <https://doi.org/10.3390/ijms231810244>
134. Trisha, A.T.; Shakil, M.H.; Talukdar, S.; Rovina, K.; Huda, N.; Zzaman, W. Tea Polyphenols and Their Preventive Measures against Cancer: Current Trends and Directions. *Foods* **2022**, 11, 3349. <https://doi.org/10.3390/foods11213349>
135. Murazov Ia.G., Nyuganen A.O., Artemyeva A.S. Evaluation of the chemopreventive potential of polyphenols from the needles of *Picea abies* L. and *Pinus sylvestris* L. using the model of prostate carcinogenesis in male Wistar rats. *Voprosy pitaniia [Problems of Nutrition]*. 2021; 90 (3): 104-115. DOI: <https://doi.org/10.33029/0042-8833-2021-90-3-104-115>
136. Lutter AH, Scholka J, Richter H, Anderer U. Applying XTT, WST-1, and WST-8 to human chondrocytes: A comparison of membrane-impermeable tetrazolium salts in 2D and 3D cultures. *Clin Hemorheol Microcirc.* 2017;67(3-4):327-342. doi: 10.3233/CH-179213. PMID: 28869462.
137. Maria Scuto, Maria Laura Ontario, Angela Trovato Salinaro, Isabella Caligiuri, Francesco Rampulla, Vincenzo Zimbone, Sergio Modafferi, Flavio Rizzolio, Vincenzo Canzonieri, Edward J. Calabrese, Vittorio Calabrese, Redox modulation by plant polyphenols targeting vitagenes for chemoprevention and therapy: Relevance to novel anti-cancer interventions and mini-brain organoid technology, *Free Radical Biology and Medicine*, Volume 179, 2022, Pages 59-75, ISSN 0891-5849, <https://doi.org/10.1016/j.freeradbiomed.2021.12.267>.
138. Diab KA, El-Shenawy R, Helmy NM, El-Toumy SA. Polyphenol Content, Antioxidant, Cytotoxic, and Genotoxic Activities of *Bombax ceiba* Flowers in Liver Cancer Cells Huh7. *Asian Pac J Cancer Prev.* 2022 Apr 1;23(4):1345-1350. doi: 10.31557/APJCP.2022.23.4.1345. PMID: 35485695; PMCID: PMC9375612.
139. Malinowski, P.; Skała, K.; Jabłońska-Trypuć, A.; Koronkiewicz, A.; Wołejko, E.; Wydro, U.; Świdorski, G.; Lewandowski, W. Comparison of the Usefulness of MTT and CellTiterGlo Tests Applied for Cytotoxicity Evaluation of Compounds from the Group of Polyphenols. *Environ. Sci. Proc.* 2022, 18, 9. <https://doi.org/10.3390/environsciproc2022018009>

140. Choi, B.H.; Kim, M.-R.; Jung, Y.N.; Kang, S.; Hong, J. Interfering with Color Response by Porphyrin-Related Compounds in the MTT Tetrazolium-Based Colorimetric Assay. *Int. J. Mol. Sci.* 2023, 24, 562. <https://doi.org/10.3390/ijms24010562>
141. Ashishkumar A. Kale, Meghsham P. Anjankar, Ashwin V., Uday V. Pawade, Anticancer Activity Of Calotropis Procera And Its Phytoconstituents: An Overview, *WORLD JOURNAL OF PHARMACY AND PHARMACEUTICAL SCIENCES SJIF Impact Factor 7.632 Volume 11, Issue 11, 410-420 Review Article ISSN 2278 – 4357*
142. Younes, M.; Mardirossian, R.; Rizk, L.; Fazlian, T.; Khairallah, J.P.; Sleiman, C.; Naim, H.Y.; Rizk, S. The Synergistic Effects of Curcumin and Chemotherapeutic Drugs in Inhibiting Metastatic, Invasive and Proliferative Pathways. *Plants* 2022, 11, 2137. <https://doi.org/10.3390/plants11162137>
143. Owczarek K., Sosnowska D., Kajszyzak D., i Lewandowska U., Evaluation of phenolic composition, antioxidant and cytotoxic activity of aronia melanocarpa leaf extracts, „*Journal of Physiology and Pharmacology*”, 2022, t.73, s. 1–11.
144. Abolmaesoomi, Mitra, Mat Junit, Sarni, Mohd Ali, Johari, Chik, Zamri Bin and Abdul Aziz, Azlina. "Effects of polyphenolic-rich extracts from Citrus hystrix on proliferation and oxidative stress in breast and colorectal cancer" *Turkish Journal of Biochemistry*, 2022. <https://doi.org/10.1515/tjb-2022-0062>
145. Maleki Dana, P., Sadoughi, F., Asemi, Z. et al. The role of polyphenols in overcoming cancer drug resistance: a comprehensive review. *Cell Mol Biol Lett* 27, 1 (2022). <https://doi.org/10.1186/s11658-021-00301-9>
146. Kapoor, S.; Damiani, E.; Wang, S.; Dharmanand, R.; Tripathi, C.; Tovar Perez, J.E.; Dashwood, W.M.; Rajendran, P.; Dashwood, R.H. BRD9 Inhibition by Natural Polyphenols Targets DNA Damage/Repair and Apoptosis in Human Colon Cancer Cells. *Nutrients* 2022, 14, 4317. <https://doi.org/10.3390/nu14204317>
147. Antony, A.; Farid, M. Effect of Temperatures on Polyphenols during Extraction. *Appl. Sci.* 2022, 12, 2107. <https://doi.org/10.3390/app12042107>
148. Tylkowski, B.; Konopka, P.; Maj, M.; Kazmierski, L.; Skrobanska, M.; Montane, X.; Giamberini, M.; Bajek, A.; Jastrzab, R. Christmas Tree Bio-Waste as a Power Source of Bioactive Materials with Anti-Proliferative Activities for Oral Care. *Molecules* 2022, 27, 6553. <https://doi.org/10.3390/molecules27196553>
149. Lin Y, Shi R, Wang X, Shen HM. Luteolin, a flavonoid with potential for cancer prevention and therapy. *Curr Cancer Drug Targets.* 2008 Nov;8(7):634-46. doi: 10.2174/156800908786241050. PMID: 18991571; PMCID: PMC2615542.
150. Prasher, P., Sharma, M., Singh, S.K. et al. Luteolin: a flavonoid with a multifaceted anticancer potential. *Cancer Cell Int* 22, 386 (2022). <https://doi.org/10.1186/s12935-022-02808-3>
151. Lovitt, C.J.; Shelper, T.B.; Avery, V.M. Advanced Cell Culture Techniques for Cancer Drug Discovery. *Biology* 2014, 3, 345-367. <https://doi.org/10.3390/biology3020345>
152. Sodek, K.L., Ringuette, M.J. and Brown, T.J. (2009), Compact spheroid formation by ovarian cancer cells is associated with contractile behavior and an invasive phenotype. *Int. J. Cancer*, 124: 2060-2070. <https://doi.org/10.1002/ijc.24188>

153. Hui-li Ma et al., Multicellular Tumor Spheroids as an In Vivo–Like Tumor Model for Three-Dimensional Imaging of Chemotherapeutic and Nano Material Cellular Penetration Molecular Imaging, Vol 11, No 6 (November–December 2012): pp 487–498.
154. Pickl, M., Ries, C. Comparison of 3D and 2D tumor models reveals enhanced HER2 activation in 3D associated with an increased response to trastuzumab. *Oncogene* 28, 461–468 (2009). <https://doi.org/10.1038/onc.2008.394>
155. Sant S, Johnston PA. The production of 3D tumor spheroids for cancer drug discovery. *Drug Discov Today Technol.* 2017 Mar;23:27-36. doi: 10.1016/j.ddtec.2017.03.002. Epub 2017 Apr 14. PMID: 28647083; PMCID: PMC5497458.
156. Richard C Bates, Nathaniel S Edwards, Jonathon D Yates, Spheroids and cell survival, *Critical Reviews in Oncology/Hematology*, Volume 36, Issues 2–3, 2000, Pages 61-74, ISSN 1040-8428, [https://doi.org/10.1016/S1040-8428\(00\)00077-9](https://doi.org/10.1016/S1040-8428(00)00077-9).
157. Nagma Khan, Dhruva J. Bharali, Vaqar M. Adhami, Imtiaz A. Siddiqui, Huadong Cui, Sameh M. Shabana, Shaker A. Mousa, Hasan Mukhtar, Oral administration of naturally occurring chitosan-based nanoformulated green tea polyphenol EGCG effectively inhibits prostate cancer cell growth in a xenograft model, *Carcinogenesis*, Volume 35, Issue 2, February 2014, Pages 415–423, <https://doi.org/10.1093/carcin/bgt321>
158. Croom K.F., Goa K.L. Levofloxacin. A review of its use in the treatment of bacterial infections in the United States. *Drugs* 2003; 63 (24): 2769-2802.
159. The Department of Pharmacy Practice, School of Pharmacy, University of Colorado Health Sciences Center, Denver, Colorado. Fluoroquinolone adverse effects and drug interactions: specific adverse effects. www.medscape.com/viewarticle/418295_2.
160. Lubasch A. Keller I. Borner K. Koeppel P. Lode H. Comparative pharmacokinetics of ciprofloxacin, gatifloxacin, grepafloxacin, levofloxacin, trovafloxacin and moxifloxacin after single oral administration in healthy volunteers. *Antimicrobial Agents and Chemotherapy*, Oct. 2000, p. 2600-2603.
161. Lal-Nag M, McGee L, Titus SA, Brimacombe K, Michael S, Sittampalam G, et al. Exploring drug dosing regimens in vitro using real-time 3D spheroid tumor growth assays. *SLAS Discov.* 2017;22(5):537–46. z: <http://dx.doi.org/10.1177/2472555217698818>
162. Fuentes-Chandía, M., Vierling, A., Kappelmann-Fenzl, M., Monavari, M., Letort, G., Höne, L., Parma, B., Antara, S. K., Ertekin, Ö., Palmisano, R., Dong, M., Böpple, K., Boccaccini, A. R., Ceppi, P., Bosserhoff, A. K., & Leal- Egaña, A.; 3D Spheroids Versus 3D Tumor-Like Microcapsules: Confinement and Mechanical Stress May Lead to the Expression of Malignant Responses in Cancer Cells. *Advanced Biology*, 2021, 5(7), [2000349]. <https://doi.org/10.1002/adbi.202000349>
163. Wade SJ, Zuzic A, Foroughi J, Talebian S, Aghmesheh M, Moulton SE, et al. Preparation and in vitro assessment of wet-spun gemcitabine-loaded polymeric fibers: Towards localized drug delivery for the treatment of pancreatic cancer. *Pancreatology.* 2017;17(5):795–804. z: doi.org/10.1016/j.pan.2017.06.001

- 164 . Mittler F, Obeid P, Rulina AV, Haguët V, Gidrol X, Balakirev MY. High-Content Monitoring of Drug Effects in a 3D Spheroid Model. *Front Oncol.* 2017 Dec 11;7:293. doi: 10.3389/fonc.2017.00293. PMID: 29322028; PMCID: PMC5732143.
165. Lee JM, Park DY, Yang L, Kim E-J, Ahrberg CD, Lee K-B, et al. Generation of uniform-sized multicellular tumor spheroids using hydrogel microwells for advanced drug screening. *Sci Rep.* 2018;8(1):17145. z: <http://dx.doi.org/10.1038/s41598-018-35216-7>
166. Zanoni M, Pignatta S, Arienti C, Bonafè M; Anticancer drug discovery using multicellular tumor spheroid models, *Expert Opinion on Drug Discovery*, 2019, 14:3, 289-301, DOI: 10.1080/17460441.2019.1570129
167. Nafiseh Moghimi, Seied Ali Hosseini, Mahla Poudineh, Mohammad Kohandel. (2022) Recent advances on cancer-on-chip models: Development of 3D tumors and tumor microenvironment. *Bioprinting* 28, pages e00238.
168. Ceron Jayme C, Ferreira Pires A, Silvestrini Fernandes D et. Al. ; DNA polymer films used as drug delivery systems to early-stage diagnose and treatment of breast cancer using 3D tumor spheroids as a model. *Photodiagnosis and Photodynamic Therapy* 2022; 37, pages 102575.
169. Fuentes-Chandía M, Vierling A, Kappelmann-Fenzl M et. Al.; 3D Spheroids Versus 3D Tumor-Like Microcapsules: Confinement and Mechanical Stress May Lead to the Expression of Malignant Responses in Cancer Cells. 2021; *Advanced Biology* 5:7, pages 2000349.